APPLICATION OF CROP MODELS IN ASSESSING IMPACT OF CLIMATE CHANGE AND IDENTIFYING ADAPTATION OPTIONS IN A TROPICAL ENVIRONMENT IN ETHIOPIA

by

HIRUT GETACHEW FELEKE

Submitted in fulfilment of the academic requirements of

Doctor of Philosophy

in Agrometeorology

School of Agricultural, Earth and Environmental Sciences

College of Agriculture, Engineering and Science

University of KwaZulu-Natal

Pietermaritzburg

South Africa

December 2021

PREFACE

The research contained in this thesis was completed by the candidate while based in the Discipline of Agrometeorology, School of Agricultural, Earth and Environmental Sciences of the College of Agriculture, Engineering and Science, University of KwaZulu-Natal, Pietermaritzburg, South Africa. The research was financially supported by Organization for Women in Science for the Developing World (OWSD) and Swedish International Development Cooperation Agency (SIDA).

The contents of this work have not been submitted in any form to another university and, except where the work of others is acknowledged in the text, the results reported are due to investigations by the candidate.

[redacted]

Signed: Professor M.J. Savage

Date: December 2021

DECLARATION 1: PLAGIARISM

I, Hirut Getachew Feleke, declare that:

(i) the research reported in this thesis, except where otherwise indicated or acknowledged, is my original work;

(ii) this thesis has not been submitted in full or in part for any degree or examination to any other university;

(iii) this thesis does not contain other persons' data, pictures, graphs or other information, unless specifically acknowledged as being sourced from other persons;

(iv) this thesis does not contain other persons' writing, unless specifically acknowledged as being sourced from other researchers. Where other written sources have been quoted, then:

a) their words have been re-written but the general information attributed to them has been referenced;

b) where their exact words have been used, their writing has been placed inside quotation marks, and referenced;

(v) where I have used material for which publications followed, I have indicated in detail my role in the work;

(vi) this thesis is primarily a collection of material, prepared by myself, published as journal articles;

(vii) this thesis does not contain text, graphics or tables copied and pasted from the Internet, unless specifically acknowledged, and the source being detailed in the thesis and in the References sections.

[redacted]

Signed: Hirut Getachew Feleke

Date: 15 December 2021

DECLARATION 2: PUBLICATIONS

This thesis is written in a manuscript format. One manuscript is published while others are in preparation. The style used in each chapter may differ depending on the Journal for which it is to be submitted for publication. My role in each paper and presentation is indicated. The * indicates corresponding author.

Chapter 3

Hirut Getachew Feleke*, MJ Savage and Kindie Tesfaye, 2021. Calibration and validation of APSIM–Maize, DSSAT CERES–Maize and AquaCrop models for Ethiopian tropical environments, South African Journal of Plant and Soil, 38:1, 36-51. DOI: 10.1080/02571862.2020.1837271.

Hirut Getachew Feleke's* role in this paper: designed the study, collected experimental data, analyzed the datasets, calibrated and evaluated the crop models and wrote the manuscript.

Chapter 4

Hirut Getachew Feleke*, MJ Savage and Kindie Tesfaye, 2021. Impact of climate change on maize (*Zea mays* L.) production and the role of cultivars, planting date and nitrogen fertilizer as an Adaptation options in Ethiopia. To be summitted for publication

Hirut Getachew Feleke's* role in this paper: designed the study, collected experimental data, downscaled climate data, analyzed the datasets, undertook crop model simulation and wrote the manuscript.

Chapter 5

Hirut Getachew Feleke*, MJ Savage and Kindie Tesfaye, 2021. Drought risk assessment in maize (*Zea may* L.) cultivated areas of Ethiopia at past and future climate change. To be summitted for publication

Hirut Getachew Feleke's* role in this paper: designed the study, downscaled climate data, analyzed the datasets and wrote the manuscript.

ACKNOWLEDGMENTS

This project would not have been possible without the support of many people. A number of individuals and organizations have been supportive in the long years of my PhD project. I recognize that many people and organizations deserve gratitude for rendering me special support and guidance. Nevertheless, I will only be mentioning few of them here and my apologies for those whom I failed to include their names. However, be assured that you all have a place in my heart.

First and foremost, I would like to praise and thank God, the almighty, who has granted countless blessing, knowledge, and opportunity to me, so that I have been finally able to accomplish my PhD.

I would like to thank the Organization for Women in Science for the Developing World (OWSD) and the Swedish International Development Agency (SIDA) for providing me scholarship and the financial means to complete the project.

I would also like to extend my special respect and gratitude to my supervisor and co-supervisor Professor MJ Savage of the University of KwaZulu-Natal (UKZN) and Dr. Kindie Tesfaye of CIMMYT respectively. Their comments and reviews greatly improved my academic writing and analytical skills.

I am highly thankful to Professor Savage for his professional support, guidance, and prompt feedback throughout my thesis writing. He has been a source of encouragement and motivation throughout my PhD journey. I am indebted to his patience, kindness, and sincere support in reading my revisions, editing, and correcting the manuscripts. I would also like to thank his wife Mrs. Meryl Savage for her kind reception and support during my visit to her office.

I also thank and appreciate Dr. Kindie Tesfaye for his constructive and invaluable comments, guidance, and support rendered throughout my thesis writing. Without this the thesis would not be a reality. I thank you.

I would also want to extend my sincere gratitude to Dr. Alistar David Clulow for his continuous support in facilitating the administrative matters in the University.

I appreciate the University of KwaZulu-Natal, Discipline of Agrometeorology, for providing a friendly environment and innumerable resources.

The institutional support of the Ambo, Bako and Melkassa Agricultural Research Centers has been invaluable contribution to the completion of my field work and data collection.

I am very grateful to Fasile Mequanint for his professional support. I would like to thank Dr. Nicholas Mbangiwa, Dr. Sheldon Strydom, Dr. Zoleka Ncoyini and Evidence Mazhawu for their professional guidance and friendly hospitality.

Being surrounded by caring friends has its own contribution while undertaking a demanding and stressful project like a PhD. In this regard, the hospitality, care, and compassion of my dear friends such as Dr. Amelework Assefa, Eyerusalem Amare and Mesi Budlue and their families deserve a special thanks for making my stay in Pietermaritzburg joyful, pleasant, and fun.

My husband, Dr. Solomon Alemu, this accomplishment would have not been possible without your love and endurance in those years. Thank you for your guidance and support through all those tough times.

Many thanks also goes to all my family members especially my mother Bogalech Tadesse, aunt Workitu Tadesse, my brother and sisters for their endless support, encouragement, and love.

Finally, I would like to extend my sincere gratitude and respect to my late father Getachew Feleke, who passed away on August 2020 while I was in the middle of my PhD journey. He was my inspiration to pursue my education. I owe him very much in all my achievements and I wish he were here with me to see another mile of my success. Love you so much.

EXTENDED SUMMARY

Ethiopia is one of the most food-insecure and famine affected countries. This is mainly due to the negative effect of climate related risks, in particular high rainfall variability and severe droughts. Anticipated climate change is expected to aggravate some of the existing challenges and impose new risks beyond the range expected. Thus, it is important to have a wide range of adaptation strategies to overcome the impact of climate change which requires an in-depth analysis of climate change sensitivity assessments on crop production.

Several climate change impact assessment methods have been developed to measure the impacts of climate change on crop production. Among these, the use of crop growth models together with climate models is one of the most applicable methods in agriculture to the impact of climate change on crops, to predict crop yield, and to support field management decisions.

The simulation of the effect of climate change on crops is based on the downscaling method of General Circulation Models (GCMs) output to match the crop model. However, the climate model outputs, and crop model inputs are the major sources of uncertainty in the assessment of the impact of climate change on crop production. The Agricultural Model Intercomparison and Improvement Project (AgMIP) has proven useful for comparing consistency among models and quantifying uncertainty in model predictions. They have reinforced the benefit of multimodel approaches, to identify sources of uncertainty associated with model parameters and model structures.

The model ensemble mean or median usually resulted as best predictors for crop yield under different climates and soils. There is therefore a growing need to use a multimodel ensemble approach to quantify model uncertainty to improve crop yield prediction for decision making. Therefore, this study aimed to calibrate three well-accepted deterministic crop models,

namely APSIM-maize, AquaCrop and DSSAT CERES-maize, to evaluate the performance of individual models and their multimodel ensemble for the tropical environment in Ethiopia. To address the objectives of the study, crop data such as date of flowering, date of maturity, canopy cover and grain yield were collected from experimental field at three different maize growing agro-ecologies namely Ambo, Bako and Melkassa in the 2017/2018 growing season. Soil data and daily precipitation, maximum and minimum air temperature data from 1995-2017 were used to calibrate and evaluate four widely grown maize hybrid varieties. The crop models were calibrated using measured data from the Bako and evaluated with independent datasets from the Ambo and Melkassa.

The calibration and evaluation result revealed that, the APSIM-maize and DSSAT CERES-maize models accurately simulated flowering and maturity date with root mean square error (RMSE) values ranging from 1.73-4.09 and 1.66-5.36 days, respectively. The AquaCrop model accurately simulated maize canopy cover for all varieties with a RMSE value of less than 10.8 % and a high (0.95) value for the index of agreement (*d*). The simulated grain yield agreed fairly well with the measured data with normalized RMSE values ranging from 13-19 %, 1-4 % and 1-17 % for APSIM, AquaCrop and DSSAT-maize models, respectively. The best performance was obtained when an ensemble of all models was considered. The ensemble mean reduced the normalized RMSE by 8 % while increasing the *d* value to more than 0.90. A multimodel approach improved the simulation of grain yield by reducing model uncertainty compared to the performance of the individual models. The approach could, therefore, provide more reliable predictions for maize varieties grown in diverse environments in the tropics.

Under- or over- estimations were observed for the simulated parameters by the individual models studied showing the need for further research to improve the robustness of the models for tropical environments. Under data scarce conditions, simpler models such as AquaCrop can be used to simulate maize yield with reasonable accuracy.

The second objective of the study was to assess the impact of climate change on maize yield and to identify possible adaptation options. To achieve this objective, downscaled daily precipitation, maximum and minimum air temperature gridded data from seven well-known General Circulation Models (GCMs) were used to assess the impact of climate change. Although, there is no difference between 4.5 and 8.5 Representative Concentration Pathways (RCPs) until the year 2050; the study only used the 8.5 RCP to assess climate change impacts at three maize growing areas. Three crop models were also used to simulate the baseline (1995-2017) and 2030s (2021-2050) maize yields. The result showed that monthly total precipitation for the *Kiremt* season (June to September) was projected to increase by up to 55 % (365 mm) for Ambo and 75 % (241 mm) for Bako respectively, whereas a significant decrease in monthly total precipitation was projected for Melkassa by 2030. The *Belg* season (March to May) total monthly precipitation was projected to decrease for all study sites. Interestingly, by 2030 the total monthly precipitation for the *Bega* season (October to February) is projected to increase for Melkassa particularly for November, December and January while the *Bega* season total monthly precipitation is projected to remain unchanged for Ambo and Bako sites.

With respect to maximum air temperature, projections from the studied GCMs indicated that average monthly maximum air temperature in the 2030s could increase by 0.3-1.7 °C, 0.7-

2.2 °C and 0.8-1.8 °C for Ambo, Bako and Melkassa compared to the historical period (1995-2017) under RCP 8.5 scenario in 2030. Similar increasing changes were projected for monthly average minimum air temperature by all models for all sites. The projected increase in monthly average minimum air temperature ranges from 0.6-1.7 °C for Ambo, 0.8-2.3 °C Bako and 0.6-2.7 °C for Melkassa in the near future. The multimodel ensemble mean projected monthly average maximum air temperature is expected to reach in the range of 24.0-29.7 °C for Ambo, 25.6-33.1 °C Bako and 27.8-32.5 °C for Melkassa and the minimum monthly average air temperature would be 10.1-13.2 °C for Ambo, 13.2-16.5 °C Bako and 11.6-18.0 °C for Melkassa compared to the historical period.

Climate change would reduce maize yield by an average of 4 % and 16 % for Ambo and Melkassa respectively with an increase by 2 % for Bako in 2030 if current maize cultivars were grown with the same crop management practices as the baseline under the future climate. At higher altitudes, early planting of maize cultivars between 15 May to 01 June would result in improved relative yields in the future climate. For Ambo, fertilizer levels between 23-150 kg ha^{-1} would result in improved yields for all maize cultivars when combined with early planting. For a mid-altitude, planting after 15 May has either no or a negative effect on maize yield. Early planting combined with a nitrogen fertilizer level of 23-100 kg ha^{-1} provided increased relative yields under the future climate. For Bako, delayed planting has a negative influence on maize production under the future climate (2030). For lower altitudes, late planting would have lower relative yields compared to early planting. Higher fertilizer levels (100-150 kg ha^{-1}) would reduce yield reductions under the future climate, but this varied among maize cultivars studied. At Melkassa, planting the Jibat cultivar between 15-30 June at increased N levels may reduce severe yield reduction of maize. Generally, future climate is expected to have a negative impact on maize yield and changes in crop management practice can alleviate the impacts on yield.

The third objective of the study was to assess the drought risk in maize (*Zea may* L.) cultivation under the past and future climate change. To this end, historical and future drought characteristics were analysed using historically observed data from 1995-2017 and an ensemble of seven Global Climate Models (GCMs) in the Coupled Model Intercomparison Project (CMIP5) under 8.5 RCP. The widely used Standardized Precipitation Index (SPI) and Standardized Precipitation Evapotranspiration Index (SPEI) were used to investigate drought characteristics. The results for Ambo indicated that increasing frequency of moderate to extremely severe drought with extended drought duration is expected to occur. The 6-month SPEI projected that Bako will experience agricultural droughts with greater severity and duration in the near future. For Melkassa, both SPI and SPEI projected increasing drought duration at short and long timescales. However, the 3- and 6-month SPEI predicted the shorter timescale to be more intensive than the longer timescale. The projected moderate to extremely severe drought for the study sites under future climate will negatively affect maize production. Therefore, developing drought resilient and improved maize varieties that are adaptable to high air temperatures and water-limited agro-ecologies is recommended to alleviate the anticipated impact of climate change. In addition, much attention needs to be directed on the substitution of maize cultivation with more drought tolerant crops, particularly for lower altitudes, is highly recommended in the near future.

ABSTRACT

In Ethiopia climate change is expected to have a negative effect on crop production. Adaptation to the impact of climate change has a significant role in reducing the negative impacts on crop production. This study aimed to assess the impact of climate change on maize (*Zea mays* L.) and identify adaptation options using a set of crop and climate models in Ethiopian tropical environments. Field experimental data from three different maize growing agro-ecologies namely Ambo, Bako and Melkassa in the 2017/2018 growing season, soil data and daily precipitation, maximum and minimum air temperature data from 1995-2017 were used to calibrate and evaluate the APSIM-maize, AquaCrop and DSSAT CERES-maize. Downscaled daily precipitation, maximum and minimum air temperature gridded data from seven well-known General Circulation Models (GCMs) under 8.5 Representative Concentration Pathway (RCP) for the year 2021-2050 were used to assess the impact of climate change for the maize growing areas. The ensemble of seven GCMs, were employed to investigate the future drought risk in maize (*Zea may* L.) cultivation using drought indices. The calibration and evaluation result showed that, the crop models accurately simulated flowering, maturity, canopy cover (AquaCrop) and grain yield against measured data. The best performance was obtained when an ensemble of all models was considered. The climate change impact assessment result indicated monthly total precipitation for the *Kiremt* season (June to September) was projected to increase for Ambo and Bako whereas a significant decrease in monthly total precipitation was projected for Melkassa by 2030. The *Belg* season (March to May) total monthly precipitation was projected to decrease for all study sites. By 2030, the *Bega* season (October to February) is projected to increase for Melkassa while the *Bega* season total monthly precipitation is projected to remain unchanged for Ambo and Bako sites. Both average monthly maximum and minimum

air temperature projected to increase for the study sites by 2030. Projection of climate change scenario showed that maize yield will decrease on average by 4 % and 16 % for Ambo and Melkassa respectively with an increase by 2 % for Bako in 2030. Future adaptation options indicates that for higher altitudes, early planting of maize cultivars combined with 23-150 kg ha^{-1} nitrogen fertilizer levels would result in improved relative yields in the future climate. For a mid-altitude, early planting combined with a nitrogen fertilizer level of 23-100 kg ha^{-1} provided increased relative yields under the future climate. For lower altitudes, late planting would have lower relative yields compared to early planting. Higher fertilizer levels (100-150 kg ha^{-1}) would reduce yield reductions under the future climate, but this varied among maize cultivars studied. The findings of this study highlight future climate are expected to have a negative impact on maize yield and changes in crop management practice can alleviate the impacts on yield. Drought risk analysis based on GCMs ensemble data indicated that an increase in the frequency of moderate to extremely severe drought in the future for the study sites. Therefore, this study recommended the development of drought resilient and improved maize varieties that are adaptable to high air temperatures and water-limited agro-ecologies for the study sites. The substitution of maize cultivation with more drought tolerant crops is highly recommended for the lower altitudes for the near future.

TABLE OF CONTENTS

Page

LIST OF TABLES

LIST OF FIGURES

CHAPTER 1: INTRODUCTION

1.1 Rationale and justification for research

Global climate variability and climate change caused by natural processes as well as anthropogenic factors are the major environmental issues that have affected the globe since the beginning of the 21st century (IPCC, 2014). For example, anthropogenic greenhouse gases such as carbon dioxide (CO_2), methane (CH_4) and nitrous oxide (N_2O) have led to global warming and changes in climate conditions such as air temperature, precipitation, soil moisture, and sea levels (IPCC, 2021; Tian et al., 2015; Kweku et al., 2017). Similarly, climatic changes has had an adverse effect on ecological systems, agricultural practices, human welfare, and the economy (IPCC, 2007; Müller et al., 2017; Tol, 2018).

Africa is considered the most vulnerable and excessively affected region in the world in terms of climate change due to widespread poverty, recurrent droughts, lowest adaptive capacity, and overdependence on rain-fed agriculture (IPCC, 1998; De Souza et al., 2015; Hoogendoorn and Fitchett, 2018).

Ethiopia is one of the largest sub-Saharan Africa countries both in terms of its land area of 1.127 million square kilometers (CSA, 2014) and human population of more than 110 million (Degu, 2019). Agriculture in Ethiopia is the basis of the economy, contributing 35.8 % of the GDP and 70 % of the population are employed in this sector (Degu, 2019). The average share of crop production in the total agricultural value is estimated to be about 60 % (CSA, 2014).

Agriculture in Ethiopia is mainly dependent on rainfall and the World Bank (2010) has ranked Ethiopia as one of the most vulnerable countries in the world to the adverse effects of climate change. This vulnerability is mainly due to its high dependence on rain-fed agriculture and low adaptive capacity (World Bank, 2010; EPCC, 2015). Due to the erratic nature of rainfall coupled with repeated droughts and low level of experience to adapt to climate change impacts, Ethiopia experienced a significant loss of crops and the population has been exposed to severe food insecurity including famine (Conway and Schipper, 2011). Furthermore, the fourth assessment report of the Intergovernmental Panel on Climate Change (IPCC) indicated that the tropics of Africa are expected to experience a significant change in the frequency and intensity of droughts in the mid to late years of the 21st century (IPCC, 2007). This is a serious concern for many developing countries including Ethiopia. Climate change is an additional burden to the already existing environmental challenges (Tesfaye et al., 2015). According to Mera (2018), the most recent drought that occurred in 2015 negatively affected the seasonal rainfall and resulted in widespread failure of seasonal crops, production of pasture and death of animals, and widespread hunger among the affected population. The aggravating impact of climate change, on the frequency and distribution of seasonal rainfall patterns in Ethiopia, is expected to change in the future (Souverijns et al., 2016). However, the impact of climate change on the productivity of major crops in Ethiopia varies with crop type, location, and future time span (Tesfaye et al., 2015).

Maize (*Zea mays* L.) is one of the major cereal food crops in Ethiopia, in terms of production (CSA, 2014). Maize is a popular crop because of its high value as a food crop as well as the growing demand for the stover as animal fodder and that it is a source of fuel for rural families. Approximately 88% of maize produced in Ethiopia is consumed as food, both as green and dry grain (Abate et al., 2015). Maize is grown under diverse agro-ecological conditions typically under rainfed production. The maize cultivating areas in Ethiopia are broadly classified into four ecological zones such as high altitude moist (1800-2400 m), mid-altitude moist (1000-1800 m), low altitude moist (below 1000 m) and moisture stressed (500-1800 m) (Twumasi-Afriyie et al., 2002). Due to the wide adaptability of maize in Ethiopia and the potential to produce more calories and food per area of land, maize is considered to be part of the national food security strategy under the government-led intensive agricultural extension program (Abate et al., 2015). However, maize productivity remains far below the potential due to various constraints caused by climate change induced problems such as drought, weeds, pests and diseases (Ertiro et al., 2017). Climate change impact assessment research using crop models together with climate models provide an option to address some of these constraints and increase maize production under a changed climate in Ethiopia (Araya et al., 2015).

Crop models are the primary tools available to assess climate change risks to crop productivity and provide a platform to describe cropping systems' response to key climate drivers (Lobell and Asseng, 2017). In recent years, crop modelling has received increasing attention and has been used to assess the impact of climate change and to increase crop yield at global (White et al., 2011), regional (Abraha and Savage, 2006; Tesfaye et al., 2015; Mbangiwa et al., 2019) and national levels (Tesfaye et al., 2018; Babel et al., 2019). However, the credibility of these models largely depends on their calibration and evaluation with reliable field experimental data within target environments (Ahmed et al., 2016). Different crop models differ in the way they simulate the dynamic process, input variables used, parameter set and output (White et al., 2011). These significant differences among crop models create large uncertainties in the simulation result. This suggests the use of multimodel simulations instead of relying on a single-model result (Palosuo et al., 2011). The literature also widely indicates research directions linking crop and climate models together with climate change scenarios and crop variety trial data for assessing the impact of future climate change on crop yield (Zhang et al., 2015; Xiao et al., 2020). According to Lapin and Melo (2004), there are four basic approaches that are used to create climate change scenarios in climate change impact studies: (i) analogue; (ii) weather generator; (iii) incremental and (iv) General Circulation Models (GCMs). GCMs are among the most advanced tools used for estimating future climate change scenarios in climate change studies (e.g., Kassie et al., 2015; Ahmadalipour et al., 2017; Deb et al., 2018; Hernandez-Ochoa et al., 2018). According to White et al. (2011), GCMs are considered to be the most popular tool in creating climate change scenarios due to their wide range of coverage of the physical processes that characterizes the climate system. Also, they have been used to examine the impact of increased greenhouse gas concentrations on global climate (White et al., 2011). The IPCC (2013) fifth assessment report developed a new set of scenarios called "Representative Concentration Pathways (RCPs)." These are a set of greenhouse gas concentrations and emissions pathways designed to support research on the impacts of potential policy responses to climate change (Moss et al., 2010; Van Vuuren et al., 2011). The RCPs are used as inputs for climate model runs and as a basis for assessment of possible climate change impacts and adaptation options.

Climate change impact assessments are subject to uncertainties related to greenhouse gas emissions (IPCC, 2007), downscaling techniques (Rötter et al., 2012) and crop models (Wang et al., 2017). Impact assessments should, therefore, be based on multimodel climate projections with crop model predictions, which are assumed to provide a more representative range of climate change impacts than single-model approaches (Meehl et al., 2007; Tao et al., 2009; Rosenzweig et al., 2013). The use of both crop and climate multimodel ensemble methods is an increasingly common approach for projecting the potential impacts of climate change (Challinor et al., 2013). Ensembles allow for a probability distribution instead of a point prediction (Harris et al., 2010). Furthermore, studies indicate that ensemble averages or medians often better reproduce observations than even the best individual model (Palosuo et al., 2011; Martre et al., 2015). It is therefore necessary to use multiple climate and crop models. Together with their ensemble approach in impact and adaptation studies, they improve the reliability of impact projections and provide an improved scientific basis for decision making in adaptation programmes.

Crop models have been used under diverse climate and soil conditions to create an improved understanding of plant-soil interactions across different regions worldwide. Models such as the Agricultural Production Systems Simulator (APSIM) (hereafter referred as APSIM-maize), FAO AquaCrop and the Decision Support System for Agrotechnology Transfer (DSSAT) (hereafter referred as DSSAT CERES-maize) are examples of models that have been used to simulate yield, development and growth of many different crops (Keating et al., 2003; Steduto et al., 2009; Hoogenboom et al., 2010 respectively). The APSIM-maize model is one of the various models embedded in APSIM. The model is considered one of the most appropriate models for use in tropical environments and crop management (Delve and Probert, 2004). The FAO AquaCrop model is a water-driven model that requires few climatic data as an input. The model is simple and robust (Steduto et al., 2009). Abi Saab et al. (2015) has shown that AquaCrop is comparable to other crop models. The DSSAT CERES-maize is one of the main crop simulation models of DSSAT. The model employs a well-developed process-oriented system which is capable of simulating crop yield, growth and development under different environments (Hoogenboom et al., 2010).

The use of multiple crop models and multiple climate models in impact and adaptation studies seems a logical approach needed to improve the reliability of impact projections and provide an improved scientific basis for decision making in adaptation planning. Previous studies on climate change in Ethiopia have often been limited to assess impacts on agricultural production without accounting for potential adaptation (Kassie et al., 2015). Only a few studies addressed both climate change impacts and adaptation in Ethiopia (e.g., Bryan et al., 2009; Kassie et al., 2015 and Tesfaye et al., 2018). Bryan et al. (2009) assessed the impact of climate change and adaptation measures based on household survey approaches. Kassie et al. (2015) applied two crop models in combination with three climate models to assess the potential impacts, adaptation options and uncertainties in climate change impact projections while Tesfaye et al. (2018) quantified climate change impacts and its adaptation by using scenarios in future climate with a hypothetical decrease in precipitation and increase in air temperatures using the DSSAT CERES-maize model. However, this study applied three crop models (APSIM-maize, AquaCrop and DSSAT CERES-maize) and seven climate models and their multimodel ensemble to assess the impact of climate change and identify possible adaptation options under different maize growing agro-ecologies (highland, mid and lowland). Furthermore, their study projected future drought on maize growing agro-ecologies using the climate models ensemble prediction. Several recent climate change impact assessment studies have based their conclusions on ensemble predictors (Asseng et al., 2015; Liu et al., 2016). Therefore, the current research extends the work of others and is therefore novel.

1.2 Research questions

This study attempts to answer the following five major research questions:

- are the APSIM-maize, AquaCrop and DSSAT CERES-maize deterministic crop models capable of simulating maize (*Zea mays* L.) growth and development for different agro-ecologies, soils, and management practices for Ethiopian tropical environments?
- can the multimodel ensemble outputs reduce uncertainties and improve maize yield simulation as compared to individual model outputs?
- can climate models be integrated into crop models for climate change assessment and adaptation options? If so, can changes in planting date, choice of cultivars and nitrogen fertilizer improve maize yield under a changed climate?
- are climate models capable of projecting drought risks induced by climate change?

1.3 Aims and objectives

The main aim of this research is to assess the impact of climate change on maize (*Zea mays* L.) yield and identify adaptation options using a set of crop and climate models in Ethiopian tropical environments.

The specific objectives include:

- the calibration of APSIM-maize, AquaCrop and DSSAT CERES-maize models for improved maize varieties and evaluation of the performance of the models and their multimodel ensemble in simulating maize yield;
- the investigation of the impact of future climate on maize yield using climate and crop models, and identify adaptation options;

- assessment of climate change induced drought risks using a climate model ensemble for maize growing areas under past and future scenarios.

1.4 Outline of thesis structure

The thesis is arranged into six chapters. Chapter 1 presents the background, justification, research questions and objectives of the study. This chapter is not structured as a manuscript and will not be sent for publication.

Chapter 2 presents a review of the related literature. This chapter presents a critical review of literature on the concept of model uncertainties, type and source of uncertainties on climate change impact assessment studies. The review also includes the role of climate and crop models and their multimodel ensemble as a tool to quantify model uncertainties.

Chapters 3, 4 and 5 present a series of related studies. These chapters are formatted as journal articles with an abstract, introduction, literature review, materials and methods, results, discussion, conclusions and references.

Chapter 3 reports on the calibration of APSIM–maize, AquaCrop and DSSAT CERES–maize models using four improved maize varieties and evaluation of the output of each model with the ensemble output of the three models. The advantage of the use of a multimodel ensemble approach over the use of single model is also investigated.

Chapter 4 presents the impact of climate change on maize (*Zea mays* L.) production using seven GCMs and three crop models (APSIM–maize, AquaCrop and DSSAT CERES–maize). Precipitation and air temperature changes under future climate and their impact on maize yield are presented. Possible adaptation strategies for the impact of climate change on maize yield are also presented.

Chapter 5 presents the drought risk assessment for the maize growing study areas using an ensemble of seven GCMs for the past and future climate conditions. Different types of projected drought characteristics under climate change are also investigated.

Chapter 6 restates the aims and objectives and presents conclusions and recommendations of the study.

1.5 References

Abate, T., Shiferaw, B., Menkir, A., Wegary, D., Kebede, Y., Tesfaye, K., Kassie, M., Bogale, G., Tadesse, B. and Keno, T., 2015. Factors that transformed maize productivity in Ethiopia. *Food Security*, *7*, pp. 965-981.

Abi Saab, M.T., Todorovic, M. and Albrizio, R., 2015. Comparing AquaCrop and CropSyst models in simulating barley growth and yield under different water and nitrogen regimes. Does calibration year influence the performance of crop growth models? *Agricultural Water Management*, *147*, pp. 21-33.

Abraha, M.G. and Savage, M.J., 2006. Potential impacts of climate change on the grain yield of maize for the midlands of KwaZulu-Natal, South Africa. *Agriculture, Ecosystems and Environment*, *115*, pp. 150-160.

Ahmadalipour, A., Rana, A., Moradkhani, H. and Sharma, A., 2017. Multi-criteria evaluation of CMIP5 GCMs for climate change impact analysis. *Theoretical and Applied Climatology*, *128*, pp. 71-87.

Ahmed, M., Akram, M.N., Asim, M., Aslam, M., Hassan, F.U., Higgins, S., Stöckle, C.O. and Hoogenboom, G., 2016. Calibration and validation of APSIM-Wheat and CERES-Wheat for spring wheat under rainfed conditions: Models evaluation and application. *Computers and Electronics in Agriculture*, *123*, pp. 384-401.

Araya, A., Hoogenboom, G., Luedeling, E., Hadgu, K.M., Kisekka, I. and Martorano, L.G., 2015. Assessment of maize growth and yield using crop models under present and future climate in southwestern Ethiopia. *Agricultural and Forest Meteorology*, *214*, pp. 252-265.

Babel, M.S., Deb, P. and Soni, P., 2019. Performance evaluation of AquaCrop and DSSAT-CERES for maize under different irrigation and manure application rates in the Himalayan Region of India. *Agricultural Research*, *8*, pp. 207-217.

Challinor, A.J., Smith, M.S. and Thornton, P., 2013. Use of agro-climate ensembles for quantifying uncertainty and informing adaptation. *Agricultural and Forest Meteorology*, *170*, pp. 2-7.

Conway, D. and Schipper, E., 2011. Adaptation to climate change in Africa. Challenges and opportunities identified from Ethiopia. *Global Environmental Change*, *21*, pp. 227-237.

CSA (Central Statistics Agency), 2014. Ethiopia socio economic survey 2013-2014. Crop and life stock product utilization. Statistics Bulletin. Addis Ababa, Ethiopia. pp. 1-8.

De Souza, K., Kituyi, E., Harvey, B., Leone, M., Murali, K.S. and Ford, J.D., 2015. Vulnerability to climate change in three hot spots in Africa and Asia: key issues for policy-relevant adaptation and resilience-building research. *Regional Environmental Change*, *15*, pp. 747-753.

Deb, P., Babel, M.S. and Denis, A.F., 2018. Multi-GCMs approach for assessing climate change impact on water resources in Thailand. *Modeling Earth Systems and Environment*, *4*, pp. 825-839.

Delve, R.J., Probert, M.E., 2004. Modelling nutrient management in tropical cropping systems. Australian Centre for International Agricultural Research (ACIAR). Centro International de Agricultura Tropical (CIAT), Canberra, AT, ACIAR proceedings no. 114, pp. 135-138.

EPCC, 2015. First Assessment Report, Working Group II Climate Change Impact, Vulnerability, Adaptation and Mitigation. Ethiopian Panel on Climate Change (EPCC). *Ethiopian Academy of Sciences*, pp. 1-126.

Ertiro, B.T., Semagn, K., Das, B., Olsen, M., Labuschagne, M., Worku, M., Wegary, D., Azmach, G., Ogugo, V., Keno, T. and Abebe, B., 2017. Genetic variation and population structure of maize inbred lines adapted to the mid-altitude sub-humid maize agro-ecology of Ethiopia using single nucleotide polymorphic (SNP) markers. *BMC Genomics*, *18*, pp. 1-11.

Harris, G.R., Collins, M., Sexton, D.M.H., Murphy, J.M. and Booth, B.B.B., 2010. Probabilistic projections for 21st century European climate. *Natural Hazards and Earth System Sciences*, *10*, pp. 2009-2020.

Hernandez-Ochoa, I.M., Asseng, S., Kassie, B.T., Xiong, W., Robertson, R., Pequeno, D.N.L., Sonder, K., Reynolds, M., Babar, M.A., Milan, A.M. and Hoogenboom, G., 2018. Climate change impact on Mexico wheat production. *Agricultural and Forest Meteorology*, *263*, pp. 373-387.

Hoogenboom, G., Jones, J.W., Wilkens, P.W., Porter, C.H., Boote, K.J., Hunt, L.A., Singh, U., Lizaso, J.L., White, J.W., Uryasev, O. and Royce, F.S., 2010. Decision support system for agrotechnology transfer (DSSAT) Version 4.5. *Honolulu: University of Hawaii*, *1*.

Hoogendoorn, G. and Fitchett, J.M., 2018. Tourism and climate change: A review of threats and adaptation strategies for Africa. *Current Issues in Tourism*, *21*, pp. 742-759.

IPCC 1998. The regional impacts of climate change: An assessment of vulnerability. Contribution of working group II. Intergovernmental Panel on Climate Change. In: Robert, T.W., Marufu, C.Z. and Richard, H.M. (Eds.). Cambridge University, United Kingdom, pp. 255-318.

IPCC, 2007. Climate change 2007: the physical science basis. In: Solomon, S., Qin, D., Manning, M., Chen, Z., Marquis, M., Averyt, K.B., Tignor, M., Miller, H.L. (Eds.), Contribution of Working Group I to the Fourth Assessment Report of the Intergovernmental Panel on Climate Change. Cambridge University Press, Cambridge, United Kingdom and New York, NY, USA. pp. 7-22.

IPCC, 2014: Climate Change 2014: Synthesis Report. Contribution of Working Groups I, II and III to the Fifth Assessment Report of the Intergovernmental Panel on Climate Change. In: Pachauri, R.K. and Meyer, L.A. (Eds.). Cambridge University. IPCC, Geneva, Switzerland, pp. 2-151.

IPCC, 2021: Climate Change 2021: The Physical Science Basis. Contribution of Working Group I to the Sixth Assessment Report of the Intergovernmental Panel on Climate Change Masson-Delmotte, V., P. Zhai, A. Pirani, S. L. Connors, C. Péan, S. Berger, N. Caud, Y. Chen, L. Goldfarb, M. I. Gomis, M. Huang, K. Leitzell, E. Lonnoy, J. B. R. Matthews, T. K. Maycock, T. Waterfield, O. Yelekçi, R. Yu and B. Zhou (Eds.). Cambridge University. IPCC, Geneva, Switzerland, pp. 2-151.

Kassie, B.T., Asseng, S., Rotter, R.P., Hengsdijk, H., Ruane, A.C. and Van Ittersum, M.K., 2015. Exploring climate change impacts and adaptation options for maize production in the

Central Rift Valley of Ethiopia using different climate change scenarios and crop models. *Climatic Change*, *129*, pp. 145-158.

Keating, B.A., Carberry, P.S., Hammer, G.L., Probert, M.E., Robertson, M.J., Holzworth, D., Huth, N.I., Hargreaves, J.N., Meinke, H., Hochman, Z. and McLean, G., 2003. An overview of APSIM, a model designed for farming systems simulation. *European Journal of Agronomy*, *18*, pp. 267-288.

Kweku, D.W., Bismark, O., Maxwell, A., Desmond, K.A., Danso, K.B., Oti-Mensah, E.A., Quachie, A.T. and Adormaa, B.B., 2017. Greenhouse effect: Greenhouse gases and their impact on global warming. *Journal of Scientific Research and Reports*, pp. 1-9.

Lapin, M. and Melo, M., 2004. Methods of climate change scenarios projection in Slovakia and selected results. *Journal of Hydrology and Hydromechanics*, *52,* pp. 224-238.

Lobell, D.B. and Asseng, S., 2017. Comparing estimates of climate change impacts from process-based and statistical crop models. *Environmental Research Letters*, *12,* pp. 1-12.

Martins, P., 2014. Structural change in Ethiopia: an employment perspective. *The World Bank*, pp. 1-40.

Martre, P., Wallach, D., Asseng, S., Ewert, F., Jones, J.W., Rötter, R.P., Boote, K.J., Ruane, A.C., Thorburn, P.J., Cammarano, D. and Hatfield, J.L., 2015. Multimodel ensembles of wheat growth: many models are better than one. *Global Change Biology*, *21*, pp. 911-925.

Mbangiwa, N.C., Savage, M.J. and Mabhaudhi, T., 2019. Modelling and measurement of water productivity and total evaporation in a dryland soybean crop. *Agricultural and Forest Meteorology*, *266*, pp. 65-72.

Meehl, G.A., Covey, C., Delworth, T., Latif, M., McAvaney, B., Mitchell, J.F., Stouffer, R.J. and Taylor, K.E., 2007. The WCRP CMIP3 multimodel dataset: A new era in climate change research. *Bulletin of the American Meteorological Society*, *88*, pp. 1383-1394.

Mera, G.A., 2018. Drought and its impacts in Ethiopia. *Weather and Climate Extremes*, *22*, pp. 24-35.

Moss, R.H., Edmonds, J.A., Hibbard, K.A., Manning, M.R., Rose, S.K., van Vuuren, D.P., Carter, T.R., Emori, S., Kainuma, M., Kram, T. and Meehl, G.A., 2010. The next generation of scenarios for climate change research and assessment. *Nature*, *463*, pp. 747-756.

Müller, B., Johnson, L. and Kreuer, D., 2017. Maladaptive outcomes of climate insurance in agriculture. *Global Environmental Change*, *46*, pp. 23-33.

Palosuo, T., Kersebaum, K.C., Angulo, C., Hlavinka, P., Moriondo, M., Olesen, J.E., Patil, R.H., Ruget, F., Rumbaur, C., Takáč, J. and Trnka, M., 2011. Simulation of winter wheat yield and its variability in different climates of Europe: a comparison of eight crop growth models. *European Journal of Agronomy*, *35*, pp. 103-114.

Rosenzweig, C., Jones, J.W., Hatfield, J.L., Ruane, A.C., Boote, K.J., Thorburn, P., Antle, J.M., Nelson, G.C., Porter, C., Janssen, S. and Asseng, S., 2013. The agricultural model intercomparison and improvement project (AgMIP): protocols and pilot studies. *Agricultural and Forest Meteorology*, *170*, pp. 166-182.

Rötter, R.P., Höhn, J.G. and Fronzek, S., 2012. Projections of climate change impacts on crop production: a global and a Nordic perspective. *Acta Agriculturae Scandinavica, Section A–Animal Science*, *62*, pp. 166-180.

Souverijns, N., Thiery, W., Demuzere, M. and Van Lipzig, N.P., 2016. Drivers of future changes in East African precipitation. *Environmental Research Letters*, *11*, pp.1-9.

Steduto, P., Hsiao, T.C., Raes, D. and Fereres, E., 2009. AquaCrop - The FAO crop model to simulate yield response to water: I. Concepts and underlying principles. *Agronomy Journal*, *101*, pp. 426-437.

Tao, F., Zhang, Z., Liu, J. and Yokozawa, M., 2009. Modelling the impacts of weather and climate variability on crop productivity over a large area: A new super-ensemble-based probabilistic projection. *Agricultural and Forest Meteorology*, *149*, pp. 1266-1278.

Tesfaye, K., Gbegbelegbe, S., Cairns J.E., Shiferaw, B., Prasanna B.M., Sonder, K., Boote, K., Makumbi, D., Robertson, R., 2015. Maize systems under climate change in sub-Saharan Africa. Potential impacts on production and food security. *International Journal of Climate Change Strategies and Management*, *7*, pp. 247-271.

Tesfaye, K., Kruseman, G., Cairns, J.E., Zaman-Allah, M., Wegary, D., Zaidi, P.H., Boote, K.J. and Erenstein, O., 2018. Potential benefits of drought and heat tolerance for adapting maize to climate change in tropical environments. *Climate Risk Management*, *19*, pp. 106-119.

Tian, H., Chen, G., Lu, C., Xu, X., Ren, W., Zhang, B., Banger, K., Tao, B., Pan, S., Liu, M. and Zhang, C., 2015. Global methane and nitrous oxide emissions from terrestrial ecosystems due to multiple environmental changes. *Ecosystem Health and Sustainability*, *1*, pp. 1-20.

Tol, R.S., 2018. The economic impacts of climate change. *Review of Environmental Economics and Policy*, *12*, pp. 4-25.

Twumasi-Afriyie, S., Zelleke, H., Yihun, K., Asefa, B. and Tariku, S., 2002. Development and improvement of highland maize in Ethiopia. *Enhancing the Contribution of Maize to Food Security in Ethiopia. EARO and CYMMIT*, pp. 31-38.

Van Vuuren, D.P., Edmonds, J., Kainuma, M., Riahi, K., Thomson, A., Hibbard, K., Hurtt, G.C., Kram, T., Krey, V., Lamarque, J.F. and Masui, T., 2011. The representative concentration pathways: an overview. *Climatic Change*, *109*, pp. 6-31.

Wang, E., Martre, P., Zhao, Z., Ewert, F., Maiorano, A., Rötter, R.P., Kimball, B.A., Ottman, M.J., Wall, G.W., White, J.W. and Reynolds, M.P., 2017. The uncertainty of crop yield projections is reduced by improved temperature response functions. *Nature Plants*, *3*, pp. 1-13.

White, J.W., Hoogenboom, G., Kimball, B.A. and Wall, G.W., 2011. Methodologies for simulating impacts of climate change on crop production. *Field Crops Research*, *124*, pp. 357-368.

World Bank, 2010. Development and Climate Change: World Development Report 2010. The World Bank, Washington DC, New York.

Xiao, D., Li Liu, D., Wang, B., Feng, P., Bai, H. and Tang, J., 2020. Climate change impact on yields and water use of wheat and maize in the North China Plain under future climate change scenarios. *Agricultural Water Management*, *238*, p. 106238.

Zhang, Y., Zhao, Y., Chen, S., Guo, J. and Wang, E., 2015. Prediction of maize yield response to climate change with climate and crop model uncertainties. *Journal of Applied Meteorology and Climatology*, *54*, pp. 785-794.

Lead to Chapter 2

In the previous chapter, the impact of climate change on agriculture was illustrated. The significance of incorporating climate and crop modelling with their multimodel ensemble in climate change assessment studies has been emphasized. However, climate change impact assessments are affected by uncertainties. Chapter 2, therefore, presents a literature review of climate and crop models and their multimodel ensemble and how the models quantify uncertainties in climate change impact studies.

CHAPTER 2: LITERATURE REVIEW

2.1 Introduction

Climate change is expected to increase the vulnerability of agricultural systems (Rosenzweig et al., 2014) by increasing air temperatures, changes in rainfall patterns, and increased frequency of extreme weather events such as drought in most parts of the world (IPCC, 2014).

Increased atmospheric concentrations of greenhouse gases is the main cause of the ongoing climate change (IPCC, 2014). Climate change is stressing ecosystems of the earth, including water cycles, agricultural and natural products and sea levels (Simonovic, 2017). Moreover, the increase in greenhouse gas concentration overstates the extreme weather patterns, which in turn increases the magnitude and frequency of drought events (Das and Umamahesh, 2017). According to Deb et al. (2015), the agricultural sector of any country is highly susceptible to climate variability as the physiological processes of plants are directly associated with meteorological inputs. Zhao et al. (2017) found that crop yield at a global scale is expected to be reduced (e.g., maize by 7.4%, wheat by 6.0%, rice by 3.2% and soybean by 3.1%) for each 1 ºC increase in the global mean air temperature. Since agricultural practices are climate-dependent and yields vary from year to year depending on climate variability, the agricultural sector is particularly exposed to changes in climate (Zhao et al., 2017).

For climate change impact assessment, crop growth models have been widely used to evaluate crop responses (development, growth and yield) by combining future climate conditions, obtained from General or Regional Circulation Models (GCMs and RCMs respectively) (Long and Ainsworth, 2005; Tao et al., 2008). However, uncertainty associated with the particular crop model, GCMs and scenarios should be ascertained while projecting for the future (Das et al., 2018). In addition, uncertainties associated with such crop and climate models are rarely assessed (Li et al., 2015). Höllermann and Evers (2017) noted that uncertainty information should be considered for climate change scenarios for improved crop yield prediction and decision-making process. Therefore, it is also necessary to examine the uncertainty in the context of a rapidly changing climate for improved policy and adaptation measures. Numerous studies have adopted different techniques for example, multimodel ensemble mean (Kundzewicz et al., 2018), Bayesian analysis (Das and Umamahesh, 2018) and sensitivity analysis (Mearns et al., 1996) to assess the uncertainty of projections in the climate change studies. This uncertainty is related to multiple factors including climate model and greenhouse gas emission scenario selection, complexities in atmosphere modelling, downscaling methods, incomplete understanding of the processes included in climate models and uncertainties in crop models (Asseng, 2013; Challinor et al., 2013; Uusitalo et al., 2015; Mason-D'Croz et al., 2016; Amin et al., 2017). Quantification of the uncertainty is one of the main steps in identifying the adaptation measures for agricultural management in the face of climate change (Hosseinzadehtalaei et al., 2017).

The construction of model uncertainty is described, focusing on the research that is needed to characterize and reduce uncertainties at various points in the climate change impact assessment studies.

2.2 Definition of uncertainty

Model uncertainty is usually related to deviations between the real world (observed) and its simplified representation (prediction) in models (Nilsen and Aven, 2003). Studies define model uncertainty in different ways. For example, Smithson (1989) defines uncertainty is related to the inaccurateness of humanly devised models and research tools to describe and represent the reality. Funtowicz and Ravetz (1990) describe uncertainty as a situation of inadequate information, which can be of inexactness, unreliability, and ignorance. The IPCC (2001) define uncertainty as an expression of the degree to which a value such as the future state of the climate system or its impact is unknown. In recent decades, uncertainty has played a prominent role in global environmental change research, including climate change science and climate change impact science. The Fifth Assessment Report of the IPCC (IPCC, 2014) defines uncertainty as a lack of complete information, as well as incomplete knowledge or disagreement on what is known and knowable. According to Kundzewicz et al. (2018), uncertainty is a lack of certainty about something, ranging from small doubts and minor imprecisions to a complete lack of definite knowledge. Walker et al. (2003) regard uncertainty as any departure from the unachievable ideal of complete determinism.

2.3 Types of uncertainty

According to Walker et al. (2003), model simulation uncertainty is classified into five types: (1) context uncertainty; (2) input uncertainty; (3) model structure uncertainty; (4) parameter uncertainty; and (5) modelling technical uncertainty. There are also a number of uncertainties in the case of crop simulation and climate change impact assessment when it applied to agricultural production.

2.3.1 Uncertainty of crop models

Crop models play an important role in agricultural management decision-making processes and they are the main tool for investigating the effects of climate change on crops (IPCC, 2007). However, the application of these models generally requires input data related to management, soil, and weather conditions as well as crop growth parameters. Numerous studies indicate that input data and parameter values are a major source of uncertainties due to the inherent variability in natural processes, imperfection in data measurement and spatial and temporal variations observed in the inputs required (Yao et al., 2011; Bi et al., 2017). Since a clear methodology is lacking, crop model uncertainties are not well addressed in most climate change impact assessments on agriculture (Müller, 2011) and climate change impact projection on crop yield (Zhang et al., 2015). Therefore, studies suggest that model input data and crop parameters should represent a particular agro-ecology and experimental field where observations are undertaken (Marin et al., 2017). Quantification of uncertainties in crop growth models cannot improve climate change projection rather with crop simulation models. (Zhang et al., 2015).

2.3.2 Uncertainty in climate projection using a climate model

Reliable information on how regional and local climates have changed in the past, and may change in the future, is important for managing climate change risks. While Global Climate Models (GCMs) can provide large-scale future climate change projections (IPCC, 2013), regional dynamic downscaling for example using Coordinated Regional Climate Downscaling Experiment (CORDEX) data (Giorgi and Gutowski, 2015) and statistical downscaling methods (Luhunga et al., 2018; Pinto et al., 2018; Ali et al., 2019) can provide spatial and temporal detail to better inform local adaptation to climate change. Nevertheless, one of the principal challenges facing the climate modelling community is the removal of systematic or structural errors in GCMs which is the bias-correction in a GCM that improve the models (Randall et al., 2007). Studies indicated that uncertainty in climate change predictions arise from three distinct sources. The first is the uncertainty arising from emission scenario of greenhouse gases such as uncertainty in the future radiative force. The second is model structure and parameter uncertainty in response to the same radiative force. The third is internal variability of the climate system, that is, the natural fluctuations that arise in the absence of any radiative forcing of the planet (Yao et al., 2011; Lovenduski et al., 2016). Moreover, the Special Report on the Emission Scenario, SRES (Nakicenovic et al., 2000), has reported different Greenhouse Gas (GHG) emission scenarios. Besides, there are many GCMs available for predicting climate scenarios, and different GCMs use a different representation of the climate system (Flato et al., 2014; Teklesadik et al., 2017). Therefore, different GCMs develop different climate projections for a single GHG emission scenario. Hence, uncertainties arise in climate projections from GCMs and GHG emission scenarios.

2.3.3 Uncertainty in crop models coupled with climate models

Process-based crop modelling can also be carried out at the scale of the climate model, provided that climate is believed to influence crop yield on that scale (Challinor et al., 2003). Climate and crop models are a particularly important tool for understanding climate change and its impacts (Challinor et al., 2009). Climate model output can be used with crop models either directly or through some post-processing. In the latter case, a weather generator can be used, and/or the change in climate simulated using a model applied to observed climate. The post-processing can use a grid that is coarse relative to the spatial scale at which field-scale crop models typically operate. Climate change impact assessment studies offer a means of quantifying uncertainties related to climate risks and provide decision-support for more sustainable crop production. Crop model yield predictions based on multiple GCMs and emission scenarios (RCPs) provide more reliable climate change impact assessments (Asseng, 2013; Rosenzweig et al., 2013). These studies were used to discover and assess the uncertainty in yield predictions and evaluate model performance (White et al., 2011; Mason-D'Croz et al., 2016).

Previous studies revealed that GCMs and RCPs are a major source of uncertainties in climate change impact quantification due to a limited capacity of GCMs to represent climate extremes and interannual climate variations. These uncertainties ultimately affect the crop growth process in crop models and lead to a false representation of climate change impacts on crop yield (Araya et al., 2015; Kassie et al., 2015). Moreover, future projections are based on alternative RCPs, each of them describing a potential future greenhouse gas concentration trajectory during the 21st century (IPCC, 2014). However, the direct use of climate predictions from GCMs is problematic due to their coarse spatial resolution resulting in biases and uncertainties at a local scale (Knutti et al., 2010). GCMs that are used to project future climate scenarios provide gridded areal average simulations while the occurrence and intensity of extreme events strongly depend on local factors (Huang et al., 2016; Ragno et al., 2018). Therefore, climatic models should be bias-corrected for climate change impact studies for accurate and reliable climate change projections (Hawkins et al., 2013).

2.4 Methods to quantify uncertainty

2.4.1 Model calibration

Calibration is referred to as tuning in the climate modelling community, a process that has a significant influence on the projections made by each modelling centre and by the IPCC (IPCC, 2013). Model calibration is the process of estimating model parameters by comparing model predictions (output) for a given set of assumed conditions with observed data for the same conditions (Moriasi et al., 2007). Despite modelers paying increasing attention to analyse and manage the different sources of uncertainty affecting model predictions, the impact of the uncertainty in the observations used for calibration has been ignored (Confalonieri et al., 2016).

Model calibration is the most important application of uncertainty quantification method for estimating model inputs to give the model output. Models are widely used for the design, optimization, and assessment of climate systems, that approximately represent the reality in their predictions and show a level of discrepancy from experimental measurements (Bi et al., 2017). Model uncertainties due to experimental measurements and parameter values can be mitigated through the well-known process of model calibration, which improve the agreement between predictions and measurements (Doebling, 1996; Farajpour and Atamturktur, 2013). After successful calibration, the degree of uncertainty in a parameter estimated using a model would be lower than the uncertainty associated with the prior estimate before calibration, and uncertainty of outputs related to a model would be reduced (Krysanova et al., 2017, 2018). Reduction of uncertainty is measured by relevance of a parameter.

2.4.2 Multimodel ensemble approach

Researchers have argued that the quantification of all aspects of model uncertainty requires multimodel ensembles. Many applications, including weather and climate prediction problems, have demonstrated that combining models outputs generally increases the skill, reliability and consistency of model predictions (Tebaldi and Knutti, 2007). Multimodel approaches can be used to estimate a broader uncertainty band so that it is more likely to include the unknown true predicted value (Rojas et al., 2010).

A model averaging technique can be used to combine predictions of multiple models. The use of the multimodel ensemble mean or median to quantify the uncertainty is nowadays common practice, within the climate community (Meehl et al., 2007), as a tool to communicate and provide policymakers with information about the uncertainty of the current model (Kundzewicz et al., 2018). Researchers have suggested the use of crop and climate multimodel ensembles to improve and to give improved estimates of uncertainty (Asseng et al., 2015; Li et al., 2015; Pirttioja et al., 2015). Furthermore, to develop climate scenarios, multimodel ensembles of GCMs are used to define the uncertainty in projections resulting from structural differences in the GCMs, as well as uncertainties in variations of initial conditions or parameterizations (Tebaldi and Knutti, 2007; Knutti et al., 2010).

Multiple models can provide more reliable decision support in climate change impact assessment and assessments of agricultural system vulnerability (Wilby et al., 2009; Asseng, 2013; Rosenzweig et al., 2013). A multimodel ensemble approach is widely used for climate impact assessment by global- and continental-scale modelling studies (Dankers et al., 2014; Gosling et al., 2017) and follows the state of the art for ensembles of GCM and RCM projections used by the IPCC (IPCC, 2014). Christensen et al. (2010) suggested that a multimodel mean is the best approach for RCM projections, because no single model is best for all variables, seasons and regions. A study by Gudmundsson et al. (2012) also indicated that a performance of a multimodel ensemble (mean or median) should be presented as the output in climate change impact studies, despite the large variations in performance of individual models.

2.4.3 Climate model downscaling

In the climate change impact assessment analysis, there are three steps involved. The first step is the selection of climate models and emission scenarios. Multiple climate models and emission scenarios have been identified in the 4th assessment (AR4) and the 5th assessment (AR5) reports of the IPCC (Stocker et al. 2013). The second step comprises the bias-correction step to modify climate model data in order to increase the correlation between model and observed data. Many bias correction methods, ranging from simple scaling techniques to more sophisticated distribution mapping techniques, have been developed to correct biased RCM outputs (Teutschbein and Seibert, 2012). The scaling approach mainly includes linear or nonlinear approaches that adjust the climatic factors based on the differences between observed and RCM means in a linear or nonlinear formula, such as the linear scaling method and the power transformation method (Teutschbein and Seibert, 2012; Crochemore et al., 2016).

Distribution mapping, involving distribution-based and distribution-free quantile-quantile mapping methods, matches the statistical distribution of RCM-simulated climatic factors to the distribution of observations. Distribution-based quantile-quantile mapping is based on the assumption that climatic factors obey a certain distribution, such as Gamma and Gaussian (White and Toumi, 2013), while the distribution-free quantile-quantile mapping technique employs the empirical distribution (Chen et al., 2013). Selecting a suitable bias-correction method is important for providing reliable inputs for impact analysis of a region.

Studies indicate that the quantile-quantile mapping technique removes the systematic bias in the GCM simulations, and it is assumed that biases relative to historical observations will be constant in the projection period (Thrasher et al., 2012; Ruiz-Ramos et al., 2016; Dosio and Fischer, 2018; Potter et al., 2020).

The third step in the climate change impact assessment analysis is downscaling of the climate model projection. Downscaling is a method used to estimate high spatial resolution climate information from low spatial resolution GCM output (Clark et al., 2016). Downscaling techniques can be broadly classified as statistical and dynamical downscaling. In statistical downscaling, a data driven relationship is derived between the predictors (GCM simulated climate variable) and predictands (regional scale variable) (Santos et al., 2016). Dynamic downscaling makes use of RCMs that transform outputs from GCMs into finer spatial and temporal resolution outputs (Dosio et al., 2015; Scinocca et al., 2016). In contrast to statistical downscaling, dynamical downscaling capabilities have evolved considerably. However, characterizing uncertainty in dynamical downscaling remains challenging (Mearns et al., 2013; Done et al., 2014). For agricultural impacts, several studies suggested that dynamical downscaling may improve projections, since the use of RCMs altered modelled crop yields by up to 20 % (Mearns et al., 1999, 2001; Adams et al., 2003; Iizumi and Nishimori, 2012).

2.5 Conclusions

Climate change impact assessment is affected by model output prediction uncertainties. Quantifying these uncertainties in agricultural research applications plays a prominent role in global environmental change research, including climate change science and climate change impact studies. There are many sources of uncertainty in projections for the future discussed in the literature. Using ensembles of climatic and crop models may allow for more robust results, for a given region. The larger the ensemble size of independent climate models considered, the more accurate the quantification of climate change uncertainty. Therefore, the application of such ensembles in climate change impact assessment is a worthwhile avenue for future research priority.

2.6 References

Adams, R.M., McCarl, B.A. and Mearns, L.O., 2003. The effects of spatial scale of climate scenarios on economic assessments: An example from US agriculture. *Climatic Change*, *60*, pp. 131-148.

Ali, S., Eum, H.I., Cho, J., Dan, L., Khan, F., Dairaku, K., Shrestha, M.L., Hwang, S., Nasim, W., Khan, I.A. and Fahad, S., 2019. Assessment of climate extremes in future projections downscaled by multiple statistical downscaling methods over Pakistan. *Atmospheric Research*, *222*, pp. 114-133.

Amin, A., Nasim, W., Mubeen, M., Kazmi, D.H., Lin, Z., Wahid, A., Sultana, S.R., Gibbs, J. and Fahad, S., 2017. Comparison of future and base precipitation anomalies by SimCLIM statistical projection through ensemble approach in Pakistan. *Atmospheric Research*, *194*, pp. 214-225.

Araya, A., Hoogenboom, G., Luedeling, E., Hadgu, K.M., Kisekka, I. and Martorano, L.G., 2015. Assessment of maize growth and yield using crop models under present and future climate in southwestern Ethiopia. *Agricultural and Forest Meteorology*, *214*, pp. 252-265.

Asseng, S., Ewert, F., Martre, P., Rosenzweig, C., Jones, J., Hatfield, J., Ruane, A., Boote, K., Thorburn, P., Rötter, R. and Cammarano, D., 2015. Benchmark data set for wheat growth models: field experiments and AgMIP multimodel simulations. *Open Data Journal for Agricultural Research*, *1*, pp. 1-5.

Asseng, S., Ewert, F., Rosenzweig, C., Jones, J.W., Hatfield, J.L., Ruane, A.C., Boote, K.J., Thorburn, P.J., Rötter, R.P., Cammarano, D. and Brisson, N., 2013. Uncertainty in simulating wheat yields under climate change. *Nature Climate Change*, *3*, pp. 827-832.

Bi, S., Prabhu, S., Cogan, S. and Atamturktur, S., 2017. Uncertainty quantification metrics with varying statistical information in model calibration and validation. *AIAA Journal*, *55*, pp. 3570-3583.

Challinor, A.J., Ewert, F., Arnold, S., Simelton, E. and Fraser, E., 2009. Crops and climate change: progress, trends, and challenges in simulating impacts and informing adaptation. *Journal of Experimental Botany*, *60*, pp. 2775-2789.

Challinor, A.J., Slingo, J.M., Wheeler, T.R., Craufurd, P.Q. and Grimes, D.I.F., 2003. Toward a combined seasonal weather and crop productivity forecasting system: determination of the working spatial scale. *Journal of Applied Meteorology*, *42*, pp. 175-192.

Challinor, A.J., Smith, M.S. and Thornton, P., 2013. Use of agro-climate ensembles for quantifying uncertainty and informing adaptation. *Agricultural and Forest Meteorology*, *170*, pp. 2-7.

Chen, J., Brissette, F.P., Chaumont, D. and Braun, M., 2013. Finding appropriate bias correction methods in downscaling precipitation for hydrologic impact studies over North America. *Water Resources Research*, *49*, pp. 4187-4205.

Christensen, J.H., Kjellström, E., Giorgi, F., Lenderink, G. and Rummukainen, M., 2010. Weight assignment in regional climate models. *Climate Research*, *44*, pp. 179-194.

Clark, M.P., Wilby, R.L., Gutmann, E.D., Vano, J.A., Gangopadhyay, S., Wood, A.W., Fowler, H.J., Prudhomme, C., Arnold, J.R. and Brekke, L.D., 2016. Characterizing uncertainty of the hydrologic impacts of climate change. *Current Climate Change Reports*, *2*, pp. 55-64.

Confalonieri, R., Bregaglio, S. and Acutis, M., 2016. Quantifying uncertainty in crop model predictions due to the uncertainty in the observations used for calibration. *Ecological Modelling*, *328*, pp. 72-77.

Crochemore, L., Ramos, M.H. and Pappenberger, F., 2016. Bias correcting precipitation forecasts to improve the skill of seasonal streamflow forecasts. *Hydrology Earth System Sciences*, *20*, pp. 3601-3618.

Dankers, R., Arnell, N.W., Clark, D.B., Falloon, P.D., Fekete, B.M., Gosling, S.N., Heinke, J., Kim, H., Masaki, Y., Satoh, Y. and Stacke, T., 2014. First look at changes in flood hazard in the Inter-Sectoral Impact Model Intercomparison Project ensemble. *Proceedings of the National Academy of Sciences*, *111*, pp. 3257-3261.

Das, J. and Umamahesh, N.V., 2017. Uncertainty and no stationarity in streamflow extremes under climate change scenarios over a river basin. *Journal of Hydrologic Engineering*, *22*, p. 04017042.

Das, J., Treesa, A. and Umamahesh, N.V., 2018. Modelling impacts of climate change on a river basin: analysis of uncertainty using REA and possibilistic approach. *Water Resources Management*, *32*, pp. 4833-4852.

Deb, P., Shrestha, S. and Babel, M.S., 2015. Forecasting climate change impacts and evaluation of adaptation options for maize cropping in the hilly terrain of Himalayas: Sikkim, India. *Theoretical and Applied Climatology*, *121*, pp. 649-667.

Doebling, S.W., 1996. Minimum-rank optimal update of elemental stiffness parameters for structural damage identification. *AIAA Journal*, *34*, pp. 2615-2621.

Done, J.M., Bruyère, C.L., Ge, M. and Jaye, A., 2014. Internal variability of North Atlantic tropical cyclones. *Journal of Geophysical Research: Atmospheres*, *119*, pp. 6506-6519.

Dosio, A. and Fischer, E.M., 2018. Will half a degree make a difference? Robust projections of indices of mean and extreme climate in Europe under 1.5 C, 2 C, and 3 C global warming. *Geophysical Research Letters*, *45*, pp. 935-944.

Dosio, A., Panitz, H.J., Schubert-Frisius, M. and Lüthi, D., 2015. Dynamical downscaling of CMIP5 global circulation models over CORDEX-Africa with COSMO-CLM: evaluation over the present climate and analysis of the added value. *Climate Dynamics*, *44*, pp. 2637-2661.

Farajpour, I. and Atamturktur, S., 2013. Error and uncertainty analysis of inexact and imprecise computer models. *Journal of Computing in Civil Engineering*, *27*, pp. 407-418.

Flato, G., Marotzke, J., Abiodun, B., Braconnot, P., Chou, S.C., Collins, W., Cox, P., Driouech, F., Emori, S., Eyring, V. and Forest, C., 2014. Evaluation of climate models. In *Climate Change 2013*: *The Physical Science Basis. Contribution of Working Group I to the Fifth Assessment Report of the Intergovernmental Panel on Climate Change*, Cambridge University Press. pp. 741-866.

Funtowicz, S.O. and Ravetz, J.R., 1990. *Uncertainty and quality in science for policy* (Vol. 15). Springer Science & Business Media.

Giorgi, F. and Gutowski Jr, W.J., 2015. Regional dynamical downscaling and the CORDEX initiative. *Annual Review of Environment and Resources*, *40*, pp. 467-490.

Gosling, S.N., Zaherpour, J., Mount, N.J., Hattermann, F.F., Dankers, R., Arheimer, B., Breuer, L., Ding, J., Haddeland, I., Kumar, R. and Kundu, D., 2017. A comparison of changes in river runoff from multiple global and catchment-scale hydrological models under global warming scenarios of 1 C, 2 C and 3 C. *Climatic Change*, *141*, pp. 577-595.

Gudmundsson, L., Wagener, T., Tallaksen, L.M. and Engeland, K., 2012. Evaluation of nine large-scale hydrological models with respect to the seasonal runoff climatology in Europe. *Water Resources Research*, *48*, pp. 1-20.

Hawkins, E., Osborne, T.M., Ho, C.K. and Challinor, A.J., 2013. Calibration and bias correction of climate projections for crop modelling: an idealised case study over Europe. *Agricultural and Forest Meteorology*, *170*, pp. 19-31.

Höllermann, B. and Evers, M., 2017. Perception and handling of uncertainties in water management—A study of practitioners' and scientists' perspectives on uncertainty in their daily decision-making. *Environmental Science and Policy*, *71*, pp. 9-18.

Hosseinzadehtalaei, P., Tabari, H. and Willems, P., 2017. Uncertainty assessment for climate change impact on intense precipitation: how many model runs do we need? *International Journal of Climatology*, *37*, pp. 1105-1117.

Huang, W.K., Stein, M.L., McInerney, D.J., Sun, S. and Moyer, E.J., 2016. Estimating changes in temperature extremes from millennial-scale climate simulations using generalized extreme value (GEV) distributions. *Advances in Statistical Climatology, Meteorology and Oceanography*, *2*, pp. 79-103.

Iizumi, T., Uno, F. and Nishimori, M., 2012. Climate downscaling as a source of uncertainty in projecting local climate change impacts. *Journal of the Meteorological Society of Japan. Ser. II*, *90*, pp. 83-90.

IPCC, 2001. Climate Change 2001: The Scientific Basis. Contribution of Working Group I to the Third Assessment Report of the Intergovernmental Panel on Climate Change [Houghton, J.T., Y. References 150 Ding, D.J. Griggs, M. Noguer, P.J. van der Linden, X. Dai, K. Maskell, and C.A. Johnson (eds.)]. Cambridge University Press, Cambridge, United Kingdom and New York, NY, USA.

IPCC, 2007. Climate Change 2007: Impacts, Adaptation and Vulnerability— Contribution of Working Group II to the Fourth assessment Report of the Intergovernmental Panel on Climate Change. Cambridge: Cambridge University Press.

IPCC, 2013. Climate Change 2013: The Physical Science Basis. Contribution of working group I to the fifth assessment report of the intergovernmental panel on climate change [Stocker, T.F., Qin, D., Plattner, G.K., Tignor, M., Allen, S.K., Boschung, J., Nauels, A., Xia, Y., Bex, V., Midgley, P.M. and Alexander, L.V.(eds)]. Cambridge University Press, Cambridge, United Kingdom and New York, NY, USA.

IPCC, 2014. Climate Change 2014: Synthesis Report. Contribution of Working Groups I, II and III to the Fifth Assessment Report of the Intergovernmental Panel on Climate Change. IPCC, Geneva, Switzerland.

Kassie, B.T., Asseng, S., Rotter, R.P., Hengsdijk, H., Ruane, A.C. and Van Ittersum, M.K., 2015. Exploring climate change impacts and adaptation options for maize production in the Central Rift Valley of Ethiopia using different climate change scenarios and crop models. *Climatic Change*, *129*, pp. 145-158.

Knutti, R., Furrer, R., Tebaldi, C., Cermak, J. and Meehl, G.A., 2010. Challenges in combining projections from multiple climate models. *Journal of Climate*, *23*, pp. 2739-2758.

Krysanova, V., Donnelly, C., Gelfan, A., Gerten, D., Arheimer, B., Hattermann, F. and Kundzewicz, Z.W., 2018. How the performance of hydrological models relates to credibility of projections under climate change. *Hydrological Sciences Journal*, *63*, pp. 696-720.

Krysanova, V., Vetter, T., Eisner, S., Huang, S., Pechlivanidis, I., Strauch, M., Gelfan, A., Kumar, R., Aich, V., Arheimer, B. and Chamorro, A., 2017. Intercomparison of regional-scale hydrological models and climate change impacts projected for 12 large river basins worldwide—a synthesis. *Environmental Research Letters*, *12*, pp. 2-12.

Kundzewicz, Z.W., Krysanova, V., Benestad, R.E., Hov, Ø., Piniewski, M. and Otto, I.M., 2018. Uncertainty in climate change impacts on water resources. *Environmental Science and Policy*, *79*, pp. 1-8.

Li, T., Hasegawa, T., Yin, X., Zhu, Y., Boote, K., Adam, M., Bregaglio, S., Buis, S., Confalonieri, R., Fumoto, T. and Gaydon, D., 2015. Uncertainties in predicting rice yield by current crop models under a wide range of climatic conditions. *Global Change Biology*, *21*, pp. 1328-1341.

Long, S.P., Ainsworth, E.A., Leakey, A.D. and Morgan, P.B., 2005. Global food insecurity. Treatment of major food crops with elevated carbon dioxide or ozone under large-scale fully open-air conditions suggests recent models may have overestimated future yields. *Philosophical Transactions of the Royal Society B: Biological Sciences*, *360*, pp. 2011-2020.

Lovenduski, N.S., McKinley, G.A., Fay, A.R., Lindsay, K. and Long, M.C., 2016. Partitioning uncertainty in ocean carbon uptake projections: Internal variability, emission scenario, and model structure. *Global Biogeochemical Cycles*, *30*, pp. 1276-1287.

Luhunga, P.M., Kijazi, A.L., Chang'a, L., Kondowe, A., Ng'ongolo, H. and Mtongori, H., 2018. Climate Change Projections for Tanzania Based on High-Resolution Regional Climate Models from the Coordinated Regional Climate Downscaling Experiment (CORDEX)-Africa. *Frontiers in Environmental Science*, *6*, p. 122.

Marin, F., Jones, J.W. and Boote, K.J., 2017. A stochastic method for crop models: including uncertainty in a sugarcane model. *Agronomy Journal*, *109*, pp. 483-495.

Mason-D'Croz, D., Vervoort, J., Palazzo, A., Islam, S., Lord, S., Helfgott, A., Havlík, P., Peou, R., Sassen, M., Veeger, M. and van Soesbergen, A., 2016. Multi-factor, multi-state, multimodel scenarios: Exploring food and climate futures for Southeast Asia. *Environmental Modelling and Software*, *83*, pp. 255-270.

Mearns, L.O., Easterling, W., Hays, C. and Marx, D., 2001. Comparison of agricultural impacts of climate change calculated from high- and low-resolution climate change scenarios: Part I. The uncertainty due to spatial scale. *Climatic Change*, *51*, pp. 131-172.

Mearns, L.O., Mavromatis, T., Tsvetsinskaya, E., Hays, C. and Easterling, W., 1999. Comparative responses of EPIC and CERES crop models to high and low spatial resolution climate change scenarios. *Journal of Geophysical Research Atmospheres*, *104*, pp. 6623-6646.

Mearns, L.O., Rosenzweig, C. and Goldberg, R., 1996. The effect of changes in daily and interannual climatic variability on CERES-Wheat: a sensitivity study. *Climatic Change*, *32*, pp. 257-292.

Mearns, L.O., Sain, S., Leung, L.R., Bukovsky, M.S., McGinnis, S., Biner, S., Caya, D., Arritt, R.W., Gutowski, W., Takle, E. and Snyder, M., 2013. Climate change projections of the North American regional climate change assessment program (NARCCAP). *Climatic Change*, *120*(4), pp. 965-975.

Meehl, G.A., Covey, C., Delworth, T., Latif, M., McAvaney, B., Mitchell, J.F., Stouffer, R.J. and Taylor, K.E., 2007. The WCRP CMIP3 multimodel dataset: A new era in climate change research. *Bulletin of the American Meteorological Society*, *88*, pp. 1383-1394.

Moriasi, D.N., Arnold, J.G., Van Liew, M.W., Bingner, R.L., Harmel, R.D. and Veith, T.L., 2007. Model evaluation guidelines for systematic quantification of accuracy in watershed simulations. *Transactions of the ASABE*, *50*, pp. 885-900.

Müller, C., 2011. Harvesting from uncertainties. *Nature Climate Change*, *1*, pp. 253-254.

Nakicenovic, N., Alcamo, J., Grubler, A., Riahi, K., Roehrl, R.A., Rogner, H.H. and Victor, N., 2000. *Special Report on Emissions Scenarios (SRES), a special report of Working Group III of the Intergovernmental Panel on Climate Change*. Cambridge University Press. pp. 3-27.

Nilsen, T. and Aven, T., 2003. Models and model uncertainty in the context of risk analysis. *Reliability Engineering and System Safety*, *79*, pp. 309-317.

Pinto, I., Jack, C. and Hewitson, B., 2018. Process-based model evaluation and projections over southern Africa from coordinated regional climate downscaling experiment and coupled model intercomparison project phase 5 models. *International Journal of Climatology*, *38*, pp. 4251-4261.

Pirttioja, N., Carter, T.R., Fronzek, S., Bindi, M., Hoffmann, H., Palosuo, T., Ruiz-Ramos, M., Tao, F., Trnka, M., Acutis, M. and Asseng, S., 2015. Temperature and precipitation effects on wheat yield across a European transect: a crop model ensemble analysis using impact response surfaces. *Climate Research*, *65*, pp. 87-105.

Potter, N.J., Chiew, F.H., Charles, S.P., Fu, G., Zheng, H. and Zhang, L., 2020. Bias in dynamically downscaled rainfall characteristics for hydroclimatic projections. *Hydrology and Earth System Sciences*, *24*, pp. 2963-2979.

Ragno, E., AghaKouchak, A., Love, C.A., Cheng, L., Vahedifard, F. and Lima, C.H., 2018. Quantifying changes in future intensity-duration-frequency curves using multimodel ensemble simulations. *Water Resources Research*, *54*, pp. 1751-1764.

Randall, D.A., Wood, R.A., Bony, S., Colman, R., Fichefet, T., Fyfe, J., Kattsov, V., Pitman, A., Shukla, J., Srinivasan, J. and Stouffer, R.J., 2007. Climate models and their evaluation.

In *Climate change 2007:* The physical science basis. Contribution of Working Group I to the Fourth Assessment Report of the IPCC (FAR), Cambridge University Press, pp. 589-662.

Rasmussen, R., Ikeda, K., Liu, C., Gochis, D., Clark, M., Dai, A., Gutmann, E., Dudhia, J., Chen, F., Barlage, M. and Yates, D., 2014. Climate change impacts on the water balance of the Colorado headwaters: High-resolution regional climate model simulations. *Journal of Hydrometeorology*, *15*, pp. 1091-1116.

Rojas, R., Kahunde, S., Peeters, L., Batelaan, O., Feyen, L. and Dassargues, A., 2010. Application of a multimodel approach to account for conceptual model and scenario uncertainties in groundwater modelling. *Journal of Hydrology*, *394*, pp. 416-435.

Rosenzweig, C., Elliott, J., Deryng, D., Ruane, A.C., Müller, C., Arneth, A., Boote, K.J., Folberth, C., Glotter, M., Khabarov, N. and Neumann, K., 2014. Assessing agricultural risks of climate change in the 21st century in a global gridded crop model intercomparison. *Proceedings of the National Academy of Sciences*, *111*, pp. 3268-3273.

Rosenzweig, C., Jones, J.W., Hatfield, J.L., Ruane, A.C., Boote, K.J., Thorburn, P., Antle, J.M., Nelson, G.C., Porter, C., Janssen, S. and Asseng, S., 2013. The agricultural model intercomparison and improvement project (AgMIP): protocols and pilot studies. *Agricultural and Forest Meteorology*, *170*, pp. 166-182.

Ruiz-Ramos, M., Rodríguez, A., Dosio, A., Goodess, C.M., Harpham, C., Mínguez, M.I. and Sánchez, E., 2016. Comparing correction methods of RCM outputs for improving crop impact projections in the Iberian Peninsula for 21st century. *Climatic Change*, *134*, pp. 283-297.

Santos, J.A., Belo-Pereira, M., Fraga, H. and Pinto, J.G., 2016. Understanding climate change projections for precipitation over western Europe with a weather typing approach. *Journal of Geophysical Research: Atmospheres*, *121*, pp. 1170-1189.

Scinocca, J.F., Kharin, V.V., Jiao, Y., Qian, M.W., Lazare, M., Solheim, L., Flato, G.M., Biner, S., Desgagne, M. and Dugas, B., 2016. Coordinated global and regional climate modeling. *Journal of Climate*, *29*, pp. 17-35.

Simonovic, S.P., 2017. Bringing future climatic change into water resources management practice today. *Water Resources Management*, *31*, pp. 2933-2950.

Smithson, M., 1989, Ignorance and Uncertainty: Emerging Paradigms, Springer-Verlag, New York.

Tao, F., Hayashi, Y., Zhang, Z., Sakamoto, T. and Yokozawa, M., 2008. Global warming, rice production, and water use in China: developing a probabilistic assessment. *Agricultural and Forest Meteorology*, *148*, pp. 94-110.

Tebaldi, C. and Knutti, R., 2007. The use of the multimodel ensemble in probabilistic climate projections. *Philosophical Transactions of the Royal Society A: Mathematical, Physical and Engineering Sciences*, *365*, pp. 2053-2075.

Teklesadik, A.D., Alemayehu, T., Van Griensven, A., Kumar, R., Liersch, S., Eisner, S., Tecklenburg, J., Ewunte, S. and Wang, X., 2017. Inter-model comparison of hydrological impacts of climate change on the Upper Blue Nile basin using ensemble of hydrological models and global climate models. *Climatic Change*, *141*, pp. 517-532.

Teutschbein, C. and Seibert, J., 2012. Bias correction of regional climate model simulations for hydrological climate-change impact studies: Review and evaluation of different methods. *Journal of Hydrology*, *456*, pp. 12-29.

Thrasher, B., Maurer, E.P., McKellar, C. and Duffy, P.B., 2012. Bias correcting climate model simulated daily temperature extremes with quantile mapping. *Hydrology and Earth System Sciences*, *16*, pp. 3309-3314.

Uusitalo, L., Lehikoinen, A., Helle, I. and Myrberg, K., 2015. An overview of methods to evaluate uncertainty of deterministic models in decision support. *Environmental Modelling and Software*, *63*, pp. 24-31.

Walker, W.E., Harremoës, P., Rotmans, J., Van Der Sluijs, J.P., Van Asselt, M.B., Janssen, P. and K., von Krauss, M.P., 2003. Defining uncertainty: a conceptual basis for uncertainty management in model-based decision support. *Integrated Assessment*, *4*, pp. 5-17.

White, J.W., Hoogenboom, G., Kimball, B.A., Wall, G.W., 2011. Methodologies for simulating impacts of climate change on crop production. *Field Crops Research*, 124, 357–368.

White, R.H. and Toumi, R., 2013. The limitations of bias correcting regional climate model inputs. *Geophysical Research Letters*, *40*, pp. 2907-2912.

Wilby, R.L., Troni, J., Biot, Y., Tedd, L., Hewitson, B.C., Smith, D.M. and Sutton, R.T., 2009. A review of climate risk information for adaptation and development planning. *International Journal of Climatology*, *29*, pp. 1193-1215.

Yao, F., Qin, P., Zhang, J., Lin, E. and Boken, V., 2011. Uncertainties in assessing the effect of climate change on agriculture using model simulation and uncertainty processing methods. *Chinese Science Bulletin*, *56*, pp. 729-737.

Zhang, Y., Zhao, Y., Chen, S., Guo, J. and Wang, E., 2015. Prediction of maize yield response to climate change with climate and crop model uncertainties. *Journal of Applied Meteorology and Climatology*, *54*, pp. 785-794.

Zhao, C., Liu, B., Piao, S., Wang, X., Lobell, D.B., Huang, Y., Huang, M., Yao, Y., Bassu, S., Ciais, P. and Durand, J.L., 2017. Temperature increase reduces global yields of major crops in four independent estimates. *Proceedings of the National Academy of Sciences*, *114*, pp. 9326-9331.

Lead to Chapter 3

Chapter 2 presented a review of uncertainties in climate change impact assessment studies. Different techniques that have been used to quantify model prediction uncertainties were also reviewed in Chapter 2. In Chapter 3, calibration of the crop models employed using different maize varieties is the focus. Individual models and their multimodel ensembles are evaluated for their performance. Chapter 3 mainly argues that multimodel ensembles reduced model uncertainty and improved simulation output accuracy compared to the outputs of individual models.

CHAPTER 3: CALIBRATION AND VALIDATION OF APSIM–MAIZE, DSSAT CERES–MAIZE AND AQUACROP MODELS FOR ETHIOPIAN TROPICAL ENVIRONMENTS [1]

Hirut Getachew Feleke [1*], M.J. Savage [1] and Kindie Tesfaye [2]

[1]Agrometeorology Discipline, Soil-Plant-Atmosphere Continuum Research Unit, School of Agricultural, Earth and Environmental Sciences, University of KwaZulu-Natal, Pietermaritzburg, South Africa

[2]International Maize and Wheat Improvement Centre (CIMMIT), Addis Ababa, Ethiopia

*Corresponding author, email: hirut_ge@yahoo.com

3.1 Abstract

Process-based crop models are popular tools to quantify the impact of changes due to climate, soil, crop management and genotype interaction. Accurate simulation of crop production for different agro-ecological conditions using an individual crop model remains a challenge due to different sources of uncertainty. Studies with ensembles of crop models can give valuable information about model accuracy and uncertainty, but such studies are limited in tropical environments including Ethiopia.

---

[1] Based on the paper: Feleke, H.G., M.J. Savage and K. Tesfaye, 2021. Calibration and validation of APSIM–Maize, DSSAT CERES–Maize and AquaCrop models for Ethiopian tropical environments. S. Afr. J. Plant Soil. 38:1, 36-51, DOI: 10.1080/02571862.2020.1837271.

Therefore, the aim of this study was to compare the performance of the outputs of three individual crop models and their ensemble mean. Three different crop models, namely, APSIM-maize, AquaCrop and DSSAT CERES-maize calibrated and evaluated them separately and in a multimodel ensemble approach using four maize varieties (BH546, BH661, Jibat and MH140) grown under rainfed conditions. Model input data were collected from field experiments conducted at three sites (Ambo, Bako and Melkassa) in the 2017/2018 crop growing season. The experiments were laid out in a randomized complete block design using a plot size of 10 m x 10 m. The crop models were calibrated using measured data from the Bako and evaluated with independent datasets from the Ambo and Melkassa. The calibration parameters used in each of the three crop models studied enabled accurate simulation of flowering, maturity, canopy cover (AquaCrop) and grain yield against measured data. Evaluation of the models indicated that APSIM-maize and DSSAT CERES-maize accurately simulated days to flowering and maturity with root mean square error (RMSE) values ranging from 1.73 – 4.09 and 1.66 – 5.36 days, respectively. However, the DSSAT CERES-maize model over-estimated the maturity period of late maturing varieties at Ambo. The AquaCrop model accurately simulated maize canopy cover for all varieties studied with a RMSE of less than 10.8 % and a high (0.95) index of agreement (*d*). The simulated grain yield agreed fairly well with the measured data with normalized RMSE values ranging from 13 – 19 %, 1 – 4 % and 1 – 17 % for APSIM, AquaCrop and DSSAT-maize models, respectively. However, the APSIM model underestimated yield for all maize varieties at Ambo (RMSE of 1.14 t ha^{-1} and *d* value of 0.50). The best performance was obtained when an ensemble of all models was considered, which reduced the RMSE values for grain yield to 0.35 t ha^{-1} at Ambo and 0.41 t ha^{-1} at Melkassa. Furthermore, the ensemble mean reduced the normalized RMSE by 8 % while increasing the *d* value to above 0.90 for both evaluation sites.

On the other hand, the ensemble results were quite similar for grain yield simulated using the AquaCrop model. It is concluded that model ensembles reduced model uncertainty and improved simulation output accuracy compared to the outputs of individual models in tropical environments.

Keywords: Ethiopia, model calibration, model evaluation, model inter-comparison, multimodel ensemble

3.2 Introduction

Process-based crop simulation models are useful tools to assess the impact of climate change. Many such models consider the interaction between plant-soil-atmosphere continuum and crop management versus their effects on crop productivity (Tian et al. 2018). In recent years, many models are being applied to study the impacts of climate change and developing adaptation strategies (MacRobert and Savage 1998; Abraha and Savage 2006; Araya et al. 2015; Deb et al. 2015; Ewert et al. 2015; Kassie et al. 2015; Shrestha et al. 2016; Jones et al. 2017; Tesfaye et al. 2018). Nevertheless, crop model applications devoted to impact assessment studies produce high uncertainties related to model structure and parameters (Palosuo et al. 2011) which have become a major concern recently in climate impact assessments (Li et al. 2015; Zhang et al. 2015).

To increase the reliability of model output and to obtain improved estimates of uncertainty, the use of crop multimodel ensembles has been suggested (Asseng et al. 2015; Li et al. 2015; Pirttioja et al. 2015). Martre et al. (2015) argued that the improvement of models in an ensemble, using good quality field-based experimental data, could substantially intensify the range of research questions to be addressed and increase the confidence in simulation results of applications under different climatic and management conditions. Furthermore, it has been empirically observed in many fields of study that ensemble averages or medians often result in improved observations than even the best individual model (Palosuo et al. 2011; Martre et al. 2015).

Moreover, the use of the multimodel ensemble mean or median to identify the uncertainty is nowadays good practice within the climate community as a tool to communicate and provide policymakers with information about the uncertainty of current models (Kundzewicz et al. 2018). However, the availability of a more detailed dataset with standard measurements, particularly for complex models, is a major concern when modelling compared to using simple models (Babel et al. 2019). Simple and user-friendly models have limitations due to a simplification of the processes involved. Thus, no single model can simulate satisfactorily all the outputs required for decision making in agricultural production. This leads to the recommendation of incorporating two or more crop models in such a way as to maximize their individual strengths and minimize their weaknesses (Kanda et al. 2018).

As a fundamental structural difference, crop simulation models are categorized as carbon-driven, solar radiation-driven or water-driven models (Todorovic et al. 2009). Among the different crop simulation models, three models namely, DSSAT-CERES-maize (radiation-driven), APSIM-maize (radiation-driven) and AquaCrop (water-driven) models were used in this study.

The Decision Support System for Agrotechnology Transfer (DSSAT) model has been adopted in a wide range of countries and continents, which indicates its strength in accommodating a wide range of climatic and agricultural conditions. For instance, Jalota and Vashish (2016) showed a decline in the future production of maize using DSSAT in India. Rezaei et al. (2015) in Iran used the DSSAT model to show maize crops could be substituted by pearl millet to counter yield reduction in the future, while other studies have shown a change of cultivar would be an option to sustain food production in the future (Ahmed et al. 2016; Lana et al. 2016). However, other studies show the model limitations indicating that the DSSAT model was not accurate in simulating water and nitrate dynamics and therefore needed to be combined with soil water and growth models for improved modelling of cropping systems (Kanda et al. 2018).

The Agricultural Production System Simulator (APSIM) model allows for a detailed description of farming system, decision, and the simulation of associated soil water and salinity dynamics, together with the interactions between maize and other crops (Radanielson et al. 2018). Most modelling studies that use APSIM involve maize as the crop. For instance, Ngugi et al. (2015) adopted APSIM for a scenario analysis of the effect of soil and water conservation practices on grain yield of improved maize varieties in Kenya. The same study indicated that the algorithm in APSIM for simulating planting date improved yield by reducing crop failures (Ngugi et al.

2015). In addition, Bacon et al. (2016) showed the potential of APSIM in determining the effect of spatial plot distribution. However, the model underestimated soil nitrogen and soil organic component and underestimation or overestimation of nitrous oxide emissions (Brilli et al. 2017).

The AquaCrop crop water productivity model was developed by the Food and Agriculture Organization of the United Nations (FAO) as a tool for irrigation engineers, extension agents, agricultural policy officers and researchers that can provide quick but accurate estimates of crop production and crop water productivity under various environmental and agronomic conditions (Hsiao et al. 2009; Raes et al. 2009; Steduto et al. 2009). The model separates evapotranspiration into crop transpiration and soil evaporation for canopy development, biomass formation and final yield. This makes the model applicable to different climates (Araya et al. 2010; Wellens et al. 2013; Babel et al. 2019). However, a weakness of AquaCrop is that it is ineffective in accurately predicting crop yield due to its single point simulation and reduced consideration of spatial differences on crop, soil and field management (Steduto et al. 2009).

Given the limitations of crop models, drawing a conclusion based on a single crop model can generate quite large biases (Asseng et al. 2013) whereas combining models increases the skill, reliability and consistency of model predictions, and make the combined result superior than a single model (Bellucci et al. 2015).

Obviously, a multimodel ensemble approach is mandatory and not an option in order to reduce uncertainties and to produce reliable output in crop model simulations (Maiorano et al. 2017). Therefore, the need to introduce a multimodel ensemble approach is crucial to farming systems, such as those in Ethiopia where maize is grown under diverse environmental and management conditions. The use of the multimodel ensemble could lead to a more reliable yield estimation and build confidence in using models for decision making in those diverse farming systems.

Therefore, the aims of this study were: (i) to calibrate three crop simulation models for improved maize varieties grown under three different agro-ecologies in Ethiopia, and (ii) to evaluate the performance of individual models and their multimodel ensemble.

3.3 Materials and methods

3.3.1 Field experiments

In Ethiopia, maize experiments were conducted under rainfed conditions at the three agricultural research centres namely Ambo (latitude 8° 57' N, longitude 38° 07' E and altitude 2225 m), Bako (latitude 9^o 12' N, longitude 37^o 04' E and altitude 1650 m), and Melkassa (latitude 8^o 42' N, longitude 39^o 32' E and altitude 1550 m) in the 2017/2018 main rain season (Figure 3.1).

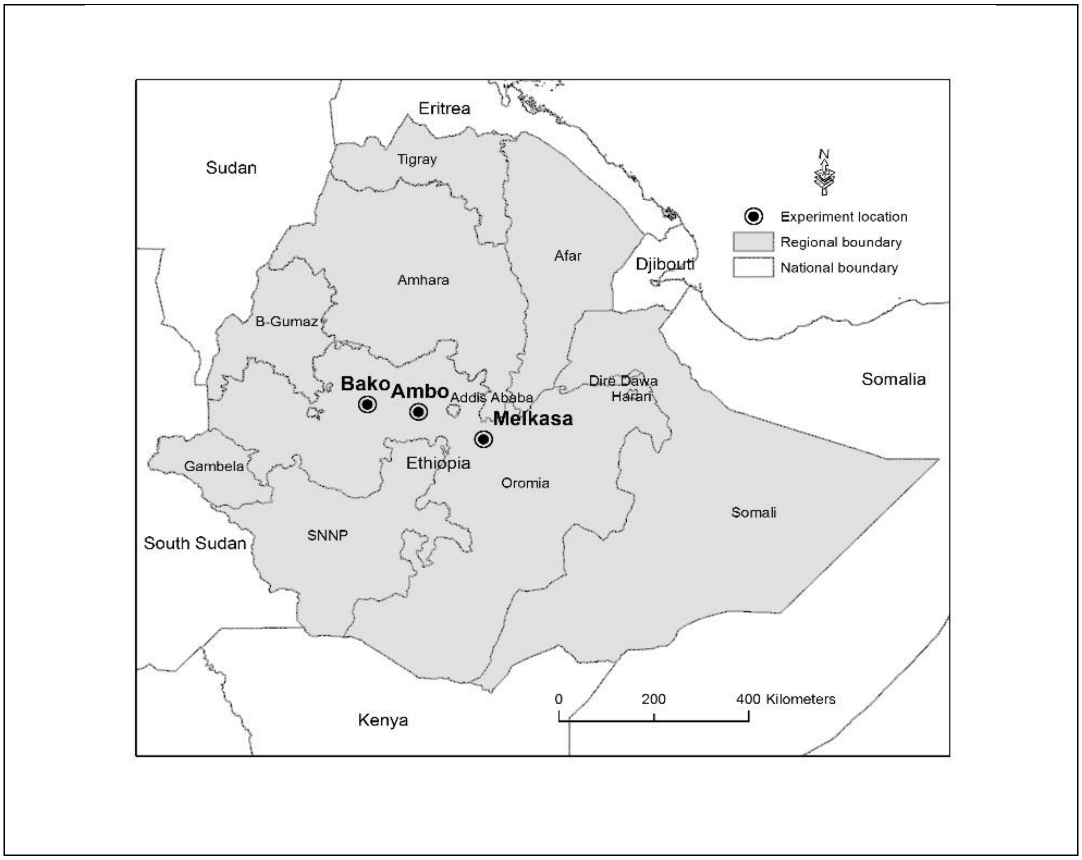

Figure 3.1: Location of the three experimental sites in Ethiopia

Data collected from Bako were used for model calibration while data from Ambo and Melkassa were used for model evaluation. Each experiment was arranged in four randomized complete blocks with three replications. The four maize cultivars were replicated three times at the three sites. Each plot consisted of 13 rows, each 10 m long, with a spacing of 250 mm between plants and 750 mm between rows. The experiments were well managed maintaining optimum conditions for plant growth and development including applying fertilizer, good management of weeds, diseases and pests as much as possible. Data were collected on crop growth and development, crop management, soil, and weather conditions as required for calibrating the cultivar coefficients of new maize varieties. The procedures described in IBSNAT (1988) and Hoogenboom et al. (1999) were followed.

The maize hybrid varieties used in all field experiments were BH546, BH661, Jibat and MH140. The highland variety Jibat was widely used at Ambo, midland varieties BH546, BH661 at Bako and MH140 lowland variety at Melkassa. These cultivars were chosen since they are widely grown by farmers in their respective areas and they have a high potential yield (Table 3.1).

Table 3.1: Agro-climate adaptation, physiological maturity and yield potential of the selected maize varieties

Variety	Year of release	Altitude (m)	Rainfall (mm)	Days to maturity	Yield (t ha^{-1})	
					Research station	Farmer's field

BH546	2013	1000-2000	1000-1500	145	8.5-11.5	6.5-7.5
BH661	2011	1600-2200	1000-1500	160	9.5-12.0	6.5-8.5
Jibat	2009	1800-2600	1000-1200	178	8.0-12.0	6.0-8.0
MH140	2013	1500-1800	800-1200	140	8.5-9.5	6.5-7.5

Source: Gissa (2016)

3.3.2 Crop measurements

The vegetative phase of the varieties was recorded by counting the leaves' collar appearance at 2-day intervals for all experiments. Flowering stage was recorded when silks were visible outside the husks on 50% of the plants of each plot. Physiological maturity was determined by regularly sampling two cobs per plot to assess the presence of black layers at the base of the grains. Above-ground biomass was measured by using destructive methods. Destructive methods were used five to six times every two weeks from a 0.75-m^2 area in order to obtain above-ground biomass. Four plants from each plot were randomly selected with all plant part samples separated into stems, leaves, ears and husks, and dried at 70 ^oC to a constant weight and the final dry weight recorded (Soler et al. 2007). Before the destruction process, plant height of the four plants was measured at two weeks intervals in order to determine the average plant height. Maximum rooting depth was measured destructively every two weeks after planting (DAP). A trench was dug to give a vertical profile face 2.0-m deep in each plot, the centre point from four plants in the row were identified and the heights were measured before the top parts were removed for dry matter analysis (Cairns et al. 2004).

The leaf area index (*LAI*) of the plant was estimated by multiplying the plant population by the leaf area per plant as described in Kar et al. (2006). First, the leaf area from eighteen plants was measured manually using a ruler and counting of plant populations was done manually from a 64-m^2 area. The *LAI* was calculated using:

$$LAI = 0.75 \times \rho \times \left(\frac{\sum_{i=1}^{m} \sum_{i=1}^{n} \left(L_{ij} \times B_{ij} \right)}{m} \right) \tag{3.1}$$

where ρ is plant density (plants m^{-2}), m is the number of measured plants, L_{ij} is leaf length (m), B_{ij} is the maximum leaf width (m), n is the number of leaves of the m^{th} plant, and the factor 0.75 is leaf area factor (Maddonni et al. 2001; Jin et al. 2014). Maize canopy cover (*CC*) was determined based on Steduto et al. (2009):

$$CC = 1 - exp^{-0.65 \times LAI} \tag{3.2}$$

The final harvest was conducted manually for the nine central rows by harvesting 8 m of the row. The number of grains per ear was counted in 15 ears per treatment. Grain weight was obtained from the average of the weight of 8 groups of 100 grains and then corrected to 0 % of moisture and converted to 1-grain weight. Yield was corrected to 0 % of moisture.

3.3.3 Weather and soil data

Daily solar radiation, maximum and minimum air temperature and precipitation for each location were obtained from the meteorological station nearest to the experimental site. Grass reference evapotranspiration (ET_O) was calculated by the FAO Penman-Monteith method (Allen et al. 1998; Allen et al. 2006; Savage 2018).

The annual total rainfall, average maximum and minimum air temperatures of the growing season for the three sites are presented in Table 3.2. During the crop growth period, analysis of monthly rainfall data at the calibration site (Bako) indicates the rain starts in April and ends in November while for Ambo and Melkassa sites rain starts in May and ends in September (see Appendix 1 Supplementary materials Figure SM3a).

The average maximum air temperature and average evapotranspiration decreases during the growing season while the average minimum air temperature shows small variation (see Figure SM3b).

Initial soil samples taken at the 200-mm depth were analyzed to calculate total nitrogen, available phosphorous, texture, pH and organic carbon before planting at the three sites (Table 3.2). Soil profile data for the three sites were obtained from reports by Liben et al. (2018) and Seyoum et al. (2018) and the International Maize and Wheat Improvement Centre (CIMMIT), Ethiopia (see Table SM3a).

Table 3.2: Weather, soil and field management data for experiments conducted at the three sites during the period 2017/2018 cropping season

Station	**Ambo**	**Bako**	**Melkassa**
Weather (1995-2017)			
Annual total rainfall (mm)	969	1600	848
Annual mean maximum temperature (^{o}C)	25.3	29.1	29.3
Annual mean minimum temperature (^{o}C)	10.6	12.7	13.9
Soil (0-200 mm)			
Texture	Sandy clay loam	Clay	Loam
Total N (%)	0.11	0.14	0.11
Available P (ppm)	11	11	17
Organic carbon (%)	1.83	1.87	1.32
Organic matter (%)	3.16	3.22	2.28
pH	7.03	4.77	6.96
Crop management			
Planting (date)	15-Jun	20-Jun	29-Jun

Harvesting (date)	15-Jan	19-Dec	06-Dec
Water management	Rainfed	Rainfed	Rainfed

3.3.4 Overview of models used

Three crop models were selected based on their different structure, complexity, global importance, and mainly their prior performance for estimating maize growth and development around the world.

3.3.4.1 APSIM-maize model

Agricultural Production System Simulator (APSIM) is a farming system model that was developed by the Agricultural Production Systems Research Unit (APSRU) to assess risk management in agricultural production (Keating et al. 2003; Holzworth et al. 2014). Within APSIM there are a series of modules that are grouped together and categorized as crop, management, soil, and the environment. The sub-modules communicate with each other via the APSIM “engine”. The “engine” passes information between modules according to a standard protocol which allows modules to be applied or removed from the “engine” depending on the specifications for the simulation task. The simulation engine module in the APSIM simulates more than 20 different crops including maize (Wang et al. 2002; Keating et al. 2003). In addition, there are also general modules for pasture, weed and forest (Huth et al. 2001; Keating et al. 2003).

The model simulates the growth and development of crops, soil characteristics, and management options by considering the cropping system. APSIM modules require input data including climate data (rainfall, solar radiation, maximum and minimum air temperature), soil and crop data together with specification of management practices. APSIM was tested against field experimental data in a wide range of growing conditions (Keating et al. 2003). APSIM was recently used to improve maize production in relation to climate variability and change across many areas, for example, in Africa (Corbeels et al. 2018), Asia (Kafatos et al. 2017), China (Xiao et al. 2020), Ethiopia (Seyoum et al. 2018), and Europe (Parent et al. 2018).

3.3.4.2 AquaCrop model

AquaCrop is a FAO (Food and Agriculture Organization of the United Nations) crop model that simulates crop and soil response to water stress under various climatic, soil, crop and management conditions (Raes et al. 2009; Steduto et al. 2009). It is a water-driven growth model with a simple structure that requires limited inputs. The model has different modules: the soil module contains the water balance, that makes the AquaCrop model different from other models; it separates the soil evaporation from crop transpiration based on the Ritchie's water balance approach (Ritchie 1972). The plant module encompasses crop growth, development, and yield processes. The atmosphere module component addresses thermal regime, rainfall, evaporative demand and CO_2 concentration (Raes et al. 2009).

AquaCrop uses different input files for simulation: daily climate file (minimum and maximum air temperature, rainfall, and short-grass reference evaporation (ET_O) or climate data from which ETo can be calculated using daily data such as solar radiation, air temperature, air humidity, sunshine and wind speed), crop file (time to emergence, maximum canopy cover, time to flowering, start of senescence, time to maturity), soil file (soil type, field capacity, permanent wilting point, saturation soil water content, saturated hydraulic conductivity), management file (field surface practices, application of mulches, effect of soil fertility), irrigation file (no irrigation, net irrigation, irrigation schedule), initial conditions (initial soil water content, soil salinity, canopy cover and rooting depth); all these inputs are user specific for the AquaCrop model.

The AquaCrop model simulates the interaction between crop and soil through considering management practices. The model crop file contains different types of crop parameters: (i) conservative crop parameters and (ii) non-conservative parameters. Conservative crop parameters are crop specific parameters, which do not change materially with time, management, geograpical locations, climate and cultivars. Conservative crop parameters are not calibrated and are valid for all cultivars and in all environments, while the non-conservative crop parameters are cultivar-specific parameters that are affected by planting mode, field management, condition in the soil profile and climate. These parameters have to be provided by the end user of the model.

Unlike many models, the AquaCrop model focuses on water, the use of ground canopy cover and water productivity values normalized for atmospheric evaporative demand and carbon dioxide concentration. The model is therefore applicable to diverse locations and seasons including future climate scenarios (Heng et al. 2009; Raes et al. 2009). AquaCrop has effectively simulated crop growth and yield for various crops including maize under different soils and environments, such as in Ethiopia (Araya et al. 2010), Europe (Yang et al. 2017), India (Babel et al. 2019), Nigeria (Akumaga et al. 2017), South Africa (Mbangiwa et al. 2019), and Vietnam (Lee and Dang 2018).

3.3.4.3 DSSAT CERES-maize model

The Decision Support System for Agrotechnology Transfer (DSSAT) is a crop simulation platform that homogenizes inputs and outputs to run several process-based models that share common modules (Jones 1986; Jones et al. 2003; Hoogenboom et al. 2012). The DSSAT research tool for crop production analysis incorporates crop-soil-weather models, and analysis tools, such as uncertainty and economic models. Supportive software such as graphics, weather data generator, GIS linkages and spatial variability analyses are used. DSSAT was designed to allow users to adapt and evaluate models for their own conditions, incorporate their own data in standard formats, provide insight into "what-if" questions about production, profitability and stability. Additionally, it assists researchers to understand responses and interactions that occur in the field.

The DSSAT CERES-maize model requires detailed input data to simulate plant growth. These include field data, soil characteristics, daily weather data, cultivar characteristics and management data. The input dataset requirement makes the model more complex and useful in drawing attention to filling the gaps in understanding, and interpreting data from field experiments in different environments (Monteith 1996).

The DSSAT CERES-maize model is widely applicable to assess the effects of climate change on crop production and it can also evaluate the best management options under changed climate scenarios (Ventrella et al. 2012). The model has been successfully used worldwide over the last 15 years in many different applications, including climate change impacts and adaptation, regional climate impact studies, diagnosing problems, such as yield gap analysis, precision agriculture and crop management, such as nitrogen fertilization, irrigation and planting or sowing date, prescribing spatially variable management, water and irrigation management, soil fertility management, yield prediction for crop management, climate variability and risk management, soil carbon sequestration, land use change analysis, early warning yield forecasting, biofuel production and risk insurance (Jones 1986; Ritchie 1998; Arora et al. 2007; Cabrera et al. 2007; Rinaldi and Ubaldo 2007; Xiong et al. 2008; Iqbal et al. 2011; Kassie et al. 2014; Araya et al. 2015; Kassie et al. 2015; Tesfaye et al. 2018; Babel et al. 2019).

3.3.5 Model calibration

The APSIM-maize model, version 7.9, AquaCrop model, version 6.0, and DSSAT CERES-maize model version 4.7 were calibrated using daily climate data, site-specific soil and management parameters, and field experimental data for the 2017/2018 cropping season, to develop cultivar specific parameters. Two independent datasets from three different sites (Ambo, Bako and Melkassa) were used. Bako is one of the major maize growing areas in Ethiopia. The collected dataset from this site was used for model calibration. The models were evaluated using independent datasets collected from the different environments (Battisti et al., 2017) such as Ambo and Melkassa sites for the 2017/2018 cropping season.

For the APSIM-maize model calibration, the input data required daily weather data (maximum air temperature, minimum air temperature, solar radiation and rainfall), soil water parameters (bulk density, air dry, drained upper limit, lower limit, saturated soil water content, root water extraction coefficient for maize), soil carbon parameters (organic carbon, microbial biomass pool - Fbiom, inert fraction - Finert), soil nitrogen parameters (soil pH, nitrate, ammonia) crop parameters (potential kernel number per plant, thermal time from emergence to the end of the juvenile stage, from the juvenile stage to floral initiation, from the flag leaf stage to flowering, flowering to start of grain filling, and from flowering to physiological maturity), management data (sowing date, plant density, date of harvest, fertilizer application).

The daily weather data files were converted into the APSIM format (.met), and annual average air temperature (tav) and annual amplitude in mean monthly air temperature (amp) were computed and incorporated into the dataset. For calibration, the cultivar coefficients were obtained step-by-step, first for phenological development and then for grain developmental parameters.

The existing cultivars, which had previously been parameterized for use in the APSIM-maize model (Keating et al. 2003) were used to simulate flowering and physiological maturity. Four hybrids whose phenology, days-to-flowering and days-to-physiological maturity matched well with the new hybrids selected for further calibration. The crop coefficients (Table SM3b) for simulated cultivars were modified using field-observed data (Table SM3c) to best represent the new cultivars and were re-named with the new cultivars.

The calibration of the AquaCrop was through an iterative process in which the values of crop specific parameters were used as already specified in the model. The non-conservative parameters (Table SM3d) were calibrated using the measured data of the maize experiment conducted during 2017/2018.

Input data required for the AquaCrop model calibration included daily weather data (maximum air temperature, minimum air temperature, ETo), cultivar specific parameters (initial canopy cover, time to 90% seedling emergence, maximum canopy cover, time to start of flowering, duration of flowering, time to beginning of canopy senescence, time to physiological maturity, maximum rooting depth, time to reach maximum rooting depth, reference harvest index), soil parameters (soil texture, bulk density, field capacity, permanent wilting point, saturated hydraulic conductivity, soil water content at saturation).

The initial canopy cover percentage (CC_O) was estimated from sowing rate, seed mass, seed number and estimated germination rate using the available options in the model. The canopy cover is a key component in calculating crop transpiration, which is directly related to *LAI* and estimated using Equation (2). The canopy cover development was determined by the model after providing the six parameters: canopy growth coefficient (CGC), canopy decline coefficient (CDC), maximum canopy cover (CC_x), days to emergence, days to senescence and days to maturity (Araya et al. 2010). The CGC governs the rate at which the canopy expands, and the CDC governs the rate at which the canopy dies off at the end of the growing season. These parameter values were determined using a repeated trial and error approach to fit the canopy cover to the measured *LAI* and CO_2 concentration. In the calibration process, the simulated canopy cover was compared to the observed canopy cover on different days after planting of the crop. The simulated yield was then compared with the observed yield for the four maize varieties at the three sites.

The calibration of the DSSAT CERES-maize model was used for the cultivar specific observation. The cultivar-specific observations were used for genetic coefficient determination. The genetic coefficients required for the DSSAT CERES-maize model are presented in Table SM2. The input data for model calibration included weather data (daily maximum and minimum air temperature, daily rainfall, daily solar radiation), soil surface information (slope, colour, drainage, presence of stones in the surface), soil profile information as a function of depth (bulk density, drained upper limit, lower limit, total nitrogen, available phosphorus, soil organic matter, cation exchange capacity, soil pH, soil texture, level of root abundance across depth), crop data (date of emergence, date of flowering, date of physiological maturity, total number of leaves per plant, maximum *LAI*, total above ground biomass, yield), growth parameters (dry biomass of leaves, stem and grain), crop management data (specification of previous crop harvested, initial soil moisture content before planting, plant density, planting date, plant population per m^2, date of harvest), fertilizer (type of fertilizer, date of application, amount applied, method of application) and type of land preparation (tillage) for the four varieties (Jibat, BH661, BH546 and MH140) at the three sites. Genetic coefficients were determined by using the Generalized Likelihood Uncertainty Estimation (GLUE), developed for estimating cultivar specific parameters for CERES maize (He et al. 2010). The GLUE software was run 6000 times for the parameters of each cultivar and then manual adjustment was applied following Boote (1999) using the same phenology and growth variables data described until an acceptable simulation fit was observed.

3.3.6 Model evaluation

The models were evaluated using flowering, maturity, canopy cover (for AquaCrop) and yield data obtained from the Ambo and Melkassa experimental sites. Maize yield from each plot and site was uased for model evaluation. As for each calibration process, a visual graphic comparison was conducted. For the three models, the goodness of fit between the simulated and observed values was evaluated by using different statistical indices, such as root mean square error (RMSE) (Ahmed et al. 2016), normalized root mean square error (NRMSE) (Ahmed et al. 2016), the prediction error (%E), *d*-index (Willmott 1981) and coefficient of determination (R^2):

$$RMSE = \left[\sum_{i=1}^{n} \frac{(Pi - Oi)^2}{n}\right]^{0.5} \tag{3.3}$$

$$\text{NRMSE} = \left[\sum_{i=1}^{n} \frac{(Pi - Oi)^2}{n}\right]^{0.5} \times \frac{100}{\bar{O}} \tag{3.4}$$

$$\%E = \frac{(Pi - Oi)}{Oi} \times 100 \tag{3.5}$$

$$d = 1 - \frac{\sum_{i=1}^{n}[(Pi - \bar{O}) - (Pi - \bar{O})^2]}{\sum_{i=1}^{n}[(|Pi - \bar{O}|) - (|Pi - \bar{O}|)^2]} \tag{3.6}$$

where *Oi* and *Pi* refer to observed and predicted values respectively for all studied variables, $\bar{O}$ is the mean of the observed variable and *n* is the number of observations.

3.3.7 Multimodel ensemble

With all models calibrated and validated, a multimodel analysis was performed by using the average of the estimated maize yields of the three models. For this analysis, the simulated yields (ensemble) were evaluated by the same statistical indices.

3.4 Results

3.4.1 Model calibration

3.4.1.1 APSIM-maize

The crop genetic coefficients for each cultivar cannot be used as constants since they are specific to the agro-ecology of the area (Ahmed et al. 2016). The crop genetic coefficients calibrated for the APSIM maize model for the newly released varieties are presented in Table 3.3.

Table 3.3: Genetic coefficients fitted for APSIM-maize and DSSAT CERES-maize models

APSIM-maize	**Cultivar**			
Parameter	BH546	BH661	Jibat	MH140
est_days_endjuv_to_init (day)	20	25	20	20
Potential kernel number per plant	460	475	378	390
Grain growth rate (mg $grain^{-1}day^{-1}$)	9.3	8.0	9.4	9.6
tt_end of juvenile stage to floral initiation (^{o}C day)	0	0	0	0
Photoperiod critical 1 (h)	12.5	12.5	12.5	12.5
Photoperiod critical 2 (h)	24	24	24	24

Photoperiod slope ($^oC\ h^{-1}$)	30	30	10	23
tt_emergence to end of juvenile (^oC day)	270	250	256	242
tt_flag leaf to flowering (^oC day)	10	80	10	10
tt_ flowering to start of grain filling (^oC day)	170	170	170	80
tt_flowering to maturity (^oC day)	897	885	910	926
tt_maturity to ripening (^oC day)	1	1	1	1
Canopy height (mm)	2550	2900	2700	2700
Stem mass (g $stem^{-1}$)	80	80	80	80
DSSAT CERES-maize				
P1	253.0	265.0	165.9	226.7
P2	0.700	0.750	0.970	0.700
P5	945.0	930.0	930.0	900.6
G2	490.5	447.0	609.8	863.0
G3	12.70	12.75	6.65	9.60
PHINT	49.00	48.00	75.00	53.00

The performance of the calibrated APSIM-maize model is shown in Table 3.4. The simulated dates of flowering and maturity agreed with that observed in the calibration dataset, with RMSE less than 2 days across all varieties at Bako. The NRMSE of flowering and maturity dates for all varieties was less than 3 %. This indicated that the APSIM-maize model could simulate well crop phenology variables for the different varieties across the different agro-environments.

The model also predicted maize yield accurately with the RMSE and NRMSE values of 0.2 t ha^{-1} and 3 % respectively. There was generally reasonable agreement between simulated and observed flowering date, maturity date and yield with the error very low (< 4.6 %) for all varieties at Bako (Table 3.4).

Table 3.4: Calibration results for APSIM-maize model for the four maize varieties using experimental data for the 2017/2018 maize cropping season

Cultivar	Flowering date (DAP)			Physiological maturity (DAP)			Maize yield (t ha^{-1})		
	Observed	Simulated	Error (%)	Observed	Simulated	Error (%)	Observed	Simulated	Error (%)
BH546	83	86	3.7	154	155	0.6	5.923	6.197	4.6
BH661	87	87	0.0	159	157	-1.3	5.399	5.421	0.4
Jibat	78	79	1.2	151	150	-0.7	5.293	5.492	3.8
MH140	77	78	1.2	151	150	-0.7	6.263	6.244	-0.3
RMSE	1.7			1.3			0.2		
NRMSE (%)	2.0			0.9			3.0		
d	0.96			0.96			0.95		
R^2	0.93			0.89			0.91		

The negative sign represents an underestimation; DAP: days after planting

3.4.1.2 AquaCrop

Calibrated crop parameters used in AquaCrop model are presented in Table 3.5. The crop parameters obtained from the model calibration (Table 3.5) were used in the evaluation simulation.

Table 3.5: AquaCrop calibration parameters and their respective values for four maize varieties

Parameters	Cultivar			
	BH546	BH661	Jibat	MH140
Base temperature (^oC)	10	10	10	10
Upper temperature (^oC)	30	30	30	30
Plant density (plants m^{-2})	5.3	5.3	5.3	5.3
Initial percentage canopy cover CCo (%)	0.26	0.26	0.26	0.26
Maximum percentage canopy cover CC_x (%)	90	90	85	85
Canopy growth coefficient CGC (% day)	7.54	8.29	7.42	8.75
Canopy decline coefficient CDC (% day)	0.13	0.12	0.08	0.06
Normalized water productivity WP (g m^{-2})	32.0	32.0	32.0	32.0
Time to maximum canopy cover (day)	116	107	116	101
Time to flowering (day)	82	86	77	76
Length of the flowering stage (day)	56	42	78	54
Time to start senescence (day)	122	122	122	122
Time to maturity (day)	154	159	151	151
Maximum rooting depth (m)	1.8	1.8	1.9	1.9
Minimum effective rooting depth (m)	0.3	0.3	0.3	0.3
Reference harvest index (%)	22	20	22	24

The simulation of percentage green crop canopy cover (CC) is a key feature of AquaCrop instead of leaf area (Steduto et al. 2009). Green CC during the growing season is presented in Figure 3.2. There is a good fit between measured and simulated values for the calibration data set for Bako.

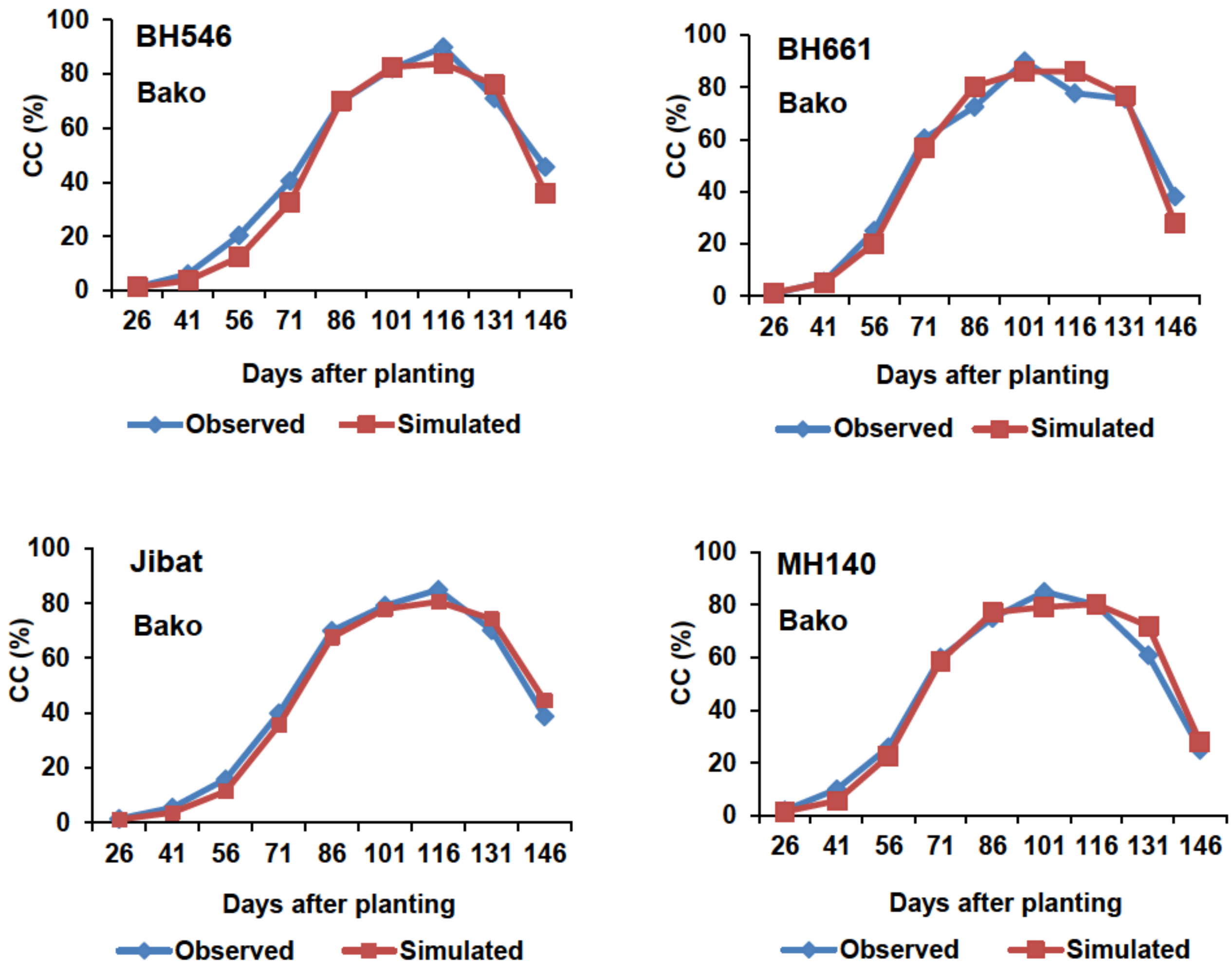

Figure 3.2: Performance of the AquaCrop model in simulating the green canopy cover (CC) of the four maize varieties grown at Bako for the 2017/2018 cropping season

The goodness of fit is supported by the statistical parameters given in Table 3.6. It can be observed that AquaCrop was able to closely simulate the canopy development across varieties at

Bako. The RMSE, *d* and R^2 value of the simulated and measured CC in Bako site were 3.6 – 8.8 %, 0.98 – 0.99 and 0.96 – 0.99 respectively for all varieties (Table 3.6).

Table 3.6: Performance of the AquaCrop model in simulating the green canopy cover (CC) of four maize varieties grown at Bako for the 2017/2018 cropping season

Cultivar	RMSE (%)	*d*	R^2
BH546	7.7	0.99	0.98
BH661	5.7	0.99	0.99
Jibat	3.6	0.99	0.99
MH140	8.8	0.98	0.96

Table 3.7 shows that the AquaCrop model successfully predicts maize yield at Bako.

Table 3.7: Performance of the AquaCrop model in simulating the grain yield (t ha^{-1}) of four maize varieties grown at Bako for the 2017/2018 cropping season

Cultivar	Observed (t ha^{-1})	Simulated (t ha^{-1})	Error (%)
BH546	5.923	5.939	0.3
BH661	5.399	5.380	-0.4

Jibat	5.293	5.233	-1.1
MH140	6.263	6.340	1.2
RMSE (t ha^{-1})	0.05		
NRMSE (%)	0.88		
d	0.99		
R^2	1.00		

3.4.1.3 DSSAT CERES-maize

The seven genetic coefficients for cultivars BH546, BH661, Jibat and MH140, which are calculated in this study, are presented in Table 3.3. The calibration result revealed that the model predicted maize flowering, maturity and yield well as the R^2 between simulated and observed values was found to be 0.87, 0.80 and 0.99 and the *d* value was 0.92, 0.93 and 0.99 respectively (Table 3.8). This implies that the model was successfully calibrated for all four maize cultivars. There was generally good agreement between observed and simulated flowering date and physiological maturity as the difference was < 3 days for all varieties. The differences in simulating yield for all four varieties were ≤ 1 t ha^{-1} (Table 3.8).

Table 3.8: Calibration results for DSSAT CERES-maize model for all four maize varieties using experimental data for the 2017/2018 maize cropping season

Cultivar	Flowering date (DAP)			Physiological maturity (DAP)			Maize yield (t ha^{-1})		
	Observed	Simulated	Error (%)	Observed	Simulated	Error (%)	Observed	Simulated	Error (%)
BH546	83	82	-1.2	154	157	1.9	5.923	5.956	0.6
BH661	87	84	-3.4	158	158	0.0	5.399	5.402	0.1
Jibat	78	77	-1.3	151	152	0.7	5.293	5.299	0.1
MH140	77	79	2.6	151	151	0.0	6.263	6.190	-1.2
RMSE	1.94			1.66			0.04		
NRMSE (%)	2.40			1.10			0.70		
d	0.92			0.93			0.99		
R^2	0.87			0.80			0.99		

The negative sign represents an underestimation; DAP: days after planting

3.4.2 *Model evaluation*

3.4.2.1 APSIM-maize

Compared to the calibration, the model slightly overestimated maturity date during evaluation. The RMSE for maturity dates ranged from 1 to 5 days, with the largest RMSE for cultivar BH661 at Ambo (Table 3.9). The simulation of flowering date was well predicted with an average RMSE value of < 3 days for the four varieties at the model evaluation sites (Table 3.9).

Table 3.9: Performance of the APSIM-maize model in simulating the flowering and physiological maturity dates (DAP) of four maize varieties grown at Ambo and Melkassa for the 2017/2018 cropping season

Site	**Cultivar**	**Flowering date (DAP)**		**Physiological maturity (DAP)**	
		Observed	Simulated	Observed	Simulated
Ambo (high altitude)	BH546	112	108	190	194
	BH661	107	108	184	193
	Jibat	97	99	183	186
	MH140	99	97	183	186
	RMSE (day)	2.50		5.36	
	d	0.95		0.53	
	R^2	0.85		0.56	
Melkassa	BH546	74	75	141	140

(low altitude)					
	BH661	78	78	138	141
	Jibat	72	70	139	139
	MH140	73	69	135	136
	RMSE (day)	2.29		1.66	
	d	0.85		0.81	
	R^2	0.80		0.55	

DAP: days after planting

The simulated and measured yields for all four varieties at the two evaluation sites are presented (Figure 3.3). The model simulated yield closely for Melkassa with a RMSE value of 0.69 t ha^{-1} and *d* value of 0.75. However, the model underestimated yield for all four varieties at Ambo with a RMSE value of 1.14 t ha^{-1} and *d* value of 0.50. Overall, the comparisons indicate that the model simulates yield reasonably well for these sites.

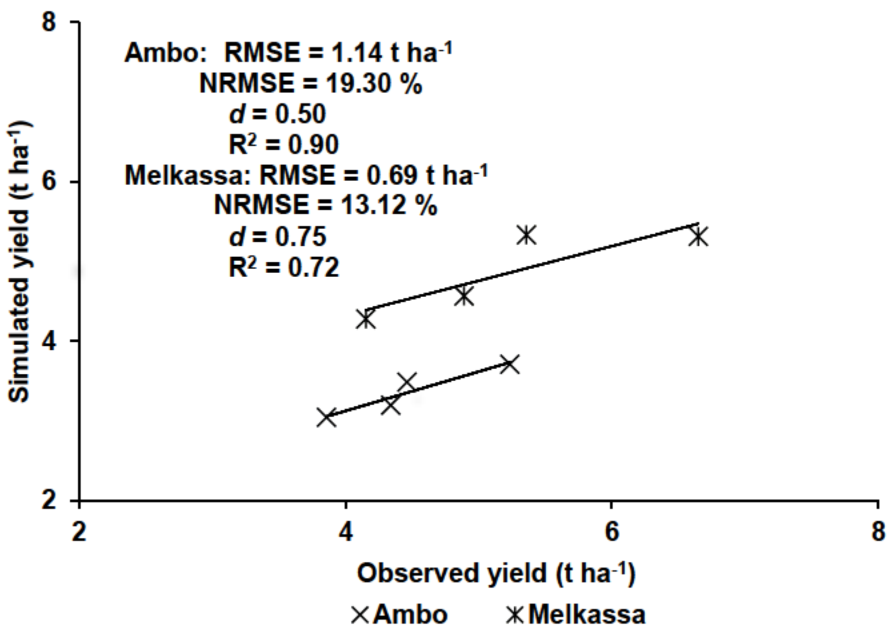

Figure 3.3: Performance of the APSIM-maize model in simulating the grain yield of four maize varieties grown at Ambo and Melkassa for the 2017/2018 cropping season

3.4.2.2 AquaCrop

The measured and simulated canopy cover for maize grown at Ambo and Melkassa for the 2017/2018 growing season is presented (Figure 3.4). It can be observed that AquaCrop was able to accurately simulate the canopy development over the season.

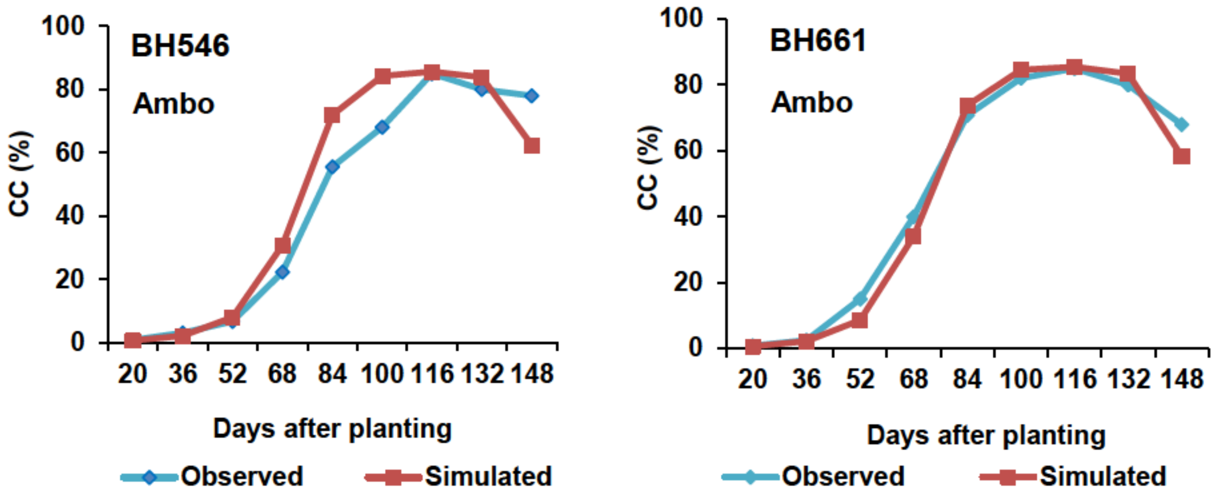

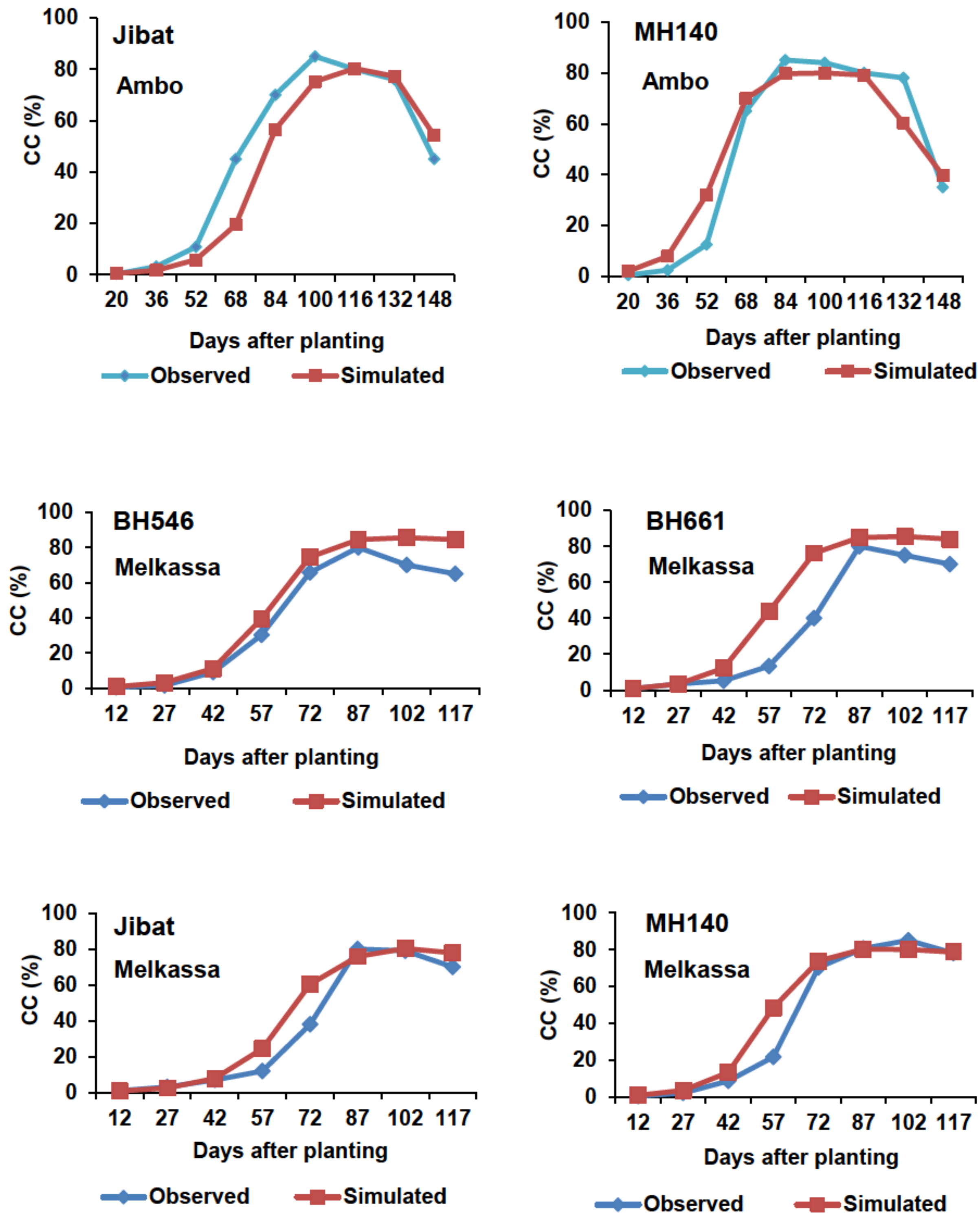
Jibat
Ambo
CC (%)
Days after planting
Observed
Simulated
MH140
Ambo
CC (%)
Days after planting
Observed
Simulated
BH546
Melkassa
CC (%)
Days after planting
Observed
Simulated
BH661
Melkassa
CC (%)
Days after planting
Observed
Simulated
Jibat
Melkassa
CC (%)
Days after planting
Observed
Simulated
MH140
Melkassa
CC (%)
Days after planting
Observed
Simulated

Figure 3.4: Performance of the AquaCrop model in simulating the green canopy cover (CC) of the four maize varieties grown at Ambo and Melkassa for the 2017/2018 cropping season

The RMSE, *d* and R^2 values of CC in the evaluation data sets ranged from 4.7 - 10.8 %, 0.97 – 0.99 and 0.96 - 0.99 respectively. The larger RMSE was found for Ambo for the Jibat variety. The smaller values of RMSE and the high values of *d* indicate an overall good agreement between the simulated and observed canopy cover (Table 3.10).

Table 3.10: Performance statistical indices of the Aquacrop model in simulating the green canopy cover (CC) of four maize varieties grown at Ambo and Melkassa for the 2017/2018 cropping season

Cultivar	Ambo (high altitude)			Melkassa (low altitude)		
	RMSE (%)	*d*	R^2	RMSE (%)	*d*	R^2
BH546	9.8	0.98	0.96	10.0	0.98	0.99
BH661	4.7	0.99	0.99	9.4	0.98	0.99
Jibat	10.8	0.97	0.96	7.0	0.99	0.98
MH140	10.0	0.98	0.97	9.8	0.98	0.97

The comparison between measured and simulated values for Ambo and Melkassa indicates that AquaCrop did simulate the yield well. This is also indicated by the high values of R^2 and *d* and low values of RMSE for all four varieties at all four sites (Figure 3.5).

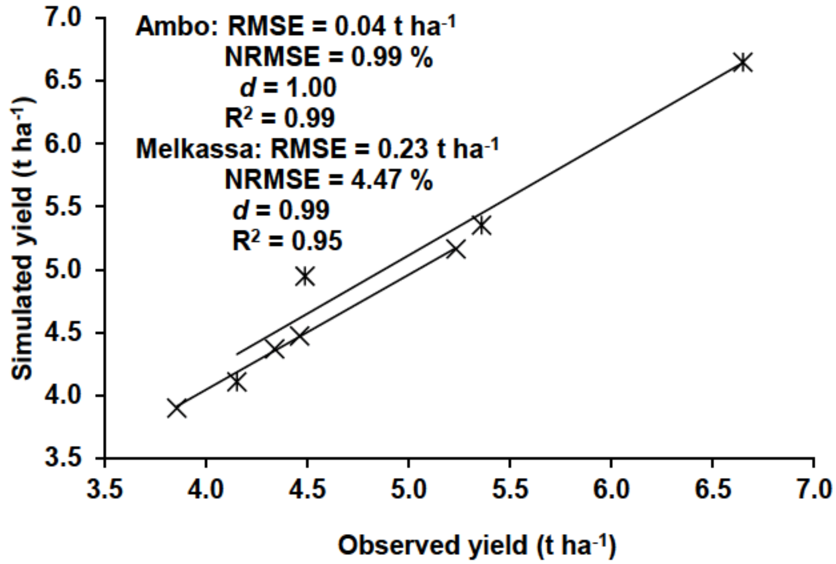

[redacted]

Figure 3.5: Performance of the AquaCrop model in simulating the grain yield of four maize varieties grown at Ambo and Melkassa for the 2017/2018 cropping season

<u>3.4.2.3 DSSAT CERES-maize</u>

For the independent evaluation datasets, there was also good agreement between simulated and observed flowering date with RMSE range of 2-4 days across all varieties (Table 3.11). The RMSE for maturity dates were 5 days for Melkassa and surprisingly large for Ambo (Table 3.11). It should be noted however, that Ambo has a highland agro-ecology and crops grown in this area have a longer maturity period.

Table 3.11: Performance of the DSSAT CERES-maize model in simulating the flowering and physiological maturity dates (DAP) of four maize varieties grown at Ambo and Melkassa for the 2017/2018 cropping season

Site	**Cultivar**	**Flowering date (DAP)**		**Physiological maturity (DAP)**	
		Observed	Simulated	Observed	Simulated
Ambo					
(high altitude)	BH546	112	105	190	208
	BH661	107	107	184	208
	Jibat	97	100	183	202
	MH140	99	102	183	200
	RMSE (day)	4.09		19.68	
	d	0.77		0.07	
	R^2	0.70		0.45	
Melkassa					
(low altitude)	BH546	74	74	141	146
	BH661	78	76	138	147
	Jibat	72	70	139	141
	MH140	73	71	135	137
	RMSE	1.73		5.33	

(day)		
d	0.87	0.50
R^2	0.87	0.53

DAP: days after planting

The DSSAT model performs well in estimating maize yield while the RMSE was found to be 0.78 t ha^{-1} and 0.58 t ha^{-1} with *d* values 0.79 and 0.84 for Ambo and Melkassa respectively (Figure 3.6). This comparison shows that the model has the potential to simulate maize yield for an independent dataset from the sites.

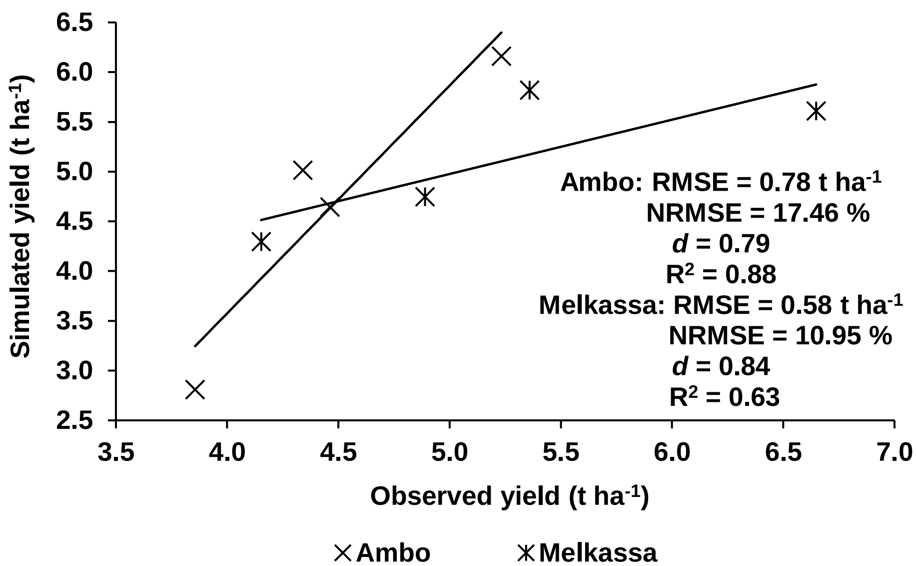

Figure 3.6: Performance of the DSSAT CERES-maize model in simulating the grain yield of four maize varieties grown at Ambo and Melkassa for the 2017/2018 cropping season

3.4.2.4 The multimodel ensemble approach

The performance of the multimodel ensemble for simulating maize yield in the evaluation phases is shown in Figure 3.7. The ensemble of the models led to improved prediction of maize yield in the evaluation phase with RMSE minimized and increased accuracy of *d* and R^2 values. As presented in Figure 3.7, the ensemble of the three models improved maize yield prediction at Ambo site with RMSE (0.35 t ha^{-1}), *d* (0.91) and R^2 (0.95) and at Melkassa site with RMSE (0.41 t ha^{-1}), *d* (0.93) and R^2 (0.90). The models' ensemble results were quite close to the grain yield simulated using the AquaCrop model (Figure 3.5). In general, the result shows that predicting maize yield with model ensemble reduces the uncertainty of yield prediction compared with any of the individual models.

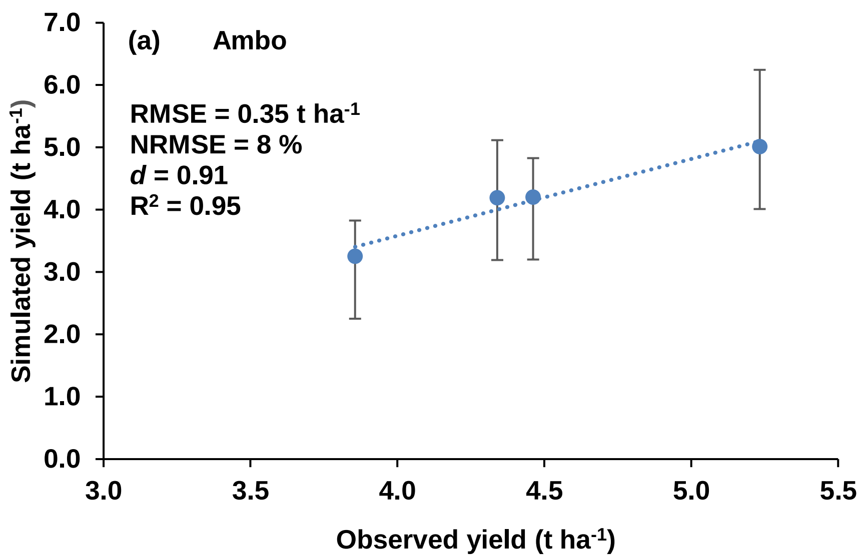

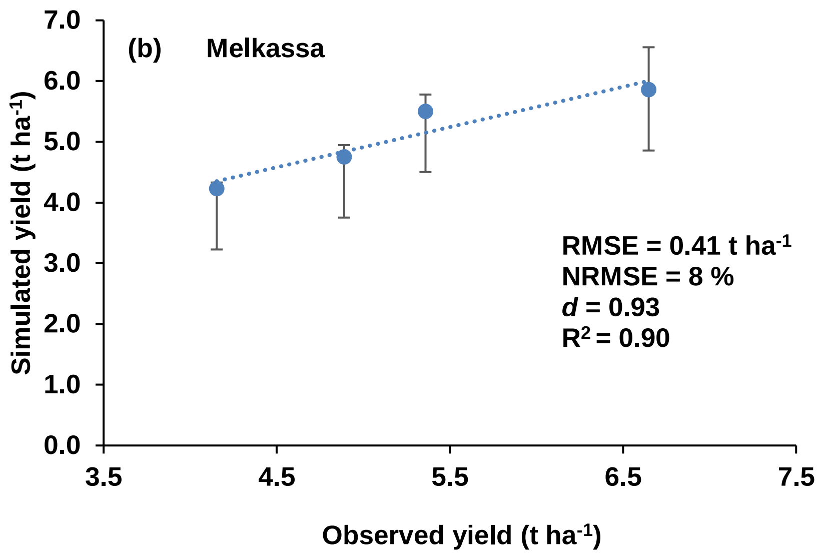

Figure 3.7: Performance of the ensemble of APSIM-maize, AquaCrop and DSSAT CERES-maize models to estimate maize yield (t ha^{-1}) during the evaluation phase at (a) Ambo and (b) Melkassa sites for the 2017/2018 cropping season

3.5 Discussion

In this study, field experiments were conducted for three different agro-ecology (highland, midland and lowland) sites in Ethiopia. Predominantly grown maize varieties were chosen and planted at each site with different planting dates. Detailed data were collected on growth and development of maize varieties to calibrate and evaluate the APSIM-maize, AquaCrop and DSSAT CERES-maize models. Calibration results show an accurate correspondence between measured values and those simulated by the models (Tables 3.4, 3.6, 3.7 and 3.8).

The results for the APSIM-maize model show that the model was able to capture a large part of the variation of the phenology of the individual varieties across the three sites of the study. Simulation of flowering dates was in agreement with the observed values and simulations of maturity dates were reasonable for all sites when compared to the DSSAT CERES-maize model. This indicated that the APSIM-maize model performed well for the three agro-ecologies in Ethiopia (Seyoum et al. 2018). Further, the evaluation indices for flowering and maturity dates confirmed the versatility of APSIM-maize to simulate phenology of maize in different environments.

On the other hand, the DSSAT CERES-maize model simulated flowering date close to the observed values in all agro-ecologies. However, the model did not accurately simulate maturity date at higher altitude areas like Ambo (late maturing varieties). The DSSAT CERES-maize model calculates maturity date based on the photoperiod (thermal time from seedling emergence to the end of the juvenile) and therefore, the model is sensitive to photoperiod estimation (Rezzoug et al. 2008). This emphasizes the need to quantify adjustments on coefficients of photoperiod sensitivity for such long-maturing varieties. This result reinforces the suggestion by Akinseye et al. (2017) that further improvement of CERES models in DSSAT is required to capture the correct photoperiod for the late maturing varieties. On the other hand, the model simulates maturity date reasonably well for Melkassa (low altitude). Overall, both the APSIM-maize and DSSAT CERES-maize models showed good performance in simulating the phenological stage of maize (Araya et al. 2015; Hammad et al. 2018) because of the use of thermal time and photoperiod sensitivity coefficients for calculating crop development rates (Specht et al. 2001).

The AquaCrop model successfully simulated canopy cover of the maize varieties studied. The crop parameters were adjusted to estimate canopy cover under different planting dates. The adjustments were made to obtain improved agreement between simulated and observed values. The results showed that the model calibration datasets (Bako) were consistent with the model evaluation datasets (Ambo and Melkassa). Good relationships were obtained between the simulated and observed canopy cover values. This indicated that the model can be used to simulate canopy cover of maize for different planting dates and environments (Greaves and Wang 2016).

The simulated grain yield agreed well with the observed data for the four maize varieties at Ambo DSSAT (d = 0.79), AquaCrop (d = 0.99) and Melkassa DSSAT (d = 0.84), APSIM (d = 0.75) and AquaCrop (d = 0.99). However, the APSIM-maize model underestimated maize yield at Ambo. The model evaluation indices RMSE, d-index and R^2 (Figures 5 and 6) confirmed the robustness of DSSAT CERES and AquaCrop models in simulating yield at higher altitudes compared to the APSIM model. This result is consistent with Babel et al. (2019). Underestimation of grain yield of maize using the APSIM-maize model at Ambo site might be caused by the fact that APSIM underestimated N uptake for maize under extended growing conditions. Another reason could be the underestimated radiation use efficiency associated with those default parameter values used in the APSIM-maize model (Archontoulis et al. 2014; Yang et al. 2018).

Unlike APSIM-maize and DSSAT CERES-maize, the FAO AquaCrop model evaluation indices for canopy cover and grain yield are satisfactory for all varieties in the three agro-ecologies with a low RMSE value, high *d* and R^2 values (Tables 3.6, 3.7 and 3.10; Figure 3.5). This indicated that AquaCrop can be used to simulate the yield of maize with improved accuracy in a tropical environment (Stricevic et al. 2011) than the other models. Some studies that focused on comparison of the performance of different crop models in predicting crop phenology (Porter et al. 1993) and grain yield (Cerrato and Blackmer 1990) revealed that some models performed better than others. However, since crop models vary in their structure of processing simulation (Asseng et al. 2013), their ensemble results are improved compared to a single model (Martre et al. 2015). In addition, different crop models have different descriptions for the simulation of crop growth under different soil, environment and management conditions. An individual model may have adequate capability to simulate a crop characteristic, nonetheless it is almost not possible to address the complexity of entire crop production systems (Huang et al. 2017). Hence, multimodel methods take advantage of the complementary strengths of individual models to generate more reliable ensemble results and minimize random errors.

Therefore, this study also considered comparing the ensemble simulated yield of the three models with the individual model simulation yield outputs. The results indicated that the performance of the models improved significantly when the multimodel approach was considered. The RMSE values were reduced and the simulation accuracy (*d* index) and precision (R^2) increased (Figure 3.7). This implies the need to use a multimodel ensemble approach to obtain reliable simulated maize yields under tropical environments which reduces the uncertainties associated with individual models while enhancing their synergy. In addition, calibration is also the most important application for quantifying model uncertainty by estimating model inputs to give the model output. So, in this study all the crop models are calibrated and evaluated before application. Hence, the calibrated models together with their ensemble result in reduction of uncertainty.

3.6 Conclusions

The APSIM-maize, DSSAT CERES-maize and AquaCrop models could reasonably simulate maize phenology, canopy cover (AquaCrop) and yield for different maturity maize varieties for different planting dates for three agro-ecologies under rainfed conditions in Ethiopia. These models showed their suitability for simulating the phenology and yield of maize in the tropical sites studied. However, under- or-over estimations were observed for the simulated parameters by the individual models studied showing the need for further work to improve the robustness of the models in tropical environments. A multimodel approach improved the simulation of grain yield by reducing model uncertainty when it was compared with the performance of the individual models studied. This approach could, therefore, provide more reliable predictions for maize varieties grown in diverse environments in the tropics. Under data scarce conditions, simpler models such as AquaCrop can be used to simulate maize yield with reasonable accuracy.

3.7 References

Abraha MG, Savage MJ. 2006. Potential impacts of climate change on the grain yield of maize for the midlands of KwaZulu-Natal, South Africa. *Agriculture, Ecosystems and Environment* 115: 150-160.

Ahmed M, Akram MN, Asim M, Aslam M, Hassan FU, Higgins S, Stöckle CO, Hoogenboom G. 2016. Calibration and validation of APSIM-Wheat and CERES-Wheat for spring wheat under rainfed conditions: Models evaluation and application. *Computers and Electronics in Agriculture* 123: 384-401.

Akinseye FM, Adam M, Agele SO, Hoffmann MP, Traore PCS, Whitbread AM. 2017. Assessing crop model improvements through comparison of sorghum (sorghum bicolor L. moench) simulation models: a case study of West African varieties. *Field Crops Research* 201: 19-31.

Akumaga U, Tarhule A, Yusuf AA. 2017. Validation and testing of the FAO AquaCrop model under different levels of nitrogen fertilizer on rainfed maize in Nigeria, West Africa. *Agricultural and Forest Meteorology* 232: 225-234.

Allen RG, Pereira LS, Raes D, Smith M. 1998. Crop evapotranspiration-Guidelines for computing crop water requirements-FAO Irrigation and drainage paper 56. *FAO, Rome* 300: 5109.

Allen RG, Pruitt WO, Wright JL, Howell TA, Ventura F, Snyder R, Itenfisu D, Steduto P, Berengena J, Yrisarry JB, Smith M. 2006. A recommendation on standardized surface resistance for hourly calculation of reference ETo by the FAO56 Penman-Monteith method. *Agricultural Water Management* 81: 1-22.

Araya A, Hoogenboom G, Luedeling E, Hadgu KM, Kisekka I, Martorano LG. 2015. Assessment of maize growth and yield using crop models under present and future climate in southwestern Ethiopia. *Agricultural and Forest Meteorology* 214: 252-265.

Araya A, Keesstra SD, Stroosnijder L. 2010. Simulating yield response to water of Teff (Eragrostis tef) with FAO's AquaCrop model. *Field Crops Research* 116: 196-204.

Archontoulis SV, Miguez FE, Moore KJ. 2014. Evaluating APSIM maize, soil water, soil nitrogen, manure, and soil temperature modules in the Midwestern United States. *Agronomy Journal* 106: 1025-1040.

Arora VK, Singh H, Singh B. 2007. Analyzing wheat productivity responses to climatic, irrigation and fertilizer-nitrogen regimes in a semi-arid sub-tropical environment using the CERES-Wheat model. *Agricultural Water Management* 94: 22-30.

Asseng S, Ewert F, Martre P, Rötter RP, Lobell DB, Cammarano D, Kimball BA, Ottman MJ, Wall GW, White JW, Reynolds MP. 2015. Rising temperatures reduce global wheat production. *Nature Climate Change* 5: 143-147.

Asseng S, Ewert F, Rosenzweig C, Jones JW, Hatfield JL, Ruane AC, Boote KJ, Thorburn PJ, Rötter RP, Cammarano D, Brisson N. 2013. Uncertainty in simulating wheat yields under climate change. *Nature Climate Change* 3: 827-832.

Babel MS, Deb P, Soni P. 2019. Performance evaluation of AquaCrop and DSSAT-CERES for maize under different irrigation and manure application rates in the Himalayan Region of India. *Agricultural Research* 8: 207-217.

Bacon SA, Mau R, Neto FM, Williams RL, Turner NC. 2016. Effect of climate warming on maize production in Timor-Leste: interaction with nitrogen supply. *Crop and Pasture Science* 67: 156-166.

Battisti, R., Sentelhas, P.C. and Boote, K.J., 2017. Inter-comparison of performance of soybean crop simulation models and their ensemble in southern Brazil. *Field Crops Research*, *200*, pp.28-37.

Bellucci A, Haarsma R, Gualdi S, Athanasiadis PJ, Caian M, Cassou C, Fernandez E, Germe A, Jungclaus J, Kröger J, and Matei D. 2015. An assessment of a multimodel ensemble of decadal climate predictions. *Climate Dynamics* 44: 2787-2806.

Boote KJ. 1999. Concepts for calibrating crop growth model. In: Hoogenboom G, Wilkens PW, and Tsuji GY (eds), *DSSAT V3, vol 4*. University of Hawaii: Honolulu, Hawaii Publisher. pp 179-220.

Brilli L, Bechini L, Bindi M, Carozzi M, Cavalli D, Conant R, Dorich CD, Doro L, Ehrhardt F, Farina R, Ferrise R. 2017. Review and analysis of strengths and weaknesses of agro-ecosystem models for simulating C and N fluxes. *Science of the Total Environment* 598: 445-470.

Cabrera VE, Jagtap SS, Hildebrand PE. 2007. Strategies to limit (minimize) nitrogen leaching on dairy farms driven by seasonal climate forecasts. *Agriculture, Ecosystems and Environment* 122: 479-489.

Cairns JE, Audebert A, Townend J, Price AH, Mullins CE. 2004. Effect of soil mechanical impedance on root growth of two rice varieties under field drought stress. *Plant and Soil* 267: 309-318.

Cerrato ME, Blackmer AM. 1990. Comparison of models for describing; corn yield response to nitrogen fertilizer. *Agronomy Journal* 82: 138-143.

Corbeels M, Berre D, Rusinamhodzi L, Lopez-Ridaura S. 2018. Can we use crop modelling for identifying climate change adaptation options? *Agricultural and Forest Meteorology* 256: 46-52.

Deb P, Shrestha S, Babel, MS. 2015. Forecasting climate change impacts and evaluation of adaptation options for maize cropping in the hilly terrain of Himalayas: Sikkim, India. *Theoretical and Applied Climatology* 121: 649-667.

Ewert F, Rötter RP, Bindi M, Webber H, Trnka M, Kersebaum KC, Olesen JE, van Ittersum MK, Janssen S, Rivington M, Semenov MA. 2015. Crop modelling for integrated assessment of risk to food production from climate change. *Environmental Modelling and Software* 72: 287-303.

Greaves GE, Wang YM. 2016. Assessment of FAO AquaCrop model for simulating maize growth and productivity under deficit irrigation in a tropical environment. *Water* 8: 557.

Hammad HM, Abbas F, Ahmad A, Farhad W, Anothai J, Hoogenboom G. 2018. Predicting water and nitrogen requirements for maize under semi-arid conditions using the CSM-CERES-Maize model. *European Journal of Agronomy* 100: 56-66.

He J, Jones JW, Graham WD, Dukes MD. 2010. Influence of likelihood function choice for estimating crop model parameters using the generalized likelihood uncertainty estimation method. *Agricultural Systems* 103: 256-264.

Holzworth DP, Huth NI, deVoil PG, Zurcher EJ, Herrmann NI, McLean G, Chenu K, van Oosterom EJ, Snow V, Murphy C, Moore AD. 2014. APSIM–evolution towards a new generation of agricultural systems simulation. *Environmental Modelling and Software* 62: 327-350.

Hoogenboom G, Jones JW, Traore PC, Boote KJ. 2012. Experiments and data for model evaluation and application. In *Improving soil fertility recommendations in Africa using the Decision Support System for Agrotechnology Transfer (DSSAT).* Springer Dordrecht: pp. 9-18.

Hoogenboom G, Wilkens PW, Tsuji GY. 1999. DSSAT version 3. *University of Hawaii*: Honolulu, Hawaii Publisher.

Hsiao TC, Heng L, Steduto P, Rajas-Lara B, Raes D, Fereres E. 2009. AquaCrop-The FAO crop model to simulate yield response to water: III. Parameterization and testing for maize. *Agronomy Journal* 101: 448-459.

Huang X, Huang G, Yu C, Ni S, Yu L. 2017. A multiple crop model ensemble for improving broad-scale yield prediction using Bayesian model averaging. *Field Crops Research* 211: 114-124.

Huth NI, Snow VO, Keating BA. 2001. Integrating a forest modelling capability into an agricultural production system modelling environment-current applications and future possibilities. Proceedings of the International Congress on Modelling and Simulation. *Aust. National University.* December. pp. 1895-1900.

IBSNAT 1988. Experimental design and data collection procedure for IBSNAT. The minimum data set for systems analysis and crop simulation IBSNAT. Technical report 1 (3rd edn). University of Hawaii: Honolulu Publisher.

Iqbal MA, Eitzinger J, Formayer H, Hassan A, Heng LK. 2011. A simulation study for assessing yield optimization and potential for water reduction for summer-sown maize under different climate change scenarios. *The Journal of Agricultural Science* 149: 129-143.

Jalota SK,Vashisht BB. 2016. Adapting cropping systems to future climate change scenario in three agro-climatic zones of Punjab, India. *Journal of Agrometeorology* 18: 48.

Jin XL, Feng HK, Zhu XK, Li ZH, Song SN, Song XY, Yang GJ, Xu XG, Guo WS. 2014. Assessment of the AquaCrop model for use in simulation of irrigated winter wheat canopy cover, biomass, and grain yield in the North China Plain. *PloS One* 9: e86938.

Jones CA. 1986. CERES-Maize: a simulation model of maize growth and development. In Jones CA, Kiniry JR (eds), *CERES-Maize a simulation model of maize growth and development*. Texas A and M Univ Pr Publisher. p 194.

Jones JW, Antle JM, Basso B, Boote KJ, Conant RT, Foster I, Godfray HCJ, Herrero M, Howitt RE, Janssen S, Keating BA. 2017. Brief history of agricultural systems modeling. *Agricultural Systems* 155: 240-254.

Jones JW, Hoogenboom G, Porter CH, Boote KJ, Batchelor WD, Hunt LA, Wilkens PW, Singh U, Gijsman AJ, Ritchie JT. 2003. The DSSAT cropping system model. *European Journal of Agronomy* 18: 235-265.

Kafatos MC, Kim SH, Lim CH, Kim J, Lee WK. 2017. Responses of agroecosystems to climate change: Specifics of resilience in the mid-latitude region. *Sustainability* 9: 1361.

Kanda EK, Mabhaudhi T, Senzanje A. 2018. Coupling hydrological and crop models for improved agricultural water management–A review. *Bulgarian Journal of Agricultural Science* 24: 380-390.

Kar G, Verma HN, Singh R. 2006. Effects of winter crop and supplemental irrigation on crop yield, water use efficiency and profitability in rainfed rice-based cropping system of eastern India. *Agricultural Water Management* 79: 280-292.

Kassie BT, Asseng S, Rotter RP, Hengsdijk H, Ruane AC, Van Ittersum MK. 2015. Exploring climate change impacts and adaptation options for maize production in the Central Rift Valley of Ethiopia using different climate change scenarios and crop models. *Climatic Change* 129: 145-158.

Kassie BT, Van Ittersum MK, Hengsdijk H, Asseng S, Wolf J, Rötter RP. 2014. Climate-induced yield variability and yield gaps of maize (Zea mays L.) in the Central Rift Valley of Ethiopia. *Field Crops Research* 160: 41-53.

Keating BA, Carberry PS, Hammer GL, Probert ME, Robertson MJ, Holzworth D, Huth NI, Hargreaves JN, Meinke H, Hochman Z, McLean G. 2003. An overview of APSIM, a model designed for farming systems simulation. *European Journal of Agronomy* 18: 267-288.

Kundzewicz ZW, Krysanova V, Benestad RE, Hov Ø, Piniewski M, Otto IM. 2018. Uncertainty in climate change impacts on water resources. *Environmental Science and Policy* 79: 1-8.

Lana MA, Eulenstein F, Schlindwein S, Guevara E, Meira S, Wurbs A, Sieber S, Svoboda N, Bonatti M. 2016. Regionalization of climate scenarios impacts on maize production and the role of cultivar and planting date as an adaptation strategy. *Regional Environmental Change* 16: 1319-1331.

Lee SK, Dang TA. 2018. Application of AquaCrop model to predict sugarcane yield under the climate change impact: A case study of Son Hoa district, Phu Yen province in Vietnam. *Research on Crops* 19: 310-314.

Li T, Hasegawa T, Yin X, Zhu Y, Boote K, Adam M, Bregaglio S, Buis S, Confalonieri R, Fumoto T, Gaydon D. 2015. Uncertainties in predicting rice yield by current crop models under a wide range of climatic conditions. *Global Change Biology* 21: 1328-1341.

Liben FM, Wortmann CS, Yang H, Lindquist JL, Tadesse T, Wegary D. 2018. Crop model and weather data generation evaluation for conservation agriculture in Ethiopia. *Field Crops Research* 228: 122-134.

MacRobert JF, Savage MJ. 1998. The use of a crop simulation model for planning wheat irrigation in Zimbabwe. In: Tsuji GY, Hoogenboom G, Thornton PK (eds), *Understanding Options for Agricultural Production*. Dordrecht, the Netherlands: Kluwer Academic Publishers. pp 205-220.

Maddonni GA, Otegui ME, Cirilo AG. 2001. Plant population density, row spacing and hybrid effects on maize canopy architecture and light attenuation. *Field Crops Research* 71: 183-193.

Maiorano A, Martre P, Asseng S, Ewert F, Müller C, Rötter RP, Ruane AC, Semenov MA, Wallach D, Wang E, Alderman PD. 2017. Crop model improvement reduces the uncertainty of the response to temperature of multimodel ensembles. *Field Crops Research* 202: 5-20.

Martre P, Wallach D, Asseng S, Ewert F, Jones JW, Rötter RP, Boote KJ, Ruane AC, Thorburn PJ, Cammarano D, Hatfield JL. 2015. Multimodel ensembles of wheat growth: many models are better than one. *Global Change Biology* 21: 911-925.

Mbangiwa NC, Savage MJ, Mabhaudhi T. 2019. Modelling and measurement of water productivity and total evaporation in a dryland soybean crop. *Agricultural and Forest Meteorology* 266: 65-72.

Monteith JL. 1996. The quest for balance in crop modeling. *Agronomy Journal* 88: 695-697.

Ngugi LW, Rao KPC, Oyoo A, Kwena K. 2015. Opportunities for coping with climate change and variability through adoption of soil and water conservation technologies in semi-arid Eastern Kenya. In: Leal Filho W, Esilaba A, Rao K, Sridhar G (eds), *Adapting African Agriculture to Climate Change*: Springer, Cham. pp. 149-157.

Palosuo T, Kersebaum KC, Angulo C, Hlavinka P, Moriondo M, Olesen JE, Patil RH, Ruget F, Rumbaur C, Takáč J, Trnka M. 2011. Simulation of winter wheat yield and its variability in different climates of Europe: a comparison of eight crop growth models. *European Journal of Agronomy* 35: 103-114.

Parent B, Leclere M, Lacube S, Semenov MA, Welcker C, Martre P, Tardieu F. 2018. Maize yields over Europe may increase in spite of climate change, with an appropriate use of the genetic variability of flowering time. *Proceedings of the National Academy of Sciences* 115: 10642-10647.

Pirttioja N, Carter TR, Fronzek S, Bindi M, Hoffmann H, Palosuo T, Ruiz-Ramos M, Tao F, Trnka M, Acutis M, Asseng S. 2015. Temperature and precipitation effects on wheat yield across a European transect: a crop model ensemble analysis using impact response surfaces. *Climate Research* 65: 87-105.

Porter JR. 1993. AFRCWHEAT2: a model of the growth and development of wheat incorporating responses to water and nitrogen. *European Journal of Agronomy* 2: 69-82.

Radanielson AM, Gaydon DS, Li T, Angeles O, Roth CH. 2018. Modeling salinity effect on rice growth and grain yield with ORYZA v3 and APSIM-Oryza. *European Journal of Agronomy* 100: 44-55.

Raes D, Steduto P, Hsiao TC, Fereres E. 2009. AquaCrop-The FAO crop model to simulate yield response to water. *FAO Land and Water Division, FAO, Rome*.

Rezaei EE, Gaiser T, Siebert S, Ewert F. 2015. Adaptation of crop production to climate change by crop substitution. *Mitigation and Adaptation Strategies for Global Change* 20: 1155-1174.

Rezzoug W, Gabrielle B, Suleiman A, Benabdeli K. 2008. Application and evaluation of the DSSAT-wheat in the Tiaret region of Algeria. *African Journal of Agricultural Research* 3: 284-296.

Rinaldi M, Ubaldo R. 2007. Simulation at regional level of irrigated wheat and tomato in a Mediterranean environment. *WIT Transactions on Ecology and the Environment* 103: 569-581.

Ritchie JT. 1972. Model for predicting evaporation from a row crop with incomplete cover. *Water Resources Research* 8: 1204-1213.

Ritchie JT. 1998. Soil water balance and plant stress. In: Tsuji GY, Hoogenboom G, Thornton PK (eds), *Understanding Options for Agricultural Production*. Dordrecht, the Netherlands: Kluwer Academic Publishers. pp 41-54.

Savage MJ. 2018. A spreadsheet for daily Penman-Monteith reference evaporation from a minimum set of meteorological data. Soil-Plant-Atmosphere Research Unit, School of Agricultural, Earth and Environmental Sciences, University of KwaZulu-Natal, Pietermaritzburg, South Africa.

Seyoum S, Rachaputi R, Chauhan Y, Prasanna B, Fekybelu S. 2018. Application of the APSIM model to exploit G×E×M interactions for maize improvement in Ethiopia. *Field Crops Research* 217: 113-124.

Shrestha S, Deb P, Bui TTT. 2016. Adaptation strategies for rice cultivation under climate change in Central Vietnam. *Mitigation and Adaptation Strategies for Global Change* 21: 15-37.

Soler T, CM, Ntelhas PC, Hoogenboom G. 2007. Application of the CSM-CERES-Maize model for planting date evaluation and yield forecasting for maize grown off-season in a subtropical environment. *European Journal of Agronomy* 27: 165-177.

Specht JE, Chase K, Macrander M, Graef GL, Chung J, Markwell JP, Germann M, Orf JH, Lark KG. 2001. Soybean response to water. *Crop Science* 41: 493-509.

Steduto P, Hsiao TC, Raes D, Fereres E. 2009. AquaCrop—The FAO crop model to simulate yield response to water: I. Concepts and underlying principles. *Agronomy Journal* 101: 426-437.

Stricevic R, Cosic M, Djurovic N, Pejic B, Maksimovic L. 2011. Assessment of the FAO AquaCrop model in the simulation of rainfed and supplementally irrigated maize, sugar beet and sunflower. *Agricultural Water Management* 98: 1615-1621.

Tesfaye K, Kruseman G, Cairns JE, Zaman-Allah M, Wegary D, Zaidi PH, Boote KJ, Erenstein O. 2018. Potential benefits of drought and heat tolerance for adapting maize to climate change in tropical environments. *Climate Risk Management* 19: 106-119.

Tian Z, Ji Y, Sun L, Xu X, Fan D, Zhong H, Liang Z, Gunther F. 2018. Changes in production potentials of rapeseed in the Yangtze River Basin of China under climate change: A multimodel ensemble approach. *Journal of Geographical Sciences* 28: 1700-1714.

Todorovic M, Albrizio R, Zivotic L, Saab MTA, Stöckle C, Steduto P. 2009. Assessment of AquaCrop, CropSyst, and WOFOST models in the simulation of sunflower growth under different water regimes. *Agronomy Journal* 101: 509-521.

Ventrella D, Charfeddine M, Giglio L, Castellini M. 2012. Application of DSSAT models for an agronomic adaptation strategy under climate change in Southern of Italy: optimum sowing and transplanting time for winter durum wheat and tomato. *Italian Journal of Agronomy*: e16-e16.

Wang E, Robertson MJ, Hammer GL, Carberry PS, Holzworth D, Meinke H, Chapman SC, Hargreaves JNG, Huth NI, McLean G. 2002. Development of a generic crop model template in the cropping system model APSIM. *European Journal of Agronomy* 18: 121-140.

Willmott CJ. 1981. On the validation of models. *Physical Geography* 2: 184-194.

Xiao D, Li Liu D, Wang B, Feng P, Bai H, Tang J. 2020. Climate change impact on yields and water use of wheat and maize in the North China Plain under future climate change scenarios. *Agricultural Water Management* 238: 106238.

Xiong W, Holman I, Conway D, Lin E, Li Y. 2008. A crop model cross calibration for use in regional climate impacts studies. *Ecological Modelling* 213: 365-380.

Yang C, Fraga H, Van Ieperen W, Santos JA. 2017. Assessment of irrigated maize yield response to climate change scenarios in Portugal. *Agricultural Water Management* 184: 178-190.

Yang X, Zheng L, Yang Q, Wang Z, Cui S, Shen Y. 2018. Modelling the effects of conservation tillage on crop water productivity, soil water dynamics and evapotranspiration of a maize-winter wheat-soybean rotation system on the Loess Plateau of China using APSIM. *Agricultural Systems* 166: 111-123.

Zhang Y, Zhao Y, Chen S, Guo J, Wang E. 2015. Prediction of maize yield response to climate change with climate and crop model uncertainties. *Journal of Applied Meteorology and Climatology* 54: 785-794.

Appendix 1:

Supplementary material (SM)

Table SM3a: Main soil properties for the study areas used in model calibration and simulation

Site	Depth (m)	Silt %	Clay %	BD (kg m^{-3})	DUL (m^3 m^{-3})	LL (m^3 m^{-3})	Saturation soil water content (m^3 m^{-3})	pH
Ambo (high altitude)	0.0-0.13	12.00	22.70	1360	0.189	0.092	0.449	6.20
	0.13-0.45	12.00	26.70	1330	0.148	0.077	0.467	6.50
	0.45-0.78	6.00	30.70	1370	0.163	0.084	0.457	6.80
	0.78-1.10	8.00	32.70	1480	0.177	0.088	0.418	6.80
	1.10-1.53	8.00	20.70	1560	0.157	0.085	0.39	7.10
	1.53-1.87	6.00	28.70	1590	0.155	0.109	0.379	7.20
Bako (mid-altitude)	0.0-0.15	24.40	40.90	1130	0.371	0.244	0.446	5.60
	0.15-0.30	23.40	43.50	1160	0.385	0.259	0.445	5.70

	0.30-0.60	22.30	45.80	1210	0.399	0.272	0.463	5.90
	0.60-1.00	21.60	45.90	1270	0.399	0.273	0.462	6.00
	1.00-2.00	21.30	44.40	1320	0.389	0.264	0.455	6.20
Melkassa (low altitude)	0.0-0.15	45.20	20.10	1190	0.343	0.094	0.393	7.30
	0.15-0.30	47.10	19.40	1230	0.337	0.188	0.387	7.50
	0.30-0.60	49.30	19.20	1240	0.348	0.162	0.398	7.60
	0.60-1.00	51.30	18.30	1250	0.352	0.186	0.401	7.80
	1.00-2.00	51.10	18.50	1240	0.378	0.209	0.428	7.90

BD refers to soil bulk density (kg m^{-3}), drained upper limit (DUL) (m^3 m^{-3}), lower limit (LL) (m^3 m^{-3}), saturation soil water content (m^3 m^{-3}) and pH (1:5 water)

Table SM3b: Definition of the cultivar coefficients of APSIM-maize and DSSAT CERES-maize model that determine maize growth, development and yield

APSIM-maize		
Coefficient	Definition	Unit
est_days_endjuv_to_init	Days from end of juvenile stage to floral initiation	day
Potential kernel number per plant		

Grain growth rate		mg $grain^{-1}day^{-1}$
tt_end of juvenile stage to floral initiation	Thermal time - end of juvenile stage to floral initiation	^{o}C day
Photoperiod critical 1		h
Photoperiod critical 2		h
Photoperiod slope		^{o}C h^{-1}
tt_emergence to end of juvenile	Thermal time - emergence to end of juvenile	^{o}C day
tt_flag leaf to flowering	Thermal time - flag leaf to flowering	^{o}C day
tt_flowering to start of grain filling	Thermal time - flowering to start of grain filling	^{o}C day
tt_flowering to maturity	Thermal time - flowering to maturity	^{o}C day
tt_maturity to ripening	Thermal time - maturity to ripening	^{o}C day
Canopy height		mm
Stem mass		g $stem^{-1}$
DSSAT CERES-maize		
P1	Thermal time from seedling emergence to the end of the juvenile phase	^{o}C day
P2	Extent to which development is delayed for each hour increase in photoperiod above the longest photoperiod at which development proceeds at maximum rate	day

P5	Thermal time from silking to physiological maturity	^{o}C day
G2	Maximum possible number of kernels per plant	
G3	Kernel filling rate during the linear grain filling stage and under optimum conditions	mg day^{-1}
PHINT	Phylochron interval; the interval in thermal time between successive leaf tip appearances	^{o}C day

Table SM3c: Observed experimental data for phenology and grain yield of four maize varieties at the three sites for the 2017/2018 cropping season

Site	Cultivar	Emergence	Flowering	Maturity	Grain yield (t ha^{-1})
Ambo (high altitude)	BH546	26-Jun	04-Oct	21-Dec	5.23
	BH661	25-Jun	29-Sep	15-Dec	4.34
	Jibat	25-Jun	19-Sep	14-Dec	3.86
	MH140	26-Jun	21-Sep	14-Dec	4.46
Bako (mid-altitude)	BH546	26-Jun	10-Sep	20-Nov	5.29
	BH661	26-Jun	04-Sep	25-Nov	5.40
	Jibat	26-Jun	05-Sep	17-Nov	5.29
	MH140	26-Jun	04-Sep	17-Nov	6.26
Melkassa (low	BH546	08-Jul	10-Sep	16-Nov	6.65

altitude)					
	BH661	08-Jul	14-Sep	13-Nov	4.15
	Jibat	08-Jul	08-Sep	14-Nov	4.89
	MH140	08-Jul	09-Sep	10-Nov	5.36

Table SM3d: Conservative and non-conservative parameters used in AquaCrop model calibration for maize crop

Parameter description	Unit
Conservative	
Base temperature	^{o}C
Upper temperature	^{o}C
Canopy growth coefficient CGC	% day^{-1}
Canopy decline coefficient CDC	% day^{-1}
Normalized water productivity WP	g m^{-2}
Nonconservative	
Plant density	plants m^{-2}
Initial canopy cover percentage CC_o	%
Maximum canopy cover percentage CC_x	%
Time to maximum canopy cover	day
Time to flowering	day
Length of the flowering stage	day
Time to start senescence	day

Time to maturity	day
Maximum rooting depth	m
Minimum effective rooting depth	m
Reference harvest index	%

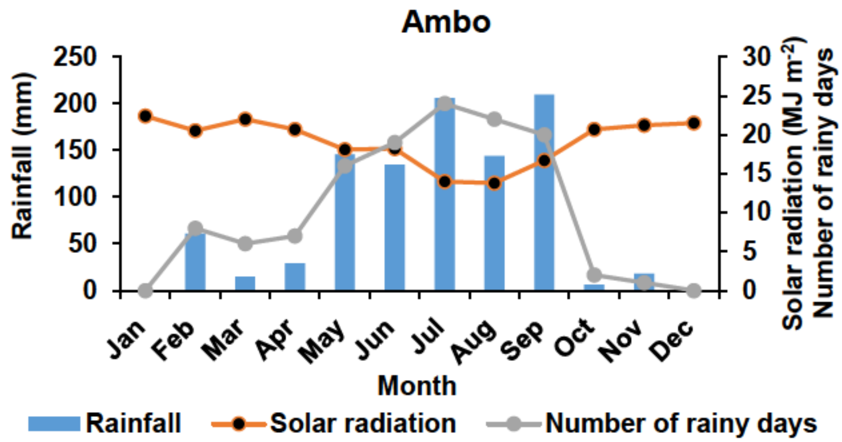
Ambo
Rainfall (mm)
Solar radiation (MJ m-2)
Number of rainy days
Jan Feb Mar Apr May Jun Jul Aug Sep Oct Nov Dec
Month
Rainfall
Solar radiation
Number of rainy days

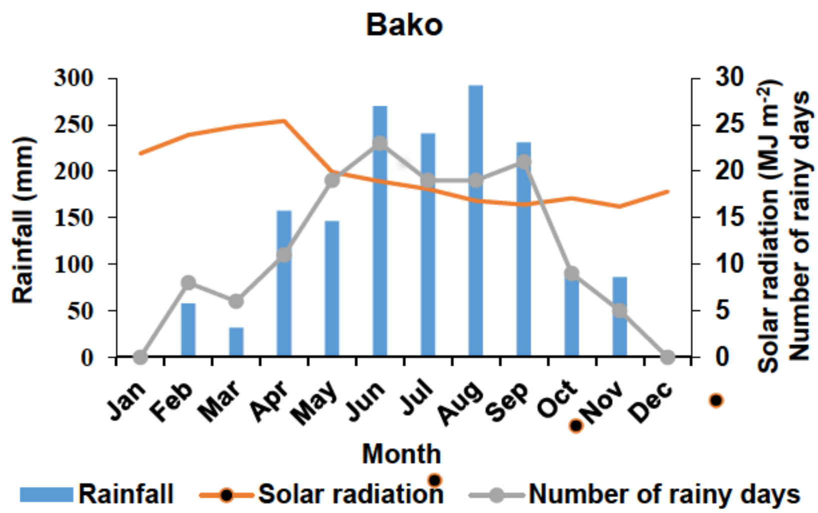
Bako
Rainfall (mm)
Solar radiation (MJ m-2)
Number of rainy days
Jan Feb Mar Apr May Jun Jul Aug Sep Oct Nov Dec
Month
Rainfall
Solar radiation
Number of rainy days

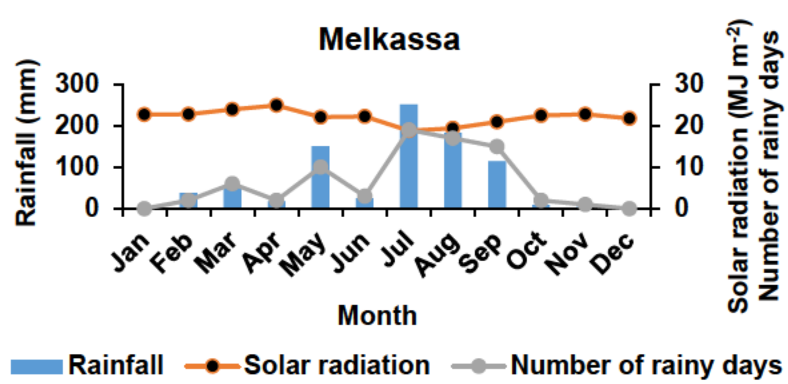
Melkassa
Rainfall (mm)
Solar radiation (MJ m-2)
Number of rainy days
Jan Feb Mar Apr May Jun Jul Aug Sep Oct Nov Dec
Month
Rainfall
Solar radiation
Number of rainy days

Figure SM3a: Monthly total rainfall, average solar radiation and number of rainy days for the crop growing season 2017/2018 for Ambo, Bako and Melkassa sites

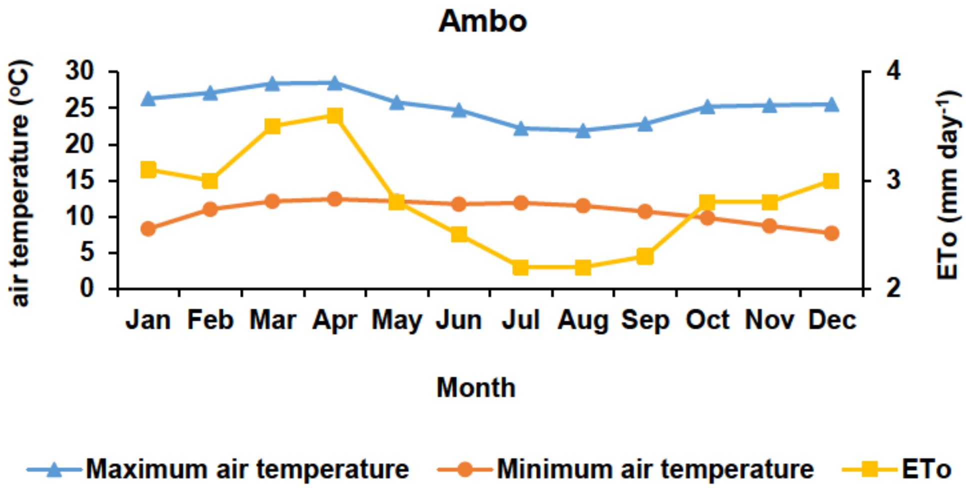

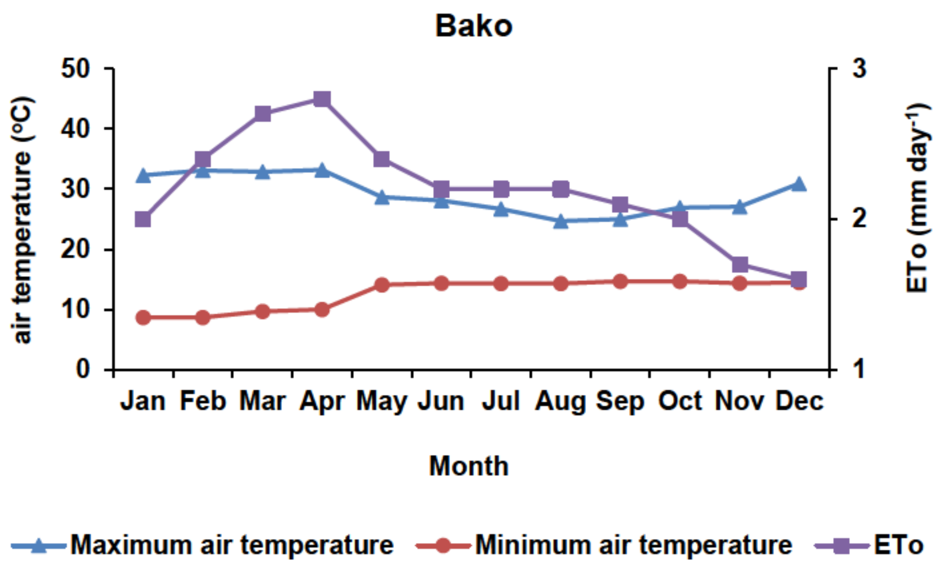

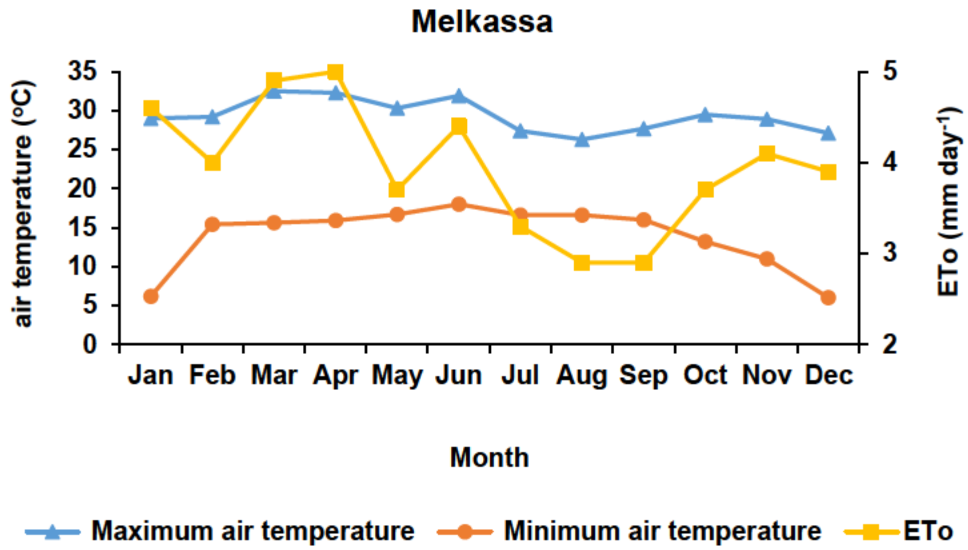

Figure SM3b: Monthly average maximum and minimum air temperature and ETo for the crop growing season 2017/2018 for Ambo, Bako and Melkassa sites

Lead to Chapter 4

Genetic coefficients of improved maize cultivars were produced through crop models calibration process and the calibrated individual model and their ensembles were evaluated in Chapter 3. In Chapter 4, climate change impact on maize yield using crop models are assessed. The daily downscaled output of General Circulation Models under 8.5 Representative Concentration Pathway scenario are used to assess the future climate change impacts. Possible adaptation measures are explored to offset the changed climate.

CHAPTER 4: THE ROLE OF CROP MANAGEMENT PRACTICES AND ADAPTATION OPTIONS TO MINIMIZE THE IMPACT OF CLIMATE CHANGE ON MAIZE (*ZEA MAYS* L.) PRODUCTION IN TROPICAL ENVIRONMENTS

Hirut Getachew Feleke [1*], M.J. Savage [1] and Kindie Tesfaye [2]

[1]Agrometeorology Discipline, Soil-Plant-Atmosphere Continuum Research Unit, School of Agricultural, Earth and Environmental Sciences, University of KwaZulu-Natal, Pietermaritzburg, South Africa

[2]International Maize and Wheat Improvement Centre (CIMMIT), Addis Ababa, Ethiopia

*Corresponding author, email: hirut_ge@yahoo.com

4.1 Abstract

Climate change impact assessment along with adaptation measures are key factors for reducing the impact of climate change on crop production. The impact of current and future climate change on maize production is investigated and evaluated the adaptation role of shifting planting dates, different level of nitrogen fertilizer rates and choice of maize cultivar as possible climate change adaptation strategies in the Ethiopian tropical environments. Future climate data were obtained from seven General Circulation Models (GCMs), namely: CanESM2, CNRM-CM5, CSIRO-MK3-6-0, EC-EARTH, HadGEM2-ES, IPSL-CM5A-MR and MIROC5 for the highest

(8.5) Representative Concentration Pathway (RCP). GCMs were bias-corrected at site level using a quantile-quantile mapping method. APSIM, AquaCrop and DSSAT models were used to simulate the baseline (1995-2017) and 2030s (2021-2050) maize yields. The result indicated that average monthly maximum air temperature in the 2030s could increase by 0.3-1.7 °C, 0.7-2.2 °C and 0.8-1.8 °C in Ambo, Bako and Melkassa, respectively. For the same sites, the projected increase in average monthly minimum air temperature was 0.6-1.7 °C, 0.8-2.3 °C and 0.6-2.7 °C in that order. While monthly total precipitation for the *Kiremt* season (June to September) projected to increase by up to 55 % (365 mm) for Ambo and 75 % (241 mm) for Bako respectively, whereas a significant decrease in monthly total precipitation is projected for Melkassa by 2030. Climate change would reduce maize yield by an average of 4 % and 16 % for Ambo and Melkassa respectively, while would increase by 2 % for Bako in 2030 if current maize cultivars were grown with the same crop management practice as the baseline under the future climate. At higher altitudes, early planting of maize cultivars between 15 May to 01 June would result in improved relative yields in the future climate. Fertilizer levels between 23-150 kg ha^{-1} would result in improved yields for all maize cultivars when combined with early planting for Ambo. For a mid-altitude, planting after 15 May has either no or negative effect on maize yield. Early planting combined with a nitrogen fertilizer level of 23-100 kg ha^{-1} provided higher relative yields under the future climate. Delayed planting has a negative influence on maize production for Bako under the future climate (2030). For lower altitudes, late planting would have lower relative yields compared to early planting. Higher fertilizer levels (100-150 kg ha^{-1}) would reduce yield reductions under the future climate, but this varied among maize cultivars studied. Generally, future climate is expected to have a negative impact on maize yield and changes in crop management practice can alleviate the impacts on yield.

Keywords: Adaptation options, Crop models, GCMs, Multimodel ensemble, Representative Concentration Pathway

4.2 Introduction

Climate change has become the major environmental and socio-economic threat to the world. Past climate change studies in Ethiopia have shown significant changes in air temperature (NMA, 2007; McSweeney et al., 2008) and precipitation patterns (Cheung et al., 2008; Williams et al., 2012) in the past decades. Climate change projection studies based on different emission scenarios indicate air temperature increases over the country (Yimer et al., 2009; Setegn et al., 2011) by the year 2050. Similarly, mean annual rainfall is expected to increase, with high uncertainty, in amount and intensity (NMA, 2007; Conway and Schipper, 2011). Climate change influences agriculture through affecting the crop physiological processes. The change in amount and distribution of precipitation and air temperature affect crop water balance by increasing evapotranspiration which in turn affects yields (Asseng et al., 2011).

Agriculture is a fundamental part of the economy in Ethiopia. With a population of more than 110 million (Alemu and Carlson, 2020), Ethiopia is the second highly populated country in Africa. Over 70 % of the population are engaged in subsistence farming (Degu, 2019). Agriculture accounts for almost one-third of the change in Gross Value Added per capita as compared to industrial sector, which contributed about 22.2 %. Agriculture in Ethiopia is the basis of the economy, contributing 35.8 % of the GDP (Degu, 2019). Despite its importance to the economy, agriculture in Ethiopia is highly affected by rainfall variability and recurrent drought, resulting in severe food insecurity (Alemu and Mengistu, 2019). Moreover, climate change seriously impacts agricultural productivity and the loss of human life and livestock (Mera, 2019). According to Viste et al. (2013), the frequency of drought and irregular precipitation occurrences has increased in recent decades and continue to increase with increased impacts under future climate change (Deressa and Hassan, 2009; Mideksa, 2010; Field et al., 2012). There is no doubt that Ethiopia's agriculture is already extremely vulnerable to climate change and consequential crop failure. It is thus very important to assess the impacts of future climate for proper adaptation mechanisms.

Maize (*Zea mays* L.) is one of the dominant cereal food crops second to tef (*Eragrostis tef*) in terms of production and area coverage. In the 2019/2020 production season, 2.3 million ha of land is under maize cultivation at the national level from which 9635735-ton ha^{-1} of yield was produced by more than 11.4 million smallholder farmers (CSA, 2020). About 88 % of maize production in the country is consumed as food, both as green and dry grain (Abate et al., 2015). However, the production of maize is seriously limited due to abiotic and biotic factors, such as drought, low soil fertility, insufficient improved varieties, pests and diseases (CSA, 2010; Shiferaw et al., 2011; Araya et al., 2015). In addition to abiotic and biotic factors, maize yield reduction in Ethiopia is exacerbated by climate change (Tesfaye et al., 2015). Recent climate projections indicate that in the near (2035) and mid future (2055), there will be an increase of air temperature in most parts of Ethiopia resulting in an average decrease of maize yield for the coming years (Tomas et al., 2019).

Adaptation is a key factor in agriculture to reduce the impacts of climate change (Yin et al., 2016; Belay et al., 2017; Tripathi and Mishra, 2017). Tomas et al. (2019) emphasized that alternative agronomic practices, such as fertilizer use, shifting planting dates, and change in cultivars as measures, are possible counters to the negative impacts of climate change with improvements to maize production in Ethiopia. Studies also revealed that adaptation options should be site-specific and need to be addressed for the various agroecological zone (Bryan et al., 2009; Tao and Zhang, 2010).

Process-based crop simulation models (hereafter referred as crop models) are commonly applied tools for multiple areas to assess the impact of climate variability and change on agricultural production (Challinor et al., 2010; Rosenzweig and Wilbanks, 2010; Rötter et al., 2011; White et al., 2011; Kassie et al., 2013; Deb et al., 2015). The coupling of crop models to climate models has been a common method for analysing the potential impact of climate change on crop production to evaluate adaptation options (Bao, 2017).

In Ethiopia, various climate change impact assessment studies have been conducted using crop models to simulate maize yield under different environments and field conditions (Kelbore, 2012; Araya et al., 2015; Kassie et al., 2015; Tesfaye et al., 2015, 2018; Tomas et al., 2019). The purpose of most of these studies was limited to climate change impacts, yield variability, and yield gap estimation of maize and did not consider the adaptation aspect. Only a few studies addressed both climate change impacts and adaptation options on maize productivity in Ethiopia, such as Kassie et al. (2015) and Tesfaye et al. (2018). Nevertheless, both studies used one or two crop model(s) to simulate maize yield which is still inadequate for a detailed analysis of crop model uncertainty. Araya et al. (2015) also recommended the multi-crop model approach and multi-GCM ensemble projections for more in depth analysis and reliable climate change sensitive assessments. In addition, there is insufficient research devoted to adaptation strategies developed based on climate change scenarios in Ethiopia (IPCC, 2014). Hence, there is a need to design climate change adaptation strategies using multiple crop and climate models under the future climate.

Therefore, the objectives of this study are to: (1) assess the impact of climate change on maize yield and to (2) identify possible adaptation mechanisms at three sites representing different agroecological zones in Ethiopia.

4.3 Materials and methods

4.3.1 The study sites

The sites used in this study are located in Central Ethiopia (Ambo), south-western Ethiopia (Bako) and Central Rift Valley of Ethiopia (Melkassa). They have different soil and climatic characteristics and hence maize cultivars that differ in their maturity period are grown across the study sites. The soils range from sandy clay loam to clay texture. The seasonal rainfall and reference evapotranspiration ranged from 587 to 1206 mm and 431 to 770 mm, respectively. The mean maximum and minimum air temperature ranges from 24.0 to 28.4 °C and 10.3 to 14.5 °C during the maize growing season in the study sites (Table 4.1). Maize field experiments were conducted under rainfed conditions for the sites. The detailed information is found in Feleke et al. (2021) (Chapter 3).

Table 4.1: Characteristics of the study sites in Ethiopia

	Ambo	Bako	Melkassa
Location			
Latitude (°)	8.57	9.12	8.42
Longitude (°)	38.07	37.04	39.32
Altitude (m)	2225	1650	1550
Soil characteristics			
Soil type	Eutric regoSol	Nitosol	Vitric andosols
Soil texture	sandy clay loam	clay	loam
Baseline climate (1995-2017)			
Seasonal total precipitation (mm)	718	1206	587
Seasonal ET_o (mm)*	543	431	770
Mean max. air temperature (°C)	24.0	24.0	28.4
Mean min. air temperature (°C)	10.3	14.5	13.9

* ET_o: grass reference evapotranspiration.

4.3.2 Data collection

4.3.2.1 Weather and soil data

Historical weather and soil data are the main input data sources used in the crop models, in addition to crop management practices such as planting date, plant density, row spacing and fertilization. For Ambo, Bako and Melkassa the daily rainfall, maximum and minimum air temperature and solar radiation data for the study sites were obtained from meteorological stations at the experimental sites and/or from the national meteorological agency where the study sites are located. Daily grass reference evapotranspiration (ET_o) were computed by the FAO Penman-Monteith method (Allen et al., 1998; Allen, 2006; Savage, 2018). For the Weather data quality control measures were undertaken and patching of missing values utilized using Allen et al. (1998) for all the study sites. The soil profile data were obtained from Liben et al. (2018), Seyoum et al. (2018), and the International Maize and Wheat Improvement Center (CIMMIT) in Ethiopia and field measurements.

4.3.2.2 Crop data

Four improved and most widely grown hybrid maize cultivars were used for this study. The hybrid maize cultivars were Jibat, BH661, BH546 and MH140. The choice of maize cultivars were based on farmers preferences. These cultivars were calibrated and evaluated for the DSSAT, APSIM and AquaCrop models (Feleke et al., 2021; Chapter 3).

4.3.3 Crop simulation models

Maize yield was simulated using three crop simulation models, namely Agricultural Production Systems Simulator (APSIM)-maize v 7.9 (Keating et al., 2003), FAO - AquaCrop v. 7.9 (Steduto et al., 2009) and Decision Support System for Agrotechnology Transfer (DSSAT) – CERES – maize v 4.7 (Hoogenboom et al., 2019) (hereafter, the crop models are referred to as APSIM, AquaCrop and DSSAT). These crop models have been used widely and provide a realistic simulation of maize yield across the world (Bassu et al., 2014; Muluneh et al., 2017; Zhao et al., 2017) under both current and future climate change conditions. The input data to run the models are daily total solar radiation, daily minimum and maximum air temperatures, and daily precipitation. Additional inputs necessary to run the crop models are soil type, cultivar type and crop management. These crop models were calibrated and validated for four maize cultivars (Jibat, BH661, BH546 and MH140) using data from field trials conducted in the 2017/18 cropping season in Ethiopia (Feleke et al., 2021).

4.3.4 Climate change projections

The daily climate data downscaled from seven Global Circulation Models (GCMs), namely, CanESM2, CNRM-CM5, CSIRO-MK3-6-0, EC-EARTH, HadGEM2-ES, IPSL-CM5A-MR and MIROC5 from the Coupled Model Intercomparison project phase 5 (CMIP5) were used to simulate maize yield in this study. The GCMs used in this study are listed in Table 4.2 together with the institutions which developed them, their country and references.

Table 4.2: Description of the global climate models (GCMs) used

GCM name	Institute	Country	References
CanESM2	CCCma: Canadian Centre for Climate Modelling and Analysis	Canada	CCCma (2017b)
CNRM-CM5	CERFACS: Centre Européen de Recherche et de Formation Avancée en Calcul Scientifique	France	Voldoire et al. (2013)
CSIRO-MK3-6-0	CSIRO: Commonwealth Scientific and Industrial Research Organization	Australia	Jeffrey et al. (2013)
EC-EARTH	ICHEC: Consortium of European research institutions and researchers	Europe	Hazeleger et al. (2010)
HadGEM2-ES	MOHC: Met Office Hadley Centre	United Kingdom	Collins et al. (2011)
IPSL-CM5A-MR	IPSL: Institut Pierre Simon Laplace	France	Dufresne et al. (2013)
MIROC5	AORI: Atmospheric and Ocean Research Institute	Japan	Watanabe et al. (2010)

The data were downscaled using the Regional Climate Model (RCM)- RCA4 (Samuelsson et al., 2011). The RCM-RCA4 simulation covers the Coordinated Regional Climate Downscaling Experiment (CORDEX)-Africa domain at a 44-km horizontal resolution in Africa for the 1951-

2100 periods which is divided into two: historical (1951-2005) and scenario (2006–2100) periods. The CORDEX initiative sets a standard grid, domain size experiment protocols, and data format allowing for direct comparison of the model outputs (Giorgi et al., 2009; Nikulin et al., 2012). The main reason for using CORDEX (44 km grid) for this study is that resources are more available with a minimum horizontal grid spacing of around 44 km was recommended (Giorgi et al., 2009). Within this framework, only models which were widely available and provide projections for the Representative Concentration Pathway (RCP) 8.5 were selected as this is deemed the highest level expected to assess future climate change impact and responses. There is no difference between RCP 4.5 and RCP 8.5 until the year 2050 (Arnell, 2004; Levy et al., 2004). The difference between the two becomes clear after 2050. Therefore, the study were used RCP 8.5 for all future climate analysis.

The data were bias-corrected using the quantile-quantile mapping procedure (Ngai et al., 2017). Atmospheric CO_2 concentrations specified for each period according to the Intergovernmental Panel on Climate Change Special Report on Emission Scenarios IPCC SRES (2014) were used: 380 $\mu L\ L^{-1}$ for the baseline (1995-2017) and 450 $\mu L\ L^{-1}$ for future (2021-2050) period. In this study, downscaled precipitation, maximum and minimum air temperature data from seven GCMs for the three study sites (Ambo, Bako and Melkassa) were evaluated. The baseline data at a daily scale (1995-2017) were used for evaluating CORDEX-Africa precipitation, maximum and minimum air temperature for future climate scenarios. The comparison between GCM's historical runs and observations was performed using average monthly values of precipitation, maximum and minimum air temperature for the reference period of 1995-2005. The performance of GCMs in simulating the observed precipitation, maximum and minimum air temperature data were evaluated statistically and presented graphically. The statistical measurements include root mean square error (RMSE) and correlation coefficient (R^2) calculated using the following equations:

$$R^2 = \frac{\sum Si \times Oi - \sum Si \times \sum Oi}{\sqrt{\sum Si^2 - (\sum Si)^2 \times \sqrt{\sum Oi^2 - (\sum Oi)^2}}} \tag{4.1}$$

$$RMSE = \sqrt{\frac{1}{n}\sum_{i=1}^{n}(Si - Oi)^2} \tag{4.2}$$

where *Si* and *Oi* represent the simulated and the observed values of the variables respectively.

4.3.5 Crop management practices for climate change adaptation

The study considered three agronomic management options: planting date shift, nitrogen fertilizer levels and maize cultivars with different maturity length. To assess the impact of climate change on maize yield the study considered the recommended planting date, nitrogen fertilizer level and cultivar for each site studied as a control treatment for the baseline period. The control treatments are planting date: 15 June for Ambo and Bako and 30 June for Melkassa. Nitrogen fertilizer: 100 kg ha^{-1} used for all sites. Maize cultivars: late maturing (Jibat) for Ambo, late (BH661) and medium (BH546) maturing for Bako and early maturing (MH140) for Melkassa. These treatments are the baseline practices used by farmers and agricultural research centres in the respective study sites. The control treatments were simulated for the baseline (1995-2017) and for future 2021-2050 (2030 s) climate. The relative yield reduction was used as a measure of climate change impact. To assess the adaptation options for the baseline and for future period, shifting planting date within the planting window (15 May to 15 July) was used. The normal planting periods 15 May to 15 June is for Ambo and Bako and 1 June to 15 July is for Melkassa (Seyoum et al., 2017).

Optimum planting dates, which provided the highest yield, were determined from simulations of the baseline and the climate change scenarios using sowing dates of two weeks intervals around the earliest and latest possible sowing date within the planting window. Hence, we adopted four different planting dates: 15 May, 1 June, 15 June and 30 June for Ambo and Bako, and 1 June, 15 June, 30 June and 15 July for Melkassa. Different nitrogen fertilizer levels below and above the recommended level (0, 23, 100, 150 and 200 kg ha^{-1}) were used with 50 % nitrogen at planting and 50 % of nitrogen at 30 days after planting. Four different maize cultivars: BH546, BH661, Jibat and MH140 under three maize agro-ecology zones were also used as future adaptation options. Maize yield was simulated for a baseline period (1995-2017) and future 2021-2050 (2030s) climatic conditions. The 2030's represents the average between 2021 and 2050. The potential impact of climate change under the RCP8.5 scenario was estimated by calculating changes in maize yield between baseline and future climates for each treatment as follows:

$$\Delta Y = \frac{\left(Y_{fi} - Y_b\right)}{Y_b} \qquad (4.3)$$

where ΔY is change of yield, Y_{fi} is yield under future climate *i* and Y_b is yield under the baseline climate.

The variability of yield (uncertainty) due to temporal variation, model or location in the climate change impact assessment were calculated based on the method described in Asseng et al. (2015) method.

4.4 Results

Monthly total precipitation and mean monthly maximum and minimum air temperatures were simulated using the seven GCMs CORDEX historical data for 1995-2005 to evaluate the model performance. The GCM models projected monthly mean maximum and minimum air temperatures very well with $R^2 > 0.99$ and RMSE ≤ 0.17 °C at all sites. In the case of monthly total precipitation, the R^2 and the RMSE range from 0.50-0.95 and 25.62-76.07 mm for Ambo, 0.67-0.97 and 54.45-75.05 mm for Bako and 0.50-0.80 and 46.35-86.24 mm for Melkassa, respectively (Appendix 2 Supplementary materials (SM) Table SM4a).

4.4.1 Changes in precipitation and maximum and minimum air temperatures in 2030

4.4.1.1 Precipitation

Projections using RCP 8.5 at Ambo, Bako and Melkassa sites clearly showed changes in monthly precipitation amount by 2030. Relative to the baseline period (1995-2017), the percentage changes in monthly total precipitation by 2030 varied among GCMs and sites. The monthly total precipitation for the most relevant months from the point of view of rainfed crop production (i.e., June to September- *Kiremt* season) projected to increase by up to 55 % (365 mm) for Ambo and 75 % (241 mm) for Bako respectively, whereas a significant decrease in monthly total precipitation is projected for Melkassa compared to the baseline period by 2030 (Figure 4.1). For the short rainy season (March to May-*Belg* season) most of the GCMs projected a decrease in monthly total precipitation for all sites except, few GCM models projected a slight increase for Bako relative to the baseline period. Interestingly, the total monthly precipitation for the dry season (October to February-*Bega* season) almost all GCM models projected a great increase for Melkassa particularly for November, December and January. Similarly, most of the GCMs projected an increase in monthly total precipitation for October and November in Ambo while the majority of the GCM models projects a decrease in monthly total precipitation for Bako in the near future (2030s) (Figure 4.1).

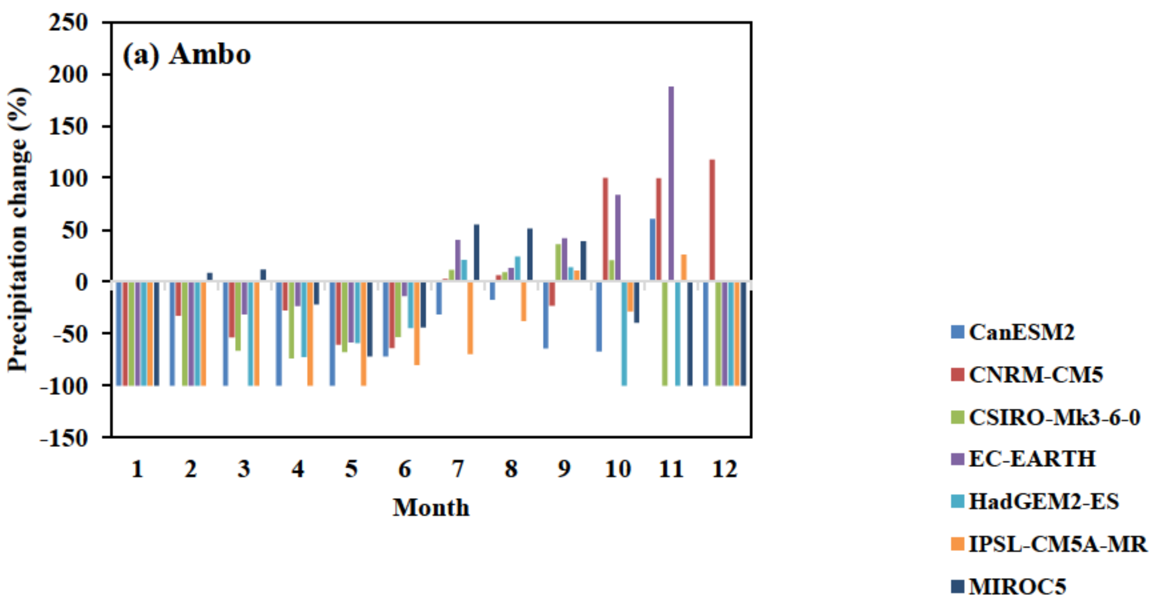

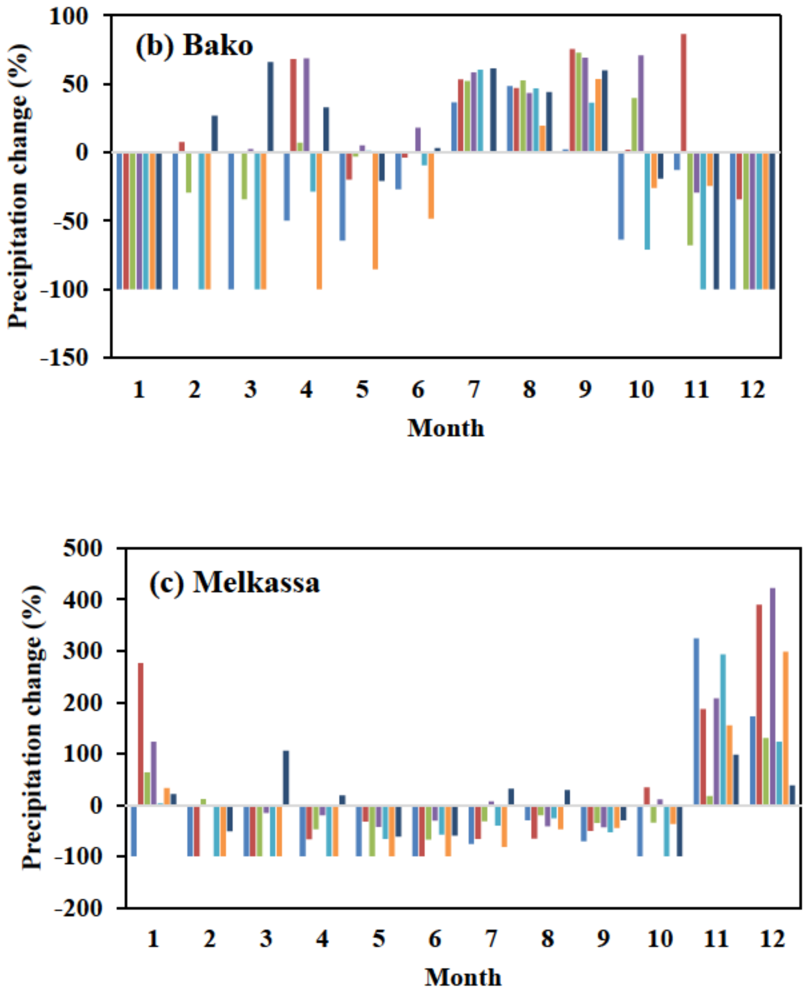

Figure 4.1: Percentage difference between monthly total precipitation as projected by seven GCMs under RCP 8.5 and that for the baseline period (1995-2017) for the three sites (a) Ambo (high altitude), (b) Bako (mid-altitude) and (c) Melkassa (low altitude)

Figure 4.2 shows the total monthly precipitation amount projected by ensemble of multiple GCMs for 2030 as compared to the observed (1995-2017) period. Results show that monthly total precipitation will remain almost the same as the baseline while the *Belg* season monthly total precipitation will decrease at Ambo under the future climate. The *Kiremt* season monthly total precipitation, on the other hand, may significantly increase at Bako in 2030. However, future monthly total precipitation projected to reduce significantly for *Belg* and *Kiremt* seasons at Melkassa by 2030 (Figure 4.2).

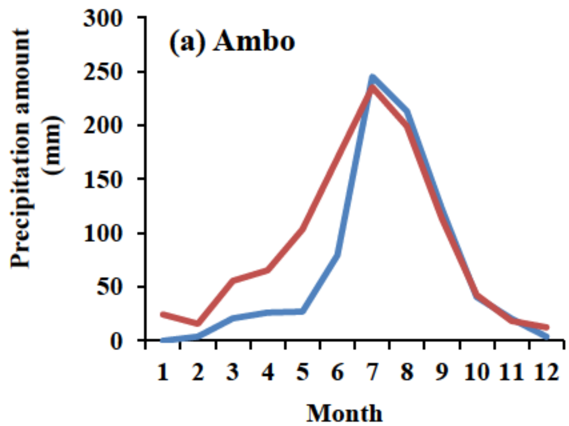

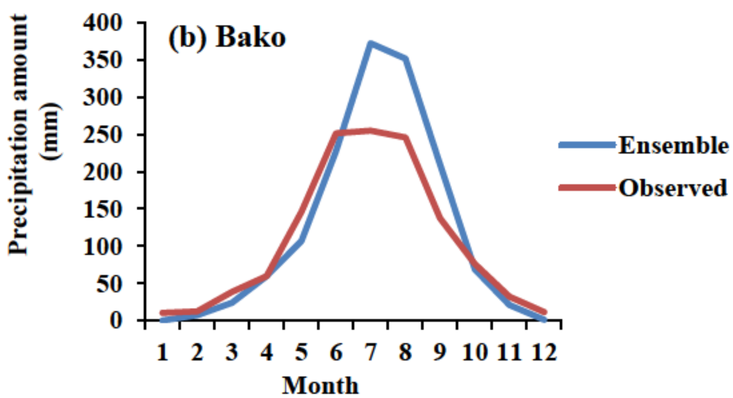

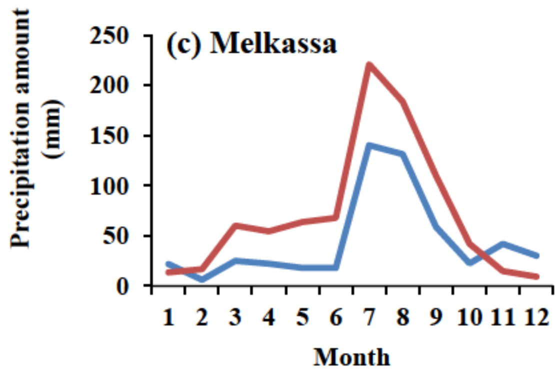

Figure 4.2: Total monthly precipitation amount projection by multimodel ensemble for 2030 compared to that observed (1995-2017) period for (a) Ambo (high altitude), (b) Bako (mid-altitude) and (c) Melkassa (low altitude)

4.4.1.2 Maximum air temperature

The projected changes in average monthly maximum air temperatures from all GCM runs are shown in Figure 4.3. The changes in average monthly maximum air temperatures projected by GCMs are quite different in magnitude, but similar in shape. All models indicate incremental changes with respect to the historical period in the near future. According to the GCM models, the average monthly maximum air temperatures would increase by 0.3-1.7 °C for Ambo, 0.7-2.2 °C for Bako and 0.8-1.8 °C for Melkassa compared to the historical period (Figure 4.3). In addition, the *Kiremt* season will experience the highest air temperature change particularly in the month of August at Ambo. Similarly, the *Bega* season will experience the highest air temperature in February and January at Bako and Melkassa respectively in 2030. Overall, for a given future period and emission scenario though, warming is found for all study sites although larger relative increases are projected for Bako.

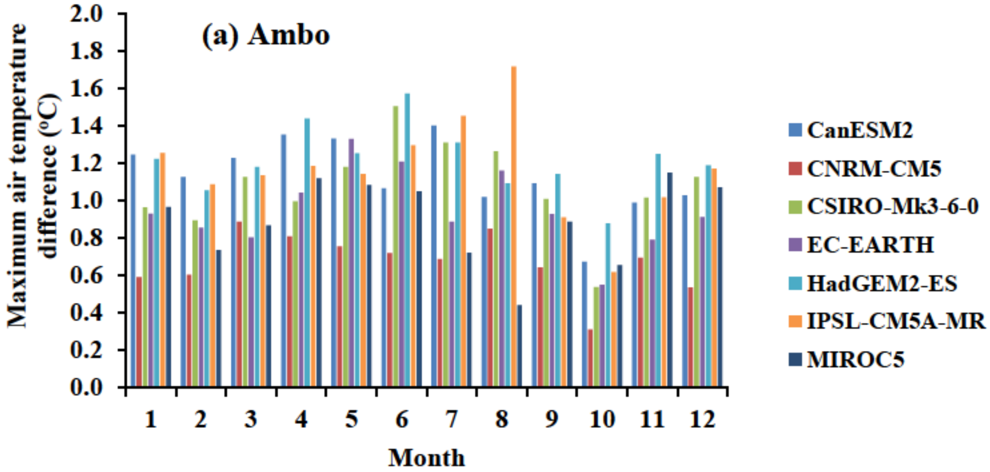
(a) Ambo
Maximum air temperature difference (ºC)
Month
CanESM2
CNRM-CM5
CSIRO-Mk3-6-0
EC-EARTH
HadGEM2-ES
IPSL-CM5A-MR
MIROC5

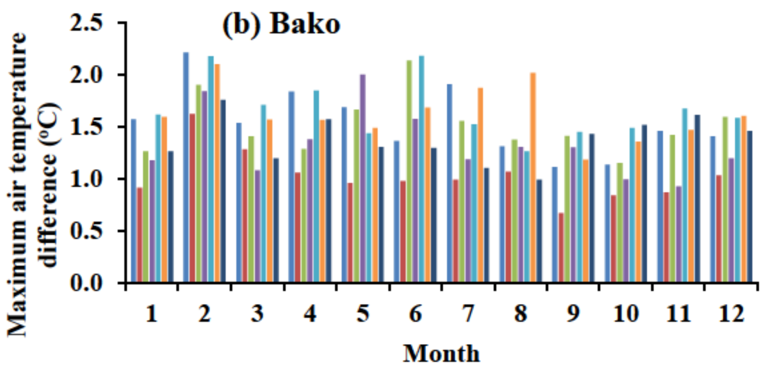
(b) Bako
Maximum air temperature difference (ºC)
Month

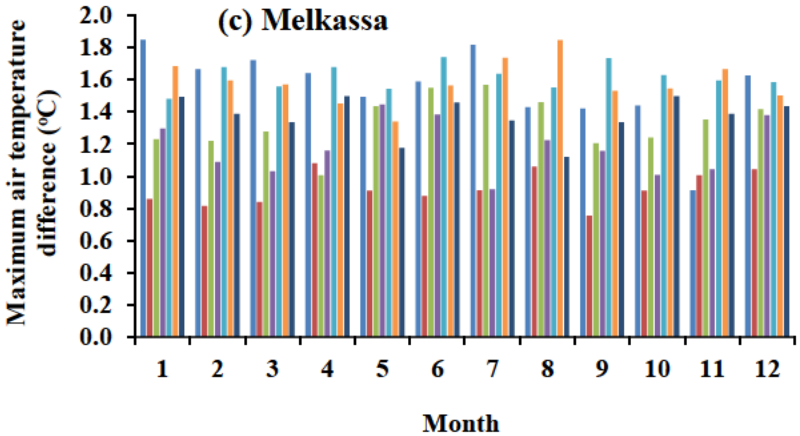

Figure 4.3: Differences in monthly average maximum air temperature (°C) as projected by seven GCMs' under 8.5 RCP for 2030 compared to the period 1995-2017 for (a) Ambo (high altitude), (b) Bako (mid-altitude) and (c) Melkassa (low altitude)

Monthly average maximum air temperature projected values obtained by the GCMs ensemble and the observed values are presented in Figure 4.4. According to the GCMs ensemble mean, the monthly average maximum air temperature is expected to increase by 24.0-29.7, 25.6-33.1 and 27.8-32.5 °C for Ambo, Bako and Melkassa respectively compared to the observed by 2030. In addition, the GCMs ensemble mean clearly indicate that the increase in monthly average maximum air temperature in the 2030 will be higher during the small rainy season (*Belg*) and the dry season (*Bega*) across all sites compared to the main rainy season (*Kiremt*) (Figure 4.4).

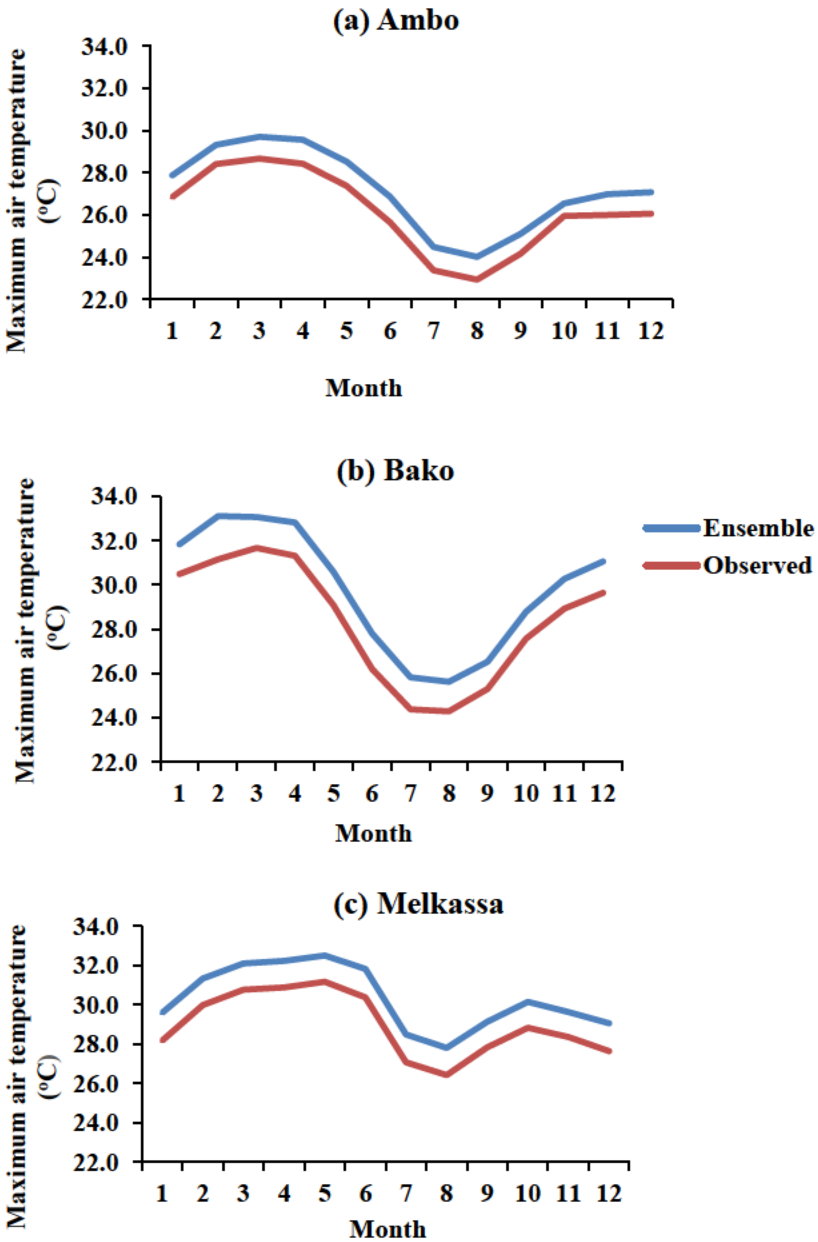

Figure 4.4: Multimodel ensemble average monthly maximum air temperature projected for 2030 compared to that observed (1995-2017) period for (a) Ambo (high altitude), (b) Bako (mid-altitude) and (c) Melkassa (low altitude)

4.4.1.3 Minimum air temperature

The results of projections for monthly average minimum air temperature are shown in Figure 4.5. The projection shows that the monthly average minimum air temperatures are projected to continue to increase by comparison to the historical period. Likewise, the monthly average minimum air temperature is projected to increase in the range of 0.6-1.7 °C for Ambo, 0.8-2.3 °C Bako and 0.6-2.7 °C for Melkassa in 2030 (Figure 4.5). This is greater than the 2 °C limit specified by the IPCC as the point beyond which ecological systems may become severely disrupted (IPCC, 2014). The result also clearly shows that the future average monthly minimum air temperature increases are similar to the results shown for average monthly maximum air temperature changes. In addition, the *Kiremt* season will experience the highest monthly average minimum air temperatures in June at Ambo for the near future. Similarly, the *Bega* season will have the greatest monthly average minimum air temperature in December and October at Bako and Melkassa respectively in 2030. Overall, for the period of 2030, there will be a clear increase in the average monthly minimum air temperature compared to the maximum air temperature change, due to climate change impacts.

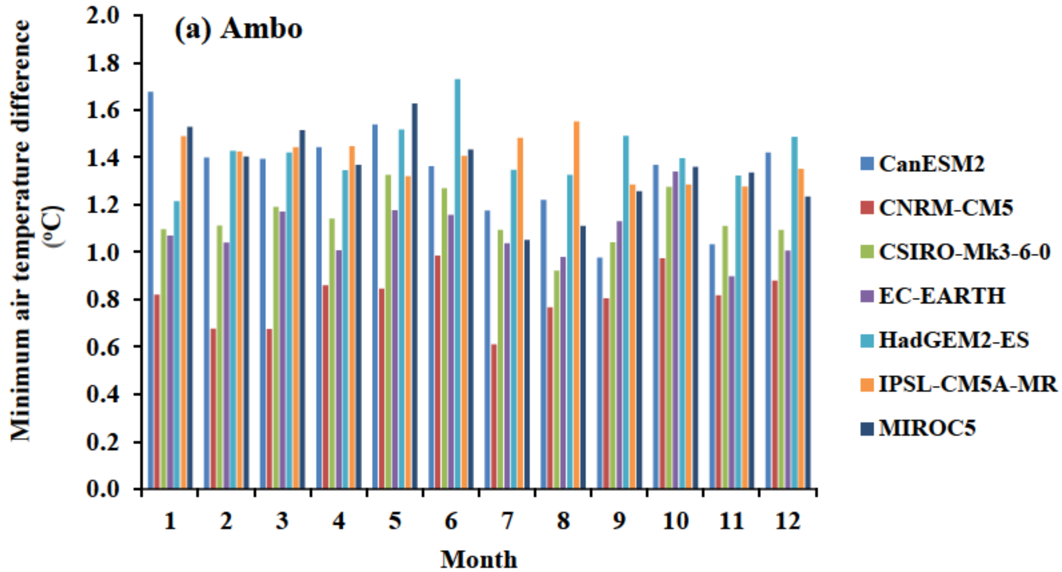
(a) Ambo
Minimum air temperature difference (°C)
Month
CanESM2
CNRM-CM5
CSIRO-Mk3-6-0
EC-EARTH
HadGEM2-ES
IPSL-CM5A-MR
MIROC5

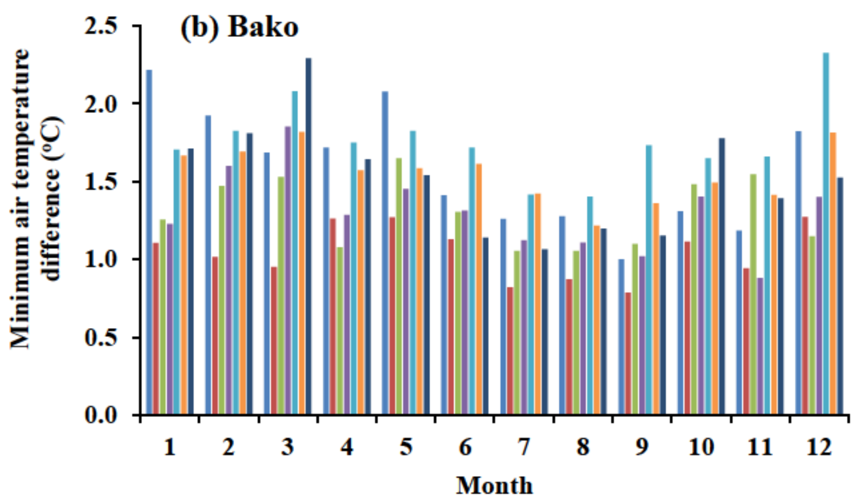
(b) Bako
Minimum air temperature difference (°C)
Month

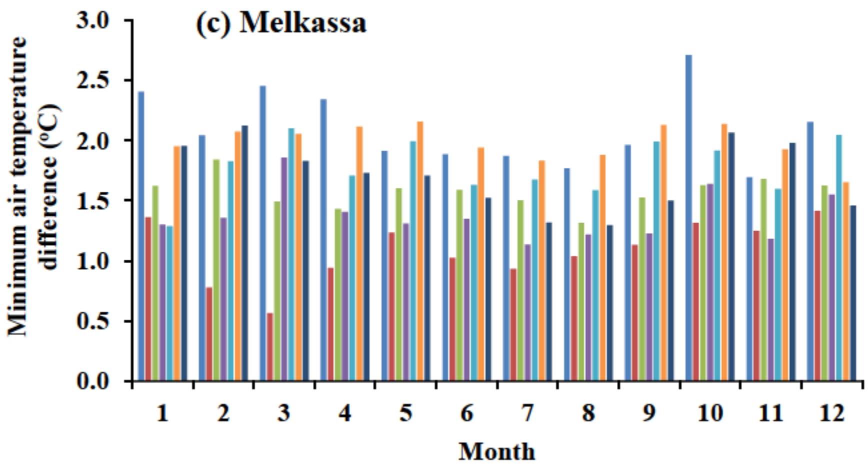

Figure 4.5: Differences between monthly mean minimum air temperature (°C) as projected by seven GCMs' under 8.5 RCP for 2030 compared to that for 1995-2017 for (a) Ambo (high altitude), (b) Bako (mid-altitude) and (c) Melkassa (low altitude)

The projected values of monthly average minimum air temperature obtained by the GCM ensembles and the observed values are presented in Figure 4.6. The ensemble GCMs were able to replicate the monthly average downward trend in minimum air temperature levels as the observed data show (Figure 4.6). Based on the GCMs ensemble projections, the monthly average minimum air temperature is expected to increase by 10.1-13.2, 13.2-16.5 and 11.6-18.0 °C for Ambo, Bako and Melkassa respectively compared to the observed in the near future. According to the GCMs ensemble mean, by 2030 the increase in monthly average minimum air temperature will be higher during the *Belg* season for all sites studied as compared to the other two seasons (Figure 4.6).

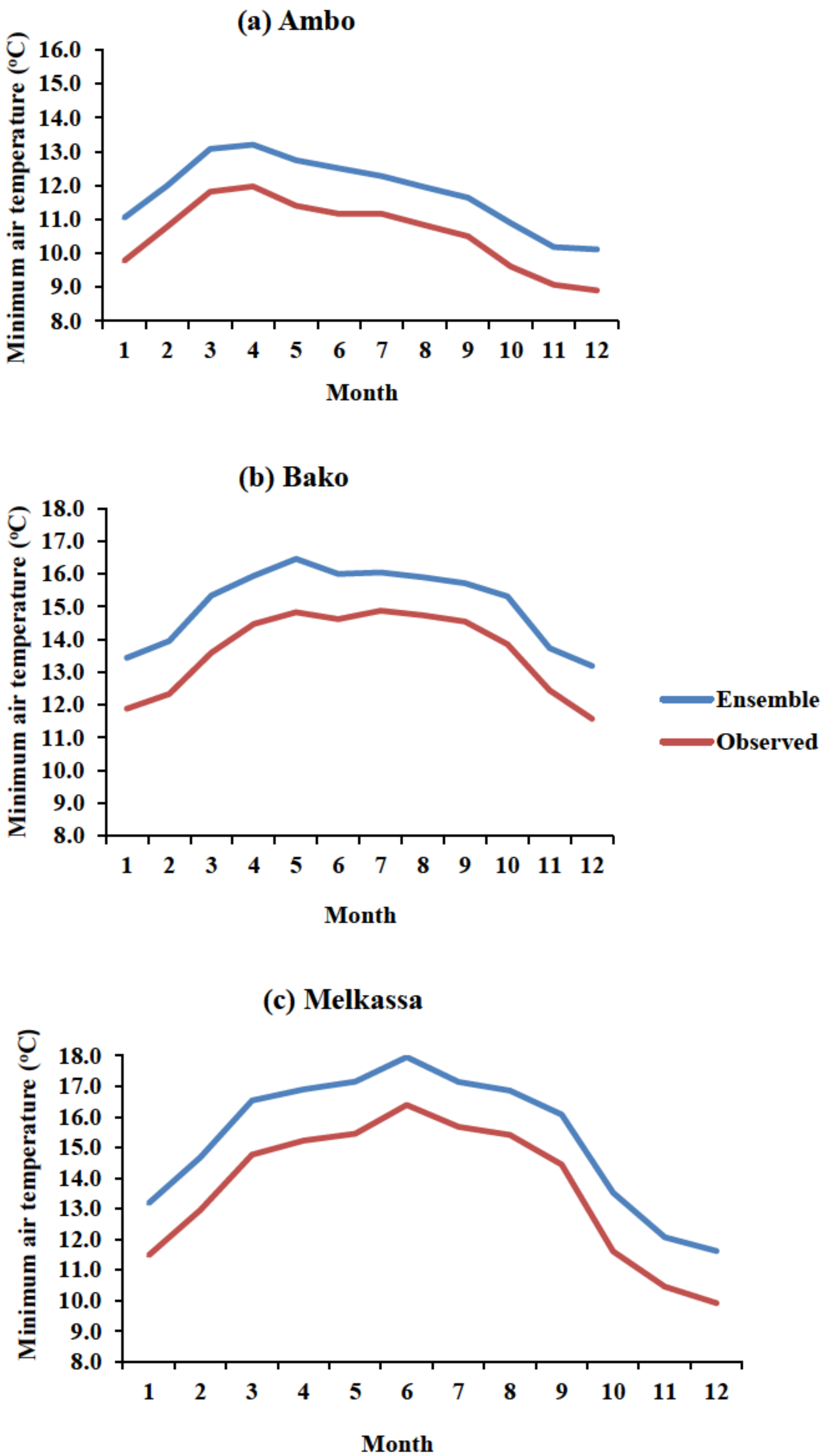

(a) Ambo
Minimum air temperature (ºC)
16.0
15.0
14.0
13.0
12.0
11.0
10.0
9.0
8.0
1 2 3 4 5 6 7 8 9 10 11 12
Month
(b) Bako
Minimum air temperature (ºC)
18.0
17.0
16.0
15.0
14.0
13.0
12.0
11.0
10.0
9.0
8.0
1 2 3 4 5 6 7 8 9 10 11 12
Month
Ensemble
Observed
(c) Melkassa
Minimum air temperature (ºC)
18.0
17.0
16.0
15.0
14.0
13.0
12.0
11.0
10.0
9.0
8.0
1 2 3 4 5 6 7 8 9 10 11 12
Month

Figure 4.6: Multimodel ensemble average monthly minimum air temperature projected for 2030 compared to that observed (1995-2017) period for (a) Ambo (high altitude), (b) Bako (mid altitude) and (c) Melkassa (low altitude)

4.4.2 Yield simulation for the baseline (1995-2017) climate

Yield simulations for the baseline period using the observed climate data indicated higher yields at mid altitude yields for Bako (Figure 4.7). Simulation of yield by all crop models suggests increased nitrogen (N) application produces an increased yield for all maize cultivars on all sites. The simulated maize yield for Ambo ranges between 2.0 and 6.7 t ha^{-1}. 2.0 and 15.5 t ha^{-1} for Bako and 2.9 and 13.1 t ha^{-1} for Melkassa for the baseline 1995-2017 period. The average of the three models provides an increased yield (up to 12.5 t ha^{-1}) as compared to the measured maize yield values (up to 6.7 t ha^{-1}) across all cultivar and sites.

(a) Ambo

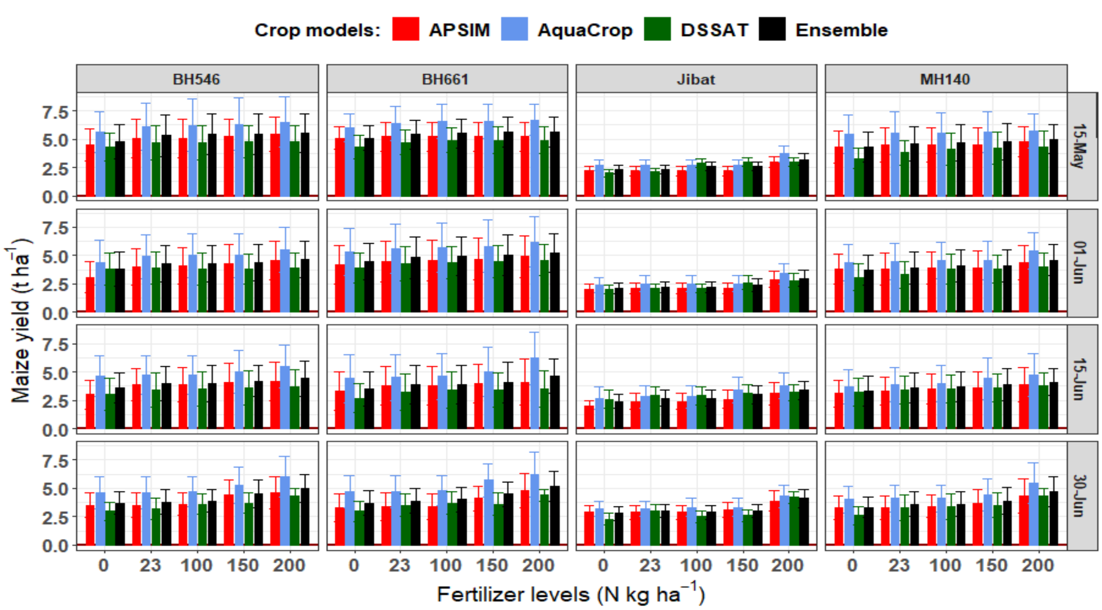

(b) Bako

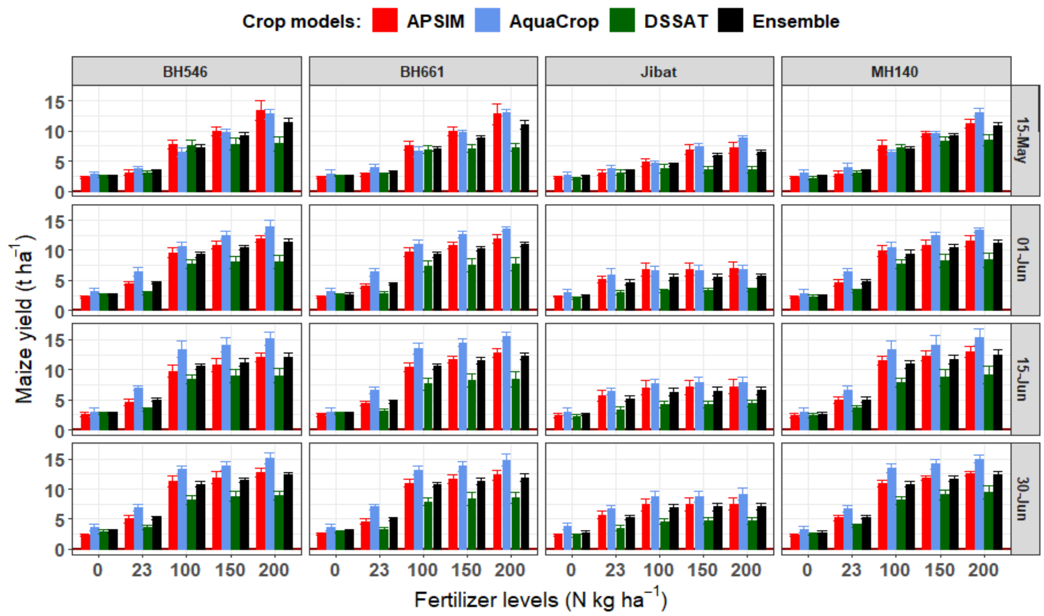

(c) Melkassa

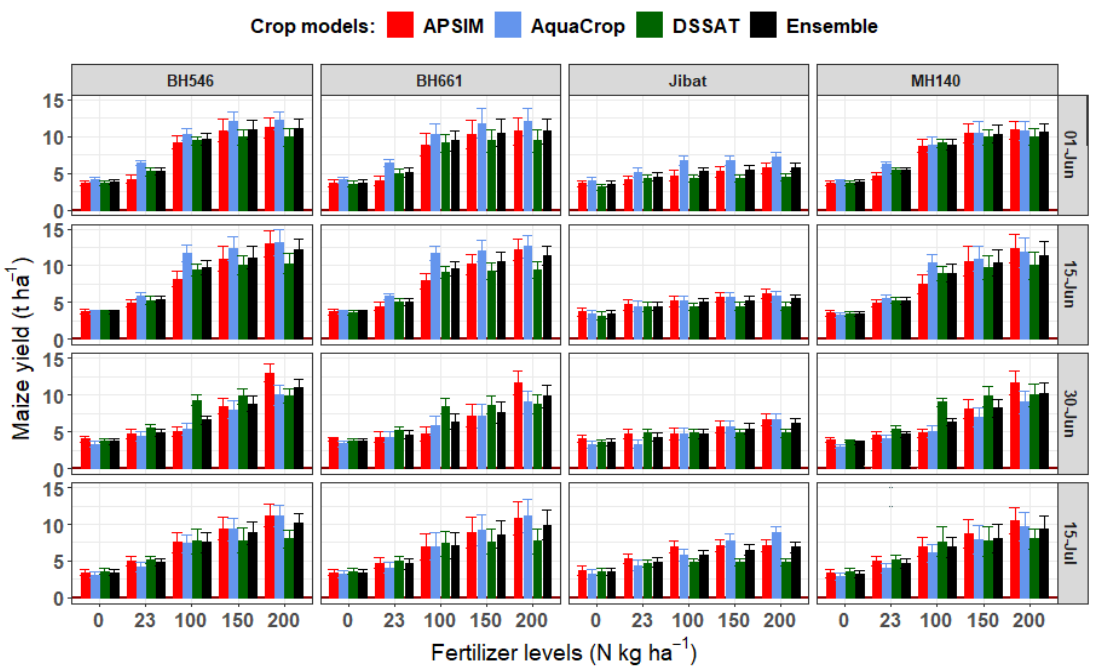

Figure 4.7: Maize yield (t ha-1) with observed climate data for the baseline period (1995–2017) as simulated with APSIM, AquaCrop and DSSAT models using different planting

dates, cultivars and nitrogen fertilizer levels for (a) Ambo (high altitude), (b) Bako (mid-altitude) and (c) Melkassa (low altitude). Error bars show the standard deviation of maize yield simulated by the crop models

4.4.3 Impact of projected climate on maize yield

Figure 4.8 presents the impact of future climate on maize yield if the existing agronomic practices used by farmers continue in 2030 in the study sites. Relative to the baseline, all the crop models showed either an increase or a decrease in maize yield depending on treatment level. However, the simulation results of the three ensemble crop models show that, mean maize yield will decrease by 4 % and 16 % for Ambo and Melkassa by 2030 respectively, while mean maize yield could increase by 2 % for Bako by 2030 if the current maize cultivars were grown with the same agronomic practice as the baseline under the future climate (Figure 4.8).

(a) Ambo

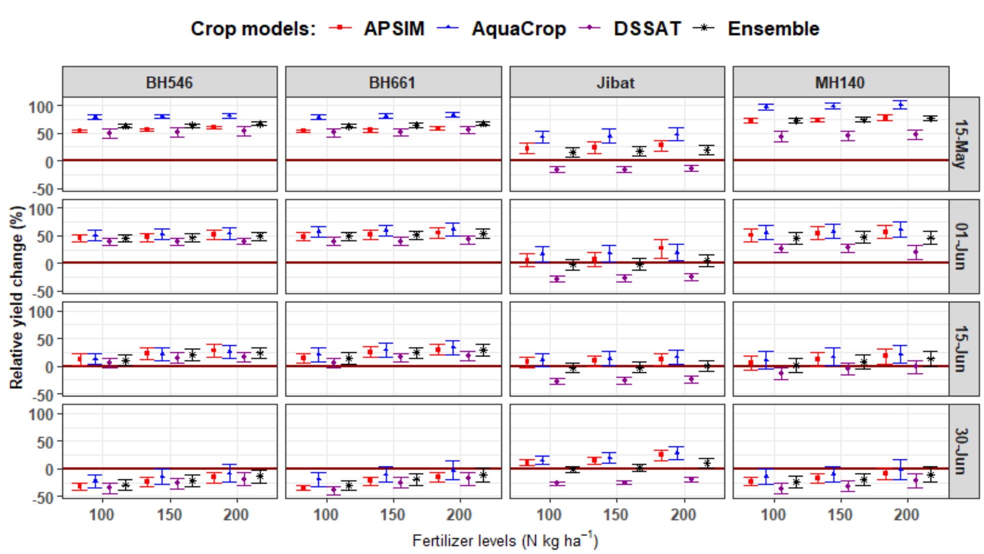

(b) Bako

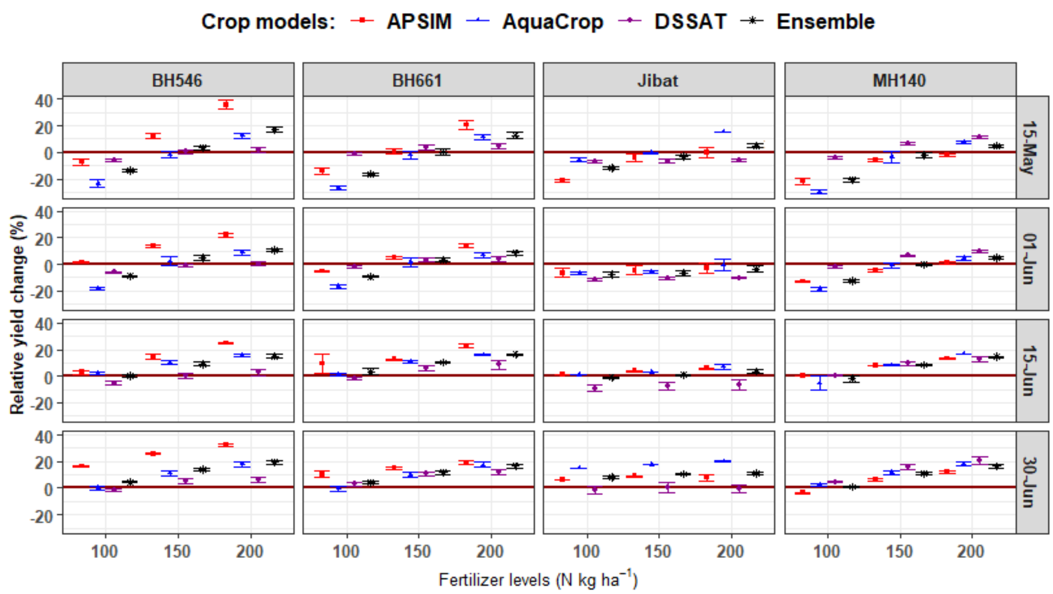

(c) Melkassa

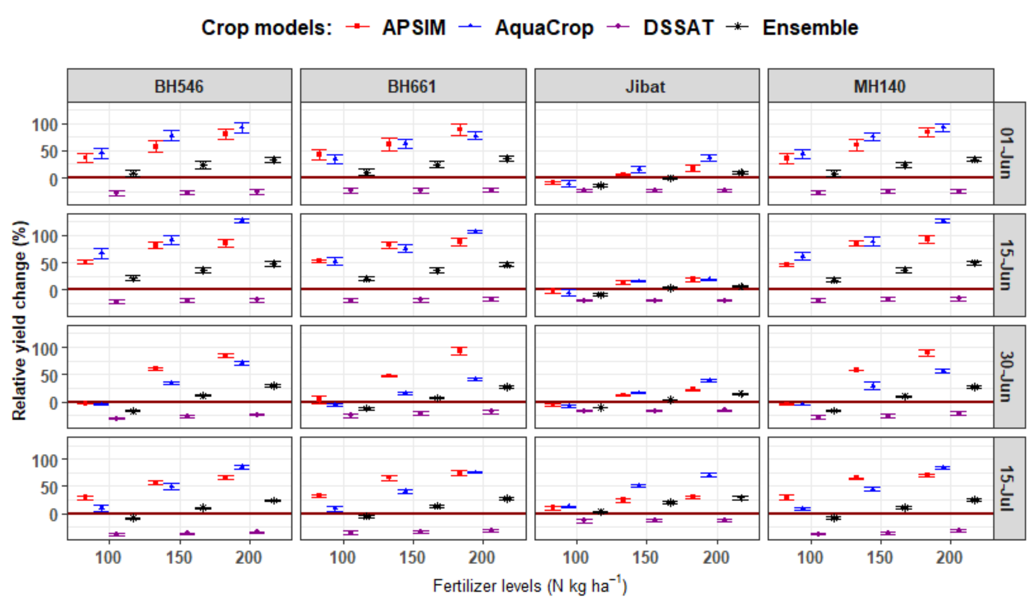

Figure 4.8: Percentage yield change in 2030 relative to the baseline control treatments as simulated with APSIM, AquaCrop and DSSAT crop models for (a) Ambo (high altitude),

(b) Bako (mid-altitude) and (c) Melkassa (low altitude). Error bars show the standard deviation of the change of maize yield simulated for multiple GCM projections

4.4.4 Crop management practices as adaptation options

According to Figure 4.9, the result indicated that for Ambo model differences in predicting maize yield are small. Planting between 15 May to 01 June would give improved relative yields for all cultivars. Fertilizer levels between 23-150 kg ha^{-1} result in increased yields for all cultivars when combined with early planting at Ambo in 2030.

For Bako, there are differences amongst the models in the relative yield of maize. Early planting increased maize yield for all cultivars under the future climate. Planting after 15 May has either no or negative effect on maize yield. All cultivars studied responded the same way to planting date shifts. Early planting combined with a nitrogen fertilizer level of 23-100 kg ha^{-1} provided increased relative yields under the future climate. Delayed planting has a negative influence on maize production for Bako under the future climate (2030).

For Melkassa, all models responded similarly to planting dates, fertilizer and cultivar levels. All planting dates considered resulted in negative relative yield. However, late planting had reduced relative yields compared to early planting. Higher fertilizer levels (100-150 kg ha^{-1}) seem to reduce yield reductions under the future climate, but this varied among maize cultivars studied.

Planting the Jibat cultivar between 15-30 June at higher N levels may reduce severe yield reduction of maize at Melkassa (Figure 4.9).

(a) Ambo

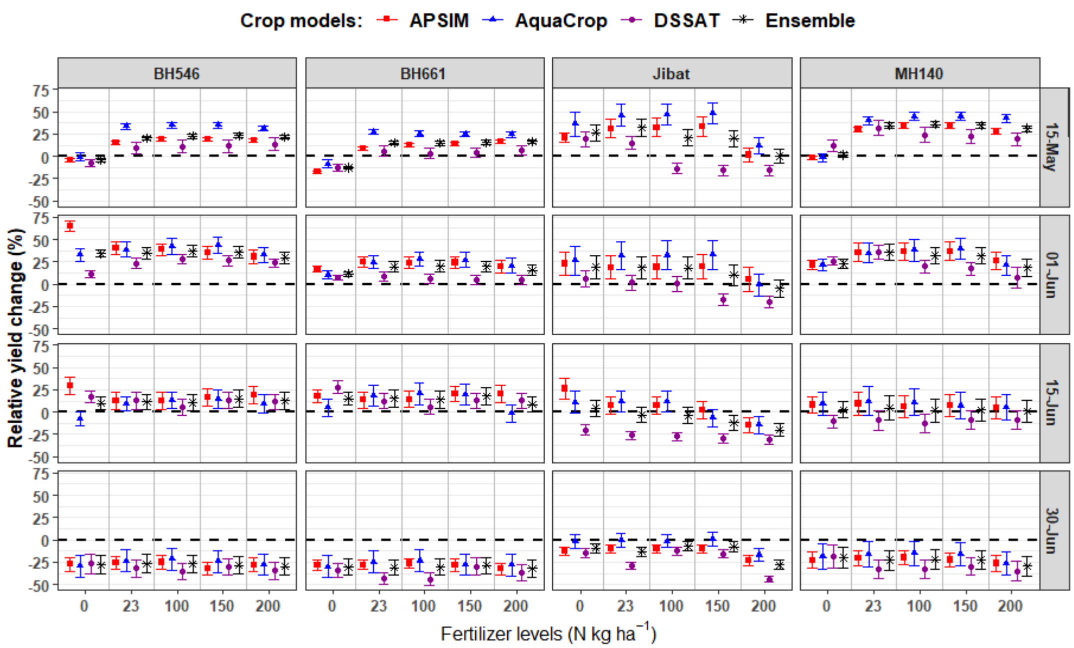

(b) Bako

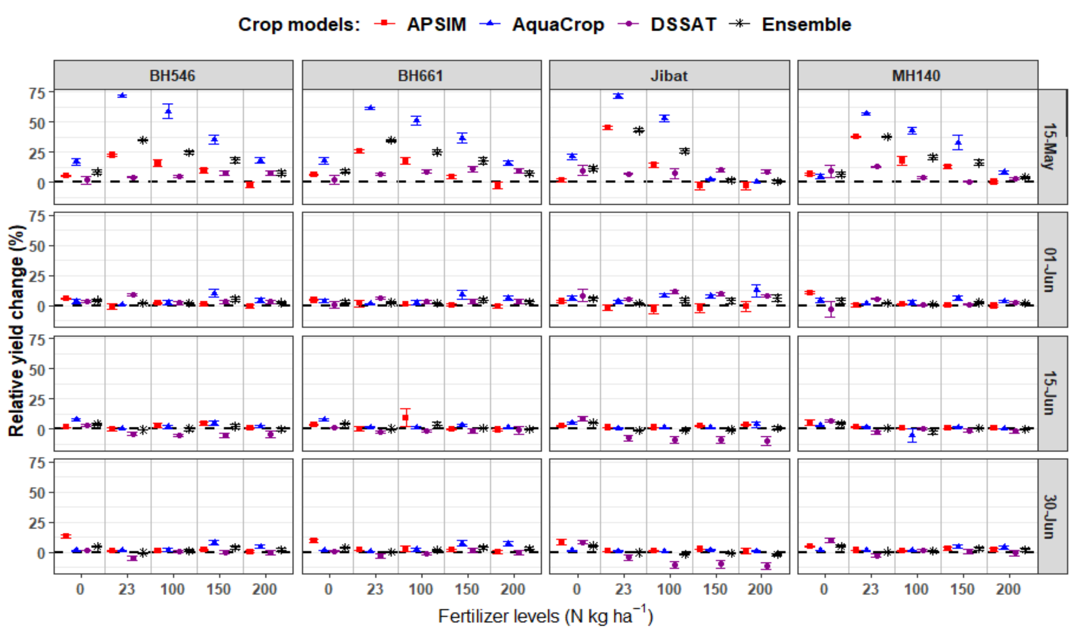

(c) Melkassa

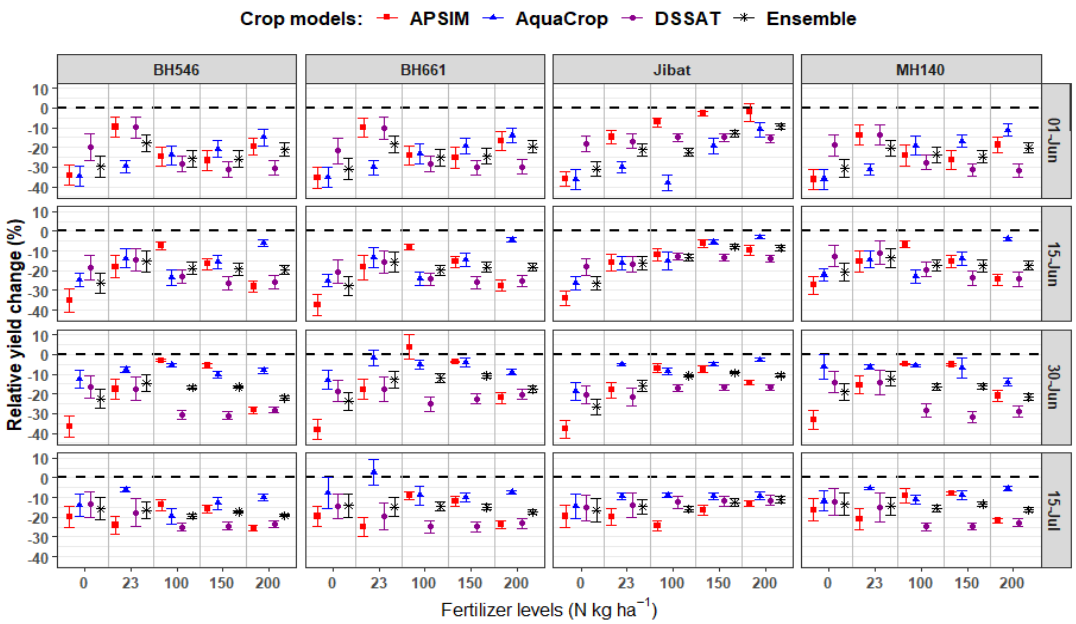

Figure 4.9: Effects of planting dates on mean maize yield under future climate change scenarios relative to the baseline for (a) Ambo (high altitude), (b) Bako (mid-altitude) and (c) Melkassa (low altitude) as simulated using the APSIM, AquaCrop and DSSAT models. Error bars show the standard deviation of the change of maize yield simulated for multiple GCM projections

4.4.5 Crop model uncertainty in yield simulation

Predicted yield differences amongst the models were noted for the higher altitude (Ambo), mid (Bako) and lower altitude (Melkassa) sites. The impact of the crop models in predicting yield varied from -38 to 38 % for Ambo, from -4 to 65 % for Bako and -12 to -36 % for Melkassa (Figure 4.10). The crop model yields were inconsistent even for the simulated mean yield change under the same climate projection. The DSSAT model projected a large mean yield reduction whereas the AquaCrop model projected a high mean yield increase for Ambo and Bako for most climate projections. The APSIM model projected both the lowest and the highest yield reduction for Melkassa for most of the climate projections (Figure 4.10). The differences in the simulated mean yield changes could to some extent be attributed to the different responses of these crop models to the projected climate conditions. Maize yield simulated using AquaCrop was generally greater than that simulated with APSIM and DSSAT.

(a) Ambo

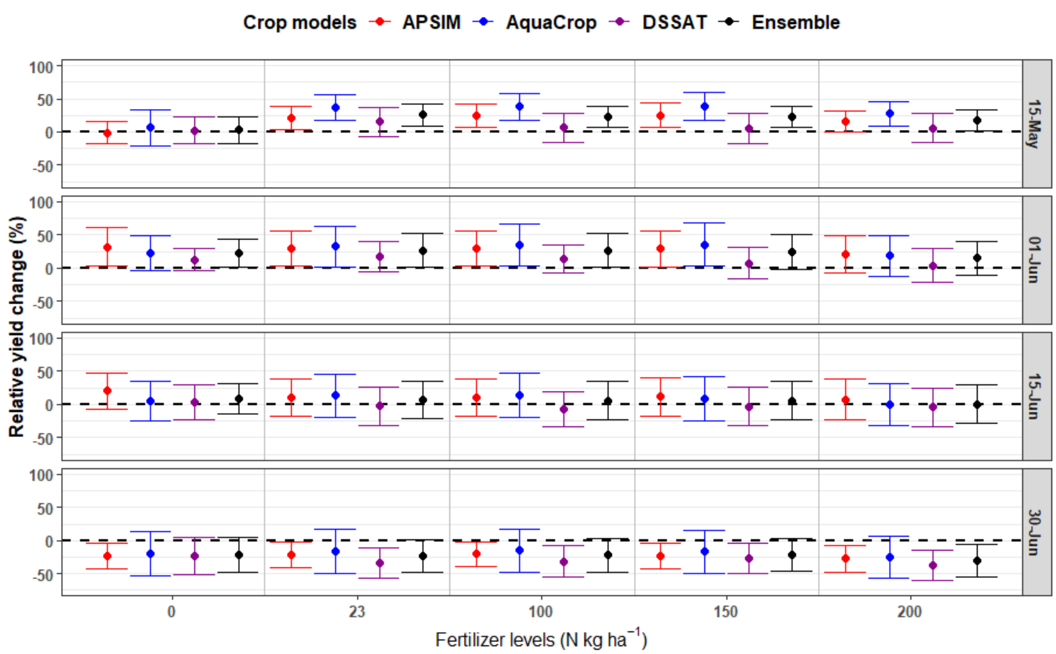

(b) Bako

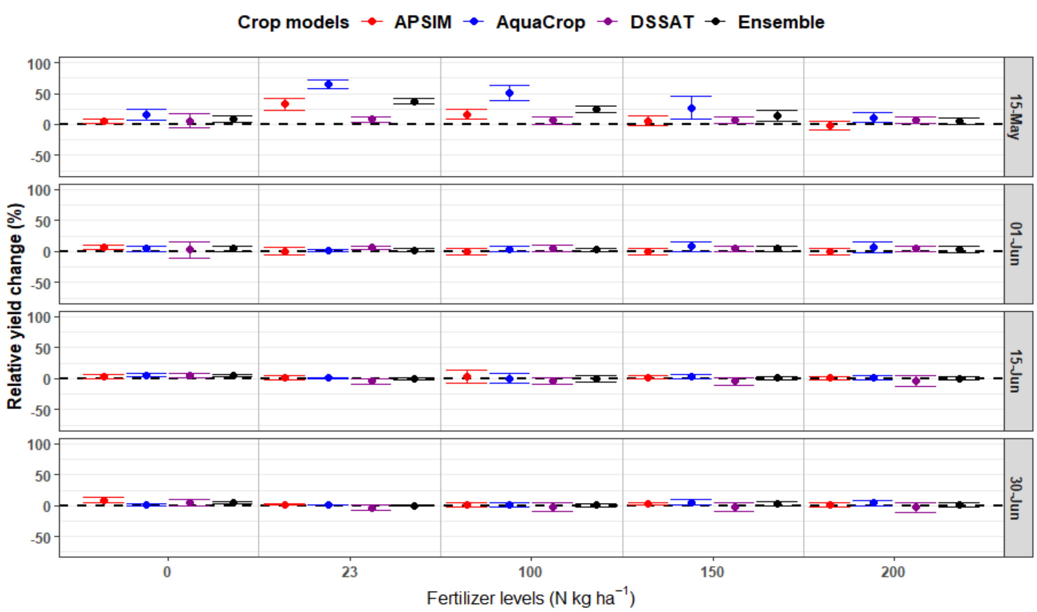

(c) Melkassa

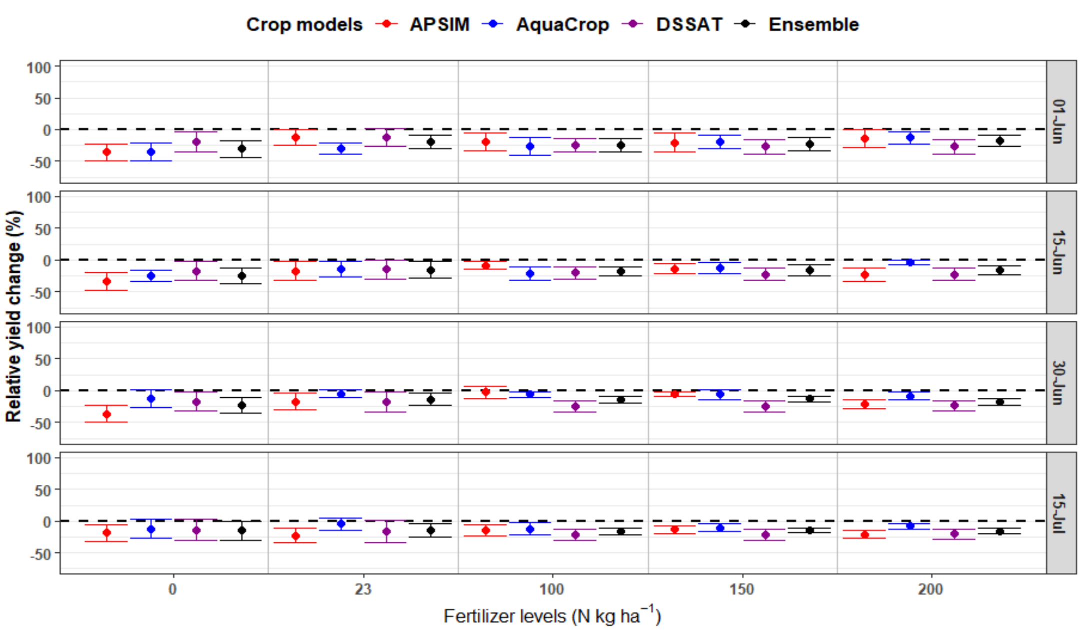

Figure 4.10: Crop model uncertainty in simulated mean maize yield for different planting dates and nitrogen fertilizer levels for (a) Ambo (high altitude), (b) Bako (mid-altitude) and

(c) Melkassa (low altitude). Error bars show the standard deviation of the change of maize yield simulated by the individual GCM projections

4.4.6 Climate model uncertainty in yield simulation

The simulated mean maize yield changes for different climate projections were quite different. For example, using the IPSL-CM5A resulted in the highest mean yield increase for both Ambo and Bako, whereas data for HadGEM2-ES and CSIRO-Mk3-6-0 models resulted in the lowest mean yield for Ambo and Bako respectively. Both the HadGEM2-ES and CSIRO-Mk3-6-0 models projected the lowest and the highest decrease in mean yield, respectively for Melkassa (Figure 4.11). Overall, the impact of the choice of GCM on yield varied from -52 to 78 % for Ambo, -5 to 41 % for Bako and -4 to -62 % for Melkassa (Figure 4.11). This result demonstrated that the yield uncertainty is greater among GCMs than crop models.

(a) Ambo

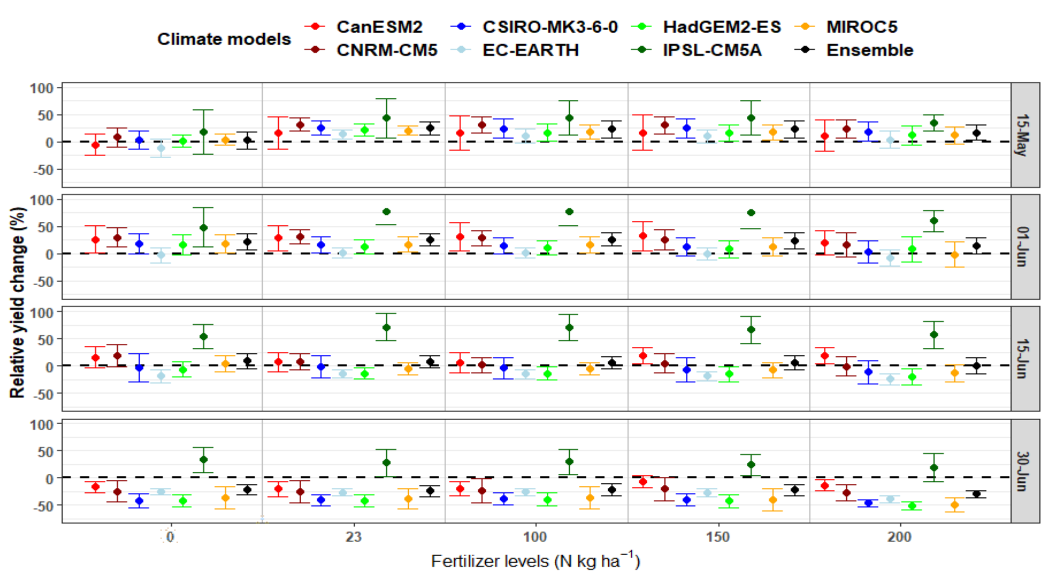

(b) Bako

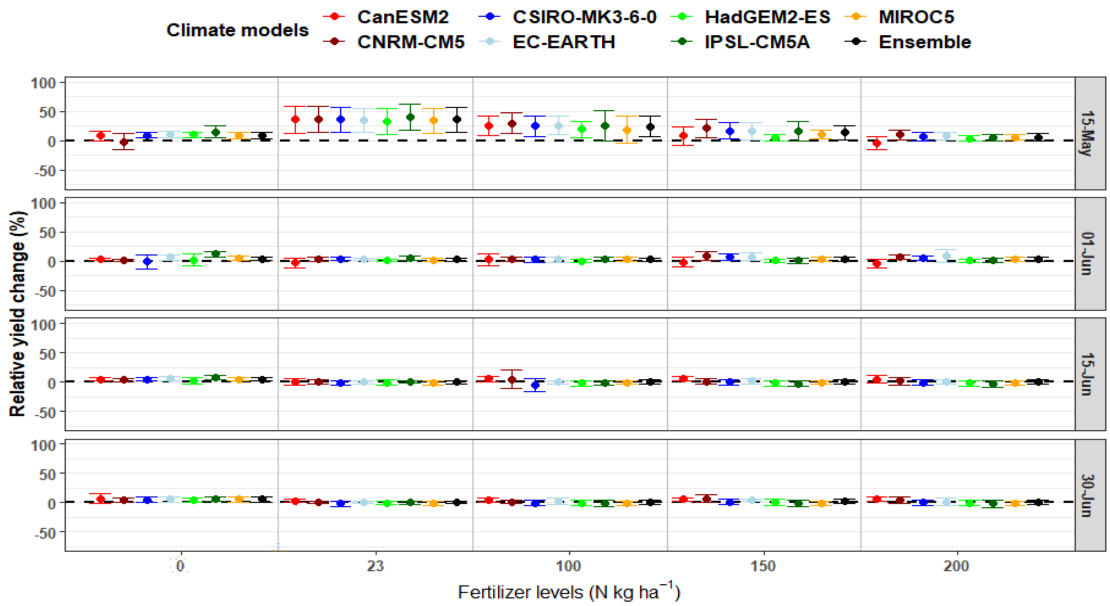

(c) Melkassa

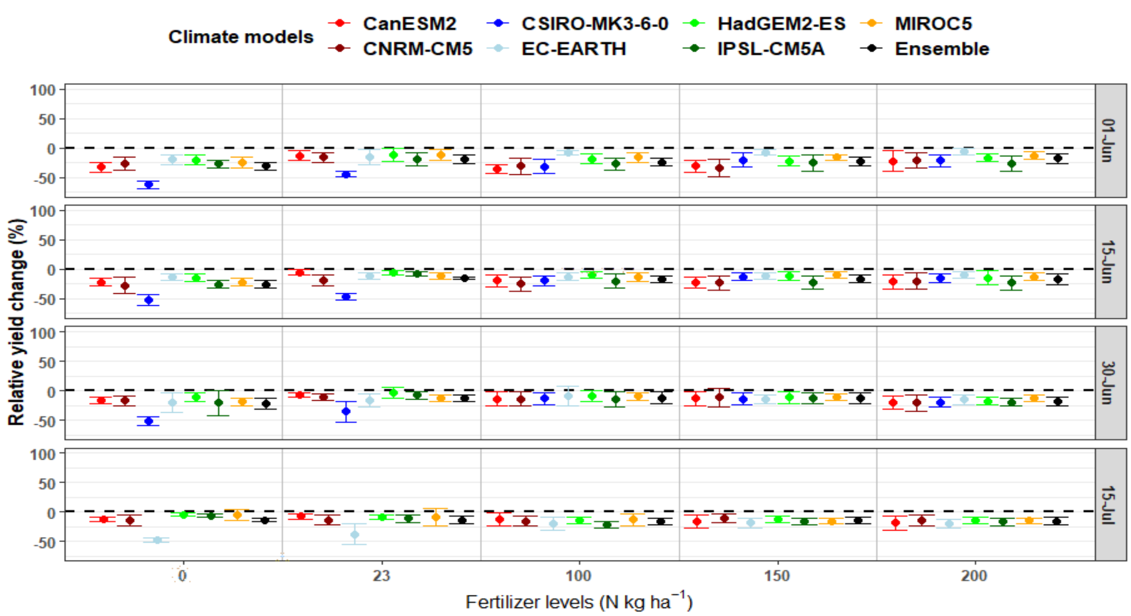

Figure 4.11: Climate model uncertainty in simulated mean maize yield for different planting dates and nitrogen fertilizer levels for (a) Ambo (high altitude), (b) Bako (mid-

altitude) and Melkassa (low altitude). Error bars show the standard deviation of maize yield change simulated for multiple GCM projections

4.5 Discussion

4.5.1 Climate change projections and impacts

Maize production is very likely to be negatively affected by climate change in Ethiopia (Kassie et al., 2015, Tesfaye et al., 2018) and there is an urgent need to develop strategies that adapt to the changing climate. Therefore, this study investigated the potential impact of climate change on maize yield for three sites (Ambo, Bako and Melkassa) in tropical environments of Ethiopia in 2030 under RCP 8.5 scenario using downscaled CORDEX-Africa domain precipitation and air temperature data. The study results indicated that both the individual GCM models and their ensemble mean projected an increase for the *Kiremt* season total monthly precipitation for Ambo and Bako while a decrease total monthly precipitation for Melkassa by 2030 as compared to the baseline period. A projected precipitation increase up to 55% (365 mm) for the *Kiremt* season at Ambo can be explained since Ambo has a highland agro-ecology and received more precipitation as compared to the mid- and low- land areas. Also, the *Kiremt* season is the main rainy season which receives most of the annual precipitation. Hence, the future climate might favour the site during this season. A future increase of the *Kiremt* total monthly precipitation at Ambo and Bako may have a positive impact on maize production though this might be changed due to an increase in air temperature for the sites that leads to an increase in evapotranspiration (Conway and Schipper, 2011).

The result from the GCMs model showed that the *Belg* season total monthly precipitation was projected to decrease for Ambo and Melkassa while projected to increase for Bako by 2030. However, the GCMs ensemble clearly indicates that the *Belg* season total monthly precipitation expected to decrease by 2030 for all sites. The decrease in the *Belg* season precipitation agrees with Muluneh et al. (2015) who investigated the impact of predicted changes in precipitation and atmospheric carbon dioxide on maize and wheat yields in the Central Rift Valley of Ethiopia.

By contrast, despite some differences in the magnitude of changes, the total monthly precipitation is projected to increase for the *Bega* season (November, December and January) for Melkassa by 2030. Even though, some of the GCMs indicated an increase of the *Bega* season total monthly precipitation for Ambo and Bako, the GCMs ensemble evidently illustrated that the total monthly precipitation would remain almost the same as the baseline for Ambo and Bako by 2030. Overall, the projected increase and decrease in precipitation for the Bako and Melkassa sites respectively is in agreement with Araya et al. (2015) and Kassie et al. (2015). Under normal conditions, the *Bega* season is a time for harvesting particularly for the lower altitude areas (Asfaw et al., 2018). Hence, the anticipated increase in monthly total precipitation mainly for November and December might affect the agricultural operation such as harvesting at Melkassa. Therefore, harvesting time should be adjusted accordingly for this site.

The projected air temperature result showed that the study region will get warmer under the future climate compared to the historical period although the magnitude of change may vary depending on the site. Across the study sites, the average monthly maximum air temperature may increase by between 0.3 and 1.7, 0.7 and 2.2 and 0.8 and 1.8 °C for Ambo, Bako and Melkassa respectively during 2030 compared to the historical period (Figure 4.3). The expected increase in monthly average maximum air temperature by 2030 is greater for Bako compared to the other sites. This agrees with previous reports that indicated future warming for the study sites (Araya et al., 2015 and Kassie et al., 2015). Similarly, the average monthly minimum air temperature may change by between 0.6 and 1.7, 0.8 and 2.3 and 0.6 and 2.7 °C for the corresponding sites for the near future (Figure 4.5). The increase in minimum air temperature is expected to be higher at lower altitude (Melkassa) compared to those in mid and higher altitudes.

Rising maximum and minimum air temperatures played a crucial role in maize yield reduction which negatively impacts on maize growth and development. For instance, increased air temperature may lead to shortening the reproductive phases and reducing the available time for radiation interception and carbon assimilation as previously reported (Wang et al., 2011; Lobell et al., 2013; Tesfaye et al., 2017). Wang et al. (2011) projected a reduced period by 10 to 30 days for the grain-filling phase and a decrease in maize yield. Lobell et al. (2013) illustrated that for maize in the USA there would be a decrease in days to flowering by 17 days and a yield loss of 13 % if air temperature increased by 2 °C. Similarly, for the March, June, and November planting season in South Asia, Tesfaye et al. (2017) projected that an increase in maximum and minimum air temperatures by 1 °C caused a yield reduction of 55, 13 and 32 % respectively while an increase by 5 °C caused a reduction of 98, 64 and 75 % for the respective months.

The GCMs ensemble mean also indicated that the average monthly maximum air temperature for the 2030 will increase to between 24.0 and 29.7, 25.6 and 33.1 and 27.8 and 32.5 °C for Ambo, Bako and Melkassa respectively. Similarly, the average monthly minimum air temperature increase by between 10.1 and 13.2, 13.2 and 16.5 and 11.6 and 18.0 °C for the corresponding sites by 2030. In addition, the GCMs ensemble mean clearly indicate that the increase in monthly average maximum air temperature in the 2030 will be less during the main rainy season (*Kiremt*) than that for the small rainy season (*Belg*) and the dry season (*Bega*) for all sites. The lower increase in average monthly air temperature during the main rainy season (*Kiremt*) may lead to reduced evaporation followed by reduced drying of the surface. Furthermore, by 2030 the monthly average minimum air temperature is expected to be higher during the *Belg* season for Ambo. Likewise, the monthly average minimum air temperature is anticipated to increase for both *Belg* and *Kiremt* seasons for Bako and Melkassa compared to the *Bega* season in 2030. The increase in maximum and minimum air temperatures for the study sites in agreement with Araya et al. (2015) and Kassie et al. (2015).

4.5.2 Impact of climate change on maize yield

If the existing agronomic practices by farmers are not improved and/or continue in the near future, the simulated mean yield indicates that maize yields are likely to be negatively impacted by climate change at Melkassa and Ambo as compared to Bako by 2030. The impact was greatest for Melkassa (low altitude) where air temperature is naturally high and precipitation is low. The projected increase in air temperature and decrease in precipitation particularly during the main rainy season (*Kirem*t) might cause a maize yield reduction. The result is consistent with other studies (Kassie et al., 2015; Tesfaye et al., 2018). Previous studies also indicated an increase in air temperature will cause to increase in maize development rate and a decrease in the total growth duration. This decrease limits the available time for the anthesis stage, and leads to a depletion of kernels per plant which subsequently reduced the simulated yield in comparison to the baseline conditions (Abraha and Savage, 2006). Tachie-Obeng et al. (2013) reported that further increases in air temperature may shorten crop life cycles and accelerate crop development rates, implying increased respiration losses, reduced biomass accumulation and reduced crop yields. Meza et al. (2008) also found that climate change will cause crops to complete their growth in a shorter period of time and this will result in a 10 to 30 % reduction in yield in the future.

Climate change is likely to reduce maize yield at Ambo by an average of 4 % in 2030 if the current varieties are grown under the existing agronomic practice in the near future. This could be associated with the decrease in precipitation and the increase in air temperature during the short rainy season (*Belg*) lead to yield reduction. Low maize yields have a direct impact on food security for the study areas. Rapid changes in basic crop management practices are necessary for the study areas and if not, farmers will be at risk to future climate shocks. Thus, improved crop management practice is needed for the maize cropping system to be more resilient to the changing environmental conditions (Cairns et al., 2013).

On the contrary, future maize yield was projected to increase slightly relative to the baseline yield for Bako. This could be attributed to the increase in precipitation in the main rainy season (*Kiremt)* and the increase in air temperature which seemed to remain favorable for maize yield for this study site. This finding agreed with Araya et al. (2015), who showed that future maize yield was slightly higher than baseline yield at Bako.

4.5.3 Crop management practices as adaptation options

The challenge to produce enough food for the fast-growing population in Ethiopia will be greater under the changing climate unless the farming systems used involve adaptation strategies and/or new technological advancements are achieved. Since rainfed maize production is vital for food security in Ethiopia (Abate et al., 2015), adapting this cropping system to a drier and warmer future climatic condition is important. In the future climate, maize would have a reduced time to flowering and to maturity due to the projected high maximum and minimum air temperature for the study sites. The suitability of early, medium, and late maturing cultivars for low- and high-rainfall environments differ. Therefore, adjusting planting date, nitrogen application level and choosing the appropriate cultivar could be considered three agronomic approaches which can be used to minimize the impact of climate change on maize and to increase yield.

Under future climate early planting between 15 May to 01 June resulted an improved relative yields for all maize cultivars for Ambo. The result is supported by Abraha and Savage (2006) who reported that early planting allows the maize crop to escape the hot weather of a future environment and increase yield compared to that for the local and late planting dates in the midlands of KwaZulu-Natal, South Africa. The increased N fertilizer level from 23-150 kg ha^{-1} resulted improved yields for all cultivars when combined with early planting at Ambo. Nitrogen fertilizer is a key nutrient for crop growth to achieve the yield potential of new cultivars (Foulkes et al., 2011).

Nitrogen management together with a shift in planting date were one of the most important adaptation strategies tested, in terms of yield impact for Bako. For example, early planting combined with a nitrogen fertilizer level of 23-100 kg ha^{-1} provided higher relative yields under the future climate. Delayed planting has a negative influence on maize production under the future climate. Our results differed from Abera et al. (2018) who suggested that combining high fertilizer levels with late planting resulted increased yields for Bako. The results from the current study suggests that improvements in crop management practices could lead to increased yields.

All planting dates considered resulted in negative relative yields for Melkassa. However, late planting had reduced relative yields compared to early planting. Higher fertilizer levels (100-150 kg ha^{-1}) seem to reduce yield reductions under the future climate, but this varied among maize cultivars studied. Planting the Jibat cultivar between 15 and 30 June at higher N levels may reduce severe yield reductions of maize at Melkassa. The result agrees with Challinor et al. (2014) who showed long-season cultivar can compensate for the reduced growth duration resulting from future increased air temperatures.

4.5.4 Crop and climate models uncertainty in yield simulation

The AquaCrop (water-driven) model over-predicted maize yield in most cases during the simulation period for the study sites (Figure 4.10a-b and see Appendix 2, Figure SM4b-c). This might be due to the simplification of complex processes in AquaCrop (Araya et al., 2017a, b) as compared to DSSAT and APSIM (radiation-driven) models. In addition, the AquaCrop model has high extrapolative capability by allowing the normalized water productivity to account for climatic condition and yield simulation (Kanda et al., 2018). Furthermore, there are several factors such as biotic and abiotic stresses (Gariby et al., 2019) as well as pedo-climatic conditions (Brilli et al., 2017) that are not accounted for in the models used and could have attributed toward the over-prediction of crop yield. On the other hand, DSSAT (radiation-driven) model underestimated maize yield for some cultivars for the study sites. This is explained by the performance of DSSAT model varied amongst locations and cultivars (Sharda et al., 2021). For this study, compared to crop models, GCM uncertainty in predicted future maize yield is relatively larger. These results are consistent with other studies of climate change impact quantification on maize crop (Kassie et al., 2015; Zhang et al., 2015). However, the result is in contrast to the findings of another study reporting that uncertainty from crop models were higher than those from GCMs (Asseng et al., 2013; Yang et al., 2014; Araya et al., 2015).

4.5.4 Conclusions

This study quantifies the impact of climate change on maize production in tropical environments of Ethiopia and the role of crop management practices as an adaptation mechanism under future climate. The analysis of climate change scenarios of seven GCM models and RCP 8.5 indicates compromised climatic conditions for maize growth. The results indicate that both average monthly maximum and minimum air temperature will increase in the study areas by 2030. GCMs ensemble show that the monthly average maximum air temperature will increase during the *Belg* and the *Bega* seasons rather than the *Kiremt* season in 2030. The monthly average minimum air temperature may increase during the *Belg* season at all sites.

Monthly total precipitation will remain almost the same as the baseline while the *Belg* season monthly total precipitation will decrease at Ambo under the future climate. The *Kiremt* season monthly total precipitation, on the other hand, may significantly increase at Bako in 2030. However, future monthly total precipitation will reduce considerably for the *Belg* and *Kiremt* seasons at Melkassa in 2030. These would result in a mean maize yield reduction of 4 and 16 % at Ambo and Melkassa respectively, and a mean maize yield increase of 2 % at Bako in 2030.

The projected climate change, with increasing air temperatures and changes in precipitation, will become a threat to Ethiopian food production unless adaptation strategies are applied. In the higher altitude (Ambo), early planting of maize cultivars between 15 May to 01 June would result in improved relative yields in the future climate. Generally, combining early planting with an increase fertilizer levels between 23-150 kg ha^{-1} will result in improved yields for all maize cultivars in Ambo. For the mid altitude (Bako), planting after 15 May has either no or negative effect on maize yield. However, early planting combined with a nitrogen fertilizer level of 23-100 kg ha^{-1} provided higher relative yields under the future climate in Bako. Delayed planting has a negative influence on maize production for Bako under the future climate (2030). For the lower altitude (Melkassa), all planting dates considered resulted in a negative relative yield. However, late planting would have lower relative yields compared to early planting. Higher fertilizer levels (100-150 kg ha^{-1}) seem to reduce yield reductions under the future climate, but this varied among maize cultivars studied. Planting the Jibat cultivar between 15-30 June at higher N levels may reduce severe yield reduction of maize at Melkassa. The output of this study is importance, since it can assist farmers to change their crop management practices and agricultural policy makers at the regional level for sustainable maize production in the study region.

4.6 References

Abate, T., Shiferaw, B., Menkir, A., Wegary, D., Kebede, Y., Tesfaye, K., Kassie, M., Bogale, G., Tadesse, B. and Keno, T., 2015. Factors that transformed maize productivity in Ethiopia. *Food Security*, *7*(5), pp. 965-981.

Abera, K., Crespo, O., Seid, J. and Mequanent, F., 2018. Simulating the impact of climate change on maize production in Ethiopia, East Africa. *Environmental Systems Research*, *7*(1), pp. 1-12.

Abraha, M.G. and Savage, M.J., 2006. Potential impacts of climate change on the grain yield of maize for the midlands of KwaZulu-Natal, South Africa. *Agriculture, Ecosystems and Environment*, *115*(1-4), pp. 150-160.

Alemu, H.W. and Carlson, A.S., 2020. Thirteen years on: The long journey of optometry in Ethiopia. *African Vision and Eye Health*, *79*(1), pp. 1-6.

Alemu, T. and Mengistu, A., 2019. Impacts of climate change on food security in Ethiopia: adaptation and mitigation options: a review. *Climate Change-Resilient Agriculture and Agroforestry*, pp. 397-412.

Allen, R.G., Pereira, L.S., Raes, D. and Smith, M., 1998. Crop evapotranspiration-Guidelines for computing crop water requirements-FAO Irrigation and drainage paper 56. *FAO, Rome*, *300*(9), p. 5109.

Allen, R.G., Pruitt, W.O., Wright, J.L., Howell, T.A., Ventura, F., Snyder, R., Itenfisu, D., Steduto, P., Berengena, J., Yrisarry, J.B. and Smith, M., 2006. A recommendation on standardized surface resistance for hourly calculation of reference ETo by the FAO56 Penman-Monteith method. *Agricultural Water Management*, *81*(1-2), pp. 1-22.

Araya, A., Hoogenboom, G., Luedeling, E., Hadgu, K.M., Kisekka, I. and Martorano, L.G., 2015. Assessment of maize growth and yield using crop models under present and future climate in southwestern Ethiopia. *Agricultural and Forest Meteorology*, *214*, pp. 252-265.

Araya, A., Kisekka, I., Gowda, P.H. and Prasad, P.V., 2017a. Evaluation of water-limited cropping systems in a semi-arid climate using DSSAT-CSM. *Agricultural Systems*, *150*, pp. 86-98.

Araya, A., Kisekka, I., Lin, X., Prasad, P.V., Gowda, P.H., Rice, C. and Andales, A., 2017b. Evaluating the impact of future climate change on irrigated maize production in Kansas. *Climate Risk Management*, *17*, pp. 139-154.

Arnell, N.W., 2004. Climate change and global water resources: SRES emissions and socio-economic scenarios. *Global Environmental Change*, *14*, pp. 31-52.

Asfaw, A., Simane, B., Hassen, A. and Bantider, A., 2018. Variability and time series trend analysis of rainfall and temperature in northcentral Ethiopia: A case study in Woleka sub-basin. *Weather and Climate Extremes*, *19*, pp. 29-41.

Asseng, S., Ewert, F., Martre, P., Rötter, R.P., Lobell, D.B., Cammarano, D., Kimball, B.A., Ottman, M.J., Wall, G.W., White, J.W. and Reynolds, M.P., 2015. Rising temperatures reduce global wheat production. *Nature Climate Change*, *5*(2), pp. 143-147.

Asseng, S., Ewert, F., Rosenzweig, C., Jones, J.W., Hatfield, J.L., Ruane, A.C., Boote, K.J., Thorburn, P.J., Rötter, R.P., Cammarano, D. and Brisson, N., 2013. Uncertainty in simulating wheat yields under climate change. *Nature Climate Change*, *3*(9), pp. 827-832.

Asseng, S., Foster, I.A.N. and Turner, N.C., 2011. The impact of temperature variability on wheat yields. *Global Change Biology*, *17*(2), pp. 997-1012.

Bao, Y., Hoogenboom, G., McClendon, R. and Vellidis, G., 2017. A comparison of the performance of the CSM-CERES-Maize and EPIC models using maize variety trial data. *Agricultural Systems*, *150*, pp. 109-119.

Bassu, S., Brisson, N., Durand, J.L., Boote, K., Lizaso, J., Jones, J.W., Rosenzweig, C., Ruane, A.C., Adam, M., Baron, C. and Basso, B., 2014. How do various maize crop models vary in their responses to climate change factors? *Global Change Biology*, *20*(7), pp. 2301-2320.

Belay, A., Recha, J.W., Woldeamanuel, T. and Morton, J.F., 2017. Smallholder farmers' adaptation to climate change and determinants of their adaptation decisions in the Central Rift Valley of Ethiopia. *Agriculture and Food Security*, *6*(1), pp. 1-13.

Brilli, L., Bechini, L., Bindi, M., Carozzi, M., Cavalli, D., Conant, R., Dorich, C.D., Doro, L., Ehrhardt, F., Farina, R. and Ferrise, R., 2017. Review and analysis of strengths and weaknesses of agro-ecosystem models for simulating C and N fluxes. *Science of the Total Environment*, *598*, pp. 445-470.

Bryan, E., Deressa, T.T., Gbetibouo, G.A. and Ringler, C., 2009. Adaptation to climate change in Ethiopia and South Africa: options and constraints. *Environmental Science and Policy*, *12*(4), pp. 413-426.

Cairns, J.E., Sonder, K., Zaidi, P.H., Verhulst, N., Mahuku, G., Babu, R., Nair, S.K., Das, B., Govaerts, B., Vinayan, M.T. and Rashid, Z., 2012. Maize production in a changing climate: impacts, adaptation, and mitigation strategies. *Advances in agronomy*, *114*, pp. 1-58.

CCCMA, 2017b. Second Generation Canadian Earth System Model [Online]. Government of Canada. Canadian Centre for Climate Mod.

http://www.ec.gc.ca/ccmaccccma/default.asp?lang=En&xml=1A3B7DF1-99BB-4EC8-B129-09F83E72D645, Accessed date: 1 July 2020.

Challinor, A.J., Simelton, E.S., Fraser, E.D., Hemming, D. and Collins, M., 2010. Increased crop failure due to climate change: assessing adaptation options using models and socio-economic data for wheat in China. *Environmental Research Letters*, *5*(3), pp.1-8.

Challinor, A.J., Watson, J., Lobell, D.B., Howden, S.M., Smith, D.R. and Chhetri, N., 2014. A meta-analysis of crop yield under climate change and adaptation. *Nature Climate Change*, *4*(4), pp. 287-291.

Cheung, W.H., Senay, G.B. and Singh, A., 2008. Trends and spatial distribution of annual and seasonal rainfall in Ethiopia. *International Journal of Climatology: A Journal of the Royal Meteorological Society*, *28*(13), pp.1723-1734.

Collins, W.J., Bellouin, N., Doutriaux-Boucher, M., Gedney, N., Halloran, P., Hinton, T., Hughes, J., Jones, C.D., Joshi, M., Liddicoat, S. and Martin, G., 2011. Development and evaluation of an Earth-System model–HadGEM2. *Geoscience Model Development Discuss*, *4*(2), pp. 997-1062.

Conway, D. and Schipper, E.L.F., 2011. Adaptation to climate change in Africa: Challenges and opportunities identified from Ethiopia. *Global Environmental Change*, *21*(1), pp. 227-237.

CSA (Central Statistical Agency), 2010. Agricultural sample survey 2009/2010. Report on farm management practices. Private peasant holdings, Meher season. Statistics Bulletin. Addis Ababa, Ethiopia. pp. 5-8.

CSA (Central Statistical Agency), 2020. Agricultural sample survey 2019/2020. Area and Production of Major Crops. Private peasant holdings, Meher season. Statistics Bulletin. Addis Ababa, Ethiopia. pp. 1-133.

Deb, P., Shrestha, S. and Babel, M.S., 2015. Forecasting climate change impacts and evaluation of adaptation options for maize cropping in the hilly terrain of Himalayas: Sikkim, India. *Theoretical and Applied Climatology*, *121*(3), pp. 649-667.

Deressa, T.T., Hassan, R.M., Ringler, C., Alemu, T. and Yesuf, M., 2009. Determinants of farmers' choice of adaptation methods to climate change in the Nile Basin of Ethiopia. *Global Environmental Change*, *19*(2), pp. 248-255.

Dufresne, J.L., Foujols, M.A., Denvil, S., Caubel, A., Marti, O., Aumont, O., Balkanski, Y., Bekki, S., Bellenger, H., Benshila, R. and Bony, S., 2013. Climate change projections using the IPSL-CM5 Earth System Model: from CMIP3 to CMIP5. *Climate Dynamics*, *40*(9-10), pp. 2123-2165.

EPCC (Ethiopian Panel on Climate Change), (2015). First assessment report, Working Group II Agriculture and Food Security, Published by the Ethiopian Academy of Sciences. pp. 1-109.

Feleke, H.G., Savage, M.J. and Tesfaye, K., 2021. Calibration and validation of APSIM–Maize, DSSAT CERES–Maize and AquaCrop models for Ethiopian tropical environments. *South African Journal of Plant and Soil*, *38*(1), pp. 36-51.

Field, C.B., Barros, V., Stocker, T.F. and Dahe, Q. eds., 2012. *Managing the risks of extreme events and disasters to advance climate change adaptation: special report of the Intergovernmental Panel on Climate Change*. Cambridge University Press.

Foulkes, M.J., Slafer, G.A., Davies, W.J., Berry, P.M., Sylvester-Bradley, R., Martre, P., Calderini, D.F., Griffiths, S. and Reynolds, M.P., 2011. Raising yield potential of wheat. III. Optimizing partitioning to grain while maintaining lodging resistance. *Journal of Experimental Botany*, *62*(2), pp. 469-486.

Garibay, V.M., Kothari, K., Ale, S., Gitz III, D.C., Morgan, G.D. and Munster, C.L., 2019. Determining water-use-efficient irrigation strategies for cotton using the DSSAT CSM CROPGRO-cotton model evaluated with in-season data. *Agricultural Water Management*, *223*, pp. 1-35.

Giorgi, F., Jones, C. and Asrar, G.R., 2009. Addressing climate information needs at the regional level: the CORDEX framework. *World Meteorological Organization (WMO) Bulletin*, *58*(3), pp. 175-183.

Hazeleger, W., Severijns, C., Semmler, T., Ştefănescu, S., Yang, S., Wang, X., Wyser, K., Dutra, E., Baldasano, J.M., Bintanja, R. and Bougeault, P., 2010. EC-Earth: a seamless earth-system prediction approach in action. *Bulletin of the American Meteorological Society*, *91*(10), pp. 1357-1364.

Hoogenboom, G., Porter, C.H., Boote, K.J., Shelia, V., Wilkens, P.W., Singh, U., White, J.W., Asseng, S., Lizaso, J.I., Moreno, L.P. and Pavan, W., 2019. The DSSAT crop modeling ecosystem. *Advances in Crop Modeling for a Sustainable Agriculture*, pp. 173-216.

IPCC (Intergovernmental Panel on Climate Change), 2014. In Core Writing Team, R. K. Pachauri, and L. A. Meyer (Eds.) Climate change: Synthesis report. The contribution of working groups I, II and III to the fifth assessment report of the intergovernmental panel on climate change. IPCC, Geneva.

Jeffrey, S.J., Rotstayn, L., Collier, M., Dravitzki, S., Hamalainen, C., Moeseneder, C., Wong, K.K. and Syktus, J., 2013. Australia's CMIP5 submission using the CSIRO-Mk3. 6 model. *Australia Meteorology Oceanography Journal*, *63*, pp. 1-13.

Kanda, E.K., Mabhaudhi, T. and Senzanje, A., 2018. Coupling hydrological and crop models for improved agricultural water management–A review. *Bulgarian Journal of Agricultural Science*, *24*(3), pp. 380-390.

Kassie, B.T., Asseng, S., Rotter, R.P., Hengsdijk, H., Ruane, A.C. and Van Ittersum, M.K., 2015. Exploring climate change impacts and adaptation options for maize production in the Central Rift Valley of Ethiopia using different climate change scenarios and crop models. *Climatic Change*, *129*(1), pp. 145-158.

Kassie, B.T., Hengsdijk, H., Rötter, R., Kahiluoto, H., Asseng, S. and Van Ittersum, M., 2013. Adapting to climate variability and change: experiences from cereal-based farming in the Central Rift and Kobo Valleys, Ethiopia. *Environmental Management*, *52*(5), pp. 1115-1131.

Keating, B.A., Carberry, P.S., Hammer, G.L., Probert, M.E., Robertson, M.J., Holzworth, D., Huth, N.I., Hargreaves, J.N., Meinke, H., Hochman, Z. and McLean, G., 2003. An overview of APSIM, a model designed for farming systems simulation. *European Journal of Agronomy*, *18*(3-4), pp. 267-288.

Kelbore, Z.G., 2012. An analysis of the impacts of climate change on crop yield and yield variability in Ethiopia. Munich Personal RePEc Archive. pp. 1-45.

Levy, P.E., Cannell, M.G.R. and Friend, A.D., 2004. Modelling the impact of future changes in climate, CO2 concentration and land use on natural ecosystems and the terrestrial carbon sink. *Global Environmental Change*, *14*, pp. 21-30.

Liben, F.M., Wortmann, C.S., Yang, H., Lindquist, J.L., Tadesse, T. and Wegary, D., 2018. Crop model and weather data generation evaluation for conservation agriculture in Ethiopia. *Field Crops Research*, *228*, pp. 122-134.

Lobell, D.B., Hammer, G.L., McLean, G., Messina, C., Roberts, M.J. and Schlenker, W., 2013. The critical role of extreme heat for maize production in the United States. *Nature Climate Change*, *3*(5), pp. 497-501.

Martins, P., 2014. Structural change in Ethiopia: an employment perspective. *World Bank Policy Research Working Paper*, 6749. pp. 3-40.

McSweeney, C., New, M. and Lizcano, G., 2008. United Nation Development Programme (UNDP) Climate Change Country Profiles–Ethiopia. J. *Meteorology Oceanography*. 63, pp. 1–13.

Mera, G.A., 2018. Drought and its impacts in Ethiopia. *Weather and Climate Extremes*, *22*, pp. 24-35.

Meza, F.J., Silva, D. and Vigil, H., 2008. Climate change impacts on irrigated maize in Mediterranean climates: evaluation of double cropping as an emerging adaptation alternative. *Agricultural Systems*, *98*(1), pp. 21-30.

Mideksa, T.K. and Kallbekken, S., 2010. The impact of climate change on the electricity market: A review. *Energy Policy*, *38*(7), pp. 3579-3585.

Muluneh, A., Biazin, B., Stroosnijder, L., Bewket, W. and Keesstra, S., 2015. Impact of predicted changes in rainfall and atmospheric carbon dioxide on maize and wheat yields in the Central Rift Valley of Ethiopia. *Regional Environmental Change*, *15*(6), pp. 1105-1119.

Muluneh, A., Stroosnijder, L., Keesstra, S. and Biazin, B., 2017. Adapting to climate change for food security in the Rift Valley dry lands of Ethiopia: supplemental irrigation, plant density and sowing date. *The Journal of Agricultural Science*, *155*(5), pp. 703-724.

Ngai, S.T., Tangang, F. and Juneng, L., 2017. Bias correction of global and regional simulated daily precipitation and surface mean temperature over Southeast Asia using quantile mapping method. *Global and Planetary Change*, *149*, pp. 79-90.

Nikulin, G., Jones, C., Giorgi, F., Asrar, G., Büchner, M., Cerezo-Mota, R., Christensen, O.B., Déqué, M., Fernandez, J., Hänsler, A. and van Meijgaard, E., 2012. Precipitation climatology in an ensemble of CORDEX-Africa regional climate simulations. *Journal of Climate*, *25*(18), pp. 6057-6078.

NMA (National Meteorological Agency of Ethiopia), 2007. Climate change national adaptation program of action (NAPA) of Ethiopia.

Raes, D., Sithole, A., Makarau, A. and Milford, J., 2004. Evaluation of first planting dates recommended by criteria currently used in Zimbabwe. *Agricultural and forest meteorology*, *125*(3-4), pp. 177-185.

Rosenzweig, C. and Wilbanks, T.J., 2010. The state of climate change vulnerability, impacts, and adaptation research: strengthening knowledge base and community. *Climatic Change*, *100*(1), pp. 103-106.

Rötter, R.P., Carter, T.R., Olesen, J.E. and Porter, J.R., 2011. Crop–climate models need an overhaul. *Nature Climate Change*, *1*(4), pp. 175-177.

Samuelsson, P., Jones, C.G., Will´ En, U., Ullerstig, A., Gollvik, S., Hansson, U.L.F., Jansson, E., Kjellstro¨ M, C., Nikulin, G. and Wyser, K., 2011. The Rossby Centre Regional Climate model RCA3: model description and performance. *Tellus A: Dynamic Meteorology and Oceanography*, *63*(1), pp. 4-23.

Savage, M. J., 2018. A spreadsheet for daily Penman–Monteith reference evaporation from a minimum set of meteorological data. Soil-Plant-Atmosphere Research Unit, School of Agricultural, Earth and Environmental Sciences, University of KwaZulu-Natal, Pietermaritzburg, South Africa.

Setegn, S.G., Rayner, D., Melesse, A.M., Dargahi, B., Srinivasan, R. and Wörman, A., 2011. Climate change impact on agricultural water resources variability in the Northern Highlands of Ethiopia. In Nile River Basin: Hydrology, climate and water use, Melesse A.M. (ed). Springler: Dordrecht, New York. pp. 241-265.

Seyoum, S., Chauhan, Y., Rachaputi, R., Fekybelu, S. and Prasanna, B., 2017. Characterising production environments for maize in eastern and southern Africa using the APSIM Model. *Agricultural and Forest Meteorology*, *247*, pp. 445-453.

Seyoum, S., Rachaputi, R., Chauhan, Y., Prasanna, B. and Fekybelu, S., 2018. Application of the APSIM model to exploit G× E× M interactions for maize improvement in Ethiopia. *Field Crops Research*, *217*, pp. 113-124.

Sharda, V., Mekonnen, M.M., Ray, C. and Gowda, P.H., 2021. Use of Multiple Environment Variety Trials Data to Simulate Maize Yields in the Ogallala Aquifer Region: A Two Model Approach. *Journal of the American Water Resources Association*, *57*(2), pp. 281-295.

Shiferaw, B., Prasanna, B.M., Hellin, J. and Bänziger, M., 2011. Crops that feed the world 6. Past successes and future challenges to the role played by maize in global food security. *Food Security*, *3*(3), pp. 307-327.

Steduto, P., Hsiao, T.C., Raes, D. and Fereres, E., 2009. AquaCrop—The FAO crop model to simulate yield response to water: I. Concepts and underlying principles. *Agronomy Journal*, *101*(3), pp. 426-437.

Tachie-Obeng, E., Akponikpe, P.B.I. and Adiku, S., 2013. Considering effective adaptation options to impacts of climate change for maize production in Ghana. *Environmental Development*, *5*, pp. 131-145.

Tao, F. and Zhang, Z., 2010. Adaptation of maize production to climate change in North China Plain: quantify the relative contributions of adaptation options. *European Journal of Agronomy*, *33*(2), pp. 103-116.

Tesfaye, K., Gbegbelegbe, S., Cairns, J.E., Shiferaw, B., Prasanna, B.M., Sonder, K., Boote, K., Makumbi, D. and Robertson, R., 2015. Maize systems under climate change in sub-Saharan Africa: potential impacts on production and food security. *International Journal of Climate Change Strategies and Management*, 7(3), pp. 247-271.

Tesfaye, K., Kruseman, G., Cairns, J.E., Zaman-Allah, M., Wegary, D., Zaidi, P.H., Boote, K.J. and Erenstein, O., 2018. Potential benefits of drought and heat tolerance for adapting maize to climate change in tropical environments. *Climate Risk Management*, *19*, pp.106-119.

Tesfaye, K., Zaidi, P.H., Gbegbelegbe, S., Boeber, C., Getaneh, F., Seetharam, K., Erenstein, O. and Stirling, C., 2017. Climate change impacts and potential benefits of heat-tolerant maize in South Asia. *Theoretical and Applied Climatology*, *130*(3), pp. 959-970.

Thomas, T.S., Dorosh, P.A. and Robertson, R.D., 2019. *Climate change impacts on crop yields in Ethiopia*. IFPRI: Paris, France. 130, pp. 3-15.

Tripathi, A. and Mishra, A.K., 2017. Knowledge and passive adaptation to climate change: An example from Indian farmers. *Climate Risk Management*, *16*, pp. 195-207.

Viste, E., Korecha, D. and Sorteberg, A., 2013. Recent drought and precipitation tendencies in Ethiopia. *Theoretical and Applied Climatology*, *112*(3), pp. 535-551.

Voldoire, A., Sanchez-Gomez, E., y Mélia, D.S., Decharme, B., Cassou, C., Sénési, S., Valcke, S., Beau, I., Alias, A., Chevallier, M. and Déqué, M., 2013. The CNRM-CM5 1 global climate model: description and basic evaluation. *Climate Dynamics*, *40*(9-10), pp. 2091-2121.

Wang, M., Li, Y., Ye, W., Bornman, J.F. and Yan, X., 2011. Effects of climate change on maize production, and potential adaptation measures: a case study in Jilin Province, China. *Climate Research*, *46*(3), pp. 223-242.

Watanabe, M., Suzuki, T., O'ishi, R., Komuro, Y., Watanabe, S., Emori, S., Takemura, T., Chikira, M., Ogura, T., Sekiguchi, M. and Takata, K., 2010. Improved climate simulation by MIROC5: Mean states, variability, and climate sensitivity. *Journal of Climate*, *23*(23), pp. 6312-6335.

White, J.W., Hoogenboom, G., Kimball, B.A. and Wall, G.W., 2011. Methodologies for simulating impacts of climate change on crop production. *Field Crops Research*, *124*(3), pp. 357-368.

Williams, A.P., Funk, C., Michaelsen, J., Rauscher, S.A., Robertson, I., Wils, T.H., Koprowski, M., Eshetu, Z. and Loader, N.J., 2012. Recent summer precipitation trends in the Greater Horn of Africa and the emerging role of Indian Ocean Sea surface temperature. *Climate Dynamics*, *39*(9-10), pp. 2307-2328.

Yang, Q., Lu, T., Yao, T. and Zhang, B., 2014. The impact of uncertainty and ambiguity related to iteration and overlapping on schedule of product development projects. *International Journal of Project Management*, *32*(5), pp. 827-837.

Yimer, G., Jonoski, A. and Griensven, A.V., 2009. Hydrological response of a catchment to climate change in the upper Beles river basin, upper Blue Nile, Ethiopia. *Nile Basin Water Engineering Scientific Magazine*, *2*(1), pp. 49-59.

Yin, X.G., Jabloun, M., Olesen, J.E., Öztürk, I., Wang, M. and Chen, F., 2016. Effects of climatic factors, drought risk and irrigation requirement on maize yield in the Northeast Farming Region of China. *The Journal of Agricultural Science*, *154*(7), pp. 1171-1189.

Zhang, J.P., He, Y.K., Wang, J., Zhao, Y.X. and Wang, C.Y., 2015. Impact simulation of drought at different growth stages on grain formation and yield of maize. *Journal of Agrometeorol*, *36*, pp. 43-49.

Zhao, C., Liu, B., Piao, S., Wang, X., Lobell, D.B., Huang, Y., Huang, M., Yao, Y., Bassu, S., Ciais, P. and Durand, J.L., 2017. Temperature increase reduces global yields of major crops in four independent estimates. *Proceedings of the National Academy of Sciences*, *114*(35), pp. 9326-9331.

Appendix 2

Supplementary materials (SM)

Table SM4a: Evaluation of GCMs outputs in simulating monthly total precipitation and mean monthly maximum and minimum air temperatures at Ambo, Bako and Melkassa for 1995- 2005 period

	Monthly total precipitation		Monthly mean maximum air temperature		Monthly mean minimum air temperature	
	R^2	RMSE (mm)	R^2	RMSE (°C)	R^2	RMSE (°C)
Ambo (high altitude)						
CanESM2	0.66	73.80	0.99	0.09	0.99	0.03
CNRM-CM5	0.81	48.30	0.99	0.09	0.99	0.03
CSIRO-Mk3-6-0	0.87	39.64	0.99	0.10	0.99	0.03
EC-EARTH	0.95	25.62	0.99	0.09	0.99	0.03
HadGEM2-ES	0.90	39.87	0.99	0.10	0.99	0.03
IPSL-CM5A-MR	0.50	76.07	0.99	0.10	0.99	0.03
MIROC5	0.88	34.51	0.99	0.09	0.99	0.03
Bako (mid altitude)						
CanESM2	0.85	56.43	0.99	0.17	1.00	0.00
CNRM-CM5	0.92	54.45	0.99	0.17	1.00	0.00
CSIRO-Mk3-6-0	0.97	65.84	0.99	0.17	1.00	0.00
EC-EARTH	0.97	64.96	0.99	0.17	1.00	0.00
HadGEM2-ES	0.94	59.67	0.99	0.17	1.00	0.00
IPSL-CM5A-MR	0.67	75.05	0.99	0.17	1.00	0.00
MIROC5	0.91	59.06	0.99	0.17	1.00	0.00
Melkassa (low altitude)						
CanESM2	0.79	75.51	1.00	0.02	1.00	0.00
CNRM-CM5	0.05	86.24	1.00	0.02	1.00	0.01
CSIRO-Mk3-6-0	0.80	48.11	1.00	0.02	1.00	0.01
EC-EARTH	0.56	49.65	1.00	0.01	1.00	0.01
HadGEM2-ES	0.79	46.35	1.00	0.02	1.00	0.01
IPSL-CM5A-MR	0.50	67.34	1.00	0.02	1.00	0.01
MIROC5	0.74	57.53	1.00	0.02	1.00	0.01

(a) Ambo

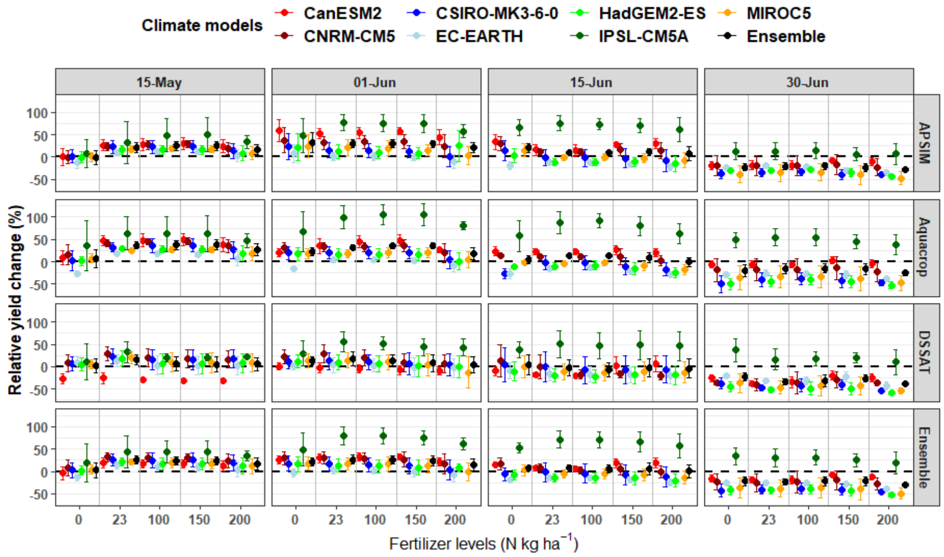

Climate models
CanESM2
CNRM-CM5
CSIRO-MK3-6-0
EC-EARTH
HadGEM2-ES
IPSL-CM5A
MIROC5
Ensemble
15-May
01-Jun
15-Jun
30-Jun
APSIM
Aquacrop
DSSAT
Ensemble
Relative yield change (%)
Fertilizer levels (N kg ha^{-1})

(b) Bako

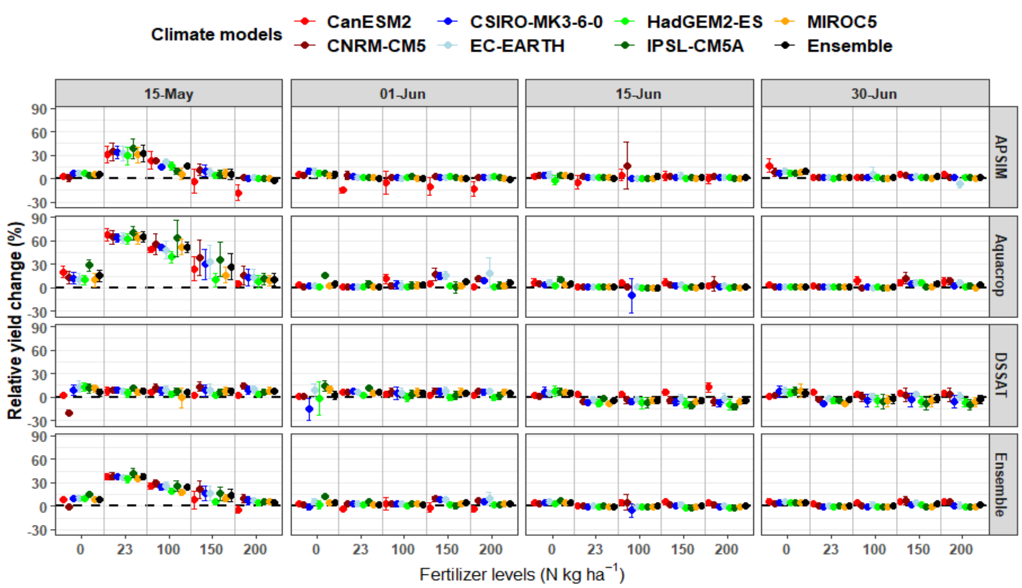

Climate models
CanESM2
CNRM-CM5
CSIRO-MK3-6-0
EC-EARTH
HadGEM2-ES
IPSL-CM5A
MIROC5
Ensemble
15-May
01-Jun
15-Jun
30-Jun
APSIM
Aquacrop
DSSAT
Ensemble
Relative yield change (%)
Fertilizer levels (N kg ha^{-1})

(c) Melkassa

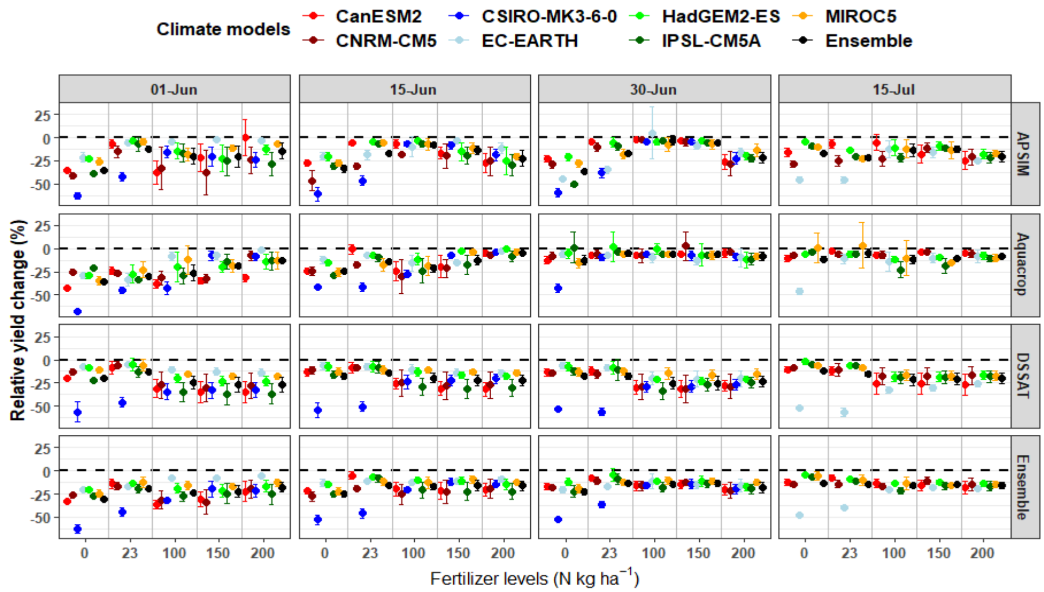

Figure SM4a: Percentage yield differences in 2030 relative to the baseline period as simulated with APSIM, AquaCrop and DSSAT crop models at different planting dates and nitrogen fertilizer levels across cultivars for (a) Ambo (high altitude), (b) Bako (mid-altitude) and (c) Melkassa (low altitude). Error bars show the standard deviation of maize yield change simulated by multiple GCMs

Ambo

(a) APSIM

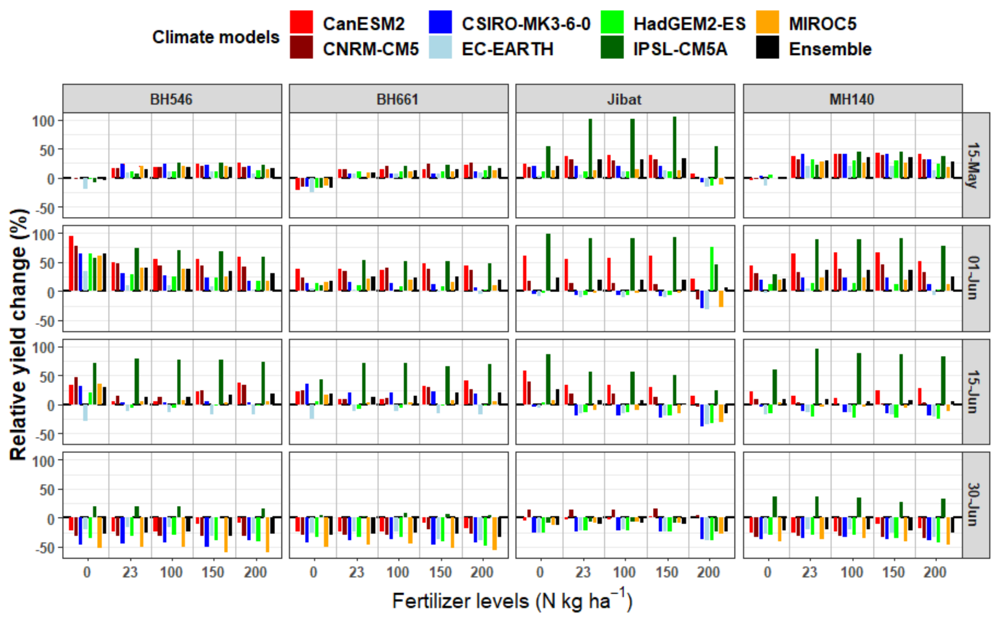

(b) AquaCrop

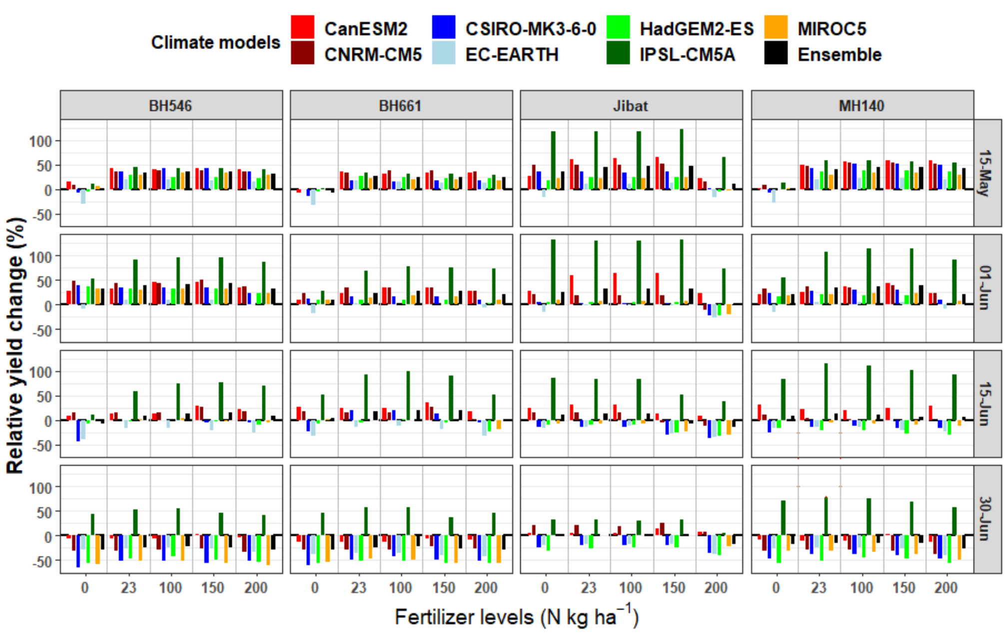

(c) DSSAT

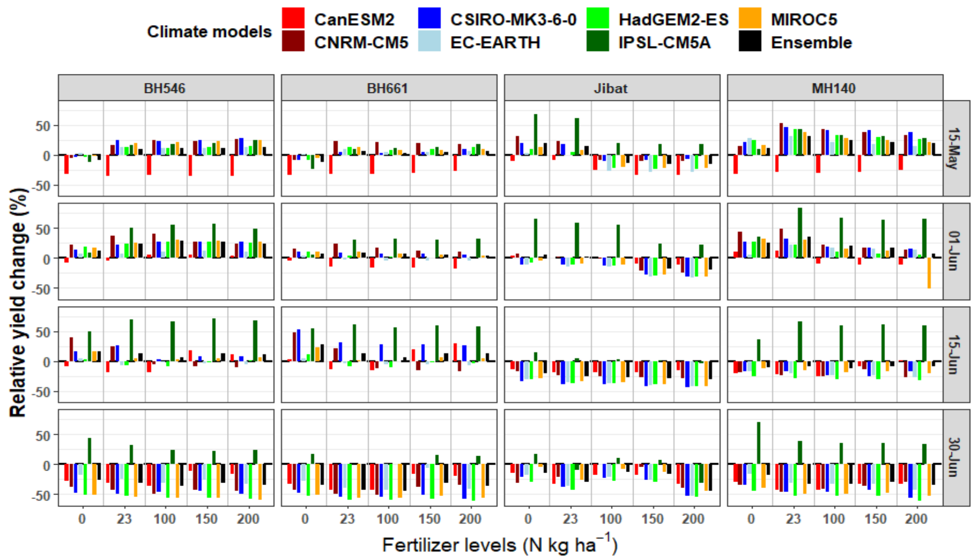

(d) Ensemble

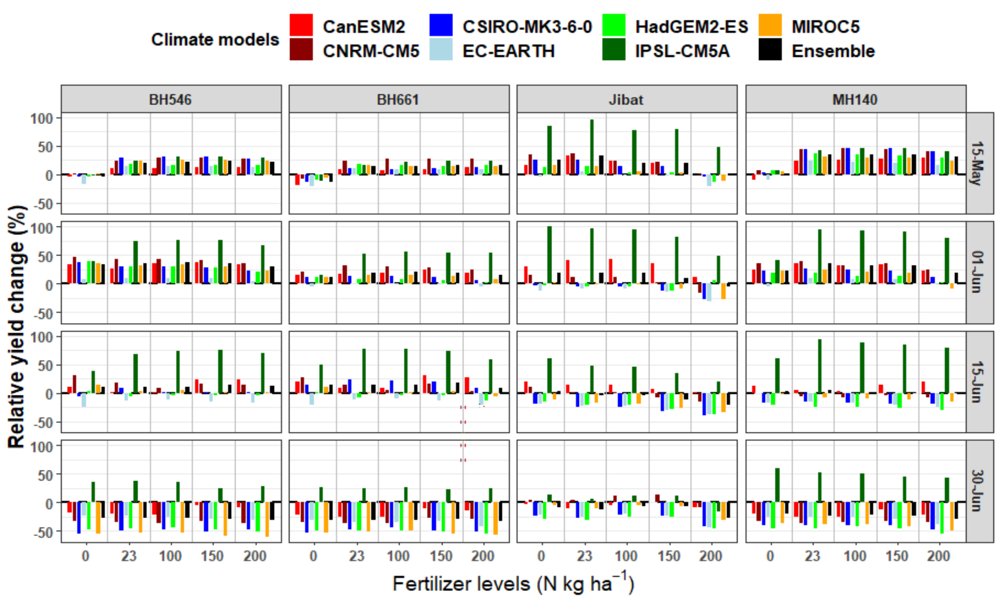

Figure SM4b: Relative mean maize yield change (%) as compared to the baseline as simulated using (a) APSIM, (b) AquaCrop, (c) DSSAT and (d) ensemble based on seven GCMs under RCP8.5 for near future (2030) for Ambo

Bako

(a) APSIM

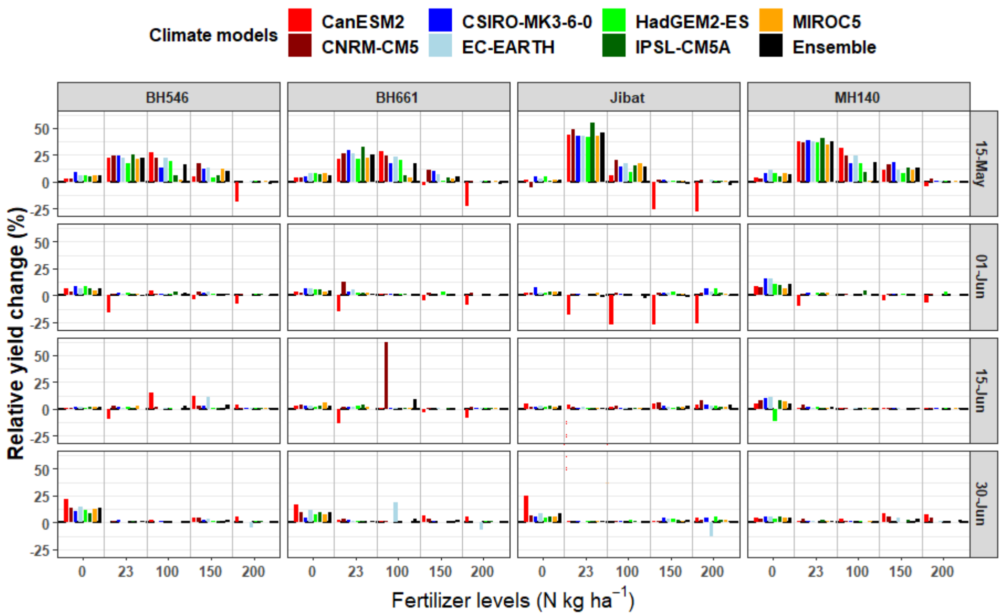

(b) AquaCrop

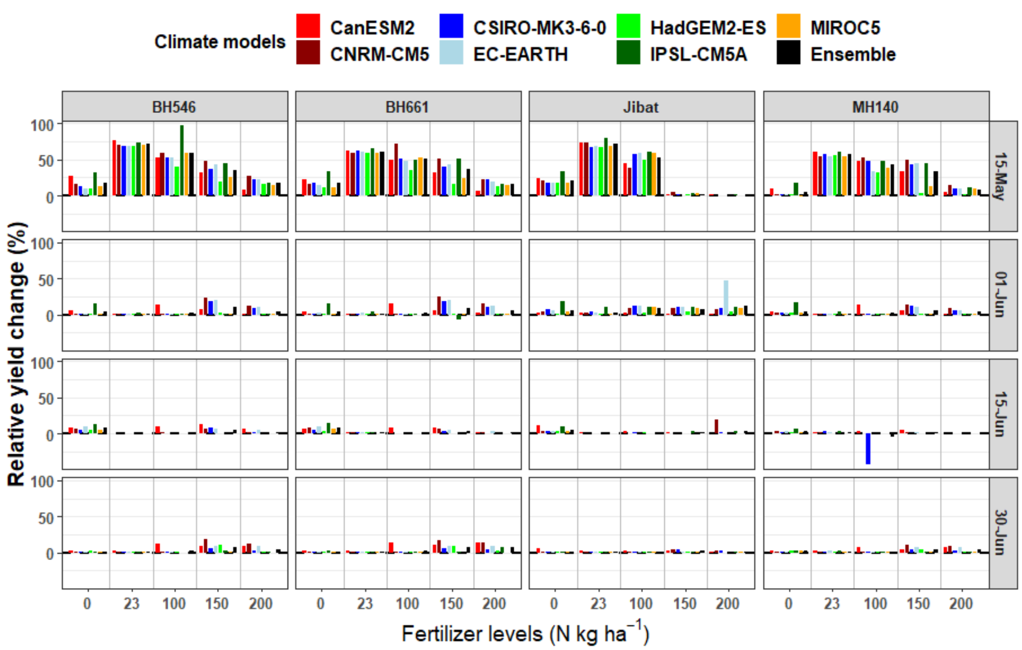

(c) DSSAT

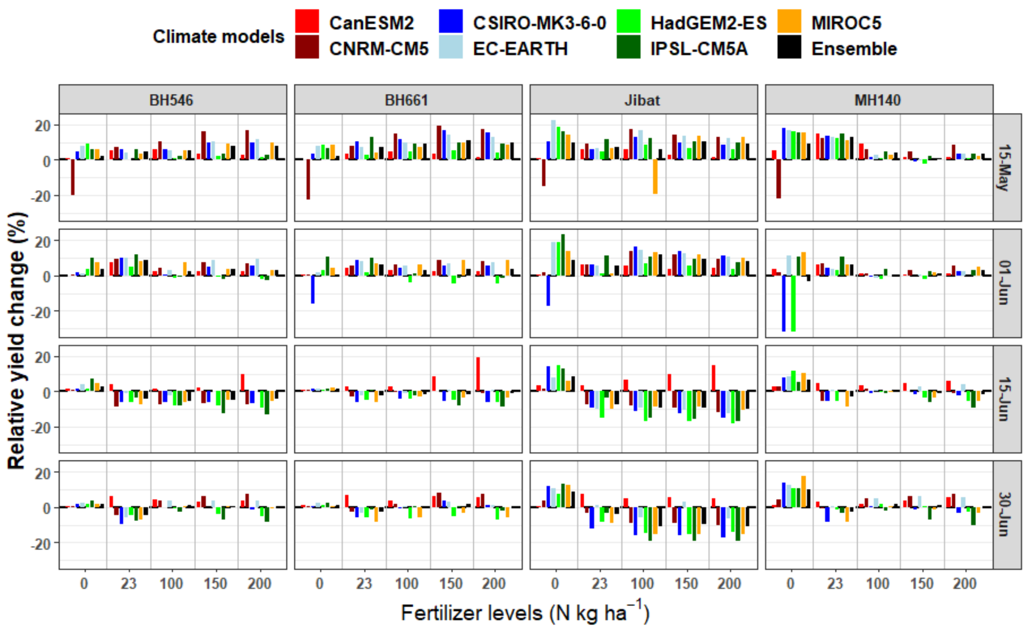

(d) Ensemble

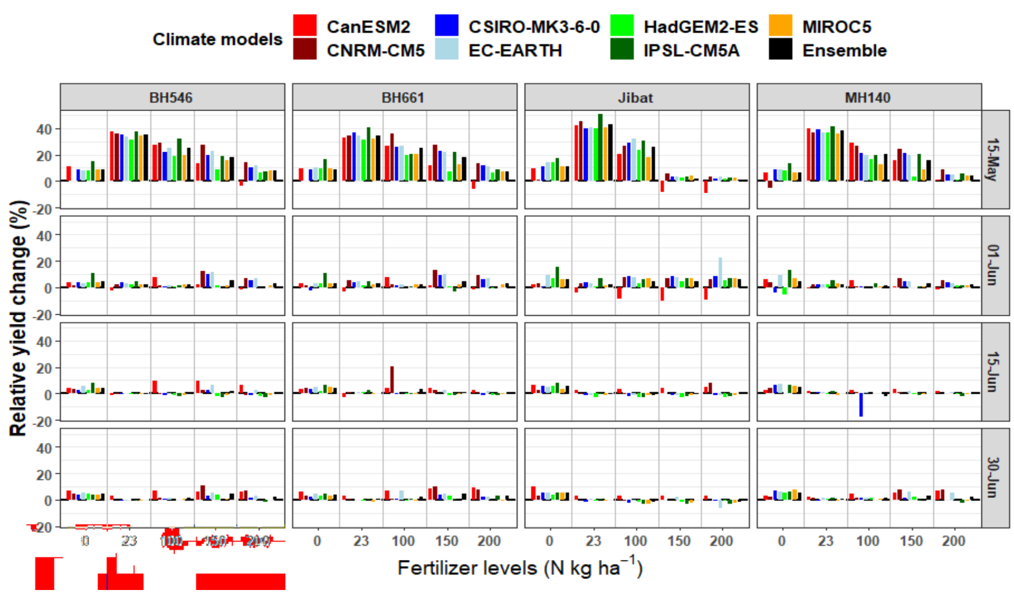

Figure SM4c: Relative mean maize yield change (%) as compared to the baseline as simulated using (a) APSIM, (b) AquaCrop, (c) DSSAT and (d) ensemble based on seven GCMs under RCP8.5 for near future (2030) for Bako

Melkassa

(a) APSIM

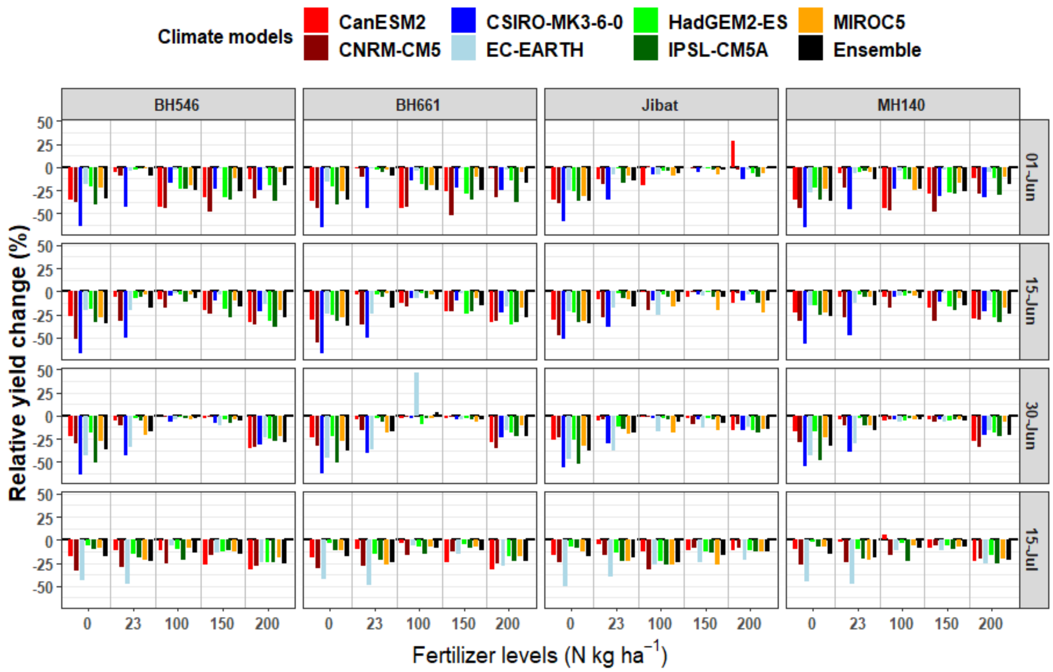

(b) AquaCrop

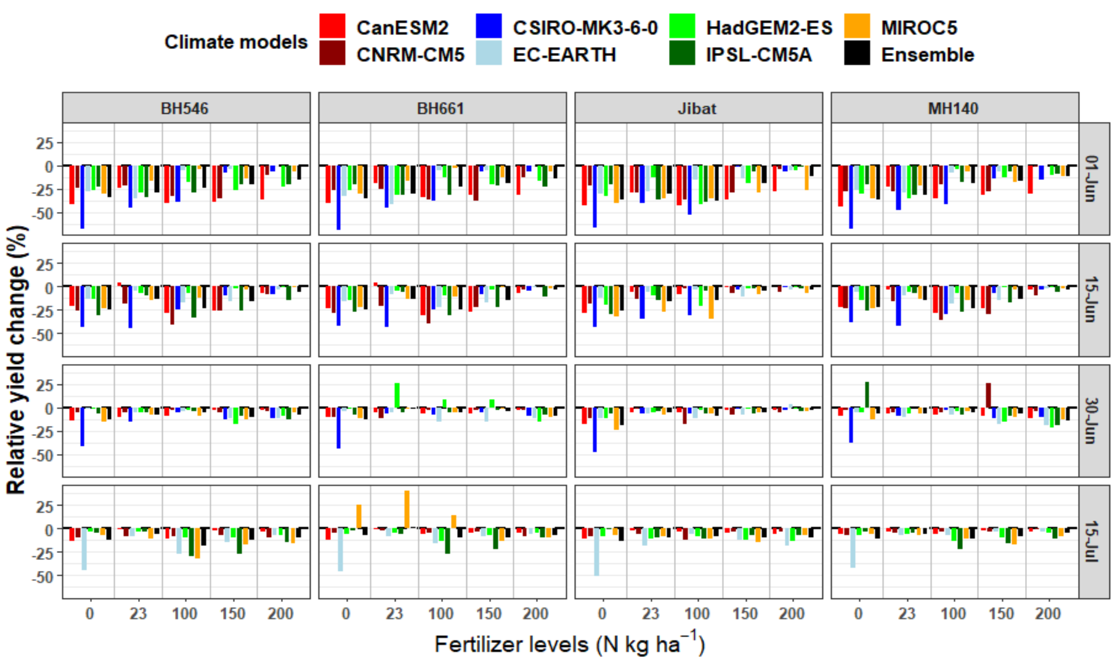

(c) DSSAT

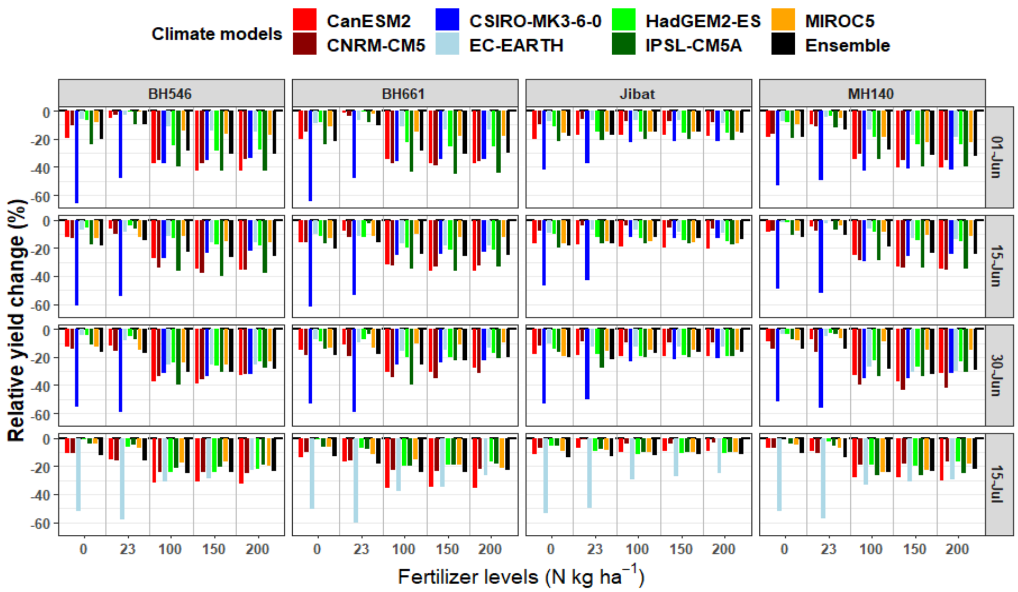

(d) Ensemble

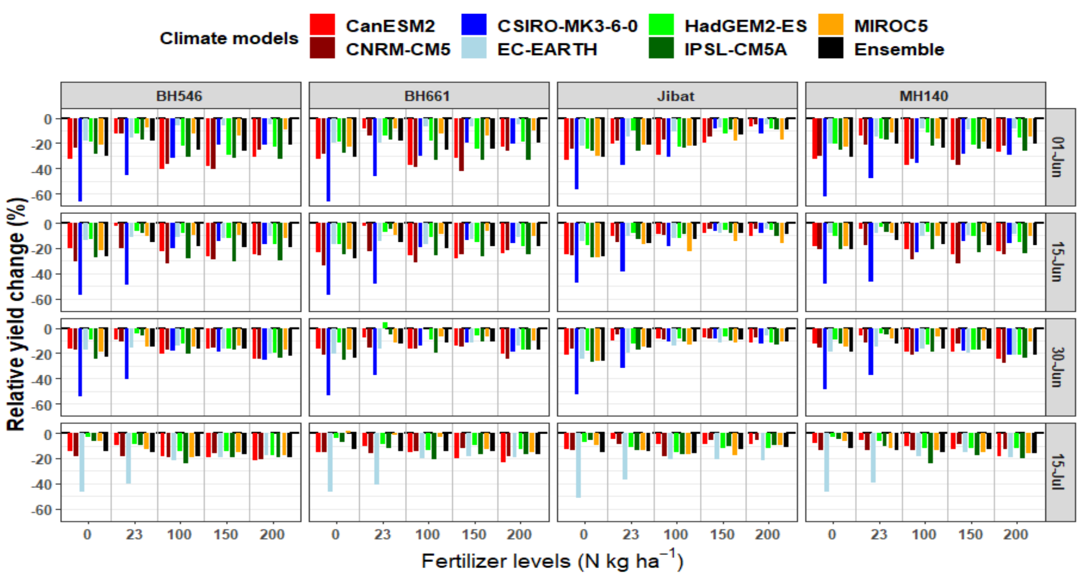

Figure SM4d: Relative mean maize yield change (%) as compared to the baseline as simulated using (a) APSIM, (b) AquaCrop, (c) DSSAT and (d) ensemble based on seven GCMs under RCP8.5 for near future (2030) for Melkassa

Lead to Chapter 5

Chapter 4 mainly focused on the impact assessment of climate change on future precipitation and air temperature and their effect on maize yield. Possible adaptation measures were also explored, to counteract the future climate. In Chapter 5, historical drought events and projected future climate change impacts on drought for the study sites are presented. The observed precipitation and air temperature data are used to assess the past drought events. Also, projected precipitation and air temperature data from the ensemble of seven GCMs are used to analyze future drought characteristics.

CHAPTER 5: DROUGHT RISK ASSESSMENT IN MAIZE (*ZEA MAYS* L.) CULTIVATED AREAS OF ETHIOPIA DUE TO CLIMATE CHANGE

Hirut Getachew Feleke [1*], M.J. Savage [1] and Kindie Tesfaye [2]

[1]Agrometeorology Discipline, Soil-Plant-Atmosphere Continuum Research Unit, School of Agricultural, Earth and Environmental Sciences, University of KwaZulu-Natal, Pietermaritzburg, South Africa

[2]International Maize and Wheat Improvement Centre (CIMMIT), Addis Ababa, Ethiopia

*Corresponding author, email: hirut_ge@yahoo.com

5.1 Abstract

Droughts negatively impact agricultural production. Thus, drought projections are vital for the development of future drought mitigation strategies. This study aimed to assess historical and future drought characteristics using historical observed data for 1995-2017 and an ensemble of seven Global Climate Models (GCMs) from Coupled Model Intercomparison Project (CMIP5) for maize growing areas of Ethiopia. Future drought characteristics were investigated under 8.5 Representative Concentration Pathway (RCP). The widely known Standardized Precipitation Index (SPI) and Standardized Precipitation Evapotranspiration Index (SPEI) were used to investigate drought characteristics. The results indicate that compared to the SPI-based analysis, the SPEI suggests more severe drought conditions over the maize-growing study sites in the

future indicating potential effects of increasing air temperatures on drought risks. The SPI and SPEI at all timescales projected the driest years in the future climate as 2027, 2039, 2042, 2048 and 2049 for Ambo, 2022, 2023, 2042, 2048 and 2049 for Bako, and 2021, 2036, 2044, 2047 and 2048 for Melkassa. SPI and SPEI showed strong correlation ($R > 0.9$) on the direction of change but the effect on drought condition was different. Increasing frequency of moderate to extremely severe drought with extended drought duration was found to occur for Ambo in the future. According to the 6-month SPEI, Bako will experience agricultural droughts with greater severity and duration in the future. Both SPI and SPEI projected increasing drought duration at short and long timescales for Melkassa. However, the 3- and 6-month SPEI predicted the shorter timescale to be more intensive than the longer timescale. The projected moderate to extremely severe drought under future climate will negatively affect maize production for the study sites. Therefore, the development of resilient-improved maize varieties for high air temperature, crop diversification, soil and water conservation, drought tolerance crops for water-limited environments are highly recommended as risk-reducing management options to offset some of the maize yield losses caused by severe drought due to climate change.

Keywords: Ensemble, Global climate models, Representative concentration pathway, SPEI, SPI

5.2 Introduction

Drought is a complex natural hazard that severely affects agriculture (Wang et al., 2014) and the ecosystem (Van Loon, 2015). Its complexity is due to the fact that it is spatially and temporally variable, region-specific and context dependent. Also, drought occurs with varying degrees of intensity, while its cumulative effect makes it difficult to detect its onset and cessation period (Tirivarombo et al., 2018).

Ethiopia is the second highly populated country in Africa, next to Nigeria. The country's population was estimated to be more than 110 million (Alemu and Carlson, 2020). The livelihood of 85 % of its population, depends on agricultural production. The farming system in the country is traditional and affected by climate related hazards including drought. Drought is considered to be the main limiting factor of food security and national sustainable development (Mera, 2018). In recent years, drought has occurred more frequently due to climate change, and this trend remains unchanged and could worsen in the future (Robinson, 2013). Therefore, increased attention to the drought risk and its future potential changes can assist with adaptation to climate change and agricultural production, especially in rain-fed agricultural regions.

Drought is a major climate related natural disaster occasionally affecting Ethiopia. About one hundred years ago, drought frequency occurrence in the country was once every 10 years (Eshetie et al., 2016). However, almost half of rural households in Ethiopia were affected by drought in a five-year period from the year 1999 to 2004 (Dercon et al., 2005). Presently, the drought cycle has become more frequent and occurred in three successive years (Mera, 2018). For example, the 2015 El Niño-induced drought caused food insecurity among 10.2 million people and was one of the most intense droughts in history (FAO, 2016). In most cases, Ethiopian droughts were associated with a failure of major rains (*Kiremt*, June to September) that account for 65–95% of the total annual rainfall, depending on the location (Suryabhagavan, 2017).

Drought is a phenomenon that exists when there is a prolonged water deficit in the atmosphere, soil and rivers (Touma et al., 2015). Drought can be classified as meteorological, agricultural, hydrological, socio-economic drought (Van Loon, 2015; Zhao et al., 2017) and ecological drought (Crausbay et al., 2017). Meteorological drought is characterized by a prolonged deficit of precipitation combined with increased potential evapotranspiration extending over a large area for a long period of time. Agricultural drought is characterized by deficits of total soil moisture and results mainly from the shortage of precipitation. Hydrological drought is related to a shortage of precipitation and/or subsurface water supply (i.e., stream flow, reservoir and lake levels, and groundwater). Socioeconomic drought is associated with the impacts of meteorological, agricultural, and hydrological droughts on the socioeconomic sectors (Van Loon, 2015). Ecological drought is an episodic deficit in water availability that drives ecosystems beyond thresholds of vulnerability, impacts ecosystem services, and triggers feedbacks in natural and/or human systems (Crausbay et al., 2017).

In previous studies, drought indices have been identified using several methods (Heim, 2002). However, so far, the most commonly used drought index is the Palmer Drought Severity Index (PDSI) (Palmer, 1965) and the Standardized Precipitation Index (SPI) (Mckee et al., 1993). The PDSI index lacks the effectiveness of spatial and temporal comparisons while, the SPI index ignores the effect of evapotranspiration changes caused by air temperature increases (Wang et al., 2019). The PDSI is based on the water balance and incorporates precipitation, runoff, moisture supply and evaporation as input parameters. On the other hand, the SPI quantifies the impact of precipitation deficit on water sources using standardized precipitation. With SPI, there is the assumption that other climate variables such as air temperature remain stationary (Vicente-Serrano et al., 2010). The fundamental strength of SPI over other indices is that it is able to detect drought at different time scales (1, 3, 6, 12 and 24 months) implying that various types of drought (meteorological, agricultural, and hydrological) can be monitored. However, in assessing the influence of climate change on drought, it is vital to incorporate both precipitation and air temperature (Vicente-Serrano et al., 2010). Several studies have also shown the role of air temperature in drought (Diffenbaugh et al., 2015; Shukla et al., 2015; Williams et al., 2016; Ahmadalipour et al., 2017). To more understand the impact of global warming on drought, it is recommended that air temperature be introduced (Jeong et al., 2014; Sun et al., 2016). For the SPI calculation air temperature is not considered, in spite of it being important for a warming climate (Liu et al., 2016). Increased air temperature leads to increased evapotranspiration (King et al., 2015). Therefore, for a projected climate, it is important to use drought indices which also account for air temperature in its formulation. For this reason, the Standardized Precipitation Evapotranspiration Index (SPEI), a newly conceptualized drought index that is similar to SPI but includes air temperature variability, was recently developed (Vicente-Serrano et al., 2010). Compared to other indices, the SPEI more reflects the impacts of drought on agriculture (Guo et al., 2019). However, the use of SPEI and SPI on the impact of drought on maize growing agro-ecologies has not been conducted in Ethiopia. Therefore, there is a critical need to more accurately predict droughts caused by climate change to assist in developing effective strategies on agricultural loss and to respond to socioeconomical crises.

Global climate models (GCMs) are valuable tools for understanding the climate process under different Representative Concentration Pathways (RCPs), increasing the reliability of drought predictions. Haile et al. (2020) investigated future drought changes using an ensemble of five GCMs in the coupled Model Intercomparison project (CMIP5) under RCPs 2.6, 4.5, and 8.5 scenarios using SPI and SPEI over East Africa. Yao et al. (2020) projected drought characteristics using SPEI and multiple GCMs under RCPs 4.5 and 8.5 scenarios in mainland China. Venkataraman et al. (2016) evaluated the performance of the ensemble of CMIP5 GCMs on drought characteristics under 2.6, 4.5 and 8.5 RCP scenarios using the SPI and SPEI in Texas.

Considering the increasing trend in global air temperatures and the impact on local climate, it has been shown that climate change may alter the frequency and severity of extreme events such as droughts (IPCC, 2013). Therefore, drought analysis with respect to the effect of climate change has received more attention over recent years in Ethiopia (Kim and Kaluarachchi, 2009; Enyew et al., 2014; Funk et al., 2016; Taye et al., 2018). However, these studies focused only on climate change impact on water resources and El Niño-associated drought impact assessment. Few studies assessed future drought (e.g., Abrha and Hagos, 2019) using a multimodel approach under climate change in the Hintalo Wejerat district of Ethiopia which is different from the current study region and not agro-ecologies of different maize growing areas. Hence, to the best of our knowledge, this is the first study that uses the SPEI and SPI indices under the 8.5 RCP scenario for drought analysis across the study areas.

The main objective of this study is firstly, to assess historical drought using observed data from 1995-2017. The second objective is to project future climate change impact on drought risk based on the ensemble mean of seven GCMs for the period of 2021-2050 under the RCP 8.5 scenario. SPI and SPEI were used to identify drought through the use of the ensemble mean monthly precipitation and air temperature data.

5.3 Materials and methods

5.3.1 Study area

Three agricultural research centres were selected to represent maize growing areas of Ethiopia: Ambo (latitude 8° 57' N, longitude 38° 07' E and altitude of 2225 m) in the central highland of Ethiopia, Bako (9^o 12' N, 37^o 04' E and 1650 m) in the western part of Ethiopia and Melkassa (8^o 42' N, 39^o 32' E and 1550 m) in the central rift valley of Ethiopia. These are the most important agricultural research centres in Ethiopia, playing key roles in the country’s food security. Ambo has a temperate (intermediate highland) agro-ecology. The maize growing season lasts from May to December depending on the variety. Bako has a mid-altitude agro-ecology with hot humid weather. The maize growing season ranges from May to November. Melkassa has an arid to semi-arid agro-ecology. The maize growing season ranges from June to November.

5.3.2 Datasets

The observation data series used in the present study includes daily precipitation, and minimum and maximum air temperature records for the period of 1995–2017 (baseline). These data were collected from the meteorological station nearest to the three agricultural research centres and/or from national meteorological agency where the study sites are located. Data from the time periods of 2021–2050 (near future) were extracted from seven GCMs namely, CNRM-CM5, CSIRO-MK3-6-0, ICHEC-EC-EARTH, IPSL-CM5A-MR, MIROC5, HadGEM2-ES and CanESM2 (Table 5.1) using the Regional Climate Model (RCM)- RCA4 (Samuelsson et al., 2011). The RCM-RCA4 simulation covers the Coordinated Regional Climate Downscaling Experiment (CORDEX)-Africa domain with a spatial resolution of 0.44^{o} and were bias-corrected using a quantile-quantile mapping approach (Ngai et al., 2017). The GCMs' ensemble mean was used to detect drought events in the near future. The RCP 8.5 (highest emissions) (Moss et al., 2010) was considered so as to analyze the projected changes in drought due to climate change. This climate scenario was designed to represent a business-as-usual scenario assuming the continuation of current trends and projected drought for the future climate in Ethiopia.

Table 5.1: List of GCMs used for this study

GCM name	Institute	References
CanESM2	CCCma: Canadian Centre for Climate Modelling and Analysis	CCCma (2017b)
CNRM-CM5	CERFACS: Centre Européen de Recherche et de Formation Avancée en Calcul Scientifique	Voldoire et al. (2013)
CSIRO-MK3-6-0	CSIRO: Commonwealth Scientific and Industrial Research Organization	Jeffrey et al. (2013)
EC-EARTH	ICHEC: Consortium of European research institutions and researchers	Hazeleger et al. (2010)
HadGEM2-ES	MOHC: Met Office Hadley Centre	Collins et al. (2011)
IPSL-CM5A-MR	IPSL: Institut Pierre Simon Laplace	Dufresne et al. (2013)
MIROC5	AORI: Atmospheric and Ocean Research Institute	Watanabe et al. (2010)

5.3.3 Assessment of drought condition using the SPI and SPEI

A comparative analysis of SPI and SPEI is carried out in order to establish whether potential evapotranspiration, used in obtaining SPEI, has an impact on the drought index. The analyses were performed at different time scales for the baseline period 1995–2017 and for the near future 2021-2050. The different time scales (3, 6 and 12 months) were computed to capture both the short-term and long-term drought. The SPI and SPEI were generated using the SPEI package (Beguería et al., 2014) found in the R software package which is free software available at http://sac.csic.es/spei.

5.3.3.1 SPI

The SPI (McKee et al., 1993) is one of the most popular indices to assess drought conditions based on probability distribution of long-term precipitation using the gamma function. Precipitation is transformed into normalized numerical values and the SPI is given as the number of standard deviations by which the observed precipitation deviates from the long-term mean (Eq. 5.1). The index gives a reliable estimate of the magnitude, severity and temporal extent of droughts. An index of zero indicates the median precipitation amount, a negative index a drought awareness, and a positive index wet conditions. As the dry or wet conditions become more severe, SPI becomes more negative or positive respectively. The index is calculated as follows:

$$SPI = \frac{x_i - \bar{x}}{\sigma} \tag{5.1}$$

where x_i is the precipitation of the selected period during the year i, $\bar{x}$ is the long term mean precipitation and σ is precipitation standard deviation for the selected period.

5.3.3.2 SPEI

The SPEI is considered an improved drought index of the SPI that is especially suited to analyse the effect of global warming on drought conditions (Beguería et al., 2014). The calculation of the SPEI in this study follows the method by Vicente-Serrano et al. (2010). The SPEI is based on a climatic water balance which is determined by the difference between monthly precipitation (P) and potential evapotranspiration (*PET*). For this study, *PET* was calculated using the Hargreaves-Samani equation (Hargreaves and Samani, 1985). The Hargreaves–Samani equation has been evaluated across different climate regions (Hargreaves and Samani, 1985; Hargreaves, 1989; Hess et al., 2001; Droogers and Allen, 2002; Hargreaves and Allen, 2003) and has been used in SPEI calculations by Rhee and Cho (2016). In addition, the Food and Agriculture Organization of the United Nations (FAO) recommends the use of the Hargreaves–Samani equation, when meteorological data are lacking, to compute the potential evapotranspiration using the Penman–Monteith equation. Therefore, in the present study, SPEI was adopted with potential evapotranspiration estimated using the Hargreaves–Samani equation. The Hargreaves–Samani (HS) equation is given as:

$$ET_{HS} = 0.0135 \times KT \times (T_{av} + 17.8) \times (T_{max} - T_{min})^2 \times R_a \times 0.408 \times d \qquad (5.2)$$

where ET_{HS} is evapotranspiration in mm decade^{-1}, KT is an empirical coefficient, T_{av} the average daily air temperature (°C), T_{max}, T_{min} are the decadal mean, maximum, and minimum air temperatures (°C), R_a is extraterrestrial radiation (MJ m^{-2}) and d is the number of days within the decade (Guo et al., 2019). The surplus accumulation of a climate water balance is calculated as the difference between the precipitation P and PET for the month i, which means deficit D_i, is calculated using:

$$D_i = P_i - PET_i \tag{5.3}$$

The calculated D_i values are aggregated at different time scales as follows:

$$D_n^k = \sum_{i=0}^{k-1} (P_{n-1} - PET_{n-1}) \tag{5.4}$$

where *k* is the timescale (months) of the aggregation and *n* is the calculation month.

The probability density function of a log-logistic distribution is given as:

$$f(x) = \frac{\beta}{\alpha}\left(\frac{x-\gamma}{\alpha}\right)^{\beta-1}\left(1+\left(\frac{x-\gamma}{\alpha}\right)^{\beta}\right)^{-2} \tag{5.5}$$

where α, β and γ are scale, shape and origin parameters respectively for $\gamma > D < \infty$ (Vicente-Serrano et al., 2010). The probability distribution function for the *D* series is then given as:

$$f(x) = \left[1+\left(\frac{\alpha}{x-\gamma}\right)^{\beta}\right]^{-1} \tag{5.6}$$

Using *f(x)*, the SPEI can be obtained as the standardized values of *f(x)* according to the method of Abramowitz et al. (1965):

$$SPEI = W - \frac{C_0 + C_1 W + C_2 W^2}{1 + d_1 W + d_2 W^2 + d_3 W^3} \tag{5.7}$$

where $W = \sqrt{-2 \, In \, P}$ for $P \leq 0.5$ (5.8)

where *P* is the probability, as a fraction, of exceeding a determined D_i value and is given as:

$P = 1 - f(x)$.

The constants of Eq. (5.7) are: C_0 = 2.515517, C_1 = 0.802853, C_2 = 0.010328, d_1 = 1.432788, d_2 = 0.189269, and d_3 = 0.001308. Positive values of SPEI indicate above-average moisture conditions while negative values indicate drier conditions. A drought event is defined when the SPEI value is less than or equal to −1 in a certain period. The drought categories according to the SPI and SPEI values are presented in Table 5.2.

Table 5.2: Categorization of drought severity using SPI/SPEI drought indices

Drought severity level	SPI, SPEI value
No drought	SPI, SPEI > -1
Moderate drought	-1.5 < SPI, SPEI ≤ -1
Severe drought	-2.0 < SPI, SPEI ≤ -1.5
Extreme drought	SPI, SPEI ≤ -2.0

Source: Haile et al., 2020

5.3.4 Analysis of drought duration, severity, intensity and frequency

Drought characteristics include various drought conditions, such as frequency, duration, severity, and intensity (Lee et al., 2017). In the current study, drought indicators SPI and SPEI were used and calculated for the different timescales 3, 6 and 12 months. To measure the duration of drought and magnitude of drought severity, a threshold value must be defined. A threshold value of −1 is usually used to identify the availability of drought conditions for the SPI and SPEI drought indices. The drought duration (*D*) is the period length for which the SPI and SPEI are continuously negative, starting from when the SPI and SPEI values equal to -1 and ends when the SPI and SPEI values are positive (Adhyani et al., 2017). The drought severity (*S*) is the cumulated SPI or SPEI values within the drought duration, and is defined by:

$$S = -\sum_{i=1}^{D} SPEI_i \tag{5.9}$$

The intensity of drought is the ratio of severity of drought to its duration. Furthermore, droughts were evaluated using drought frequency *F* (%) given as:

$$F = \frac{n_m}{N_m} \times 100 \quad (5.10)$$

where n_m is the number of drought months and N_m the total number of months. The comparison of SPI and SPEI, that determines if both indices show the same pattern (irrespective of their magnitude), is assessed using the Pearson correlation coefficient, *r*, which measures the strength of the linear relationship between the SPI and SPEI. This coefficient establishes whether a linear relationship exists between the indices at the 95% confidence. The relationship coefficient (*r*) takes values between 1 (positive relationship) and −1 (negative relationship). An *r* value ≥ 0.5 is deemed to be a strong correlation (Taylor, 1990) and is calculated as follows:

$$r_{xy} = \frac{\sum_{i=1}^{n}(x_i - \bar{x})(y_i - \bar{y})}{\sqrt{\sum_{i=1}^{n}(x_i - \bar{x})^2 \ (y_i - \bar{y})^2}} \quad (5.11)$$

where: n is the number of observations. For this study *x* and *y* represent the SPEI and SPI values, respectively.

5.4 Results

5.4.1 Assessment of historical drought conditions using the SPI and SPEI

The time series (1995–2017) of the drought indices were produced for the three study sites. To demonstrate the temporal variation of drought at different time scales (3, 6 and 12 months) for Ambo, Bako and Melkassa, the SPIs and SPEIs historic drought events were generated and are presented in Figures 5.1 - 5.3. In general, and for all the sites, both indices show the same pattern of variability for each timescale, but they differ in the duration, magnitude, and intensity of the drought. Variability in the droughts can be attributed to the fact that the study sites experienced high interannual variability in climate. Moreover, the frequency of occurrence of the droughts is greater for the shorter timescale compared to the longer timescale. This implies that a shorter timescale (3-6-months) of an existing dry condition leads to agricultural drought, which has high temporal variability for the study sites, whereas at a longer timescale (12-month), the frequency of dry spells considerably decreased. Hence, the agricultural droughts (3-6-month timescale) show the highest frequency of occurrence. However, at the longer timescales, the drought lasts longer, and their magnitude increases. Several drought periods occurred across the study sites during the period 1995–2017. Investigations of the historical drought conditions confirmed that four to five significant drought periods occurred for all study sites. According to SPI and SPEI (3-, 6- and 12-month) timescale drought events which have a duration of more than two months occurred in 1999-2000, 2002, 2009 and 2015-2016 for Ambo (Figure 5.1) while for Bako and Melkassa in 1996, 2002-2003, 2008-2009, 2012-2013 and 2015; and 1999, 2002, 2009 and 2015-2016 respectively (Figures 5.2 and 5.3).

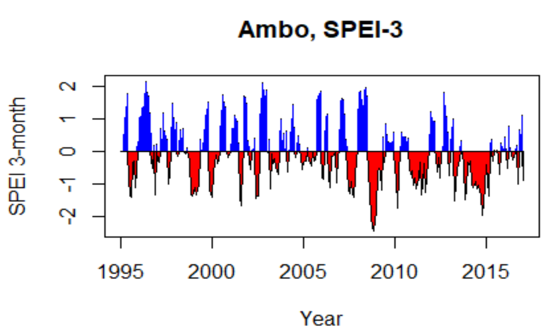

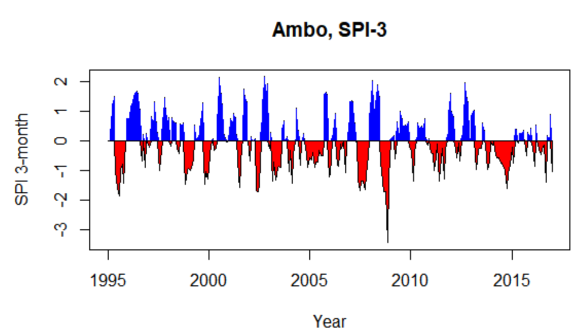

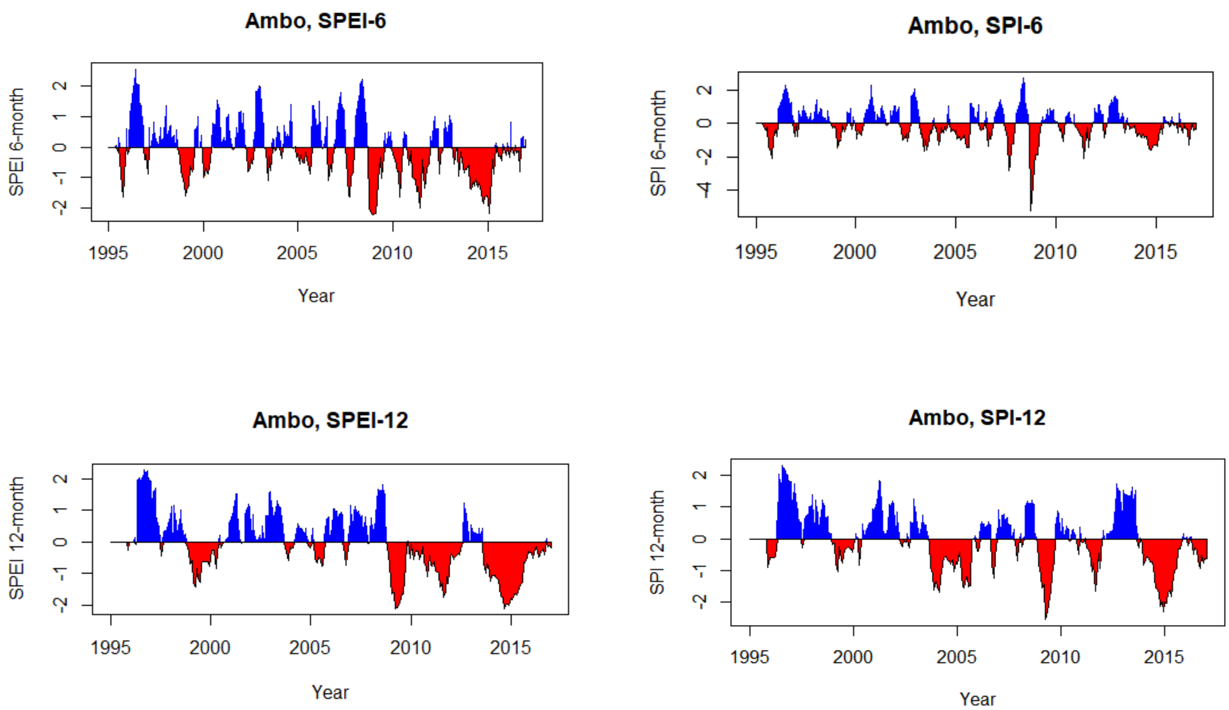

Figure 5.1: SPI and SPEI at different timescales for Ambo for 1995-2017

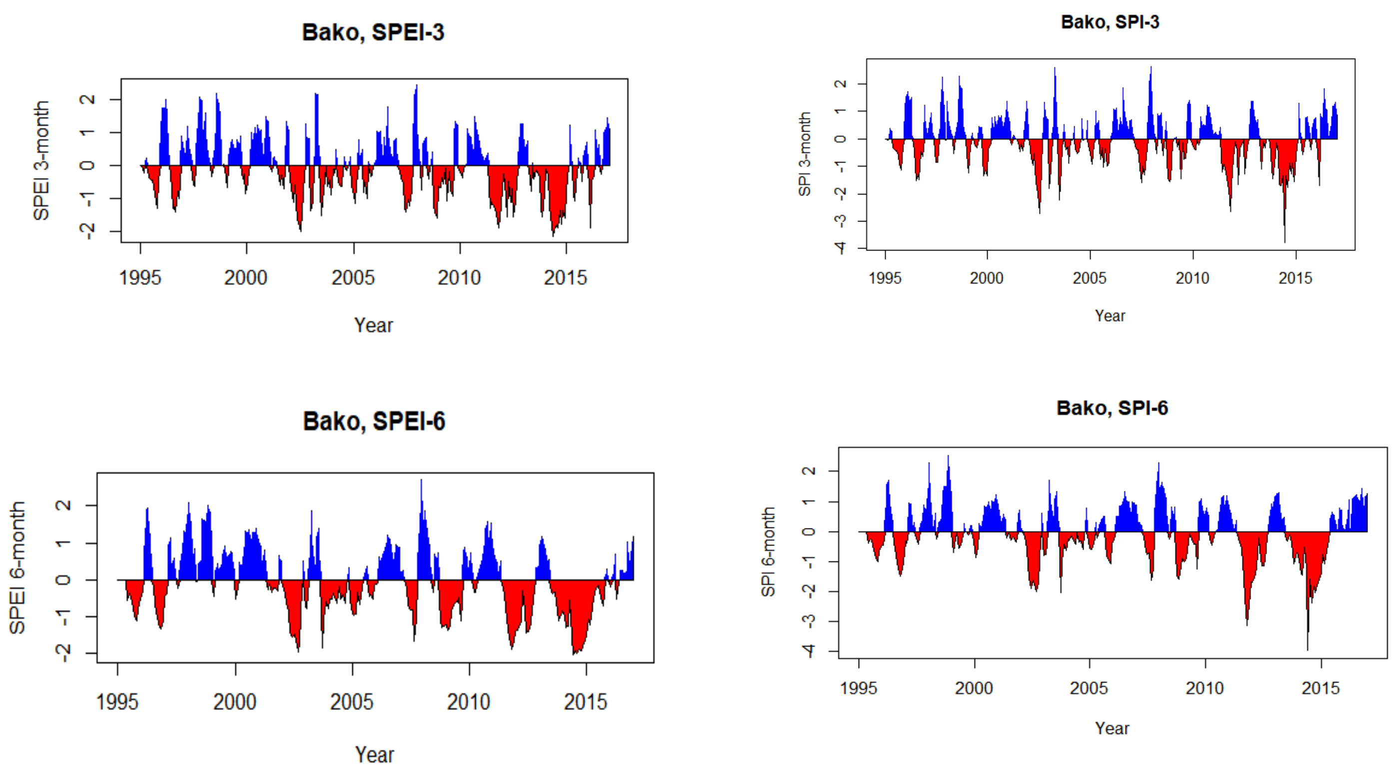

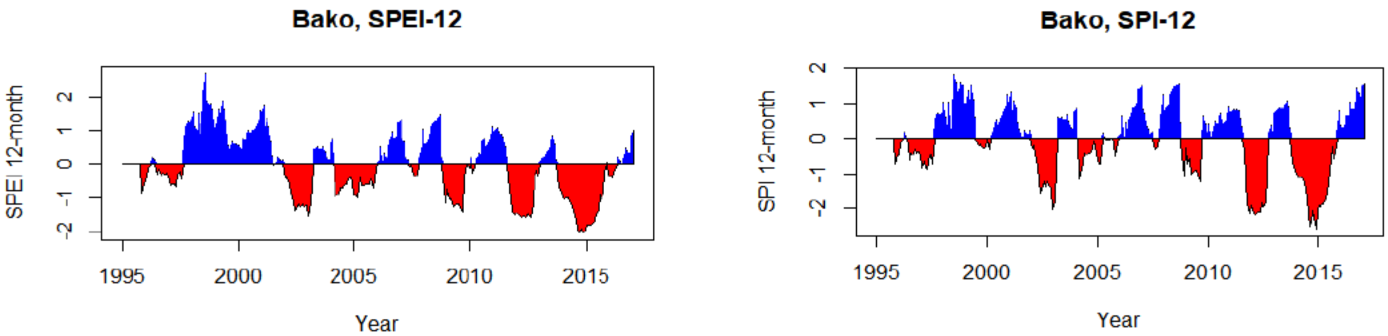

Figure 5.2: SPI and SPEI at different timescales for Bako for 1995-2017

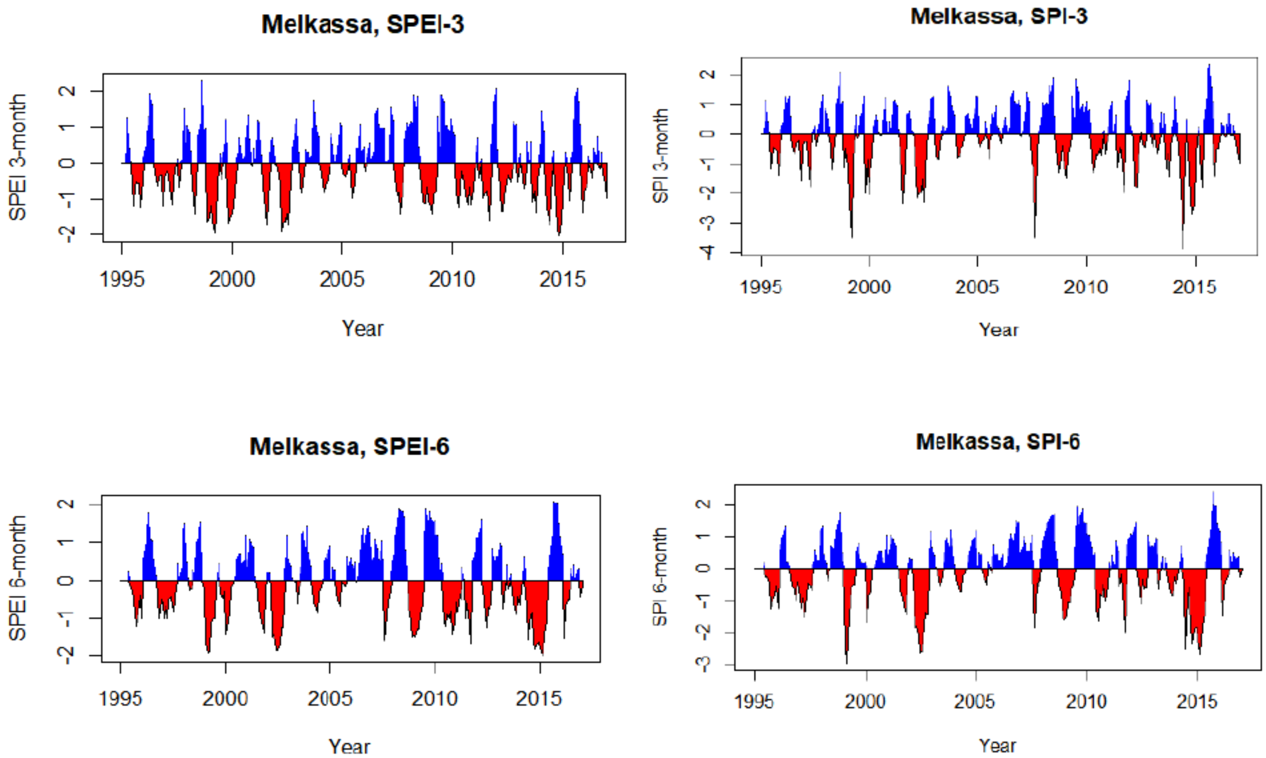

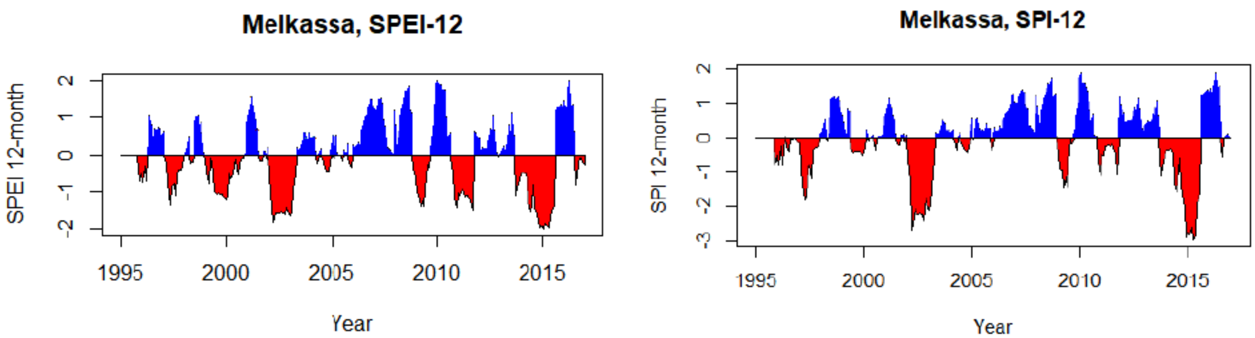

Figure 5.3: SPI and SPEI at different timescales for Melkassa for 1995-2017

5.4.2 Historical drought events, duration, severity, and intensity

Combining Figures 5.1, 5.2 and 5.3, yearly historical drought characteristic values were further counted in Table 5.3. The results of the SPI also produced similar time series when compared to the SPEI. The SPEI adequately reproduced the historical drought events as moderately dry, severely dry, and extremely dry periods. However, SPEI identified more droughts than SPI under the moderate to extremely dry drought categories for all sites and for all timescales except for the 12-month timescale for Bako (Table 5.3). This provides evidence about the suitability of identifying and monitoring droughts using an index that considers precipitation and air temperature data. Moreover, the result shows the advantage of the SPEI over the SPI since the different timescales over which the SPEI can be calculated allow for the identification of different drought types. However, SPI identified more extreme drought values for Bako and Melkassa. For the period under observation (1995–2017), the most common agricultural and hydrological droughts were observed during the years 2002, 2009, 2012 and 2015 for all study sites (Table 5.3).

Table 5.3: Historical drought years and drought categories of SPEI and SPI for the period 1995-2017 at different timescales for the (a) Ambo, (b) Bako and (c) Melkassa stations. (M: moderate, S: severe, E: extreme)

(a) Ambo

	SPEI-3				SPI-3				SPEI-6				SPI-6				SPEI-12				SPI-12			
Year	M	S	E	Σ	M	S	E	Σ	M	S	E	Σ	M	S	E	Σ	M	S	E	Σ	M	S	E	Σ
1995	3	_	_	3	1	2	_	3	1	1	_	2	1	1	1	3	_	_	_	_	_	_	_	_
1996	1	_	_	1	_	_	_	_	_	_	_	_	_	_	_	_	_	_	_	_	_	_	_	_
1997	_	_	_	_	1	_	_	1	_	_	_	_	_	_	_	_	_	_	_	_	_	_	_	_
1998	_	_	_	_	_	_	_	_	_	_	_	_	_	_	_	_	_	_	_	_	_	_	_	_
1999	6	_	_	6	3	_	_	3	4	1	_	5	3	_	_	3	4	_	_	4	1	_	_	1
2000	3		_	3	3	_	_	3	1	_	_	1	_	_	_	_	_	_	_	_	_	_	_	_
2001	1	1	_	2	1	1	_	2	_	_	_	_	_	_	_	_	_	_	_	_	_	_	_	_
2002	3	_	_	3	1	2	_	3	_	_	_	_	1	_	_	1	_	_	_	_	_	_	_	_
2003	1	_	_	1	2	_		2	1	_		1	1	2	_	3	_	_	_	_	_	_	_	_
2004	_	_	_	_	2	_	_	2	_	_	_	_	1	_	_	1	_	_	_	_	3	3	_	6
2005	_	_	_	_	_	_	_	_	_	_	_	_	1	_	_	1	_	_	_	_	3	2	_	5
2006	1	_	_	1	2	_	_	2	_	_	_	_	4	_	_	4	_	_	_	_	1	1	_	2
2007	1	_	_	1	2	_	_	2	1	_	_	1	1	_	_	1	_	_	_	_	1	_	_	1
2008	3	_		3	3	2	_	5	_	2		2	2	2	_	4	_	_	_	_	_	_	_	_
2009	2	2	2	6	2	2	1	5	1	1	5	7	_	2	3	5	1	2	2	5	2	1	2	5
2010	1	_	_	1	1	_	_	1	1	_	_	1	_	_	_	_	_	4	_	4	_	_	_	_
2011	2	_	_	2	_	_	_	_	3	1	_	4	1	_	_	1	1	_	_	1	_	_	_	_
2012	3	_	_	3	2	_	_	2	4	_	1	5	2	_	1	3	5	2	_	7	2	1	_	3
2013	_	_	_	_	_	_	_	_	_	_	_	_	2	1	_	3	_	_	_	_	_	_	_	_
2014	3	_	_	3	_	_	_	_	2	_	_	2	_	_	_	_	3	_	_	3	_	_	_	_
2015	7	2	_	9	1	1	_	2	6	5	1	12	6	1	_	7	4	6	2	12	_	4	4	8
2016	_	_	_	_	_	_	_	0	1	_	_	1	_	_	_	_	3	3	_	6	2	3	_	5
2017	_	_	_	_	2	_	_	2	_	_	_	_	1	_	_	1	_	_	_	_	_	_	_	_
Total	41	5	2	48	29	10	1	40	26	11	7	44	26	8	4	38	21	17	4	42	15	15	6	36

(b) Bako

Year	SPEI-3 M	SPEI-3 S	SPEI-3 E	SPEI-3 Σ	SPI-3 M	SPI-3 S	SPI-3 E	SPI-3 Σ	SPEI-6 M	SPEI-6 S	SPEI-6 E	SPEI-6 Σ	SPI-6 M	SPI-6 S	SPI-6 E	SPI-6 Σ	SPEI-12 M	SPEI-12 S	SPEI-12 E	SPEI-12 Σ	SPI-12 M	SPI-12 S	SPI-12 E	SPI-12 Σ
1995	2	_	_	2	1	_	_	1	1	_	_	1	1	_	_	1	_	_	_	_	_	_	_	_
1996	4	_	_	4	2	1	_	3	3	_	_	3	3	_	_	3	_	_	_	_	_	_	_	_
1997	_	_	_	_	_	_	_	_	1	_	_	1	1	_	_	1	_	_	_	_	_	_	_	_
1998	_	_	_	_	_	_	_	_	_	_	_	_	_	_	_	_	_	_	_	_	_	_	_	_
1999	_	_	_	_	1	_	_	1	_	_	_	_	_	_	_	_	_	_	_	_	_	_	_	_
2000	_		_	_	3	_	_	3	_	_	_	_	_	_	_	_	_	_	_	_	_	_	_	_
2001	_	_	_	_	_	_	_	_	_	_	_	_	_	_	_	_	_	_	_	_	_	_	_	_
2002	2	3	_	5	1	2	1	4	2	2	_	4	_	4	_	4	4	_	_	4	3	1	_	4
2003	4	_	_	4	2	1	1	4	_	2		2	_	1	1	2	5	1	_	6	4	1	1	6
2004	_	_	_	_	_	_	_	_	1	1	_	2	1	_	1	2	_	_	_	_	1	_	_	1
2005	1	_	_	1	_	_	_	_	_	_	_	_	_	_	_	_	_	_	_	_	_	_	_	_
2006	_	_	_	_	1	_	_	1	_	_	_	_	1	_	_	1	_	_	_	_	_	_	_	_
2007	1	_	_	1	1	_	_	1	_	_	_	_	_	_	_	_	_	_	_	_	_	_	_	_
2008	3	_		3	2	1	_	3	1	1		2	1	1	_	2	_	_	_	_	_	_	_	_
2009	2	1	_	3	2	1	_	3	6	_	_	6	3	1	_	4	5	_	_	5	2	_	_	2
2010	1	_	_	1	1	_	_	1	1	_	_	1	1	_	_	1	4	_	_	4	2	_	_	2
2011	_	_	_	_	_	_	_	_	_	_	_	_	_	_	_	_	_	_	_	_	_	_	_	_
2012	5	3	_	8	3	3	1	7	5	3	_	8	1	4	3	8	4	3	_	7	1	2	4	7
2013	2	1	_	3	1	_	_	1	3	_	_	3	2	_	_	2	2	4	_	6	1	3	2	6
2014	1	1	_	2	3	_	_	3	3	_	_	3	2	_	_	2	1	_	_	1	2	_	_	2
2015	3	6	1	10	3	4	1	8	2	8	1	11	3	3	4	10	4	6	2	12	4	2	6	12
2016	1	_	_	1	_	_	_	_	1	_	_	1	1	_	_	1	_	_	_	_	1	3	_	4
2017	_	1	_	1	1	_	_	1	_	_	_	_	_	_	_	_	_	_	_	_	_	_	_	_

Total	32	16	1	49	28	13		4	45	30	17	1	48	21	14	9	44	29	14	2	45	21	12	13	46

(c) Melkassa

	SPEI-3				SPI-3				SPEI-6				SPI-6				SPEI-12				SPI-12			
Year	M	S	E	Σ	M	S	E	Σ	M	S	E	Σ	M	S	E	Σ	M	S	E	Σ	M	S	E	Σ
1995	2	_	_	2	2	_	_	2	2	_	_	2	1	_	_	1	_	_	_	_	_	_	_	_
1996	1	_	_	1	_	1	_	1	2	_	_	2	1	_	_	1	_	_	_	_	_	_	_	_
1997	1	_	_	1	_	1	_	1	1	_	_	1	2	_	_	2	3	_	_	3	2	2	_	4
1998	1	_	_	1	1	_	_	1	_	_	_	_	_	_	_	_	_	_	_	_	_	_	_	_
1999	2	4	_	6	2	_	2	4	2	3	_	5	1	_	2	3	4	_	_	4	_	_	_	_
2000	2	2	_	4	1	1	1	3	2	_	_	2	_	1	_	1	4	_	_	4	_	_	_	_
2001	2	1	_	3	2	_	1	3	_	_	_	_	_	_	_	_	_	_	_	_	_	_	_	_
2002	1	4	_	5	_	3	2	5	4	4	_	8	2	2	4	8	1	6	_	7	1	6	_	7
2003	_	_	_	_	_	_	_	_	2	_		2	2	_	_	2	1	5	_	6	1	3	3	7
2004	_	_	_	_	_	_	_	_	_	_	_	_	_	_	_	_	_	_	_	_	_	_	_	_
2005	_	_	_	_	_	_	_	_	_	_	_	_	_	_	_	_	_	_	_	_	_	_	_	_
2006	_	_	_	_	_	_	_	_	_	_	_	_	_	_	_	_	_	_	_	_	_	_	_	_
2007	_	_	_	_	_	_	_	_	_	_	_	_	_	_	_	_	_	_	_	_	_	_	_	_
2008	_	1	_	1	1	_	1	2	_	1		1	_	1	_	1	_	_	_	_	_	_	_	_
2009	5	_	_	5	4	_	_	4	5	_	_	5	3	2	_	5	4	_	_	4	2	_	_	2
2010	1	_	_	1	1	_	_	1	_	_	_	_	_	_	_	_	1	_	_	1	1	_	_	1
2011	2	_	_	2	1	_	_	1	4	_	_	4	2	1	_	3	4	_	_	4	1	_	_	1
2012	2	1	_	3	2	2	_	4	2	1	_	3	1	1	_	2	6	_	_	6	1	_	_	1
2013	1	_	_	1	_	1	_	1	1	_	_	1	1	_	_	1	_	_	_	_	_	_	_	_
2014	2	_	_	2	2	_	_	2	_	_	_	_	_	_	_	_	1	_	_	1	1	_	_	1
2015	2	4	1	7	1	_	5	6	1	7	_	8	3	4	_	7	3	6	_	9	3	2	4	9
2016	2	_	_	2	1	_	1	2	2	1	_	3	1	1	1	3	1	5	_	6	3	3	_	6
2017	_	_	_	_	_	_	_	_	_	1	_	1	1	_	_	1	_	_	_	_	_	_	_	_
Total	29	17	1	47	21	9	13	43	30	18	_	48	21	13	7	41	33	22	_	55	16	16	7	39

Table 5.4 shows the summary results of duration, severity, and intensity for each site for the timescales 3-, 6- and 12- months. The result indicates the 6- and 12-month SPEI for 2015 was the longest (12-month drought duration) and most intense (-20.061 index value) for Ambo (Table 5.4). Similarly, 2015 was the longest and the most severe drought year for Bako as indicated by the SPI and SPEI 12-month timescale. Likewise, the SPI and SPEI 12-month timescale for Melkassa showed that 2002 was the longest drought year with a duration of 7 months and the highest severity with an SPI of -15.045 (extremely dry). This result indicates that droughts identified using the SPEI were also identified as droughts with the SPI which could also detect a drought condition that was identified with SPEI within the same historical period. The magnitude of the drought intensity in one period has a high severity and a short duration. For SPI-6, the highest intensity that occurred for Ambo was -3.055 for May to September 2009 with a severity of -15.277 for a five-month duration while the highest intensity for SPI-6 was recorded in Bako of about -1.974 with severity of -17.762 and duration of nine months which occurred in March to November 2015. On the other hand, SPI-3 gives the results that Melkassa had the highest intensity of about -2.515 in February to April 2015 with a value of severity of -7.546 for a three-month duration.

Table 5.4: The longest, strongest, and highest drought events for SPI and SPEI for timescales of 3, 6 and 12 months for the period 1995-2017 for Ambo, Bako and Melkassa

Site	Time Scale	Longest		Strongest		Highest	
		Year	Duration	Year	Severity	Year	Intensity
Ambo	SPEI 3	2015	7	2009	-9.807	2009	-1.961
	SPEI 6	2015	12	2015	-17.787	2009	-1.943
	SPEI 12	2015	12	2015	-20.061	2010	-1.801
	SPI 3	2008 - 2009	5	2009	-9.429	2009	-1.886
	SPI 6	2015	7	2009	-15.277	2009	-3.055
	SPI 12	2015	8	2015	-15.293	2015	-1.912
Bako	SPEI 3	2015	10	2015	-16.879	2015	-1.688
	SPEI 6	2015	10	2015	-17.203	2003	-1.841
	SPEI 12	2015	12	2015	-19.825	2015	-1.652
	SPI 3	2015	6	2015	-11.606	2015	-1.934
	SPI 6	2015	9	2015	-17.762	2015	-1.974
	SPI 12	2015	12	2015	-22.466	2012	-1.914
Melkassa	SPEI 3	1999	6	1999	-9.362	2015	-1.712
	SPEI 6	2002 and 2015	6	2015	-10.520	2015	-1.753
	SPEI 12	2002	7	2002	-10.798	2015	-1.775
	SPI 3	2002	5	2002	-9.845	2015	-2.515
	SPI 6	2002 and 2015	6	2002	-13.108	1999	-2.258
	SPI 12	2002	7	2002	-15.045	2016	-2.288

The drought frequency for 1995-2017 was analyzed. According to SPEI-3 and SPEI-12 month drought indices, during the past period, the frequency of occurrence of moderate drought was very high (14.9 %) for Ambo as compared to Bako (11.6 %) and Melkassa (12 %). On the other hand, the frequency of occurrence of severe drought was 8 % at Melkassa while it was 6.2 % for Ambo and Bako indicated by SPEI-6 and SPEI-12. However, the frequency of extreme drought occurrence is relatively reduced. SPI-3 and SPI-12 values revealed that the frequency of extreme drought occurrence was 4.7 % for Bako and Melkassa while SPEI-6 indicated 2.5 % at Ambo (Table 5.5). The result shows that SPI indicated more extreme drought than SPEI.

Table 5.5: Drought frequency of SPI and SPEI for 1995-2017 and under future climate (2021-2050) for 3- 6- 12-month timescales for Ambo, Bako and Melkassa

Time series		Ambo			Bako			Melkassa		
		Drought frequency (%)								
		Moderate	Severe	Extreme	Moderate	Severe	Extreme	Moderate	Severe	Extreme
1995-2017	SPEI-3	14.9	1.8	0.7	11.6	5.8	0.4	10.5	6.2	0.4
	SPI-3	10.5	3.6	0.4	10.1	4.7	1.4	7.6	3.3	4.7
	SPEI-6	9.4	4.0	2.5	10.9	6.2	0.4	10.9	6.5	0.0
	SPI-6	9.4	2.9	1.4	7.6	5.1	3.3	7.6	4.7	2.5
	SPEI-12	7.6	6.2	1.4	10.5	5.1	0.7	12.0	8.0	0.0
	SPI-12	5.4	5.4	2.2	7.6	4.3	4.7	5.8	5.8	2.5
2021-2050	SPEI-3	14.2	3.9	0.6	11.1	6.1	0.6	15.8	2.5	0.8
	SPI-3	10.6	2.8	1.9	9.4	5.3	1.4	13.1	1.7	0.6
	SPEI-6	13.6	4.4	0.8	9.4	0.1	0.6	9.4	5.8	1.1
	SPI-6	8.6	2.5	1.9	8.3	5.3	0.8	10.3	5.0	0.0
	SPEI-12	12.8	5.0	0.8	11.1	7.2	0.0	10.8	6.1	0.0
	SPI-12	6.9	1.4	3.3	10.8	5.3	1.1	10.0	4.2	0.0

Figure 5.4 shows the correlation between SPEI and SPI at 3-, 6-and 12 month timescales. The correlation between the SPEI and SPI was high and positive (R > 0.9) for the 1995-2017 series, independently of the timescale analyzed; the exceptions were Ambo and Bako, where correlations decreased at the longest timescales. Under climatic conditions with low inter-annual variability in air temperature compared to the variability in precipitation, the results imply that both indices will generally respond more to the variations in precipitation. The differences observed between SPI and SPEI for some months suggest that inclusion of potential evapotranspiration is important especially given that evaporative water demand is important in determining water availability and in view of it being a major component of the hydrological and soil water balance.

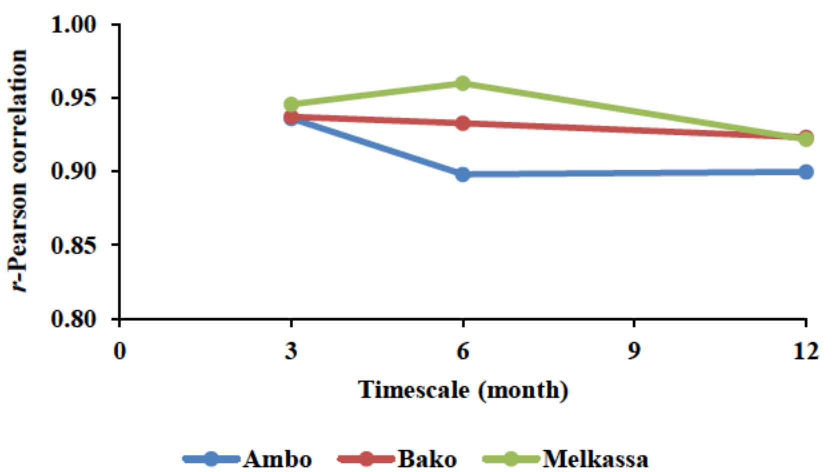

Figure 5.4: Correlation between series for the SPI and SPEI of (3-, 6- and 12-month) for Ambo, Bako and Melkassa during 1995-2017

5.4.3 Projection of drought under future climate using SPI and SPEI

Figures 5.4, 5.5 and 5.6 show the projected SPI and SPEI time series drought values under 8.5 RCP scenario for climate of the three sites for the future period (2021–2050). With respect to the projected SPI and SPEI 3-, 6- and 12-month patterns under the RCP 8.5 scenario, it is observed that drought is expected to increase during the future period for all timescales for all sites compared to that for the historical period. The SPEI projection from the ensemble means of the seven GCMs shows a consistent projection of more drought years than the SPI which may be due to increased air temperature in the future. Both the SPEI and SPI indicated that the short- to long-term drought conditions will be less severe for Ambo and Melkassa than for Bako compared to the historical period. The drying values fluctuated between -2 and -3 at Ambo, -2 and -4 at Bako and -1 and -3 at Melkassa. As with the historical period, there is a downward trend towards the value of -4 at shorter timescales (3-month) at Bako indicating there will be a severe dry period in the near future (Figure 5.6). According to the index SPI and SPEI 3- and 6- month, all study sites show two distinct severe dry periods during the near future, at the beginning of 2020s, and late 2040s. It is noticeable that the seven GCMs ensemble mean provides a clear dry period at the end of the near future period. It starts after 2045 and it becomes gradually more intense in time. On the other hand, indices with a longer timescale (12-month) are not influenced by frequent drought resulting foreseeable less drought occurrence with longer duration.

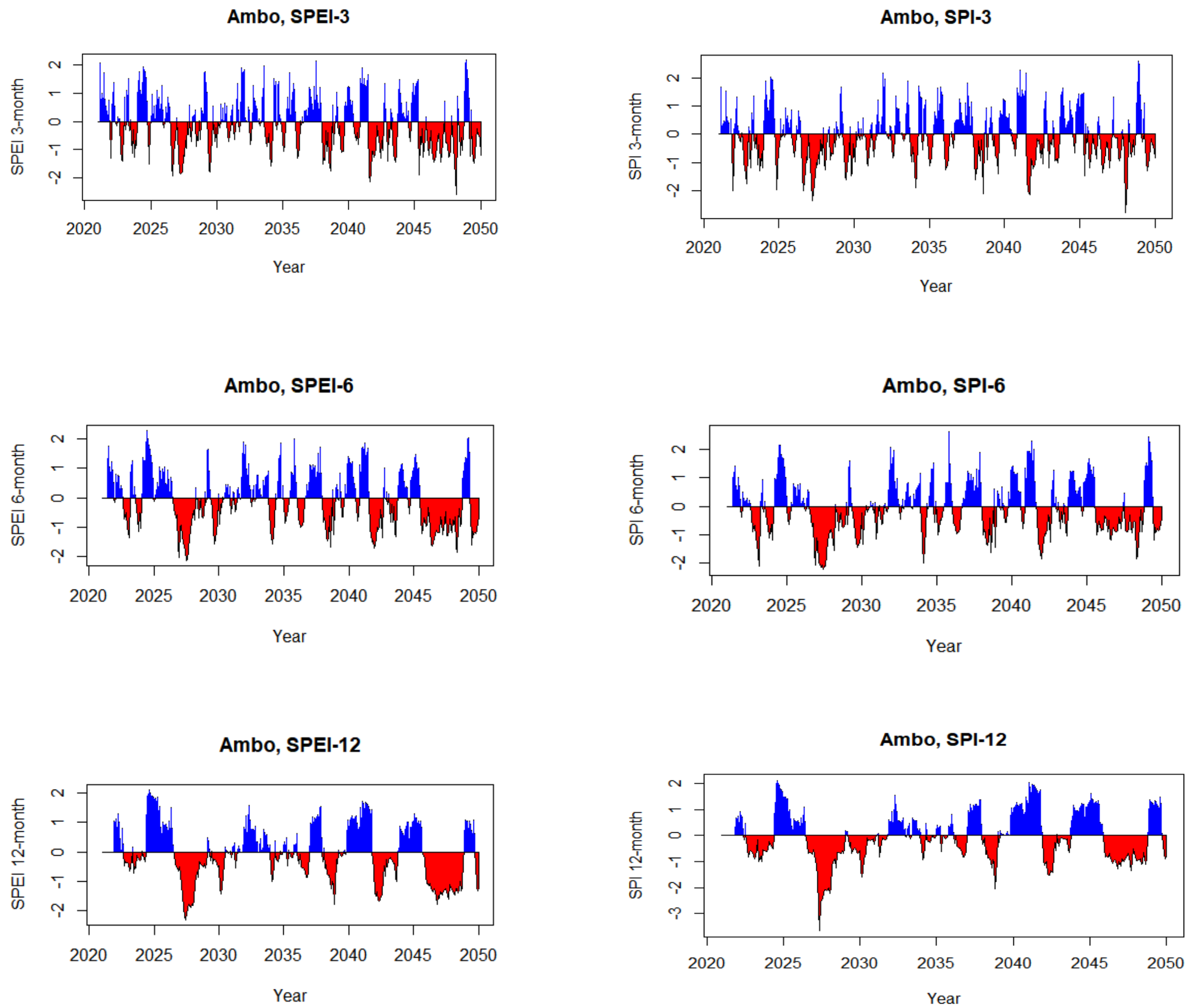

Figure 5.5: SPI and SPEI at different timescales for Ambo for 2021-2050

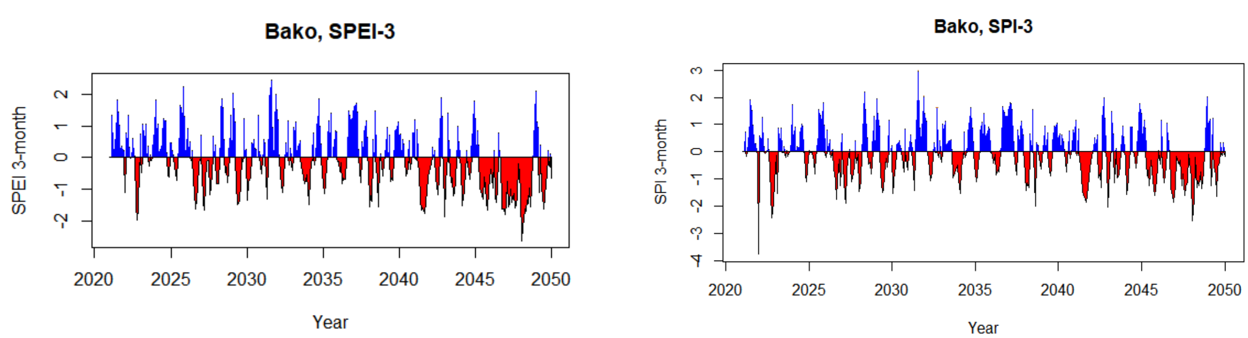

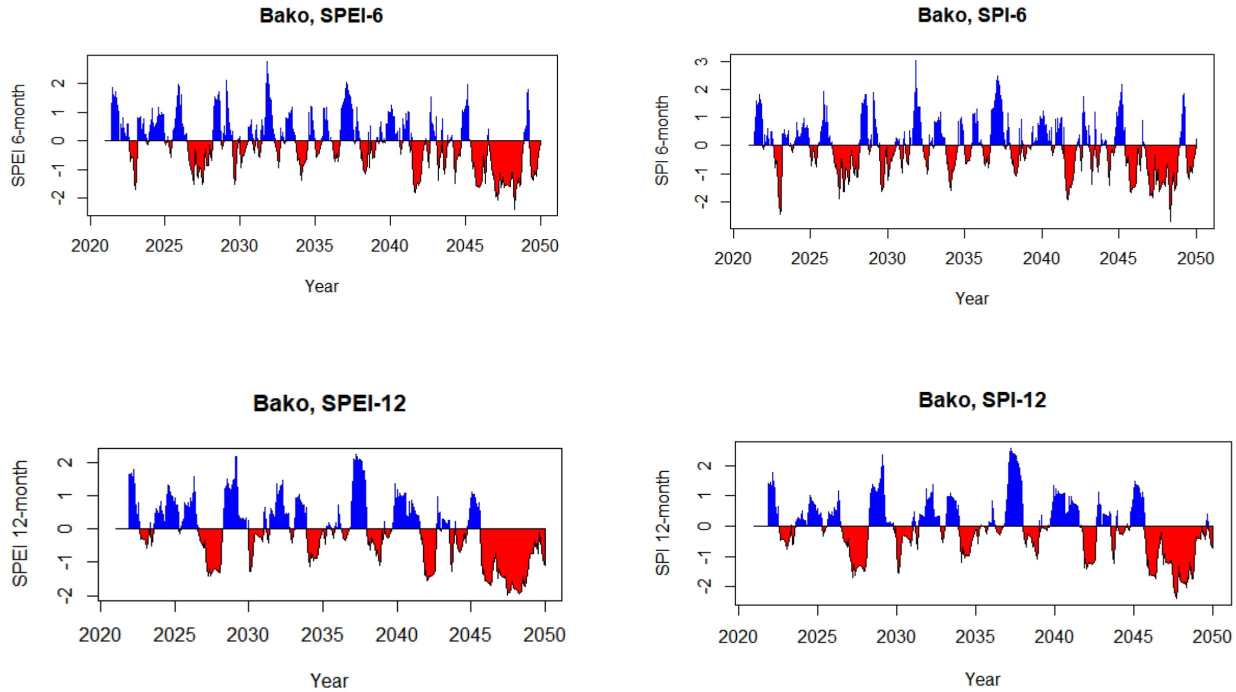

Figure 5.6: SPI and SPEI at different timescales for Bako for 2021-2050

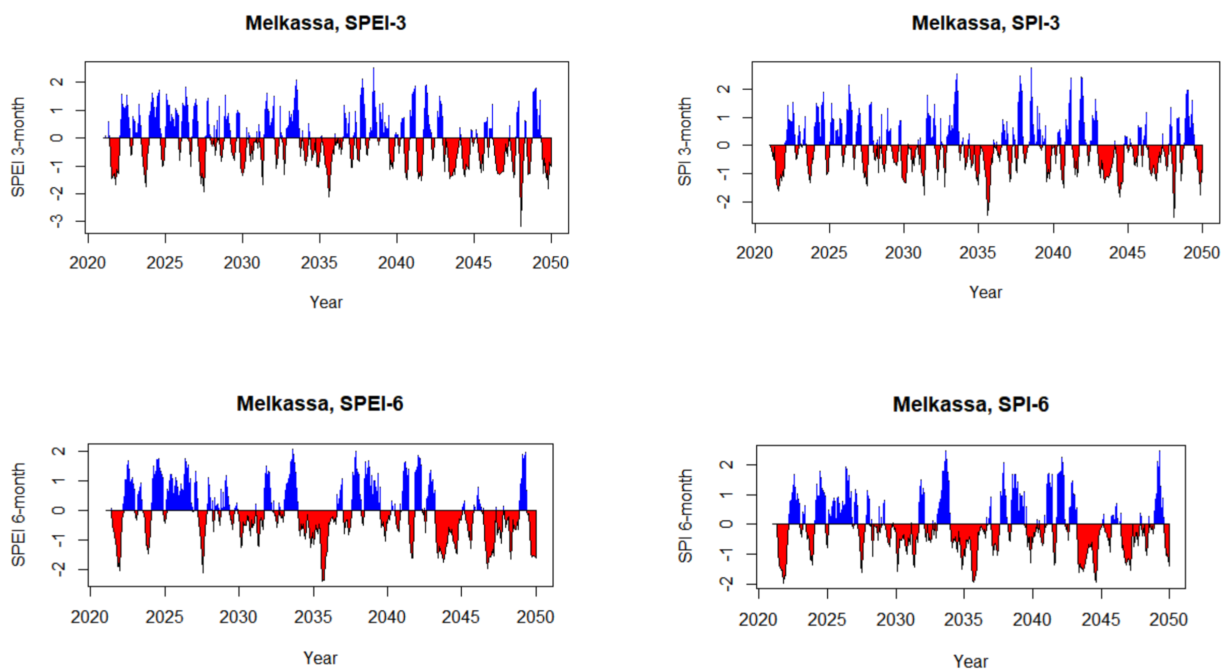

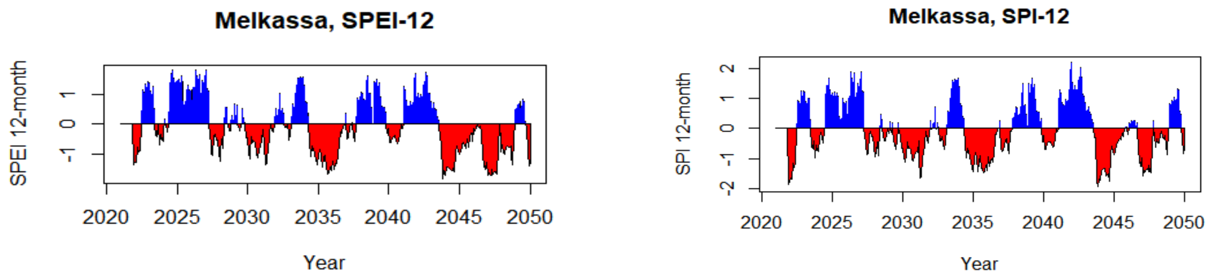

Figure 5.7: SPI and SPEI at different timescales for Melkassa for 2021-2050

5.4.4 Projected drought events, frequency duration, severity, and intensity

Analysis of drought frequency under future climate was undertaken to further understand how frequently drought is likely to occur for the study sites. Changes in frequency of projected drought provides meaningful measurement criterion to understand the influence of climate change on future drought for the study sites. To address this issue, the study compares the number of future projected drought events for a 50-year period with the number of counterpart events during the historical period (Table 5.5). The increasing frequency of future drought events is found for the Ambo and Bako sites under the RCP 8.5 scenario (Table 5.5). Except for the 6-month SPI, the frequency occurrence of moderate to extremely severe drought is expected to increase at Ambo for all-timescales under future climate. Similarly, an increasing frequency (5.3-11.1 %) of moderate to severe drought is projected to occur in Bako for SPI-6, SPEI and SPI 12-month. Surprisingly, the SPI and SPEI projected a much reduced severe to extreme drought frequency percentage at Melkassa compared to the historical period. The SPI and SPEI short and long-timescales only projected increasing moderate drought frequency by 10-15.8 % at Melkassa.

The drought duration, severity and intensity for the future periods was also investigated for the study sites. Table 5.6 presents projected future longest, strongest, and highest drought years for 2021-2050. The duration of the drought is the lifespan of droughts in months under climate change. According to the SPEI-6 and SPI-12, the longest droughts (12 months) are predicted to occur for Ambo in 2027, 2047 and 2048 while the longest dry year (2048) is projected for Bako. In the case of Melkassa, SPEI-12 projected the longest drought event for 2036. Among all categories of drought, moderate to severe droughts are projected across the study sites in most cases. Average-term droughts (3-6 months) are considered as agricultural droughts. According to SPEI and SPI 3-, 6-, and 12-month for future climate, both indices for all sites projected the five strongest and highest intensity drought years to occur in 2027, 2039, 2042, 2048 and 2049 for Ambo, 2022, 2023, 2042, 2048 and 2049 for Bako, and 2021, 2036, 2044, 2047 and 2048 for Melkassa. SPI 6- and 12-month projected the most severe (-21.457) and the highest drought intensity (-2.308) to occur in 2027 for Ambo.

On the other hand, SPI 6- and SPEI 12-month projected the highest intensity (-2.130) and the strongest drought with severe index (-20.436) expected to occur in 2023 and 2048 respectively for Bako. In the case of Melkassa, SPEI 3- and 12-month projected the strongest drought with a severity index value of -16.998 and highest intensity -2.130 anticipated to occur in 2036 and 2048 respectively (Table 5.6).

Table 5.6: Future longest, strongest and highest drought characteristics projected to occur under RCP 8.5 scenario for the period 2021-2050 for Ambo, Bako and Melkassa sites

Site	Time	Longest		Strongest		Highest	
	Scale	Year	Duration	Year	Severity	Year	Intensity
Ambo	SPEI 3	2042	7	2042	-10.359	2039	-1.573
	SPEI 6	2047	10	2027	-13.643	2049	-1.756
	SPEI 12	2047-2048	12	2047	-16.466	2027	-1.849
	SPI 3	2027	6	2027	-9.976	2027	-1.663
	SPI 6	2027	12	2027	-21.457	2049	-1.798
	SPI 12	2027	8	2027	-18.464	2027	-2.308
Bako	SPEI 3	2048	8	2048	-10.837	2022	-1.674
	SPEI 6	2048	12	2048	-18.296	2049	-1.596
	SPEI 12	2048	12	2048	-20.436	2048	-1.703
	SPI 3	2042	5	2042	-7.994	2022	-1.945
	SPI 6	2042, 2046 and 2048	6	2042	-9.455	2023	-2.130
	SPI 12	2048	12	2048	-20.093	2049	-1.686
Melkassa	SPEI 3	2047	7	2047	-8.603	2048	-2.130
	SPEI 6	2047	7	2044	-12.709	2036	-1.802
	SPEI 12	2036	12	2036	-16.998	2048	-1.623
	SPI 3	2021 and 2044	6	2021	-7.546	2036	-1.887
	SPI 6	2044	9	2044	-12.288	2036	-1.6803
	SPI 12	2048	7	2044	-9.938	2044	-1.656

Table 5.7 presents the temporal future drought events (2021–2050) including the number of droughts per year and the drought categories for Ambo, Bako and Melkassa. Under RCP 8.5, the most common agricultural drought projected by SPEI and SPI are 2022-2023, 2026-2028, 2034, 2038, 2042 and 2047-2050 for Ambo, 2022, 2027, 2038, 2044 and 2046-2049 for Bako and 2021, 2027, 2030, 2035-2036, 2041-2042, 2044-2045, 2047-2048 and 2050 for Melkassa.

Table 5.7 also shows that SPEI projected more droughts than SPI under the moderate to severe drought categories for all sites and for all timescales. The results show that even though reduced precipitation is the major driver of droughts, the effect of air temperature through evaporative water demand has a role to play in the determination of droughts. On the other hand, SPI projected more extreme drought as compared to SPEI at all timescales for Ambo and Bako. This indicates that considering precipitation alone, more droughts are classified as extreme compared to when including potential evapotranspiration. Overall, Table 5.7 shows that, Melkassa will experience the highest number of droughts for the 3-month timescale while Ambo and Bako will experience 6- and 12-month timescale droughts, respectively.

Table 5.7: Projected drought years and drought categories of SPI and SPEI under the RCP 8.5 scenario for 2021-2050 at different timescales for (a) Ambo, (b) Bako and (c) Melkassa. (M: moderate, S: severe, E: extreme)

(a) Ambo

	SPEI-3				SPI-3				SPEI-6				SPI-6				SPEI-12				SPI-12			
Year	M	S	E	Σ	M	S	E	Σ	M	S	E	Σ	M	S	E	Σ	M	S	E	Σ	M	S	E	Σ
2021	_	_	_	_	_	_	_	_	_	_	_	_	_	_	_	_	_	_	_	_	_	_	_	_
2022	4	_	_	4	2	1	1	4	_	_	_	_	_	_	_	_	_	_	_	_	_	_	_	_
2023	2	_	_	2	3	_	_	3	4	_	_	4	3	_	1	4	_	_	_	_	2	_	_	2
2024	_	_	_	_	1	_	_	1	1	_	_	1	1	_	_	1	_	_	_	_	_	_	_	_
2025	1	_	_	1	_	1	_	1	_	_	_	_	_	_	_	_	_	_	_	_	_	_	_	_
2026	1	2	_	3	2	_	1	3	_	_	_	_	_	_	_	_	_	_	_	_	_	_	_	_
2027	3	3	_	6	3	2	2	7	2	5	3	10	3	3	6	12	2	3	3	8	1	1	6	8
2028	_	_	_	_	2	_	_	2	1	_	_	1	2	1	_	3	1	5	_	6	3	_	5	8
2029	1	2	_	3	2	1		3	1	1		2	2	_	_	2	_	_	_	_	_	_	_	_
2030	_	_	_	_	2	_	_	2	2	_	_	2	4	_	_	4	3	_	_	3	2	1	_	3
2031	_	_	_	_	2	_	_	2	_	_	_	_	1	_	_	1	_	_	_	_	_	_	_	_
2032	_	_	_	_	_	_	_	_	_	_	_	_	_	_	_	_	_	_	_	_	_	_	_	_
2033	_	_	_	_	_	_	_	_	_	_	_	_	_	_	_	_	_	_	_	_	_	_	_	_
2034	2	1		3	2	1	_	3	2	1		3	2	1	_	3	_	_	_	_	_	_	_	_
2035	1	_	_	1	1	_	_	1	_	_	_	_	_	_	_	_	_	_	_	_	_	_	_	_
2036	2	_	_	2	2	_	_	2	_	_	_	_	_	_	_	_	_	_	_	_	_	_	_	_
2037	_	_	_	_	_	_	_	_	_	_	_	_	_	_	_	_	_	_	_	_	_	_	_	_
2038	3	1	_	4	2	1	_	3	2	_	_	2	2	_	_	2	_	_	_	_	_	_	_	_
2039	1	1	_	2	_	_	1	1	2	1		3	2	1	_	3	4	1	_	5	2	_	1	3
2040	2	_	_	2	1	_	_	1	_	_	_	_	_	_	_	_	_	_	_	_	_	_	_	_

2041	_	_	_	_	_	_	_	_	_	_	_	_	_	_	_	_	_	_	_	_	_	_	_	_
2042	4	2	1	7	2	2	1	5	7	2		9	4	1	_	5	2	2	_	4	2	1	_	3
2043	3	_	_	3	2	_	_	2	2	_	_	2	1	_	_	1	1	3	_	4	2	2	_	4
2044	4	_	_	4	1	_	_	1	2	_	_	2	1	_	_	1	_	_	_	_	_	_	_	_
2045	_	_	_	_	_	_	_	_	_	_	_	_	_	_	_	_	_	_	_	_	_	_	_	_
2046	2	1		3	2	_	_	2	2	_	_	2	_	_	_	_	2	_	_	2	_	_	_	_
2047	6	_	_	6	3	_	_	3	7	3		10	2	_	_	2	9	3	_	12	5	_	_	5
2048	2	1		3	_	_	1	1	7	_	_	7	_	_	_	_	11	1	_	12	3	_	_	3
2049	2	_	1	3	_	1	_	1	_	2	_	2	_	2	_	2	8	_	_	8	3	_	_	3
2050	5	_	_	5	1	_	_	1	5	1	_	6	1	_	_	1	3	_	_	3	_	_	_	_
Total	51	14	2	67	38	10	7	55	49	16	3	68	31	9	7	47	46	18	3	67	25	5	12	42

(b) Bako

	SPEI-3				SPI-3				SPEI-6				SPI-6				SPEI-12				SPI-12			
Year	M	S	E	Σ	M	S	E	Σ	M	S	E	Σ	M	S	E	Σ	M	S	E	Σ	M	S	E	Σ
2021	_	_	_	_	_	_	_	_	_	_	_	_	_	_	_	_	_	_	_	_	_	_	_	_
2022	2	2	_	4	_	2	2	4	_	_	_	_	_	_	_	_	_	_	_	_	_	_	_	_
2023	_	_	_	_	1	1	_	2	2	1	_	3	_	1	2	3	_	_	_	_	_	_	_	_
2024	_	_	_	_	_	_	_	_	_	_	_	_	_	_	_	_	_	_	_	_	_	_	_	_
2025	_	_	_	_	1	_	_	1	_	_	_	_	_	_	_	_	_	_	_	_	_	_	_	_
2026	1	1	_	2	1	1	_	2	1	_	_	1	1	_	_	1	_	_	_	_	_	_	_	_
2027	2	1	_	3	2	2	_	4	4	2	_	6	3	3	_	6	8	_	_	8	6	2	_	8
2028	_	_	_	_	2	_	_	2	_	_	_	_	3	_	_	3	4	_	_	4	4	_	_	4
2029	2	_	_	2	1	1	_	2	1	1	_	2	1	1	_	2	_	_	_	_	_	_	_	_
2030	1	_	_	1	_	1	_	1	1	_	_	1	2	_	_	2	3	_	_	3	2	1	_	3
2031	1	_	_	1	1	_	_	1	_	_	_	_	_	_	_	_	_	_	_	_	_	_	_	_
2032	1	_	_	1	1	_	_	1	_	_	_	_	_	_	_	_	_	_	_	_	_	_	_	_

2033	_	_	_	_	_	_	_	_	_	_	_	_	_	_	_	_	_	_	_	_	_	_	_	_
2034	1	_	_	1	1	1	_	2	2	_	_	2	1	1	_	2	1	_	_	1	2	_	_	2
2035	1	_	_	1	1	_	_	1	_	_	_	_	_	_	_	_	_	_	_	_	_	_	_	_
2036	_	_	_	_	_	_	_	_	_	_	_	_	_	_	_	_	_	_	_	_	_	_	_	_
2037	_	_	_	_	_	_	_	_	_	_	_	_	_	_	_	_	_	_	_	_	_	_	_	_
2038	2	1	_	3	3	_	_	3	2	_	_	2	1	_	_	1	_	_	_	_	_	_	_	_
2039	_	1	_	1	_	_	1	1	_	_	_	_	_	_	_	_	1	_	_	1	1	_	_	1
2040	_	_	_	_	_	_	_	_	_	_	_	_	_	_	_	_	_	_	_	_	_	_	_	_
2041	_	_	_	_	_	_	_	_	_	_	_	_	_	_	_	_	_	_	_	_	_	_	_	_
2042	3	4	_	7	2	3	_	5	4	4	_	8	3	3	_	6	4	2	_	6	6	_	_	6
2043	1	1	_	2	1	_	1	2	_	_	_	_	1	_	_	1	4	_	_	4	4	_	_	4
2044	3	1	_	4	2	1	_	3	1	_	_	1	_	_	_	_	1	_	_	1	1	_	_	1
2045	1	_	_	1	_	_	_	_	1	_	_	1	1	_	_	1	_	_	_	_	_	_	_	_
2046	4	1	_	5	3	1	_	4	2	5	_	7	3	3	_	6	2	3	_	5	2	3	_	5
2047	3	3	_	6	3	2	_	5	3	2		5	1	2	_	3	5	4	_	9	4	3	_	7
2048	7	2	1	10	3	1	1	5	3	8	1	12	6	3	_	9	3	9	_	12	5	4	3	12
2049	2	3	1	6	4	1	_	5	2	5	1	8	2	2	1	5	2	8	_	10	2	6	1	9
2050	2	1	_	3	1	1	_	2	5	_	_	5	1	_	_	1	2	_	_	2	_	_	_	_
Total	40	22	2	64	34	19	5	58	34	28	2	64	30	19	3	52	40	26	_	66	39	19	4	62

(C) Melkassa

	SPEI-3				SPI-3				SPEI-6				SPI-6				SPEI-12				SPI-12			
Year	M	S	E	Σ	M	S	E	Σ	M	S	E	Σ	M	S	E	Σ	M	S	E	Σ	M	S	E	Σ
2021	4	1	_	5	5	1	_	6	2	2	_	4	2	4	_	6	1	_	_	1	_	1	_	1
2022	1	_	_	1	1	_	_	1	_	1	1	2	_	1	_	1	3	_	_	3	3	3	_	6
2023	1	1	_	2	2	_	_	2	2	_	_	2	2	_	_	2	_	_	_	_	_	_	_	_
2024	_	_	_	_	1	_	_	1	1	_	_	1	1	_	_	1	_	_	_	_	_	_	_	_
2025	_	_	_	_	_	_	_	_	_	_	_	_	_	_	_	_	_	_	_	_	_	_	_	_

2026	1	_	_	1	_	_	_	_	_	_	_	_	_	_	_	_	_	_	_	_	_	_	_	_
2027	1	3	_	4	3	_	_	3	1	1	1	3	1	1	_	2	1	_	_	1	_	_	_	_
2028	_	_	_	_	_	_	_	_	_	_	_	_	1	_	_	1	1	_	_	1	_	_	_	_
2029	_	_	_	_	_	_	_	_	_	_	_	_	_	_	_	_	_	_	_	_	_	_	_	_
2030	4	_	_	4	4	_	_	4	2	_	_	2	1	1	_	2	1	_	_	1	2	_	_	2
2031	1	1	_	2	1	1	_	2	2	_	_	2	2	_	_	2	3	_	_	3	1	2	_	3
2032	1	_	_	1	1	_	_	1	_	_	_	_	_	_	_	_	_	_	_	_	_	_	_	_
2033	1	_	_	1	1	_	_	1	_	_	_	_	_	_	_	_	_	_	_	_	_	_	_	_
2034	_	_	_	_	_	_	_	_	_	_	_	_	_	_	_	_	1	_	_	1	_	_	_	_
2035	3	_	_	3	3	_	_	3	3	_	_	3	2	1	_	3	8	_	_	8	6	_	_	6
2036	1	1	1	3	1	1	1	3	1	3	2	6	1	5	_	6	7	5	_	12	10	_	_	10
2037	2	_	_	2	2	_	_	2	_	_	_	_	2	_	_	2	_	_	_	_	_	_	_	_
2038	_	_	_	_	_	_	_	_	_	_	_	_	_	_	_	_	_	_	_	_	_	_	_	_
2039	_	_	_	_	_	_	_	_	_	_	_	_	_	_	_	_	_	_	_	_	_	_	_	_
2040	2	_	_	2	2	_	_	2	1	_	_	1	1	_	_	1	_	_	_	_	_	_	_	_
2041	3	_	_	3	3	_	_	3	_	_	_	_	_	_	_	_	_	_	_	_	_	_	_	_
2042	3	1	_	4	2	_	_	2	2	_	_	2	2	_	_	2	_	_	_	_	_	_	_	_
2043	1	_	_	1	1	_	_	1	_	_	_	_	_	_	_	_	_	_	_	_	_	_	_	_
2044	5	_	_	5	6	_	_	6	5	4	_	9	7	2	_	9	2	4	_	6	2	4	_	6
2045	4	_	_	4	4	1	_	5	4	_	_	4	2	2	_	4	4	3	_	7	2	4	_	6
2046	2	_	_	2	_	_	_	_	1	_	_	1	_	_	_	_	_	_	_	_	_	_	_	_
2047	7	_	_	7	3	_	_	3	3	4		7	5	_	_	5	3	3	_	6	3	1	_	4
2048	3	_	1	4	_	_	1	1	1	1	_	2	_	1	_	1	_	7	_	7	7	_	_	7
2049	2	_	1	3	1	1	_	2	2	1	_	3	1	_	_	1	2	_	_	2	_	_	_	_
2050	4	1	_	5	_	1	_	1	1	4	_	5	4	_	_	4	2	_	_	2	_	_	_	_
Total	57	9	3	69	47	6	2	55	34	21	4	59	37	18	_	55	39	22	_	61	36	15	_	51

Figure 5.8 shows the correlation between the 2021-2050 series for 3-, 6- and 12-monthly SPI and SPEI for each of the study sites. As indicated, there is a statistically positive strong correlation between the SPI and SPEI, with *r* values greater than 0.94 for all timescales. Correlation increased at the timescale of 3-months for Ambo and Bako and 12-months for Ambo and Melkassa. A similar strong positive correlation result with *r* values of greater than 0.96 was found for the timescale of 6-months for all sites. These results indicated that the main explanatory variable for droughts is precipitation. This is particularly obvious at those sites where the evolution of air temperature was stationary during the analysis period. However, correlation decreased at 12-months timescales.

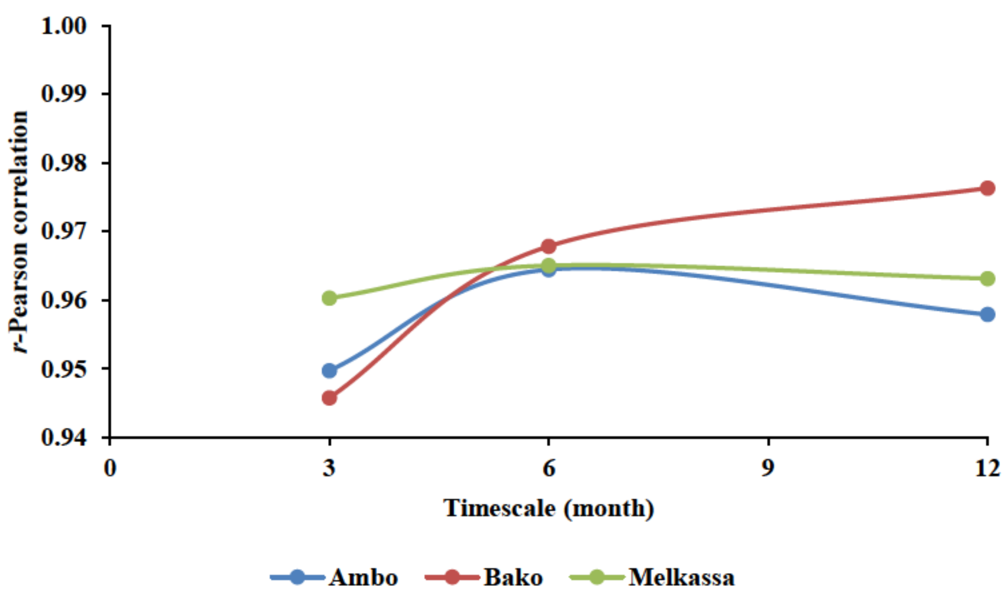

Figure 5.8: Correlation between SPI and SPEI (3-, 6- and 12-month) for Ambo, Bako and Melkassa for 2021 to 2050

5.5 Discussion

This study investigated the temporal variation of drought characteristics, at different timescales (3-, 6- and 12 months) for Ambo, Bako and Melkassa. Long maturing cultivars especially in the mid and highland areas benefited from *Bega* season moisture the study explored also the drought characterstics for the three agricultural seasons for the sites. The results of SPEI and SPI drought indices compared well for the historical period (1995-2017) and under future climate (2021-2050). Future climate data were based on the outputs of an ensemble mean of seven GCMs also used by the Coupled Model Intercomparison Project (CMIP5) using RCP 8.5. The data were downscaled using a quantile-quantile mapping bias correction procedure (Ngai et al., 2017).

According to the SPEI and SPI values, the major dry periods for 1995-2017 were 2002, 2009 and 2015-2016, among which 2015 had the longest and most severe drought for all study sites. The result agrees with the finding from various studies (Legesse and Suryabhagavana, 2014; Hundera et al., 2016; Mere, 2018) confirming that the years mentioned experienced extreme droughts. These prolonged droughts had adverse effects on the agricultural and water resource sectors across the country. Moreover, droughts have threatened widespread cropping areas. For example, drought in 2002 was very severe and in this cropping season, nearly all areas experienced agricultural drought, and agricultural yield was reduced by 80 % (Legesse and Suryabhagavana, 2014). Mere (2018) reported that successive droughts occurred in Ethiopia in 2015 and 2016. According to this report, the number of districts that required lifesaving food aid in the 2015/2016 drought increased from 192 to 228 (30 % of the country). Hundera et al. (2016) reported 2009 was a drought period based on SPI. However, a severe drought was experienced in

2015 and caused hunger for about 10 million people. The Food and Agricultural Organization (FAO, 2016) reported that an El Niño event occurred in 2015. Drought in Ethiopia and much of the Horn of Africa is usually associated with the occurrence of a warm sea surface temperature (SST) observed in the equatorial pacific east. This in turn leads to El Niño-induced droughts causing excessive dryness and major rainfall failures in many parts of the country (Korecha et al., 2007).

The different timescales of the SPI and SPEI demonstrated differences in magnitude and duration of droughts. Shorter timescales showed a reduced severity and shorter duration of droughts than the longer timescales. As compared to the historical period, the SPEI projects more drought events than the SPI at all timescales at all sites suggesting an increase in *PET* as compared to precipitation in the future. Moreover, the results also highlight the inability of the SPI to capture air temperature-controlled droughts. This finding is supported by Vicente-Serrano et al. (2011) who stated that a crucial advantage of the SPEI was its multi-scalar characteristics and comprehensiveness, which enable identification of different drought types and effects in the context of global warming. Under global warming conditions, differences were found between the SPEI and the SPI for the three sites where air temperature increased over the analysis period (Tirivarombo et al., 2018). This indicated that air temperature is the main explanatory variable for droughts. Therefore, under the future climate conditions, the inclusion of air temperature as a variable to quantify potential evapotranspiration (*PET*) in the SPEI does provide much additional information. However, SPI projected more extreme drought under future climate particularly for Ambo and Bako. As compared to Bako, Ambo would experience more extreme drought conditions in the future (Table 5.7). Based on the SPI and SPEI time series, the drought duration, frequency, severity, and intensity were analyzed. Both SPI and SPEI at all timescales projected longer drought duration (7-12 months) for Melkassa than Ambo and Bako while SPI and SPEI 6-month timescale projected longer duration on mid-timescales for Ambo and Bako compared to the historical period (Tables 5.4 and 5.6).

The different timescales of the SPI and SPEI demonstrated differences in magnitude and duration of droughts. Longer timescales (12-months) showed a greater severity and longer duration of droughts than the short timescales (3-6 months). In addition, compared to historical drought, the future drought frequency is shown to increase in the shorter timescale as compared to longer timescales. Although there are differences in the drought periods for each drought index, the longest and most extreme drought predicted by both drought indices is for the mid and end of the 2050s. In general, the SPI and SPEI 3- and 6-month timescale drought projection at all sites indicated that the further into the future, the more frequently droughts with great intensity will occur in the near future. The projected longer droughts for the study sites, would adversely affect the stability of agricultural production, for example the growth rate of maize, the low water levels of rivers and water provision (Potopová et al., 2018).

With respect to drought frequency, both SPI and SPEI revealed that moderate to extremely severe drought frequency can be expected to increase for Ambo and Bako while only moderate drought can be expected to increase for Malkassa. According to SPI and SPEI projected values, the lower altitudes such as Melkassa tend to show relatively decreasing severe drought frequency compared to the mid (Bako) and the higher altitude (Ambo) under future climate. Changes in drought characteristics for the lower altitude can therefore be explained by increasing drought duration and frequency of moderate drought occurrences under future climate (Tables 5.5 and 5.6).

Drought severity increased for all study sites. The SPEI 6- and 12-month for Bako and Melkassa and SPI 6- and 12-month for Ambo showed that the severity of six-month droughts in future climate will be greater compared to the historical period (Tables 5.4 and 5.6). Severe drought reduces the yield of rainfed crops, in particular the anthesis-silking stage for maize, the jointing-booting stage for sorghum, the flowering-podding stage for soybean, and the sowing-milking stage for millet (Chen et al., 2016). Furthermore, a sustained drought of 10 to 40 days at the seedling stage has a negative impact on maize grain filling and eventually leads to a decline in yield. A long duration of a drought prolongs the filling period, which causes serious yield reduction (Zhang et al., 2015). This has been used to study the frequency and duration of drought spell during the maize growing period (Kassie et al., 2014). Moreover, for maize, depending on the severity of drought and stage of occurrence, yield reduction was 10-76 % due to drought (Windhausen et al., 2012; Cairns et al., 2013). Therefore, development of improved drought tolerant maize varieties together with supplementary irrigation are critical for future climate for the study sites.

Drought intensity for all timescales was also investigated for the three study sites. The 12-month timescale for both SPI and SPEI show Ambo will experience an increased drought intensity (-1.8 to -2.3 index value) under future climate than Bako and Melkassa. On the other hand, there would be high intensity droughts expected at both short and long timescales for Bako, but it will not be as intense as that for Ambo. The SPEI -3 and -6 revealed that Melkassa will experience high intensity drought at shorter timescale (agricultural drought) (Table 5.6). Intensity of drought is consistent with the duration and frequency of droughts (Tables 5.5 and 5.6) where the study sites that will receive higher and frequent drought are likely to experience a higher intensity of drought. Thus, it is essential to understand how intensified drought is persisting in a specific area for a given period.

The correlation between the SPI and the SPEI was good at shorter timescales (3 months) and decreased at longer timescales (12-month) for 1995-2017. This indicates that precipitation is a dominant driver of drought conditions. For 2021-2050, the correlation between the SPEI and SPI shows positive high correlation at 6 months and relatively close correlation at 3 months and a decreasing correlation at the longer timescale. The positively correlated indices at 3- and 6-month explains the occurrence of agricultural drought for the future period in the study areas. Overall, the correlation results demonstrated that changes in precipitation were not the only dominant driver causing the long-term drought variations but increasing air temperatures in terms of *PET* are also responsible for drought severities. Even though the SPI is recommended by the World Meteorological Organization (Hayes et al., 2011) as a universal index, a single indicator may be inadequate to characterize a complicated drought (Hao and Singh, 2015).

5.6 Conclusions

Drought risk assessment indices relative to the aspects of drought duration, severity, intensity and frequency are used to assess the maize growing period drought risk during 1995–2017 and predictions for 2021–2050. Change in drought duration, severity, intensity and frequency patterns, caused by climate change, will increase the likelihood of maize crop failure and long-term production declines in the near future. It is anticipated that climate change will increase water scarcity in the coming decades in maize growing areas investigated. The study assessed both historical and future droughts for three sites namely Ambo (high altitude), Bako (mid-altitude) and Melkassa (low altitude) in Ethiopia. The study used weather data for 1995-2017 as the reference, and ensemble mean of seven GCMs downscaled from CORDEX-Africa data from 2021-2050 under the RCP 8.5 scenario. The Standardized Precipitation Index (SPI) and the Standardized Precipitation Evapotranspiration Index (SPEI) with potential evapotranspiration estimated using the Hargreaves–Samani equation.

The SPEI showed for the study sites, more drought conditions in the future were noted when using the SPEI when compared to the SPI. Thus, in the context of global warming future drought risks can be accurately estimated by incorporating *PET* data in drought quantification rather than using only precipitation. The drought event, frequency, duration, severity and intensity have shown that the frequency and duration of moderate to extremely severe drought would increase for the higher altitude (Ambo) in the future. In addition to the frequent occurrence of moderate to severe drought SPEI-6 showed that the severity and duration of six-month droughts in future will be high for the mid-altitude site (Bako). In particular, for drought duration identified by SPEI and SPI at all timescales, the lower altitude site (Melkassa) will experience long drought duration in the future compared to the historical period. However, SPEI -3 and -6 projected the short timescale drought to be more intensive than the long timescales. Therefore, in addition to causing more severe and frequent drought, climate change will also result in longer duration droughts for the study sites.

The short-term drought at Bako and Melkassa and long-term drought at Ambo will be more influenced by climate change. Overall, the lower altitude site (Melkassa) will be the most affected site in the future compared to the other two sites due to the longer anticipated drought duration (7-12 month) together with high intensity drought. Therefore, decision makers should pay attention to the severe problems that are anticipated for the study areas in the future. Furthermore, irrigation, the development of improved and drought tolerance maize cultivars for increased air temperatures and water-limited environments are risk-reducing management options that might have the potential to offset some of the maize yield losses caused by severe drought due to climate change. Much attention needs to be directed to the substitution of maize cultivation with more drought tolerant crops, particularly for the lower altitude site, is highly recommended in the near future.

5.7 References

Abramowitz, M., Irene, A., Stegun, I.A. (Eds.), 1965. Handbook of Mathematical Functions with Formulas, Graphs, and Mathematical Tables. National Bureau of Standards Applied Mathematics Series 5. Library of Congress Catalog Card Number: 64-60036 5.

Abrha, H. and Hagos, H., 2019. Future drought and aridity monitoring using multimodel approach under climate change in Hintalo Wejerat district, Ethiopia. *Sustainable Water Resources Management*, *5*(4), pp. 1963-1972.

Adhyani, N.L., June, T. and Sopaheluwakan, A., 2017, March. Exposure to drought: duration, severity and intensity (Java, Bali and Nusa Tenggara). In *IOP conference series: earth and environmental science* (Vol. 58, pp. 1755-1315).

Ahmadalipour, A., Moradkhani, H. and Svoboda, M., 2017. Centennial drought outlook over the CONUS using NASA-NEX downscaled climate ensemble. *International Journal of Climatology*, *37*(5), pp. 2477-2491.

Alemu, H.W. and Carlson, A.S., 2020. Thirteen years on: The long journey of optometry in Ethiopia. *African Vision and Eye Health*, *79*(1), pp. 1-6.

Beguería, S., Vicente-Serrano, S.M., Reig, F. and Latorre, B., 2014. Standardized precipitation evapotranspiration index (SPEI) revisited: parameter fitting, evapotranspiration models, tools, datasets and drought monitoring. *International Journal of Climatology*, *34*(10), pp. 3001-3023.

Cairns, J.E., Crossa, J., Zaidi, P.H., Grudloyma, P., Sanchez, C., Araus, J.L., Thaitad, S., Makumbi, D., Magorokosho, C., Bänziger, M. and Menkir, A., 2013. Identification of drought, heat, and combined drought and heat tolerant donors in maize. *Crop Science*, *53*(4), pp. 1335-1346.

CCCMA, 2017b. Second Generation Canadian Earth System Model [Online]. Government of Canada. Canadian Centre for Climate Mod. http://www.ec.gc.ca/ccmaccccma/default.asp?lang=En&xml=1A3B7DF1-99BB-4EC8-B129-09F83E72D645, Accessed date: 1 July 2020.

Chen, T., Xia, G., Liu, T., Chen, W. and Chi, D., 2016. Assessment of drought impact on main cereal crops using a standardized precipitation evapotranspiration index in Liaoning Province, China. *Sustainability*, *8*(10), pp. 2-16.

Collins, W.J., Bellouin, N., Doutriaux-Boucher, M., Gedney, N., Halloran, P., Hinton, T., Hughes, J., Jones, C.D., Joshi, M., Liddicoat, S. and Martin, G., 2011. Development and evaluation of Earth-System model–HadGEM2. *Geoscientific Model Development*, *4*(4), pp. 1051-1075.

Crausbay, S.D., Ramirez, A.R., Carter, S.L., Cross, M.S., Hall, K.R., Bathke, D.J., Betancourt, J.L., Colt, S., Cravens, A.E., Dalton, M.S. and Dunham, J.B., 2017. Defining ecological drought for the twenty-first century. *Bulletin of the American Meteorological Society*, *98*(12), pp. 2543-2550.

Dercon, S., 2005. Risk, poverty and vulnerability in Africa. *Journal of African Economies 14*(4), pp. 483-488.

Diffenbaugh, N.S., Swain, D.L. and Touma, D., 2015. Anthropogenic warming has increased drought risk in California. *Proceedings of the National Academy of Sciences*, *112* (13), pp. 3931-3936.

Droogers, P. and Allen, R.G., 2002. Estimating reference evapotranspiration under inaccurate data conditions. *Irrigation and Drainage Systems*, *16*(1), pp.33-45.

Dufresne, J.L., Foujols, M.A., Denvil, S., Caubel, A., Marti, O., Aumont, O., Balkanski, Y., Bekki, S., Bellenger, H., Benshila, R. and Bony, S., 2013. Climate change projections using the IPSL-CM5 Earth System Model: from CMIP3 to CMIP5. *Climate Dynamics*, *40*(9-10), pp. 2123-2165.

Enyew, B.D., Van Lanen, H.A.J. and Van Loon, A.F., 2014. Assessment of the impact of climate change on hydrological drought in Lake Tana catchment, Blue Nile basin, Ethiopia. *J. Geology and Geosciences*, *3*(6), pp. 1-17.

Eshetie, S.M., Demisse, G.B. and Suryabhagavan, K.V., 2016. Evaluation of vegetation indices for agricultural drought monitoring in East Amhara, Ethiopia. *International Journal of Scientific Research*, *5*(10), pp. 535-540.

FAO, 2016. Ethiopia El Niño Response Plan. Food and Agricultural Organization (FAO), Rome, Italy, *4*, pp. 1-22.

Frank, A., Armenski, T., Gocic, M., Popov, S., Popovic, L. and Trajkovic, S., 2017. Influence of mathematical and physical background of drought indices on their complementarity and drought recognition ability. *Atmospheric Research*, *194*, pp. 268-280.

Funk, C., Harrison, L., Shukla, S., Korecha, D., Magadzire, T., Husak, G., Galu, G. and Hoell, A., 2016. Assessing the contributions of local and east Pacific warming to the 2015 droughts in Ethiopia and Southern Africa. *Bulletin of the American Meteorological Society*, *97*(12), pp. S75-S80.

Guo, X., Yang, Y., Li, Z., You, L., Zeng, C., Cao, J. and Hong, Y., 2019. Drought trend analysis based on the Standardized Precipitation–Evapotranspiration Index using NASA’s earth exchange global daily downscaled projections, high spatial resolution Coupled Model Intercomparison Project Phase 5 projections, and assessment of potential impacts on China’s crop yield in the 21st century. *Water*, *11*(12), pp. 1-19.

Haile, G.G., Tang, Q., Hosseini-Moghari, S.M., Liu, X., Gebremicael, T.G., Leng, G., Kebede, A., Xu, X. and Yun, X., 2020. Projected impacts of climate change on drought patterns over East Africa. *Earth's Future*, *8*(7), p. e2020EF001502.

Hao, Z. and Singh, V.P., 2015. Drought characterization from a multivariate perspective: A review. *Journal of Hydrology*, *527*, pp. 668-678.

Hargreaves, G.H., 1989. Accuracy of estimated reference crop evapotranspiration. *Journal of Irrigation and Drainage Engineering*, *115*(6), pp. 1000-1007.

Hargreaves, G.H. and Allen, R.G., 2003. History and evaluation of Hargreaves evapotranspiration equation. *Journal of Irrigation and Drainage Engineering*, *129*(1), pp. 53-63.

Hargreaves, G.H. and Samani, Z.A., 1985. Reference crop evapotranspiration from temperature. *Applied Engineering in Agriculture*, *1*(2), pp. 96-99.

Hayes, M., Svoboda, M., Wall, N. and Widhalm, M., 2011. The Lincoln declaration on drought indices: universal meteorological drought index recommended. *Bulletin of the American Meteorological Society*, *92*(4), pp. 485-488.

Hazeleger, W., Severijns, C., Semmler, T., Ştefãnescu, S., Yang, S., Wang, X., Wyser, K., Dutra, E., Baldasano, J.M., Bintanja, R. and Bougeault, P., 2010. EC-Earth: a seamless earth-system prediction approach in action. *Bulletin of the American Meteorological Society*, *91*(10), pp. 1357-1364.

Heim, R.R., 2002. A review of twentieth-century drought indices used in the United States. *Bulletin of the American Meteorological Society*, *83*(8), pp. 1149-1166.

Hess, A., Iyer, H. and Malm, W., 2001. Linear trend analysis: a comparison of methods. *Atmospheric Environment*, *35*(30), pp. 5211-5222.

Hundera, H., Berhan, G. and Bewuket, W., 2016. Remote sensing and GIS based agricultural drought risk assessment in east Shewa zone, central Rift Valley region of Ethiopia. *Remote Sensing*, *6*(7), pp. 48-54.

IPCC, 2012. Managing the Risks of Extreme Events and Disasters to Advance Climate Change Adaptation, C.B. Field, V. Barros, T.F. Stocker, D. Qin, D.J. Dokken, K.L. Ebi, M.D.

Mastrandrea, K.J. Mach, G.K. Plattner, S.K. Allen, M. Tignor, and P.M. Midgley (Eds.) Cambridge University Press. The Edinburg Building, Shaftesbury Road, Cambridge CB2 8RU England, pp. 582.

https://www.ipcc.ch/pdf/ special-reports/srex/SREX_Full_Report.pdf.

IPCC, 2013. The physical science basis. In: Contribution of working group I to the fifth assessment report of the Intergovernmental Panel on Climate Change. Cambridge UK: Cambridge University Press, pp. 1535.

Jeffrey, S.J., Rotstayn, L., Collier, M., Dravitzki, S., Hamalainen, C., Moeseneder, C., Wong, K.K. and Syktus, J., 2013. Australia's CMIP5 submission using the CSIRO-Mk3. 6 model. *Australia Meteorology Oceanography Journal*, *63*, pp. 1-13.

Jeong, D.I., Sushama, L. and Khaliq, M.N., 2014. The role of temperature in drought projections over North America. *Climatic Change*, *127*(2), pp. 289-303.

Kassie, B.T., Rötter, R.P., Hengsdijk, H., Asseng, S., Van Ittersum, M.K., Kahiluoto, H. and Van Keulen, H., 2014. Climate variability and change in the Central Rift Valley of Ethiopia: challenges for rainfed crop production. *The Journal of Agricultural Science*, *152*(1), pp. 1-17.

Kim, U. and Kaluarachchi, J.J., 2009. Climate Change Impacts on Water Resources in the Upper Blue Nile River Basin, Ethiopia 1. *JAWRA Journal of the American Water Resources Association*, *45*(6), pp. 1361-1378.

King, D.A., Bachelet, D.M., Symstad, A.J., Ferschweiler, K. and Hobbins, M., 2015. Estimation of potential evapotranspiration from extraterrestrial radiation, air temperature and humidity to assess future climate change effects on the vegetation of the Northern Great Plains, USA. *Ecological Modelling*, *297*, pp. 86-97.

Korecha, D. and Barnston, A.G., 2007. Predictability of June-September rainfall in Ethiopia. *Monthly Weather Review*, *135*(2), pp. 628-650.

Lee, S.H., Yoo, S.H., Choi, J.Y. and Bae, S., 2017. Assessment of the impact of climate change on drought characteristics in the Hwanghae Plain, North Korea using time series SPI and SPEI: 1981–2100. *Water*, *9*(8), pp. 1-19.

Legesse, G and Suryabhagavana, K.V., 2014. Remote sensing and GIS based agricultural drought assessment in East Shewa Zone, Ethiopia. *Tropical Ecology* 55 (3), pp. 349-363.

Liu, Z., Wang, Y., Shao, M., Jia, X. and Li, X., 2016. Spatiotemporal analysis of multiscalar drought characteristics across the Loess Plateau of China. *Journal of Hydrology*, *534*, pp. 281-299.

McKee, T.B., Doesken, N.J. and Kleist, J., 1993, January. The relationship of drought frequency and duration to time scales. In *Proceedings of the 8th Conference on Applied Climatology*, *17*(22), pp. 179-183.

Mera, G.A., 2018. Drought and its impacts in Ethiopia. *Weather and Climate Extremes*, *22*, pp. 24-35.

Moss, R.H., Edmonds, J.A., Hibbard, K.A., Manning, M.R., Rose, S.K., Van Vuuren, D.P., Carter, T.R., Emori, S., Kainuma, M., Kram, T. and Meehl, G.A., 2010. The next generation of scenarios for climate change research and assessment. *Nature*, *463*(7282), pp. 747-756.

Ngai, S.T., Tangang, F. and Juneng, L., 2017. Bias correction of global and regional simulated daily precipitation and surface mean temperature over Southeast Asia using quantile mapping method. *Global and Planetary Change*, *149*, pp. 79-90.

Palmer, W.C., 1965. *Meteorological drought*. US Department of Commerce, Weather Bureau, *30*, pp. 1-58.

Potopová, V., Štěpánek, P., Zahradníček, P., Farda, A., Türkott, L. and Soukup, J., 2018. Projected changes in the evolution of drought on various timescales over the Czech Republic according to Euro-CORDEX models. *International Journal of Climatology*, *38*, pp. e939-e954.

Rhee, J. and Cho, J., 2016. Future changes in drought characteristics: regional analysis for South Korea under CMIP5 projections. *Journal of Hydrometeorology*, *17*(1), pp. 437-451.

Robinson, S., Strzepek, K. and Cervigni, R., 2013. The cost of adapting to climate change in Ethiopia: Sector-wise and macro-economic estimates. *Ethiopia Strategy Support Program II (ESSP) working Paper*, *53*. IFPRI ESSP WP. http://www.ifpri.org/sites/default/files/publications/esspwp53.pdf

Samuelsson, P., Jones, C.G., Will´ En, U., Ullerstig, A., Gollvik, S., Hansson, U.L.F., Jansson, E., Kjellstro¨ M, C., Nikulin, G. and Wyser, K., 2011. The Rossby Centre Regional Climate model RCA3: model description and performance. *Tellus A: Dynamic Meteorology and Oceanography*, *63*(1), pp. 4-23.

Schwalm, C.R., Anderegg, W.R., Michalak, A.M., Fisher, J.B., Biondi, F., Koch, G., Litvak, M., Ogle, K., Shaw, J.D., Wolf, A. and Huntzinger, D.N., 2017. Global patterns of drought recovery. *Nature*, *548*(7666), pp. 202-205.

Shukla, S., Safeeq, M., AghaKouchak, A., Guan, K. and Funk, C., 2015. Temperature impacts on the water year 2014 drought in California. *Geophysical Research Letters*, *42*(11), pp. 4384-4393.

Sun, B., Zhao, H. and Wang, X., 2016. Effects of drought on net primary productivity: Roles of temperature, drought intensity, and duration. *Chinese Geographical Science*, *26*(2), pp. 270-282.

Suryabhagavan, K.V., 2017. GIS-based climate variability and drought characterization in Ethiopia over three decades. *Weather and Climate Extremes*, *15*, pp. 11-23.

Taye, M.T., Dyer, E., Hirpa, F.A. and Charles, K., 2018. Climate change impact on water resources in the Awash basin, Ethiopia. *Water*, *10*(11), pp. 1-16.

Taylor, R., 1990. Interpretation of the correlation coefficient: a basic review. *Journal of Diagnostic Medical Sonography*, *6*(1), pp. 35-39.

Thornthwaite, C.W., 1948. An approach toward a rational classification of climate. *Geographical Review*, *38*(1), pp. 55-94.

Tirivarombo, S., Osupile, D. and Eliasson, P., 2018. Drought monitoring and analysis: standardised precipitation evapotranspiration index (SPEI) and standardised precipitation index (SPI). *Physics and Chemistry of the Earth, Parts A/B/C*, *106*, pp. 1-10.

Touma, D., Ashfaq, M., Nayak, M.A., Kao, S.C. and Diffenbaugh, N.S., 2015. A multimodel and multi-index evaluation of drought characteristics in the 21st century. *Journal of Hydrology*, *526*, pp. 196-207.

Van Loon, A.F., 2015. Hydrological drought explained. *Wiley Interdisciplinary Reviews: Water*, *2*(4), pp. 359-392.

Venkataraman, K., Tummuri, S., Medina, A. and Perry, J., 2016. 21st century drought outlook for major climate divisions of Texas based on CMIP5 multimodel ensemble: Implications for water resource management. *Journal of Hydrology*, *534*, pp. 300-316.

Vicente-Serrano, S.M., Beguería, S. and López-Moreno, J.I., 2010. A multiscalar drought index sensitive to global warming: the standardized precipitation evapotranspiration index. *Journal of Climate*, *23*(7), pp. 1696-1718.

Vicente-Serrano, S.M., López-Moreno, J.I., Drumond, A., Gimeno, L., Nieto, R., Morán-Tejeda, E., Lorenzo-Lacruz, J., Beguería, S. and Zabalza, J., 2011. Effects of warming processes on droughts and water resources in the NW Iberian Peninsula (1930− 2006). *Climate Research*, *48*(2-3), pp. 203-212.

Voldoire, A., Sanchez-Gomez, E., y Mélia, D.S., Decharme, B., Cassou, C., Sénési, S., Valcke, S., Beau, I., Alias, A., Chevallier, M. and Déqué, M., 2013. The CNRM-CM5 1 global climate model: description and basic evaluation. *Climate Dynamics*, *40*(9-10), pp. 2091-2121.

Wang, F., Wang, Z., Yang, H., Zhao, Y., Zhang, Z., Li, Z. and Hussain, Z., 2019. Copula-based drought analysis using Standardized Precipitation Evapotranspiration Index: A case study in the Yellow river basin, China. *Water*, *11*(6), pp. 1-20.

Wang, Q., Wu, J., Lei, T., He, B., Wu, Z., Liu, M., Mo, X., Geng, G., Li, X., Zhou, H. and Liu, D., 2014. Temporal-spatial characteristics of severe drought events and their impact on agriculture on a global scale. *Quaternary International*, *349*, pp. 10-21.

Watanabe, M., Suzuki, T., O'ishi, R., Komuro, Y., Watanabe, S., Emori, S., Takemura, T., Chikira, M., Ogura, T., Sekiguchi, M. and Takata, K., 2010. Improved climate simulation by MIROC5: Mean states, variability, and climate sensitivity. *Journal of Climate*, *23*(23), pp. 6312-6335.

Williams, A.P., Seager, R., Abatzoglou, J.T., Cook, B.I., Smerdon, J.E. and Cook, E.R., 2015. Contribution of anthropogenic warming to California drought during 2012–2014. *Geophysical Research Letters*, *42*(16), pp. 6819-6828.

Windhausen, V.S., Wagener, S., Magorokosho, C., Makumbi, D., Vivek, B., Piepho, H.P., Melchinger, A.E. and Atlin, G.N., 2012. Strategies to subdivide a target population of environments: Results from the CIMMYT-led maize hybrid testing programs in Africa. *Crop Science*, *52*(5), pp. 2143-2152.

Yao, N., Li, L., Feng, P., Feng, H., Li Liu, D., Liu, Y., Jiang, K., Hu, X. and Li, Y., 2020. Projections of drought characteristics in China based on a standardized precipitation and evapotranspiration index and multiple GCMs. *Science of the Total Environment*, *704*, pp. 5430-5447.

Zhang, J. P., Yong-Kun, H.E., Jing, W.A.N.G., Yan-Xia, Z.H.A.O. and Chun-Yi, W.A.N.G., 2015. Impact simulation of drought at different growth stages on grain formation and yield of maize. *Chinese Journal of Agrometeorology*, *36*(01), p.43-49.

Zhang, L., Jiao, W., Zhang, H., Huang, C. and Tong, Q., 2017. Studying drought phenomena in the Continental United States in 2011 and 2012 using various drought indices. *Remote Sensing of Environment*, *190*, pp. 96-106.

Zhao, H., Gao, G., An, W., Zou, X., Li, H. and Hou, M., 2017. Timescale differences between SC-PDSI and SPEI for drought monitoring in China. *Physics and Chemistry of the Earth, Parts A/B/C*, *102*, pp. 48-58.

Lead to Chapter 6

Previous Chapters (1 and 2) presented the importance of climate-crop modelling with their multimodel ensemble and uncertainties in climate change assessment studies. Chapters (3 and 4) mainly focused on crop models calibration, evaluation and climate change impact and adaptation options. Chapter 5 presented historical and future drought events for the study sites. Chapter 6 provides conclusions and recommendations of the previous chapters for further research.

CHAPTER 6: CONCLUSIONS AND RECOMMENDATIONS

FOR FURTHER RESEARCH

6.1 Introduction

Maize growing smallholder farmers in Ethiopia are vulnerable to the impact of climate change due to local weather variability, the rainfed nature of the farming system and their low adaptive capacity. Maize production is highly dependent on precipitation. Small changes in precipitation distribution or amount could potentially affect maize productivity under future climate. In Ethiopia, it is expected that climate change has already and will further increase climatic variability and the frequency and severity of extreme weather events. With the increasing climate persuaded risks, rainfed agriculture in most places particularly in maize growing regions of Ethiopia, is projected to become further constrained. Thus, climate change impact assessments are needed to investigate the potential impacts of climate change on crop production. Identification and evaluation of different on-farm adaptation strategies that might minimize the climate change risk on the impacts on crop phenology and grain yield are also needed. Although previous research on climate change impact on maize production has been conducted, most studies focused on economic aspects, yield variability and yield gap of maize. In addition, previous researches of climate change’s impact on crop yield were investigated by setting a hypothetical decrease in precipitation and an increase in air temperatures in the future climate. However, due to the complex interactions among weather variables and radiative forcing of the climate system, the temporal pattern and variability of the current climate will not be the same as that for the future climate. Therefore, climate change data from global climate models (GCMs) is an important approach for use as an input for process-based crop models for climate change impact assessment investigations on crop yield. However, due to the uncertainty in different emission scenarios, and individual model structure, the use of a single model can result in under- or over-estimation of climate variables and crop yield at regional scales in the future climate. Thus, the use of multiple climate and crop models, together with their ensemble, may provide an improved result in projecting future climate.

The main motivation for this research is to have an improved understanding of the impact of climate change on future maize yield and to explore ways of improving maize production by developing suitable adaptation strategies for future climate.

6.2 Revisiting the research question, aims and objectives

The overall aim of the research undertaken was to assess the impact of past and future climate on maize (*Zea mays* L.) production and identify adaptation options using a set of crop and climate models in Ethiopian tropical environments. As such, several research questions were developed.

Research questions included:

1. Are the APSIM-maize, AquaCrop and DSSAT CERES-maize deterministic crop models capable of simulating maize (*Zea mays* L.) growth and development for different agro-ecologies, soils, and management practices in Ethiopian tropical environments?

2. Can the multimodel ensemble outputs reduce uncertainties and improve maize yield simulation when compared to the use of individual model outputs?
3. Can climate models be integrated into crop models for climate change assessment and adaptation options? Yes, it can be integrated. Can changes in planting date, choice of cultivars and nitrogen fertilizer improve maize yield under a changed climate?
4. Are climate models capable of projecting drought risks?

The specific objectives were to:

- calibrate APSIM-maize, AquaCrop and DSSAT CERES-maize models and evaluate the performance of the models and their multimodel ensemble in simulating maize yield;
- investigate the impact of future climate on maize yield using climate and crop models, and identify adaptation options;
- assessment of climate change induced drought risks using a climate model ensemble for maize growing areas under past and future scenarios.

6.3 Study findings

Calibrating the APSIM-maize, AquaCrop and DSSAT CERES-maize models and the evaluation of the performance of the models and their multimodel ensemble in simulating maize yield addressed the first two research questions. Using daily climate data, site-specific soil and management parameters, and field experimental data, the APSIM-maize, AquaCrop and DSSAT CERES-maize models were calibrated for the newly released maize varieties. Results indicated that each of the three crop models used enabled accurate simulation of flowering, maturity, canopy cover (AquaCrop) and grain yield against measured data. Evaluation of the models indicated that APSIM-maize and DSSAT CERES-maize accurately simulated days to flowering and maturity with a root mean square error (RMSE) values ranging from 1.73 – 4.09 and 1.66 – 5.36 days, respectively. However, the DSSAT CERES-maize model over-estimated the maturity period of late maturing varieties at Ambo. The AquaCrop model accurately simulated maize canopy cover for all varieties studied with a RMSE of less than 10.8 % and a high (0.95) value of index of agreement (*d*). The simulated grain yield agreed reasonably well with the measured data with normalized RMSE values ranging from 13 – 19 %, 1 – 4 % and 1 – 17 % for APSIM, AquaCrop and DSSAT maize models, respectively. However, the APSIM model underestimated yield for all maize varieties for Ambo (RMSE of 1.14 t ha^{-1} and *d* value of 0.50). The best performance was obtained when an ensemble of all models was considered, which reduced the RMSE values for grain yield to 0.35 t ha^{-1} for Ambo and 0.41 t ha^{-1} for Melkassa. Furthermore, the ensemble mean reduced the normalized RMSE by 8 % while increasing the *d* value to above 0.90 for both evaluation sites. Model ensembles reduced model uncertainty and improved simulation output accuracy compared to the outputs of individual models in tropical environments.

The impact of future climate on maize yield was investigated using climate and crop models and adaptation options identified.

This study, addressing the third research question, utilized downscaled precipitation and air temperature data from seven bias-corrected GCMs (CanESM2, CNRM-CM5, CSIRO-MK3-6-0, EC-EARTH, HadGEM2-ES, IPSL-CM5A-MR and MIROC5) under the RCP8.5 scenario. The result of climate change impact assessments indicated that in 2030, the average monthly maximum air temperature may increase by 0.3-1.7 °C, 0.7-2.2 °C and 0.8-1.8 °C for Ambo, Bako and Melkassa respectively. GCMs revealed the increase in average monthly minimum air temperature by 0.6-1.7 °C, 0.8-2.3 °C and 0.6-2.7 °C for the corresponding sites for 2030. Similarly, monthly total precipitation for *Kiremt* season (June to September) projected to increase by up to 55 % (365 mm) for Ambo and 75 % (241 mm) for Bako respectively, whereas a significant decrease in monthly total precipitation is projected for Melkassa by 2030. The *Belg* season (March to May) total monthly precipitation is projected to decrease for all study sites. Interestingly, by 2030 the total monthly precipitation for the *Bega* season (October to February) is projected to increase for Melkassa particularly for November, December and January while *Bega* season total monthly precipitation will remain unchanged for Ambo and Bako compared to the baseline period.

Climate change could reduce maize yield by an average of 4 % and 16 % for Ambo and Melkassa respectively, while maize yield is projected to increase by 2 % for Bako in 2030 if farmers continue employing the existing agronomic practice with the current maize cultivars for future climate (2030). The climate change adaptation result using a shift in planting date, nitrogen fertilizer application and a change in cultivar revealed that for the higher altitude site (Ambo), early planting of maize cultivars between 15 May to 01 June would result in improved relative yields in the future climate. Fertilizer levels between 23-150 kg ha^{-1} would result in improved yields for all maize cultivars when combined with early planting for Ambo. For a mid-altitude (Bako), planting after 15 May has either no or negative effect on maize yield. Early planting combined with a nitrogen fertilizer level of 23-100 kg ha^{-1} provided an increased relative yields under the future climate. Delayed planting has a negative influence on maize production for Bako under the future climate (2030). For lower altitudes (Melkassa), late planting would have lower relative yields compared to early planting. Higher fertilizer levels (100-150 kg ha^{-1}) would reduce yield reductions under the future climate, but this varied among maize cultivars studied. Planting the Jibat cultivar between 15-30 June at higher N levels may reduce severe yield reduction of maize at Melkassa. Generally, future climate is expected to have a negative impact on maize yield and changes in crop management practice for the near future can alleviate the impacts on maize yield.

Historical and future drought characteristics using historical observed data from 1995-2017 and an ensemble of seven Global Climate Models (GCMs) in the Coupled Model Intercomparison Project (CMIP5) for maize growing areas of Ethiopia were assessed. This study addressed the fourth research question. The widely known Standardized Precipitation Index (SPI) and Standardized Precipitation Evapotranspiration Index (SPEI) were used to investigate drought characteristics. The results indicate that compared to the SPI-based analysis, use of the SPEI suggests more drought conditions for the maize-growing study sites in the future indicating potential effects of increasing air temperatures on drought risks. The SPI and SPEI at all timescales projected 2027, 2039, 2042, 2048 and 2049 for Ambo, 2022, 2023, 2042, 2048 and

2049 for Bako, and 2021, 2036, 2044, 2047 and 2048 for Melkassa as the driest years in the future climate. SPI and SPEI have a strong correlation (R > 0.9) on the direction of change but the effect on the drought condition was different. Increasing frequency of moderate to extremely severe drought with extended drought duration is expected to occur for Ambo in the future. According to the 6-month SPEI, Bako will experience agricultural droughts with greater severity and duration in the future. Both SPI and SPEI projected increasing drought duration at short and long timescales for the Melkassa site. However, the 3- and 6-month SPEI predicted the shorter timescale droughts to be more intense than the longer timescale.

6.4 Contributions to new knowledge

The specific contributions of this research to new knowledge are listed below:

1. This research provided the first insights on using three different deterministic crop growth simulation models to simulate maize yield in Ethiopian tropical environments. This is one of the innovative features of the methodology used in this thesis. Previous research efforts on modelling crop-climate interactions in Ethiopia used a maximum of two crop models with limited regions (usually Central Rift valley and other lowland areas) to simulate crop growth and yield processes. These previous studies therefore do not provide an in-depth analysis to produce more comprehensive and reliable climate change sensitivity assessments. The study also contributed towards new knowledge in providing insights on the use of a multmodel ensemble approach in reducing model uncertainty and improved simulation output accuracy compared to the outputs of individual models for a tropical environment. This could provide important lessons to

other researchers on the added value of using multimodel ensemble in simulation studies. The study also developed new genetic coefficients for new local maize cultivars through a calibration process of the APSIM-maize, AquaCrop and DSSAT CERES-maize models and the crop models were evaluated for local conditions.

2. While climate change impact assessments have for decades been studied, very few studies have actively quantified the adaptation strategies in Ethiopia. The research presented here is the first of its kind to quantify both impacts and adaptation strategies of climate change in the maize growing agroecology of Ethiopia using multiple crop-climate models and their ensembles. The study illustrated that the seven GCMs could model future changes in precipitation and air temperature under RCP 8.5 scenario for the three sites in Ethiopia. The study findings also demonstrated that there will be a clear increase of average monthly minimum air temperature compared to the maximum air temperature change, suggesting that minimum air temperatures will experience the greatest impact from climate change in the period of 2030 for the study sites. Furthermore, the study also contributed towards new knowledge in providing insights into the impact of climate change on maize yield for the study sites in the near future, and thus also provides insights on scientifically based effective adaptation options for farmers and policymakers to mitigate the adverse effects of future climate change. In addition, adaptation recommendations are site specific, not general. Several adaptation studies have been undertaken for Ethiopia but these studies did not use the methodologies used in this research. The study contributed agro-ecological climate change adaptation mechanism

with multiple crop, climate models and their ensemble outputs which most studies lack in Ethiopia.

3. As with current climate research, research aiming to analyze drought risks has been focused on specific regions and/or the whole country at a wider scale and has somewhat neglected agroecological aspects of maize growing areas. Using the ensemble of seven GCMs the study provided new information describing the impact of RCP8.5 climate scenarios on drought on maize growing areas, a study that has never been conducted for Ethiopia until now.

6.5 Challenges and research limitations encountered

Crop-climate modelling is an effective and advanced method of understanding crop-soil-climate interactions and evaluating various agronomic adaptation strategies. However, the success of such approaches depends on the quality of input data used. For this research, acquiring high quality long-term daily meteorological data proved to be the greatest challenge. While data were available for several stations in Ethiopia, the quality of the data came into question. Missing and unlikely values within the datasets are likely attributed to a failure to maintain meteorological instruments and a lack of close supervision of the stations. Though, missing values required extensive and time-consuming gap filling, patching of missing values utilizing accepted methods proved to be accurate.

Limited access to climate data is another challenge for climate research. At present, there are difficulties in obtaining climate data due to constraining data use policies. The observed data obtained for this study were from the National Meteorological Agency of Ethiopia through long administrative processes. Climate data need to be considered as a public good provided that it is used for research purpose.

For obvious reasons, COVID-19 was a great challenge to the academic community and researchers all over the world, including myself.

It has become standard practice to use several climate models to characterize uncertainty in future climate. This study is only use a multimodel ensemble approach to quantify uncertainty then it is necessary to use additional uncertainty quantifying methods. In addition, until 2050 at least there is relatively little or no difference in climate change between the different RCP emissions scenarios. It is therefore a reasonable approach to apply climate changes with other future socio-economic aspects in order to characterise the full range of possible future impacts of climate change.

6.6 Recommendations

- Based on the study results, a multimodel approach improved the simulation estimates of maize yield by reducing model uncertainty when compared to the result when individual models were applied. This approach could, therefore, provide more reliable predictions for maize cultivars grown in diverse environments in the tropics.

- Increasing air temperature in the future for the study sites would demand the use of new cultivars with more heat tolerant traits. Hence breeders need to consider robustness to climate change in their programs.

- A combination of different planting dates and increased N fertilizer levels with different maturity date of maize varieties is strongly recommended for the study sites to offset the adverse effects of future climate change on maize yield.

- Changing the planting date is one of the suitable adaptation strategies for future climate for the study sites. However, changing the planting date is site- and variety-specific and its effectiveness may vary from site to site. Different GCMs and emission pathways may also respond differently. Therefore, it should be tested for each specific site using an ensemble mean of multiple GCMs to increase the certainty of shifting in planting date strategy.

- The projected moderate to extremely severe drought under future climate will negatively affect maize production for the study sites. Therefore, the development of resilient improved maize varieties for increased air temperature, crop diversification, food reserve, crop insurance, soil and water conservation, drought tolerance for water-limited environments are highly recommended as risk-reducing management options to offset some of the maize yield losses caused by severe drought due to climate change.

- The anticipated longer drought durations together with high intensity droughts for a lower altitude needs increased attention on the substitution of maize cultivation with more drought tolerant crops such as sorghum and millet in the near future.

- Comparision of several crop models with more scenarios are recommended for further research in the study sites.

6.7 Future research opportunities

The results of this study have shown that the APSIM-maize, AquaCrop and DSSAT CERES-maize deterministic crop models are suitable for simulating the phenology and yield of maize for the tropical sites studied. However, under-or over-estimations were observed for the simulated parameters by the individual models studied. There is a need for future research to improve the robustness of models used in tropical environments.

Although the research presented in this thesis provides a useful insight into the impacts of climate change and its adaptation on maize production in Ethiopia, further research is needed. Adaptation options such as nitrogen fertilization may include significant expenses and will require additional feasibility concerning economics aspects and sustainability assessments.

Future research is necessary to include the socio-economic impacts of the different adaptation management options.

Future research should also be undertaken by breeders on developing new drought and heat tolerant cultivars for lowland maize growing areas in order to compensate for future climate change impacts.

6.8 Final comments and summary conclusions

Generally, the findings of the study highlight the impacts and adaptations of climate change on maize growing areas of Ethiopia. The results of the study conclude that:

- Based on the findings of crop model calibration and validation, the APSIM-maize, DSSAT CERES-maize and AquaCrop models could reasonably simulate maize phenology, canopy cover (AquaCrop) and yield for different maturity maize varieties for three agro-ecologies under rainfed conditions in Ethiopia;

- The multimodel approach employed improved the simulation of grain yield by reducing model uncertainty when it was compared to the performance of the individual models studied.

- Under data scarce conditions, simpler models such as AquaCrop could be used to simulate maize yield with reasonable accuracy.

- A significant projected decrease in monthly total precipitation, during the main rainy season (*Kiremt*) for Melkassa. However, an increase in monthly total precipitation was projected for Ambo and Bako relative to the baseline for 2030s.

- Total monthly precipitation for the short rainy season (*Belg*) is projected to decrease for all study sites by 2030.

- The total monthly precipitation for the dry season (*Bega*) would expect to increase for Melkassa particularly for November, December, and January while *Bega* season total monthly precipitation will remain unchanged for Ambo and Bako by 2030 compared to the baseline period.

- An increasing trend in average monthly maximum and minimum air temperature was observed in all sites for the future time period. Minimum air temperatures will cause the greatest impact from climate change in the study sites.

- Simulation of the mean yield for current maize cultivars under future air temperature and precipitation conditions in 2030 indicates that maize yield will increase by 2 % for Bako while, maize yield is projected to decrease by 4 % and 16 % for Ambo and Melkassa respectively relative to the baseline.

- Early planting of maize cultivars between 15 May to 01 June would result in improved relative yields in the future climate. Fertilizer levels between 23-150 kg ha^{-1} would give improved yields for all maize cultivars when combined with early planting for Ambo.

- Planting after 15 May has either no or negative effect on maize yield for Bako. Early planting combined with a nitrogen fertilizer level of 23-100 kg ha^{-1} provided increased relative yields under the future climate. Delayed planting had a negative influence on maize production for Bako under the future climate (2030).

- Late planting would have lower relative yields compared to early planting at Melkassa. Higher fertilizer levels (100-150 kg ha^{-1}) would reduce yield reductions under the future climate, but this varied among maize cultivars studied. Planting the Jibat cultivar between 15-30 June at higher N levels may reduce severe yield reduction of maize at Melkassa.

- In the prediction of maize yield GCMs uncertainty is relatively higher than the corresponding crop models uncertainty.